Agronomy Research

Established in 2003 by the Faculty of Agronomy, Estonian Agricultural University

Aims and Scope:
Agronomy Research is a peer-reviewed international Journal intended for publication of broad-spectrum original articles, reviews and short communications on actual problems of modern biosystems engineering incl. crop and animal science, genetics, economics, farm- and production engineering, environmental aspects, agro-ecology, renewable energy and bioenergy etc. in the temperate regions of the world.

***Agronomy Research* online:**
Agronomy Research is available online at: https://agronomy.emu.ee/

Acknowledgement to Referees:
The Editors of *Agronomy Research* would like to thank the many scientists who gave so generously of their time and expertise to referee papers submitted to the Journal.

Abstracted and indexed:
SCOPUS, EBSCO, DOAJ, CABI Full Paper and Clarivate Analytics database: (Zoological Records, Biological Abstracts and Biosis Previews, AGRIS, ISPI, CAB Abstracts, AGRICOLA (NAL; USA), VINITI, INIST-PASCAL.)

Subscription information:
Institute of Forestry and Engineering,
Estonian University of Life Sciences
Fr.R. Kreutzwaldi Str. 56,
51006 Tartu,
ESTONIA
e-mail: timo.kikas@emu.ee

ISSN 1406-894X

CONTENTS

Agronomy Research **24**(S1), 4–17, 2026
https://doi.org/10.15159/AR.25.105

Breaking new ground: floristic diversity and conservation implications in Bordj Bou Arreridj Forests, Algeria

S. Belloula*, N. Khababa, R. Tiet and R. Amara Korba

Mohamed El Bachir El Ibrahimi University, Faculty of Life and Natural Sciences and of Earth and Universe Sciences, Department of Ecology and Environment, DZ34000 Bordj Bou Arreridj, Algeria
*Correspondence: salima.beloula@univ-bba.dz

Received: July 29th, 2025; Accepted: November 27th, 2025; Published: December 3rd, 2025

Abstract. This study assessed the floristic diversity and conservation status of two ecologically significant forests in Bordj Ghedir region, southeastern Bordj Bou Arreridj, Algeria: Ouled Hanneche (10,221.69 ha) and Ouled Khelouf (8,580.47 ha), covering a combined area of 18,802.16 hectares. Field inventories conducted in March 2023 across 13 stations, with 13 plots collected using random sampling methods. We identified 71 plant species from 32 families and 64 genera. The *Asteraceae* and *Lamiaceae* families were dominant. Hemicryptophytes and Therophytes were the most abundant life forms, and chorological analysis indicated a predominance of Mediterranean elements. Ecological indices (Shannon H' up to 3.602; Simpson 1-D up to 0.97) confirmed high species richness and diversity, particularly in the Ouled Hanneche forest. Despite this richness, the ecosystems face threats from overgrazing, wildfires, and insect pests. The findings provide a critical baseline for conservation and underscore the need for sustainable management strategies, including protected area enforcement and community engagement, to preserve this unique Mediterranean biodiversity hotspot.

Key words: Bordj Bou Arreridj, forest of bordj ghedir, biodiversity indices, floristic diversity.

INTRODUCTION

Aquatic and terrestrial ecosystems support a diverse array of organisms, including animals, plants, and microorganisms. Over the past decades, biodiversity within these ecosystems has faced significant pressures, such as climate change and human activities (Brondízio et al., 2019; Muposhi, 2024). Additionally, biological diversity is increasingly threatened by overexploitation, leading to the decline and disappearance of species. Protecting these living species is essential not only for preserving biodiversity but also for maintaining the ecosystems that provide vital natural resources (Díaz et al., 2019; Bilassé et al., 2023; Isbell et al., 2023).

The Convention on Biological Diversity (CBD), established in 1992, represents a landmark global effort to address these challenges through conservation, sustainable use of resources and equitable sharing of benefits (Convention on Biological Diversity, 1992).

Despite international commitments, biodiversity loss continues, particularly in key habitats such as forests, which have lost around 6.5 million hectares per year since 2010. Forest degradation not only reduces carbon storage and biodiversity, but also disrupts ecosystem services essential to human livelihoods (Hansen et al., 2013). This decline can be attributed to various environmental changes (like climate change) and human activities (such as logging, agriculture, and urbanization) (Gibbs et al., 2010; Hosonuma et al., 2012 and Gustave, 2022).

Among the world's biodiversity hotspots, the Mediterranean basin stands out for its exceptional plant diversity and high endemism. This region faces severe anthropogenic and environmental stressors, including an increased frequency and intensity of wildfires driven by climate change (hotter, drier summers) and human negligence (Batllori et al., 2019; Fayad, 2023 and Moreno et al., 2023). These fires lead to direct species loss, soil erosion, and long-term alteration of ecosystem structure and function (Bowd et al., 2019; Nolan et al., 2021; Thom, 2023 and Navarro-Cano et al., 2024). However, comprehensive data on Mediterranean endemic species is still scarce, which hampers the effectiveness of conservation strategies (Fenu et al., 2020; Fady, 2022; Mendoza-Fernandez et al., 2022; Pipinis et al., 2022; Heba et al., 2023 and Lanzas et al., 2024). In Algeria, forests cover less than 2% of the country's surface area, with continuing losses due to fires, overgrazing and unsustainable land use (DGF, 2022). The Ouled Hanneche and Ouled Khelouf forests (Bordj Bou Arriridj, Algeria) illustrate these pressures, representing ecologically important but vulnerable areas within the Tellian and Saharan Atlas ranges (Forest conservation of Bordj Bou Arreridj, 2023).

Floristic studies are essential for understanding species diversity, guiding conservation and informing sustainable management (Dajoz, 2000; Ludovicy et al., 2022; Elgadi et al., 2024 and Ribeiro et al., 2024). However, gaps persist in regional assessments, particularly in Bordj Bou Arreridj, where climatic and anthropogenic impacts are increasingly threatening endemic flora.

This study aims to assess plant diversity and community structure in the Ouled Hanneche and Ouled Khelouf forests, evaluate environmental and anthropogenic impacts, and provide actionable insights for their conservation aligned with national and global biodiversity targets.

MATERIALS AND METHODS

Study area

Bordj Ghedir is located on the high plateaus in the southeastern of Bordj Bou Arreridj, with geographical coordinates of 36°04′23″ North latitude and 4°45′39″ East longitude (WGS84) (Fig. 1). The research focused on two state forests: Ouled Hanneche and Ouled Khelouf. The Ouled Hanneche forest, part of the Hodna Mountains, spans an area of 10,221.69 hectares across the wilayas of Bordj Bou Arreridj and Sétif. The Ouled Khelouf forest is situated entirely within Bordj Bou Arreridj, covering 8,580.47 hectares (Bordj Bou Arreridj conservation, 2023). The region is characterized by a semi-arid climate and mountainous terrain.

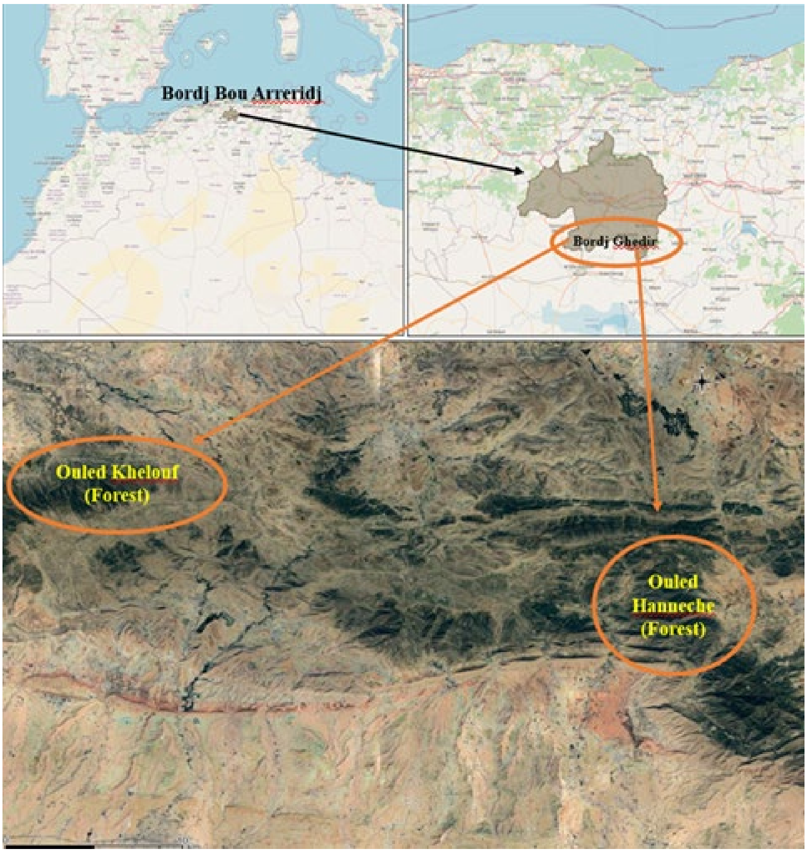

Figure 1. Location of the study area, including the Ouled Hanneche and Ouled Khelouf forests, in the Bordj Bou Arreridj Wilaya, Algeria.

Field methodology, choice of stations and sampling

Two study sites were selected for their ecological significance and representation of the region's forest diversity: the Ouled Khelouf forest and the Ouled Hanneche forest known for its richer floristic diversity in a semi-arid zone. The Ouled Hanneche forest features two exposures (north and south) with an altitudinal range from 1,200 to 1,733 meters, while the Ouled Khelouf forest ranges from 1,341 to 1,700 meters.

During scientific outings in March 2023, a total of 13 stations were established across both forests (4 in Ouled Khelouf forest and 9 in Ouled Hanneche forest). A total of 13 plots were surveyed using the random quadrat method to ensure a representative inventory of the plant community. Station selection was based on environmental factors such as altitude, slope exposure, and vegetation type to capture the ecological heterogeneity in each forest.

Methods for processing results

The results were analyzed using several methods. Ecological composition analysis employed key metrics such as Species Richness (S.R.), Absolute Abundance (Aa), Relative Abundance (RA), and Relative Frequency (RF) to assess species distribution and ecosystem dynamics (Ramade, 1984; Krebs, 1999; Magurran, 2004). Ecological structure analysis utilized indices like the Shannon-Weaver index (H') (Shannon & Weaver, 1949), Simpson index (D) (Simpson, 1949), Piélou's equitability index (J) (Pielou, 1966), and Berger-Parker index (D/B) (Berger & Parker, 1970) to evaluate species diversity, evenness, and community structure. Additionally, diversity estimators, including Chao 1 and Chao 2 (Chao, 1984), were applied to further analyze biodiversity patterns. Together, these methods provided comprehensive insights into ecosystem composition, structure, and diversity.

Mathematical formulae for ecological indices

- Shannon-Weaver Index (H′): $H' = -\sum(pi \cdot \ln(pi))$ (Magurran, 2013).

Where pi is the proportion of individuals belonging to species i, and S is the total number of species. Range: 0 (low diversity) to > 4 (high diversity).

- Simpson Index (1-D): $D = \sum(pi^2)$ (Magurran, 2013).

Range: 0 (low diversity) to 1 (high diversity).

- Piélou's Equitability (J): J = $J = \frac{H'}{\ln(S)}$

Range: 0 (dominance) to 1 (perfect evenness).

- Berger-Parker Index (D): $d = \frac{Nmax}{N}$

Where NmaxNmax is the number of individuals in the most abundant species, and NN is the total number of individuals. Range: 0 (low dominance) to 1 (high dominance).

- Chao1 Estimator: $S_{chao1} = S_{ods} + (F_1^2/2F_2)$.

Where S_{obs} is the number of observed species, F1 is the number of singletons, and F2 is the number of doubletons.

RESULTS

Taxonomic hierarchy of species

In this study, a floristic inventory was conducted across various zones of the two forests mentioned earlier. The inventory included 71 species and 64 genera, belonging to 32 families, as illustrated in Table 1 and Fig. 2.

The histogram (Fig. 2) displays the distribution of plant families in the study area. The most dominant families are *Asteraceae* and *Lamiaceae*, each represented by 10 species. Families with a less represented number of species (only 1 specie) include *Amaranthaceae, Amaryllidaceae, Anacardiaceae, Compositae, Cupressaceae, Fabaceae, Fagaceae, Iridaceae, Liliaceae, Malvaceae, Oleaceae, Papaveraceae, Papilionaceae, Resedaceae, Rutaceae*, and *Thymelaeaceae*. Families represented by 2 species are *Apiaceae, Boraginaceae, Caryophyllacées, Crassulaceae, Geraniaceae, Pinaceae, Rubiaceae.* Families with a

Table 1. Chorological type of species in the study area

Type	Number of species	Percentage %
Mediterranean-Atlantic	5	4%
Mediterranean	35	70%
Western Mediterranean	7	6%
Eastern Mediterranean	2	2%
Cosmopolitan	7	7%
Southern European	6	4%
Eurasian	5	4%
European	2	1%
Southern Eurasian	2	2%

medium number of species (3 or 4 species) include *Asparagaceae* and *Brassicaceae* (4 species each), as well as *Cistaceae, Plantaginaceae, Poaceae,* and *Rosaceae* (3 species each).

This taxonomic hierarchy highlights the diversity and distribution of plant families within the study area, with Asteraceae and Lamiaceae being the most prominent.

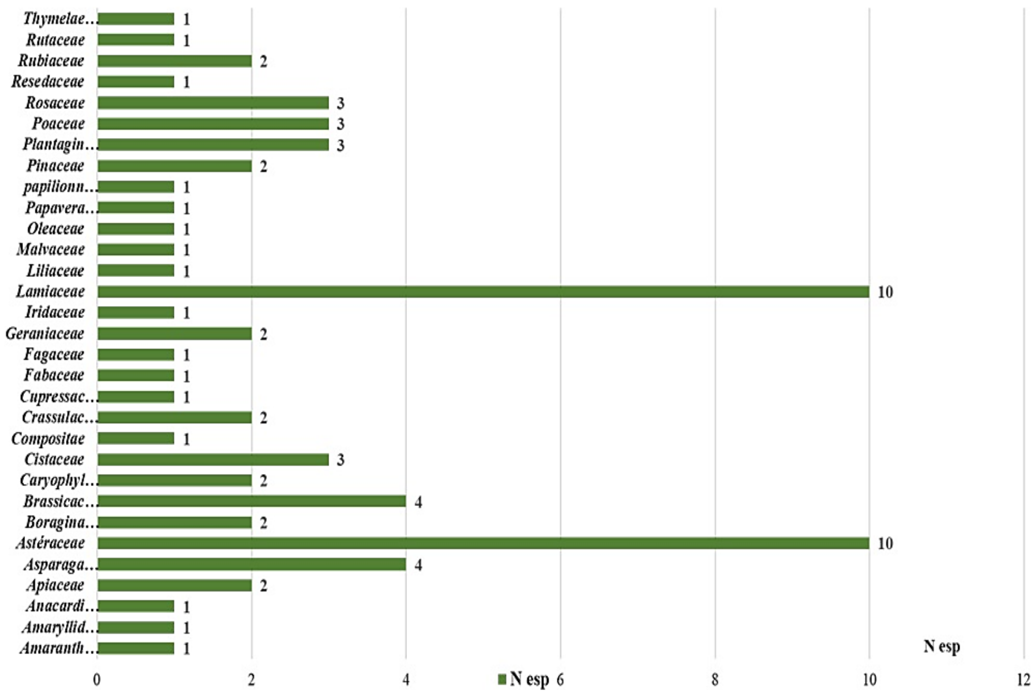

Figure 2. Histogram of plant family distribution in the study area.

The circular diagram (Fig. 3) illustrates the overall biological spectrum of all species in the study area. The most dominant life form is hemicryptophytes, representing 30% of the species. This is followed by therophytes at 25%, chamaephytes at 15%, and geophytes at 14%. Nanophanerophytes account for 10%, while the least represented life forms are microphanerophytes (4%) and mesophanerophytes (2%).

This distribution highlights the prevalence of hemicryptophytes and therophytes in the study area, reflecting the adaptation of plant species to the local environmental conditions.

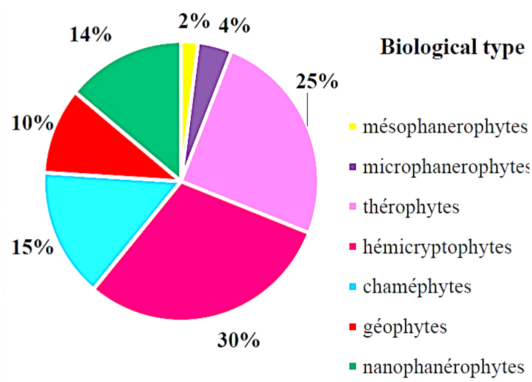

Figure 3. Overall biological spectrum of the study area.

Morphological plant analysis

Analysis of the vegetation in the Bordj Ghedir region, focusing on the two forests, indicates a significant overall presence of herbaceous species. There are 45 herbaceous species, which cover 60% of the green space. The tree and shrub component covers 15% of the space, with 5 tree species and 6 shrub species. Shrubs and sub-shrubs cover a combined 10% of the green space, with shrubs representing 6.8% (9 species) and sub-shrubs representing 3.2% (6 species).

Chorological type

The phytogeographical element according to Braun Blanquet (1919) *sensu* Rivas-Martinez (2017), corresponds to the floristic and phytosociological expression of a well-defined extended territory; it encompasses the species and phytogeographical collectives characteristic of a given region or domain. Chorology is the discipline that studies the delimitation and distribution of species, including those of genera, families, orders, and beyond (Lomolino et al., 2017).

Table 1 shows the chorological type of species in the study area. The most prevalent type is Mediterranean, comprising a high percentage of 70% and a greater number of species (35). The other chorological types have lower percentage (1–7%).

Results of analysis using ecological composition indices

The species richness (Table 2) in the two forests is almost identical in terms of the values recorded across all stations, with a differentiation of families and species from one station to another. This also demonstrates the influence of stationary factors (exposure, altitude, and direction) on forest richness.

Table 2. Stationary variations in species richness in two forests

Forest	Ouled Khelouf				Ouled Hanneche								
Station	1	2	3	4	1	2	3	4	5	6	7	8	9
RS	23	18	23	19	34	35	32	32	32	30	38	32	22

Upon the completion of our field surveys in the forest, we found around 272 individuals recorded in the 3 stations of the Ouled Khelouf forest, with the highest number of individuals being 82 at station 3 (El-Ghebaire). In the Ouled Hanneche forest, we found approximately 1,102 individuals recorded across the 7 stations, with the highest number of individuals being 157 at station 7 (Zbire) (Table 3).

Table 3. Absolute abundance of the two forests

Forest	Ouled Khelouf				Ouled Hanneche								
Station	1	2	3	4	1	2	3	4	5	6	7	8	9
Aa	78	52	82	60	107	133	111	127	118	113	157	122	114

Table 4 presents the relative abundance of individuals in the Ouled Khelouf and Ouled Hanneche forests. In Ouled Khelouf, a total of 272 individuals were recorded, with the highest number (82) recorded at the El-Ghebaire station, reflecting the greatest relative abundance, where the sum of station values equals 1. In Ouled Hanneche, a total of

1,102 individuals were recorded, with the highest number (157) observed at the Zbire station, also indicating the greatest relative abundance, with all station values summing to 1.

Table 4. Relative abundance of the two forests

Forest	Station	N	Aa	AR
Ouled Khelouf	1	272	78	0.286765
	2		52	0.191176
	3		82	0.301471
	4		60	0.220588
Ouled Hanneche	1	1102	107	0.097096
	2		133	0.12069
	3		111	0.100726
	4		127	0.115245
	5		118	0.107078
	6		113	0.102541
	7		157	0.142468
	8		122	0.110707804
	9		114	0.103448

Table 5. Relative frequency of two forests

Forest	Splots	AR	FR (%)
Ouled Khelouf	1	0.286765	28.67647
	2	0.191176	19.11765
	3	0.301471	30.14706
	4	0.220588	22.05882
Ouled Hanneche	1	0.097096	9.709619
	2	0.12069	12.06897
	3	0.100726	10.0726
	4	0.115245	11.5245
	5	0.107078	10.7078
	6	0.102541	10.25408
	7	0.142468	14.24682
	8	0.110707804	11.0707804
	9	0.103448	10.34483

Table 5 shows the relative frequency for the Ouled Khelouf and Ouled Hanneche forests. In Ouled Khelouf, the highest relative frequency is 30.147% at station 3 (El-Ghebaire), while in Ouled Hanneche, the highest relative frequency is 14.246% at station 7 (Zbire), with the total relative frequency for both forests summing to 100%.

Results of analysis using ecological structure indices

From Table 6, the Shannon diversity index (H) was calculated for both Ouled Khelouf and Ouled Hanneche forests, where a higher value of H indicates greater community diversity. In Ouled Khelouf, the index values are nearly identical across all stations (1, 2, 3, and 4), with the highest value of 2.874 recorded at station 3 (El-Ghebaire). Similarly, in Ouled Hanneche, the index values are almost the same across all stations (1, 2, 3, 4, 5, 6, 7, 8, and 9), with the highest value of 3.602 recorded at station 7 (Zbire).

Table 6. Ecological structure indices for the Ouled Khelouf and Ouled Hanneche forests

Forest	Station	Shannon (H')	Simpson (1-D)	Piélou (J)	Berger-Parker (D)
Ouled Khelouf	1	2.871	0.921	0.915	0.192
	2	2.772	0.917	0.959	0.192
	3	2.874	0.907	0.916	0.268
	4	2.47	0.852	0.838	0.333
Ouled Hanneche	1	3.446	0.960	0.977	0.140
	2	3.466	0.963	0.974	0.112
	3	3.360	0.960	0.969	0.090
	4	3.342	0.960	0.964	0.078
	5	3.359	0.960	0.969	0.084
	6	3.349	0.961	0.984	0.088
	7	3.602	0.970	0.990	0.089
	8	3.416	0.964	0.985	0.081
	9	3.041	0.950	0.983	0.087

Table 6 represents the Simpson 1-D index for both Ouled Khelouf and Ouled Hanneche forests, where the index ranges from 0 (minimum diversity) to 1 (maximum diversity). In Ouled Khelouf, the results show that the maximum diversity is found in the Chouchet Naima and

El-Ghebaire stations, while the minimum diversity is observed in the Laayoun station. Similarly, in Ouled Hanneche, the Simpson 1-D index indicates maximum diversity across all stations (1, 2, 3, 4, 5, 6, 7, 8, and 9).

Table 6 shows the species equirepartition index (Piélou's equitability index) for both Ouled Khelouf and Ouled Hanneche forests, with values ranging from 0 (dominance of one species) to 1 (equirepartition of species). In Ouled Khelouf, the results are nearly identical across stations 1, 2, 3, and 4, with the highest value of 0.959 recorded at the Chouchet Naima station. Similarly, in Ouled Hanneche, the index values are very close across all stations (1, 2, 3, 4, 5, 6, 7, 8, and 9), with the highest value of 0.990 observed at the Zbire station.

Berger-Parker index (Table 6) which measures the proportion of the community represented by the most abundant species, for both Ouled Khelouf and Ouled Hanneche forests. In Ouled Khelouf, the highest value of 0.333 is recorded at the Laayoun station, while in Ouled Hanneche, the highest value of 0.140 is observed at the Agar station compared to the other stations.

Analysis of biodiversity indices for Ouled Khelouf and Ouled Hanneche forests

The analysis of forest diversity utilized several ecological indices, with results summarized in Table 6. The findings for each index are as follows:

Shannon Diversity Index (H'), this index increases with higher species richness and evenness. In Ouled Khelouf, the index values were very consistent across all four stations, with the highest value (H' = 2.874) recorded at station 3 (El-Ghebaire). A similar pattern of high uniformity was observed in Ouled Hanneche across its nine stations, where the maximum diversity (H' = 3.602) was found at station 7 (Zbire).

Simpson's Diversity Index (1-D), Ranging from 0 (minimal diversity) to 1 (maximal diversity), this index measures dominance. In Ouled Khelouf, the highest diversity was found at the Chouchet Naima and El-Ghebaire stations, while the Laayoun station showed the lowest diversity. In contrast, the Simpson index indicated consistently high diversity across all stations in Ouled Hanneche.

Pielou's Evenness Index (J'), this index ranging from 0 (dominance by one species) to 1 (perfect species evenness), showed little variation across stations in both forests. In Ouled Khelouf, the values were nearly identical, peaking at 0.959 in Chouchet Naima. Similarly, Ouled Hanneche exhibited very uniform and high evenness, with a maximum of 0.990 at the Zbire station.

Berger-Parker Index, this index measures the proportional dominance of the most abundant species. A higher value indicates greater dominance. In Ouled Khelouf, the Laayoun station had the highest dominance value (0.333). In Ouled Hanneche, the Agar station showed the highest level of dominance (0.140) compared to the other stations.

Analysis results using diversity estimators

Table 7 presents the diversity estimators, including Chao1 and Chao2, which estimate the number of unobserved species based on those observed once or twice, for both Ouled Khelouf and Ouled Hanneche forests. In Ouled Khelouf, the Laayoun station has the highest values for Chao1 (32.52) and Chao2 (41.1) compared to the other stations, while the values for stations 1, 2, 3, and 4 are nearly identical and closely aligned, suggesting similar levels of unobserved species. In Ouled Hanneche, the Zbire station records the highest values for Chao1 (38) and Chao2 (38.06), whereas the values across stations 1, 2, 3, 4, 5, 6, 8, and 9 are very similar and closely grouped, indicating consistent levels of unobserved species across these areas.

Table 7. Diversity estimators for two forests

Forest	Ouled Khelouf				Ouled Hanneche								
Station	1	2	3	4	1	2	3	4	5	6	7	8	9
Chao1	26.46	18.27	24.27	32.52	35.73	37.13	35.47	33.35	33.86	30.09	38	32.3	22
Chao2	28.27	18.44	25.46	41.1	36.73	38.02	36.53	33.79	34.55	30.2	38.06	32.5	22
RS	23	18	23	19	34	35	32	32	32	30	38	32	22

Notable plant species and photographic documentation

The study identified several ecologically and medicinally significant plant species. Among the most widespread and notable species are (Fig. 5):

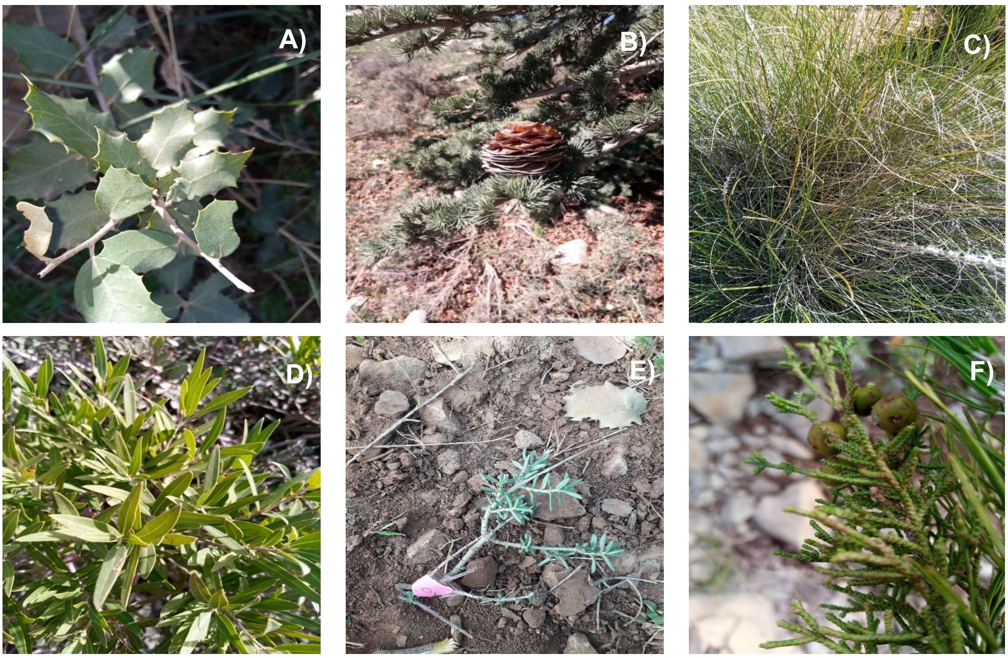

Figure 4. Photographs of key plant species in the study area: A) *Quercus ilex*, B) *Cedrus atlantica*, C) *Stipa tenacissima*, D) *Olea europaea*, E) *Thymus vulgaris* L., F) *Juniperus phoenica* L.

DISCUSSION

This study represents one of the first comprehensive assessments of floristic diversity in the Bordj Ghedir forests, a region that has been underrepresented in biodiversity research despite its ecological significance. Focusing on the Ouled Khelouf and Ouled Hanneche forests, this research inventoried vegetation and analyzed floristic diversity across 10,221.69 hectares. By documenting 71 plant species from 32 families and 64 genera.

This work fills a critical gap in the understanding of Algeria's plant biodiversity. The findings reveal notable floristic richness, with *Asteraceae* and *Lamiaceae* being the most dominant families, each represented by ten species. Other significant families include *Amaranthaceae*, *Fabaceae*, *Rosaceae*, and *Oleaceae*, among others. Notable species recorded include ecologically and culturally significant taxa such as the Holm oak (*Quercus ilex*), Atlas cedar (*Cedrus atlantica*), and medicinal plants like Olive (*Olea europaea* L.), Mastic tree (*Pistacia lentiscus* L.), and Rosemary (*Rosmarinus officinalis* L.). A significant finding was the first recorded presence of *Ruscus aculeatus* in the Bordj Bou Arreridj region. While no strongly invasive alien species were dominant in the surveyed plots, the presence of disturbance-indicator species, such as *Stipa tenacissima* L., signals ecosystem degradation and potential vulnerability to plant invasions, a factor that requires monitoring. This study not only enhances the scientific documentation of the region's flora but also provides a baseline for future biodiversity monitoring and conservation efforts in this ecologically important area.

The study reveals no significant difference in species richness (S.R.) between the Ouled Hanneche and Ouled Khelouf forests, suggesting minimal unobserved species. However, Ouled Hanneche exhibits greater biodiversity compared to Ouled Khelouf. Comparisons with other regions, such as Boussaada & Bensid'houm (2020), show that the diversity in these forests surpasses that of the Bordj Bou Arreridj region, which has a Shannon index (H) of 3.359, Simpson's index (1-D) of 0.9456, and Piélou's equitability index (J) of 0.8586, indicating high plant coverage and equitable species distribution. Similarly, Taibaoui et al. (2020) reported lower diversity levels in other vegetation units, with Shannon-Weaver index values ranging from 3.34 to 2.40 and Pielou index values of 0.55 and 0.39, while this study shows higher equitability.

The Biological spectrum, Hemicryptophytes dominate the forest ecosystem at 30%, followed by therophytes (25%), offers key insights into the prevailing environmental conditions. The proportion of Chamaephytes (15%) is a classic indicator of a Mediterranean climate with a pronounved dry season, but it can also signal ecosystem disturbance and overgrazing, as thes species complete their life cycle quickly to avoid summer drought and herbivory (Allen, 2014; Valerio et al., 2022). The proportion of Geophytes is (14%). Nanophanerophytes account for 10%, while microphanerophytes and mesophanerophytes are less represented, at 4% and 2%, respectively. The vegetation is predominantly herbaceous, with 45 species covering 60% of the area. Trees and shrubs collectively account for 15%, including five tree species and six shrub species. Chorological analysis highlights the Mediterranean element as the dominant biogeographical influence. Hermaphroditism is the most prevalent plant sexuality, observed in 52 species, followed by autogamous pollination in 49 species. Barochory (seed dispersal by gravity) is the dominant dissemination mechanism, accounting for 60% of the species.

The Bordj Ghedir study area exhibits significant plant cover in both forests, with high biodiversity indicated by ecological indices. In the Ouled Khelouf forest, the Shannon index (H) is 2.874, the Simpson index (1-D) is 0.92, and the Piélou equitability index (J) is 0.95, reflecting significant diversity. The Berger-Parker dominance index is 0.333, and diversity estimators Chao 1 and Chao 2 are 32.52 and 41.1, respectively. Similarly, the Ouled Hanneche forest shows even greater diversity, with a Shannon index (H) of 3.602, a Simpson index (1-D) of 0.97, and a Piélou equitability index (J) of 0.99.

The Berger-Parker dominance index is 0.14, and diversity estimators Chao 1 and Chao 2 are 38 and 38.06, respectively.

Despite this richness, the forests face significant threats from overgrazing, wildfires, and the cedar processionary caterpillar (*Thaumetopoea bonjeani*), which are reducing vegetation cover and accelerating degradation. The presence of *Stipa tenacissima* L. signals ecosystem degradation and advanced successional regression, particularly in the Ouled Khelouf forest, where it is more abundant.

Conservation efforts, such as those documented by Salemkour et al. (2017), demonstrate the potential for restoring floristic richness through resting practices. The study area hosts numerous medicinal species, including *Olea europaea* L., *Pistacia lentiscus* L., and *Rosmarinus officinalis* L., many of which are used in traditional medicine. Notably, *Ruscus aculeatus* was recorded for the first time in the Bordj Bou Arreridj region The first recorded presence of Ruscus aculeatus (Butcher's broom) in the Bordj Bou Arreridj region is a significant finding. This shade-tolerant, evergreen subshrub typically indicates well-preserved forest understories with stable microclimates (Bricca et al., 2021). Its discovery suggests the existence of small, ecologically mature refugia within these forests. Field observations also identified critical ecological factors, such as the presence of the Holm oak (*Quercus ilex*), including a notable specimen in Ouled Hanneche, and the Atlas cedar (*Cedrus atlantica*) at Zbire station.

To address these challenges, a comprehensive approach is needed, integrating on-the-ground conservation strategies with advanced decision-support tools. This includes preserving forest heritage by protecting ecological and cultural values, adopting sustainable silvicultural practices (e.g., selective harvesting and replanting) to enhance regeneration and resilience, and conducting targeted research to optimise medicinal plant use. Spatial decision-support systems, such as AHP models, are particularly effective for assessing forest resource sustainability (Pedro & Quinta-Nova, 2024), while remote sensing can directly inform these efforts by identifying priority protection zones, modelling regeneration scenarios, and quantifying extraction-conservation trade-offs (Belloula & Beghami, 2018; Moreira et al., 2025). Community education programmes can use GIS-based tools to visualise ecosystem vulnerabilities, and stricter enforcement of biodiversity regulations ensures a science-based, long-term balance in forest management.

CONCLUSION

This study provides a foundational assessment of the floristic diversity in the Bordj Ghedir forests, documenting 71 plant species from 32 families and 64 genera. The most significant results confirm the area's high ecological value, characterized by a strong Mediterranean influence with dominant families including *Asteraceae* and *Lamiaceae*. Key findings include a high diversity (Shannon index up to 3.602 in Ouled Hanneche) and equitable species distribution (Piélou index up to 0.99). The prevalence of hemicryptophytes (30%) and therophytes (25%) reflects adaptation to the local semi-arid climate. The first recorded presence of *Ruscus aculeatus* in the region and the identification of key tree species like *Quercus ilex* and *Cedrus atlantica* are also notable. However, this biodiversity is under threat from anthropogenic pressures such as overgrazing, wildfires, and forest pests.

By implementing these strategies such as sustainable forest management, fire prevention, invasive species control, and community engagement threats to biodiversity can be mitigated, ensuring the sustainable management of these forests.

To build on these findings, further research is recommended, including increasing the number of sampling stations and extending inventory periods. These efforts will deepen our knowledge of forest ecosystems and contribute to the development of more effective conservation strategies for this critical area, ensuring the preservation of this unique and biodiverse region for future generations. The findings emphasize the urgent need for integrated conservation strategies. Future efforts should focus on sustainable forest management, fire prevention, invasive species monitoring, and active community engagement.

ACKNOWLEDGEMENTS. We sincerely thank the officials of the Bordj Ghedir district (Bordj Bou Arreridj, Algeria) for their invaluable support during fieldwork. We are especially grateful to Mr. Belgoumri A. for his essential assistance and for providing critical regional insights that greatly facilitated this research.

REFERENCES

Allen, H. 2014. *Mediterranean ecogeography*. Routledge, 286 pp.

Batllori, E., De Cáceres, M., Brotons, L., Ackerly, D.D., Moritz, M.A. & Lloret, F. 2019. Compound fire-drought regimes promote ecosystem transitions in Mediterranean ecosystems. *Journal of Ecology* **107**(3), 1187–1198.

Belloula, S. & Beghami, Y. 2018. Assessment of the Dynamics of Atlas Cedar Decline (*Cedrus atlantica* Manetti) by Remote Sensing in the Aurès area, Algeria. *The Arab World Geographer* **21**(2–3), 154–167.

Berger, W.H. & Parker, F.L. 1970. Diversity of planktonic Foraminifera in deep-sea sediments. *Science* **168**(3937), 1345–1347.

Bilassé, Z., Nebnoma, R.T., Benjamin, K., Sérigne, M.S., Moussa, D. & Amadé, O. 2023. Ecosystem biodiversity and natural resource exploitation in the context of climate change. *International Journal of Biological and Chemical Sciences* **17**(1), Special Issue. ISSN 1991-8631 (Print), ISSN 1997-342X (Online), 1p. (in French).

Boussaada, B. & Bensid'houm, S. 2020. *Qualitative and quantitative assessment of the floristic composition of the wilaya of Bordj Bou Arreridj*. Université Mohamed El Bachir El Ibrahimi, Bordj Bou Arreridj. 47 pp. (in French).

Bowd, E.J., Banks, S.C., Strong, C.L. & Lindenmayer, D.B. 2019. Long-term impacts of wildfire and logging on forest soils. *Nature Geoscience* **12**(2), 113–118.

Bricca, A., Carranza, M.L., Varricchione, M., Cutini, M. & Stanisci, A. 2021. Exploring plant functional diversity and redundancy of Mediterranean high-mountain habitats in the Apennines. *Diversity* **13**(10), 466 pp.

Brondízio, E.S., Settele, J., Diaz, S. & Ngo, H.T. 2019. Global assessment report on biodiversity and ecosystem services of the Intergovernmental Science-Policy Platform on Biodiversity and Ecosystem Services. https://doi.org/10.5281/zenodo.3831673

Chao, A. 1987. Estimating the Population Size for Capture-Recapture Data with Unequal Catchability. *Biometrics* **43**(4), 783–791.

Convention on Biological Diversity. 1992. *Text of the Convention on Biological Diversity*. United Nations.

Dajoz, R. 2000. *Ecology handbook*. Dunod, 615 pp. (in French).

DGF. Direction Générale des Forêts, 2022. *Programme d'Action National sur la lutte contre la Désertification*, 104 pp.

Díaz, S., Settele, J., Brondízio, E.S., Ngo, H.T., Agard, J., Arneth, A., ... & Zayas, C.N. 2019. Pervasive human-driven decline of life on Earth points to the need for transformative change. *Science* **366**(6471), eaax3100. https://doi.org/10.1126/science.aax3100

Elgadi, S., Zine, H., Dallahi, Y. & Ouhammou, A. 2024. Unveiling floristic diversity in the High Atlas: Insights from a protected reserve in a global Mediterranean biodiversity hotspot. *Biosystems Diversity* **32**(4), 416–425.

Fady, B., Esposito, E., Abulaila, K., Aleksic, J.M., Alia, R., Alizoti, P., ... & Westergren, M. 2022. Forest genetics research in the Mediterranean Basin: Bibliometric analysis, knowledge gaps, and perspectives. *Current Forestry Reports* **8**(3), 277–298.

Fayad, J. Numerical studies of extreme fires (Doctoral dissertation, Pascal Paoli University). MNT: 2023CORT0015, tel-04461572. (in Frensh).

Fenu, G., Bacchetta, G., Christodoulou, C.S., Cogoni, D., Fournaraki, C., Gian Pietro, G.D.G. ... & de Montmollin, B. 2020. A common approach to the conservation of threatened island vascular plants: First results in the Mediterranean Basin. *Diversity* **12**(4), 157.

Forest conservation of Bordj Bou Arreridj. 2023. Organisme.

Gibbs, H.K., Ruesch, A.S., Achard, F., Clayton, M.K., Holmgren, P., Ramankutty, N. & Foley, J.A. 2010. Tropical forests were the primary sources of new agricultural land in the 1980s and 1990s. *Proceedings of the National Academy of Sciences* **107**(38), 16732–16737. https://doi.org/10.1073/pnas.0910275107

Gustave, Ch.L. 2022. Impact of Abiotic Factors on the Growth of Reforestation Trees in the Fight Against Global Warming in Beni/Lubero. *Multidisciplinary Research Academic Journal (MDRAJ)* **7**, 42–67 (in Frensh).

Hansen, M.C., Potapov, P.V., Moore, R., Hancher, M., Turubanova, S.A., Tyukavina, A., ... & Townshend, J.R.G. 2013. High-resolution global maps of 21st-century forest cover change. *Science* **342**(6160), 850–853.

Heba, B., Kamal, Sh., Marwa, W. & Halmy, A. 2023. A critical inventory of the Mediterranean endemics in the Egyptian flora. *Biodiversity and Conservation* **32**, 1327–1351. https://doi.org/10.1007/s10531-023-02561-7

Hosonuma, N., Herold, M., De Sy, V., De Fries, R. S., Brockhaus, M., Verchot, L., ... & Romijn, E. 2012. An assessment of deforestation and forest degradation drivers in developing countries. *Environmental Research Letters* **7**(4), 044009.

Isbell, F., Balvanera, P., Mori, A.S., He, J.S., Bullock, J.M., Regmi, G.R., ... & Palmer, M.S. 2023. Expert perspectives on global biodiversity loss and its drivers and impacts on people. *Frontiers in Ecology and the Environment* **21**(2), 94–103. https://doi.org/10.1002/fee.2536

Krebs, C.J. 1999. *Ecological Methodology* (2nd ed.). Addison-Wesley Educational Publishers, 656 pp.

Lanzas, M., Pou, N., Bota, G., Pla, M., Villero, D., Brotons, L., ... & Hermoso, V. 2024. Detecting management gaps for biodiversity conservation: An integrated assessment. *Journal of Environmental Management* **354**, 120247.

Lomolino, M.V., Riddle, B.R. & Whittaker, R.J. 2017. *Biogeography*. (5e éd.). Sinauer Associates, 150 pp.

Ludovicy, S., Noroozi, J., Semenchuk, P., Moser, D., Wessely, J., Talebi, A. & Dullinger, S. 2022. Protected area network insufficiently represents climatic niches of endemic plants in a Global Biodiversity Hotspot. *Biological Conservation* **275**, 109768.

Magurran, A.E. 2004. *Measuring Biological Diversity*. Blackwell Publishing, 215 pp.

Magurran, A.E. (2013). *Ecological diversity and its measurement*. Springer Science & Business Media.

Mendoza-Fernández, A.J., Fernández-Ceular, Á., Alcaraz-Segura, D., Ballesteros, M. & Peñas, J. 2022. The fate of endemic species specialized in island habitat under climate change in a Mediterranean high mountain. *Plants* **11**(23), 3193. doi: 10.3390/plants11233193

Moreira, A.N.H., Ciappina, A.H., Andrade, R.R., Casaroli, D., Rossi, G., Conti, L. & Bambi, G. 2025. Temporal analysis of pasture vegetation cover in central-western Brazil using remote sensing. *Agronomy Research* **23**(S1), 151–163.

Moreno, M., Bertolín, C., Arlanzón, D., Ortiz, P. & Ortiz, R. 2023. Climate change, large fires, and cultural landscapes in the mediterranean basin: An analysis in southern Spain. *Heliyon* **9**(6).

Muposhi, V.K. 2024. Biodiversity Conservation in the Anthropocene. *Environmental Change and Biodiversity Conservation in Sub-Saharan Africa: Volume* **1**, 418.

Navarro-Cano, J.A., Goberna, M., Pérez-Valera, E. & Verdú, M. 2024. Decoupling of trait and species turnover in fire-prone Mediterranean plant communities. *Journal of Ecology* **112**(9), 2043–2056.

Nolan, R.H., Collins, L., Leigh, A., Ooi, M.K., Curran, T.J., Fairman, T.A., ... & Bradstock, R. 2021. Limits to post-fire vegetation recovery under climate change. *Plant, cell & environment* **44**(11), 3471–3489.

Pedro, N. & Quinta-Nova, L.C. 2024. GIS-based analytic hierarchy process model for a forest residuals biorefinery site selection. *Agronomy Research* **22**(3), 1254–1265.

Pielou, E.C. 1966. The measurement of diversity in different types of biological collections. *Journal of Theoretical Biology* **13**, 131–144.

Pipinis, E., Hatzilazarou, S., Kostas, S., Bourgou, S., Megdiche-Ksouri, W., Ghrabi-Gammar, Z., ... & Krigas, N. 2022. Facilitating conservation and bridging gaps for the sustainable exploitation of the Tunisian local endemic plant Marrubium aschersonii (Lamiaceae). *Sustainability* **14**(3), 1637.

Ramade, F. 1984. *Elements of Ecology: Fundamental Ecology*. Paris: McGraw-Hill. 379 pp. (in French).

Ribeiro, João, Camilo Alves, Constança & Ribeiro, Nuno. 2024. The protective role of canopy cover against cork oak decline in the face of climate change. *Central European Forestry Journal* **70**, 133–143. 10.2478/forj-2024-0011

Rivas-Martínez, S., Penas, Á., del Río, S., Díaz González, T.E. & Rivas-Sáenz, S. 2017. Bioclimatology of the Iberian Peninsula and the Balearic Islands. *The Vegetation of the Iberian Peninsula: Volume* **1**, 29–80. https://doi.org/10.1007/978-3-319-54784-8_2

Salemkour, N., Fadlaoui, H. & Lebidi, A. 2017. Restoration of richness and floral diversity through fallowing in a *Stipa tenacissima* (L.) steppe in the M'Sila region of Algeria. *Afrique Science* **3**(4), 369–380.

Shannon, C.E. & Weaver, W. 1949. *The Mathematical Theory of Communication*. University of Illinois Press. (LCCN 49-11922).

Simpson, E.H. 1949. Measurement of diversity. *Nature* **163**(4148), 688.

Taibaoui, B., Douaoui, A. & Bouxin, G. 2020. Floristic diversity of the southern Algerian steppe: the case of the Djelfa region (Algeria). *Lejeunia, Revue de Botanique* **203**, 1–41.

Thom, D. 2023. Natural disturbances as drivers of tipping points in forest ecosystems under climate change–implications for adaptive management. *Forestry* **96**(3), 305–315.

Valerio, M., Ibáñez, R., Gazol, A. & Götzenberger, L. 2022. Long-term and year-to-year stability and its drivers in a Mediterranean grassland. *Journal of Ecology* **110**(5), 1174–1188.

Agronomy Research **24**(S1), 18–40, 2026
https://doi.org/10.15159/AR.25.107

Effect of different date palm (*Phoenix dactylifera*) compost modalities on soil parameters in the Algerian Semi-Arid Zone

M. Rebai[1,2,*], K. Guimeur[1,2], N. Boulelouah[3,2], H. Bedjaoui[1,2] and D. Haddad[4]

[1]University of Biskra, Faculty of Exact Sciences, Natural and Life Sciences, Department of Agronomic Sciences, S BP 145 RP, 07000, Algeria
[2]Laboratory for Ecosystem Diversity and Agricultural Production Systems Dynamics in Arid Zones (DEDSPAZA), University of Biskra, Algeria
[3]University of Batna 1, Department of Agricultural Sciences, Allées 19 mai, Route de Biskra, Batna 05000, Algeria
[4]University Batna2, department of Health and Safety, Faculty of Engineering Sciences, Fesdis, 05078 Batna, Algeria
[*]Correspondence: messaouda.rebai@univ-Biskra.dz

Received: August 22nd, 2025; Accepted: November 27th, 2025; Published: December 5th, 2025

Abstract. In the vast regions of eastern Algeria, the calcareous soils are characterised by low fertility. Moreover, these soils frequently lack organic matter and essential nutrients, limiting sustainable yield potential. This study aimed to assess the impact of using locally sourced date palm compost with mineral fertilisers on the improvement of soil fertility in a cereal-based system. A field experiment was arranged in a randomised complete block design (RCBD) with 11 treatments: date palm compost applied at three rates (C1: 30 t ha^{-1}, C2: 50 t ha^{-1}, C3: 70 t ha^{-1}), either alone or combined with monoammonium phosphate (C1M, C2M, C3M: 100 kg ha^{-1} MAP) or urea (C1U, C2U, C3U: 50 kg ha^{-1} urea), one treatment with sheep manure at 45 t ha^{-1}, and an untreated control.. The study evaluated the effects of varying rates of date palm compost and mineral fertilisers on soil chemical characteristics at two depths (0–20 cm and 20–40 cm). Results indicated that elevated compost rates, whether applied alone or combined with mineral fertilisers, significantly improved organic matter content, nutrient availability, and soil chemical balance at both depths. Combined treatments C3U (70 t ha^{-1} compost + 50 kg ha^{-1} urea) and C3M (70 t ha^{-1} compost + 100 kg ha^{-1} MAP) showed the greatest improvements, with C3M identified as the optimal treatment. Integrated date palm compost fertilisation is well-suited to the region's calcareous soils, enhancing nutrient availability, improving soil fertility, and efficiently utilising a locally available resource. These findings suggest that integrating date palm compost with mineral fertilisers is a sustainable approche to improving soil fertility in semi-arid mediterranean systems.

Key words: calcareous soils, compost, date palm, integrated fertilisation, semi-arid zone, soil fertility.

INTRODUCTION

In the semi-arid regions of eastern Algeria, cereal production is severely constrained by climate variability and limited soil fertility. The prevailing climatic conditions, marked by insufficient and erratic rainfall, significantly reduce agricultural productivity and grain yield (Smadhi et al., 2017; Amirouche et al., 2021). These areas are dominated by calcareous and alkaline soils with low organic matter, weak cation exchange capacity, and poor availability of nitrogen and phosphorus (Benabderrahim et al., 2017; Kavvadias et al., 2024). Moreover, inadequate irrigation often aggravates water salinisation, leading to further degradation of agroecological productivity (Devkota et al., 2022).

To counteract these constraints, intensive fertilisation with monoammonium phosphate (MAP) and urea (46% N) is frequently applied. However, calcareous soils exhibit reduced fertiliser efficiency due to nitrogen volatilisation losses (Adnan et al., 2025), resulting in structural decline and organic matter depletion (Brownrigg et al., 2022; Bontpart et al., 2024). Integrated fertilisation combining mineral and organic sources has therefore been recognised as a promising option to restore soil fertility and enhance productivity (Saber et al., 2024; Ejigu et al., 2025).

Organic fertilisers such as compost and sheep manure improve both physical and chemical soil properties (Lanno et al., 2020; Šařec et al., 2020) by enhancing water retention, microbial activity, and carbon sequestration (Al-Suhaibani et al., 2020; Bayu, 2020). Mixing organic materials with mineral fertilisers increases nutrient efficiency while reducing volatilisation and leaching losses, thus lowering dependence on synthetic products (Manzoor, 2024). Among locally available residues, date palm (*Phoenix dactylifera* L.), a keystone of oasis agriculture–generates large volumes of unused biomass such as dry fronds and spadices (Abid & Ammar, 2022; Arroussi et al., 2022; Habchi et al., 2022; Kavvadias et al., 2024).

The growing accumulation and burning of palm residues highlight an important need for their valorisation as part of sustainable agricultural transitions (Bhatia & Sindhu, 2024). Composting these by-products offers a promising route, improving soil fertility while supporting a circular bioeconomy (Benabderrahim et al., 2017; Faiad et al., 2022; El Janati et al., 2023; Kavvadias et al., 2024). Blending date palm compost with organic (e.g., sheep manure) and mineral (e.g., MAP) fertilisers enhances crop growth, nutrient availability (Badawi, 2022; Hakimi et al., 2024; Kavvadias et al., 2024), and disease control (Istifadah et al., 2020).

For soil fertility conservation, these composts help maintain soil organic matter, stabilise pH, and mitigate toxic accumulations (Ghouili et al., 2022). They also improve plant tolerance to water stress by promoting root growth and hormonal balance (Ding et al., 2020; Siebielec et al., 2020; El-Aziz et al., 2025; Li et al., 2025). This is highly beneficial as it contributes to reducing pollution from burning, greenhouse gas (GHG) emissions, and valorisation of agriculturally useful waste (Al-Suhaibani et al., 2020; Saber et al., 2024). Combining date palm fronds with organic sources (e.g., manure or olive pomace) or mineral inputs (rock phosphate) produces high-quality composts suited to dryland soils (El Janati et al., 2023; Kavvadias et al., 2024). The present study aims to assess the effects of varying application rates of palm compost and integrated fertilisation strategies on calcareous soil properties in cereal systems, contributing to sustainable soil management in semi-arid environments (Gomez-Muñoz et al., 2012; Ameziane et al., 2020; Badagliacca et al., 2024; Kavvadias et al., 2024).

MATERIALS AND METHODS

Site description and climate

The field trial was carried out under a semi-arid climate, implemented at the farm of Abdessamed Salah (Timgad) (35°31'12.1"N 6°29'24.7"E) at an altitude of 1,100 m (Fig. 1) during the 2021–2022 growing season.

Figure 1. Location of the experimental site within Batna province (Algeria).

Climatic conditions were very unfavourable for crop growth in the Timgad region (Batna) during the 2021–2022 agricultural season (Fig. 2). Cumulative annual rainfall reached approximately 105 mm, which is significantly below the average recorded over the last twenty years.

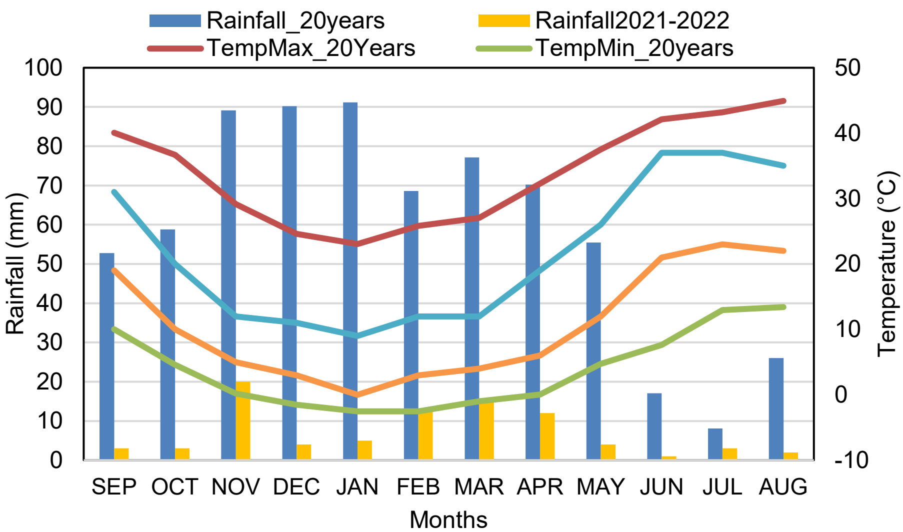

Figure 2. Monthly distribution of rainfall and minimum and maximum temperature during the growing season (2021/2022) and averaged over a 20 years period (DSA-Batna, 2023) and (NASA POWER, 2025).

Monthly rainfall was also very low throughout the year, not exceeding 18 mm, with particularly marked deficits in autumn and winter, which are generally wetter periods.

Maximum temperatures, which were above seasonal averages, reached 40 °C in June and July. Minimum temperatures, particularly from May to August, also exceeded historical averages, with values in July approaching 20 °C, compared to a usual average of around 15 °C over the last twenty years. This persistent water deficit, combined with abnormally high maximum and minimum temperatures, reflects the severe climatic stress experienced by the Timgad region during this growing season.

Experimental design and treatments

The treatment was a randomised complete block design (RCBD) with four replications. It was implemented on land allocated for planting durum wheat. Each block or replication was sub-divided into 11 sub-plots (each corresponding to a fertilisation treatment and covering an area of 31 m²). The total area of the experimental plot was 527 m², including inter-block (1 m²) and inter-plot (1m²) spacing. There were forty-four sub-plots in total (11 treatments × 4 blocks) (Fig. 3).

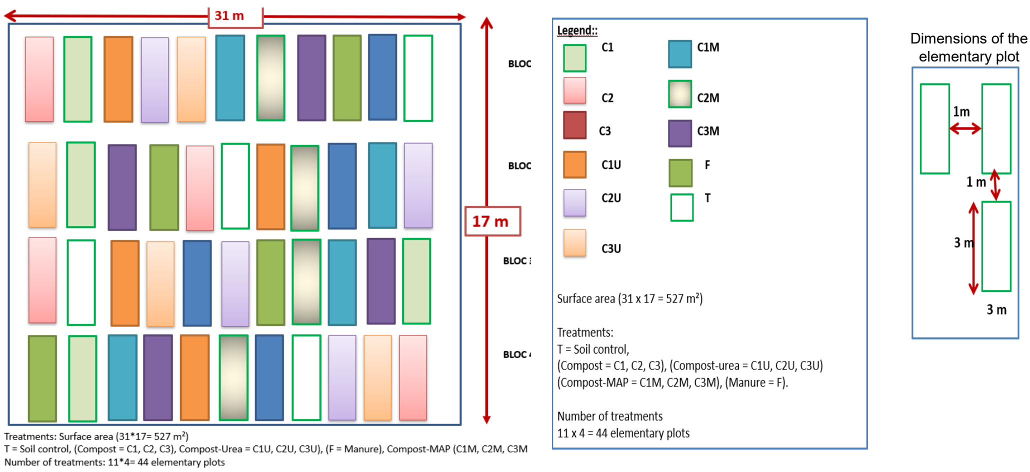

Figure 3. Experimental design.

The 11 fertilisation and organic amendment treatments are shown in Table 1. The selected treatments in this study were chosen based on the mineral fertilisers available, particularly urea (46%) and monoammonium phosphate (MAP), which are readily available on the Algerian market for cereal production. These mineral fertilisers were combined with organic amendments derived from date palm residues as compost, with the aim of increasing soil fertility.

The date palm (*Phoenix dactylifera* L.), is a dioecious monocotyledonous plant widely cultivated in arid and semi-arid regions, primarily for its edible fruit known as dates. It commonly propagates through offshoots or lateral shoots, a method that allows the faithful preservation of the mother plant's genetic traits. Renowned for its remarkable adaptability to harsh climatic conditions such as drought and high temperatures, the date palm plays a vital role as both a food source and an economic resource in dryland areas (Ashraf & Hamidi-Esfahani., 2011; Sharma et al., 2025).

The composting of date palm waste involves several key steps. First, the preparation and mixing of raw materials include collecting the main wastes such as dry leaves, stems, trunks, and sometimes fruit residues. These materials are shredded to hasten decomposition and often mixed with other organic materials like animal manure or green waste to balance the carbon-to-nitrogen (C/N) ratio, which is essential for effective composting. The mixtures are then piled into windrows or heaps to allow adequate aeration. During the thermophilic phase, temperatures rapidly rise up to approximately 45.7 °C before gradually falling back to ambient levels around 21 °C, indicating maturation. Maintaining moisture content between 50 and 60% and regular turning of the piles ensures oxygen supply and prevents anaerobic fermentation. Throughout the process, physico-chemical parameters such as pH, electrical conductivity, and organic carbon loss (typically 8.9 to 10.5%) are monitored to gauge microbial activity and organic matter breakdown. The matured compost has a natural earthy smell and uniform brown colour, with spectroscopic analyses (UV-visible, FTIR) confirming the transformation of organic compounds. A final C/N ratio below 20 indicates the compost has reached maturity and is suitable for use as an organic soil amendment (Habchi et al., 2020; Aydi et al., 2023).

Table 1. Treatments of organic and commercial fertilisation rate

Treatment	Control (T)	Sheep manure (F)	Compost (C) t ha^{-1}	MAP (M) kg ha^{-1}	Urea (U) kg ha^{-1}
T	0	0	0	0	0
F	0	45	0	0	0
C1	0	0	30	0	0
C2	0	0	50	0	0
C3	0	0	70	0	0
C1M	0	0	30	100	0
C2M	0	0	50	100	0
C3M	0	0	70	100	0
C1U	0	0	30	0	50
C2U	0	0	50	0	50
C3U	0	0	70	0	50

Legend: t (Control: Soil without amendment) – F (Sheep manure). Compost rate (C1-C2-C3). Compost-MAP combinations (C1M-C2M-C3M). Compost-Urea 46% combinations (C1U-C2U-C3U). Mineral fertilizer: MAP. Mono Ammonium Phosphate: ($NH_4H_2PO_4$): commercial fertilizer with 12% N and 52% P. U: Urea 46%.

Table 2. Physicochemical characteristics of compost

Settings (units)	Values
Organic C (%)	33.72
OM (%)	58
N total (%)	3 .18
C/N	10.60
Ph	7.47
K exchangeable (ppm)	164.1
K total (%)	0.41
Available phosphorus (ppm)	20.85
Total phosphorus (%)	0.27
EC (ms/cm)	5.22

Legend: OM = Organic Matter; TN = Total Nitrogen; TP = Total Phosphorus; AP = Available Phosphorus; TK = Total Potassium; EK = Exchangeable Potassium; OC = Organic Carbon; CEC = Cation Exchange Capacity; R = C/N Ratio; EC = Electrical Conductivity.

The compost is produced from date palm residues by a private company called PALM COMPOST. This company is located in Biskra, in a typical oasis environment of south-eastern Algeria. Physicochemical characteristics of compost were presented in Table 2.

The EC of compost from date palm fronds is 5.22 mS/cm, which implies a considerable degree of salinity. This value indicates a significant amount of soluble salts which may have effects on the physical, chemical and biological characteristics when applied to soil. Abundant high salinity could raise the content of Na^+ and Cl^- which would directly cause particles dispersion, soil structure impairment, acceleration for the water retention losses and sodicity. These alterations lead to impaired water and nutrient acquisition of plants, resulting in reduced growth and yields, as well as ionic imbalance and toxicity effects. In addition, high salt leads to reduced diversity and activity of soil microorganisms, which slows down the mineralisation of organic matter and decreases availability of essential nutrients, and eventually impacts on soil health and plant resistance to environmental stress conditions.

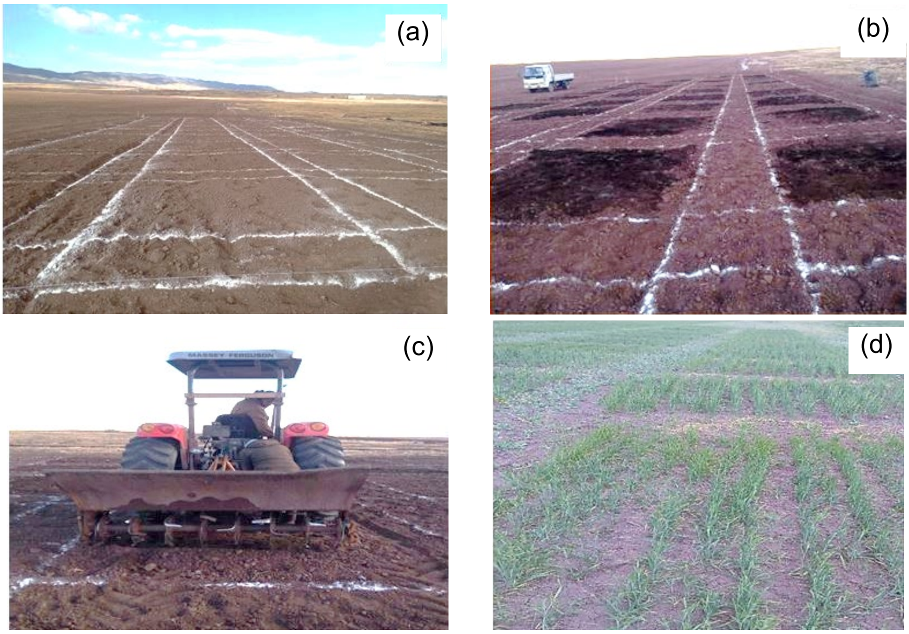

Figure 4. Different stages of experimental setup implementation: (a) Monitoring of the trial (b) Compost application, (c) Compost mixture (d) The wheat crop.

All fertilisation/organic amendments were applied before sowing on 8 January 2022 and mixed mechanically into the top 20 cm using a rotary tiller (Fig. 4).

On 18 December 2021, an initial soil sample (Fig. 5, a) was taken at a depth of 20 cm for an initial soil characterisation analysis (Table 3).

Figure 5. Soil sampling: (a) before sowing (b) after harvest (c) sampling location.

Physicochemical analysis of the soil reveals a loamy texture characterised by 47.82% silt, 30.43% sand and 21.75% clay, giving the soil good water retention capacity but making it susceptible to compaction (Rabot et al., 2018). The organic matter content is 1.83%, which is considered low according to European agronomic standards (Dignac et al., 2017), with a C/N ratio of 6.10 indicating rapid mineralisation of organic matter (Moinet et al., 2020). The total nitrogen content is 0.18%, which is in the average range, while the assimilable phosphorus content is very high at 54.34 ppm, well above the optimal thresholds of 15–30 ppm (Withers et al., 2019). Exchangeable potassium (0.51 meq per 100 g) remains at an average level, and the cation exchange capacity (CEC) of 19.02 meq per 100 g reflects good nutrient retention capacity (Mattila & Rajala, 2021).

Table 3. Initial soil characterisation analysis (before sowing)

Settings (units)	Values
Texture	Silty
Sand (%)	30.43
Silt (%)	47.82
Clay (%)	21.75
OM (%)	1.83
TN (%)	0.18
P (ppm)	54.34
K (meq per 100 g)	0.51
OC (%)	0.79
CEC (meq per 100 g)	19.02
R(C/N)	6.10
Ph	8.04
CT (%)	46.88
CA (%)	21.44
EC (dS/m)	1.45
Ca (meq per 100 g)	12.14
Mg (meq per 100 g)	2.99
Na (meq per 100 g)	0.90

Legend: OM = Organic Matter; TN = Total Nitrogen; P = Available Phosphorus; K = Exchangeable Potassium; OC = Organic Carbon; CEC = Cation Exchange Capacity; R = C/N Ratio; Total $CaCO_3$ Active $CaCO_3$; EC = Electrical Conductivity; Ca = Exchangeable Calcium; Mg = Exchangeable Magnesium; Na = Exchangeable Sodium.

The alkaline pH of 8.04 is explained by exceptionally high levels of total limestone (46.88%) and active limestone (21.44%), which are characteristic of Mediterranean calcareous soils and can lead to micronutrient deficiencies, particularly iron and zinc (Marschner & Rengel, 2023). The electrical conductivity of 1.45 dS m^{-1} indicates slight salinity, with a sodium content of 0.90 meq per 100 g exceeding the critical threshold of 0.5 meq per 100 g, suggesting a potential risk of sodisation (Qadir et al., 2014). The exchangeable cations show a dominance of calcium (12.14 meq per 100 g) and an average level of magnesium (2.99 meq per 100 g), reflecting the influence of the calcareous parent material on the chemical composition of the soil (Tucker, 1954).

After the wheat crop was harvested, a new soil sampling as (Fig. 5, b) carried out at the centre of each elementary plot (Fig. 5, c), at two different horizons: 0–20 cm and 20–40 cm. Each elementary plot measured 3 m × 3 m, and the distance between plots was 1 meter.

Thus, the distance between two adjacent sampling points (center to center) is 4 meters (3 m plot width + 1 m spacing). The samples taken were dried in the open air and then sieved using a 2 mm sieve to obtain a homogeneous fraction suitable for chemical characterisation analyses (Tables 5 and 6).

Statistical analysis

In the RStudio/2025.05.01+513 environment, the collected data were subjected to rigorous statistical analysis to identify significant differences between groups. Analysis of variance (ANOVA) was employed to test these differences, followed by post-hoc comparisons to specify pairwise contrasts. Tukey's honestly significant difference (HSD) test at a 5% significance level, implemented via the **agricolae** package. Relationships among variables were explored through correlation matrices using the **FactoMineR** and **corrplot** packages. Additionally, treatments were characterised using principal component analysis (PCA) and hierarchical clustering (HCA). Finally, simple linear regressions were conducted to determine the most influential explanatory variables for the parameters studied using a program in Matlab (version 2017).

RESULTS AND DISCUSSION

The opposite effects of treatments on nutrient availability and soil chemical properties are evident in analytical results. Treatment effects were assessed by analysis of physical and chemical parameters from two soil depths (0–20 cm, 20–40 cm) (Tables 4 and 5) after six months of applying organic and commercial fertilisers.

Table 4. Soil analysis methods

Measured parameters	Methods used	References
pH	pH meter with a soil/water ratio of 1/2.5	Mathieu & Pieltain, 2003
EC	Conductivity meter with a soil/water ratio of 1/5 is expressed in dS m^{-1} at 25 °C).	Estefan et al., 2013
Total CaCO3	Bernard Method	Estefan et al., 2013
Active CaCO3	Drouineau-Galet Method	Estefan et al., 2013
Organic matter OM	Walkley-Black Method	Estefan et al., 2013.
Organic carbon OC	Walkley-Black Method	Estefan et al., 2013
Total nitrogen	Kjeldahl Method	Estefan et al., 2013
Exchangeable Potassium	Extraction (pH 8.2) with ammonium acetate	Mathieu & Pieltain, 2003
Exchangeable calcium	Extraction (pH 8.2) with ammonium acetate	Mathieu & Pieltain, 2003
Exchangeable magnesium	Extraction (pH 8.2) with ammonium acetate	Mathieu & Pieltain, 2003
Exchangeable sodium	Extraction (pH 8.2) with ammonium acetate	Mathieu & Pieltain, 2003
available phosphorus	Olsen Method	Estefan et al., 2013
CEC	Extraction (pH 8.2) with ammonium acetate	Mathieu & Pieltain, 2003

Legend: OM = Organic Matter; TN = Total Nitrogen; P = Available Phosphorus; K = Exchangeable Potassium; OC = Organic Carbon CEC = Cation Exchange Capacity; Total CaCO3 C/N Ratio; Active Total CaCO3 EC = Electrical Conductivity; Ca = Exchangeable Calcium; Mg = Exchangeable Magnesium; Na = Exchangeable Sodium.

Effect of different date palm compost modalities on soil fertility

The findings in Tables 5(a) and 5(b) reveal several important trends. First, the combined application of date palm compost and mineral fertilisers significantly increased organic matter content, with the highest values observed in treatment C2M (3.79%) in the surface soil (0–20 cm) and in treatment C3U (4.00%) in the subsurface soil (20–40 cm). This finding is consistent with recent reports by Kumari & Purakayastha (2020), who demonstrated that combined organic inputs are highly effective in building organic matter stocks in semi-arid calcareous soils.

Table 5. (a) and 5(b). Results of the ANOVA for the Effect of different date palm compost modalities on soil fertility two depths: 0–20 cm and 20–40 cm

Table 5(a)

Treatments	OM (%)	OC (%)	CEC (meq per 100 g)	C/N (ratio)	pH	EC (dS m^{-1})
T	2.43 ± 0.26 abc	1.06 ± 0.11 abc	21.04 ± 3.52 a	5.81 ± 5.48 a	8.04 ± 0.30 a	1.32 ± 1.20 a
F	3.13 ± 0.36 abc	1.36 ± 0.16 abc	24.24 ± 3.60 a	2.52 ± 0.65 a	7.98 ± 0.13 a	1.47 ± 1.03 a
C1	1.86 ± 0.46 c	0.81 ± 0.20 c	18.77 ± 5.58 a	2.17 ± 1.32 a	7.91 ± 0.14 a	1.69 ± 1.18 a
C2	2.95 ± 0.47 abc	1.28 ± 0.20 abc	19.30± 2.36 a	2.05 ± 0.56 a	7.90 ± 0.09 a	1.51 ± 0.72 a
C3	3.40 ± 0.23 ab	1.48 ± 0.10 ab	19.71 ± 0.51 a	1.66 ± 0.75 a	7.94 ± 0.21 a	1.49 ± 1.00 a
C1M	2.93 ± 0.46 abc	1.27 ± 0.20 abc	21.11 ± 4.67 a	3.23 ± 1.54 a	7.91 ± 0.08 a	1.62 ± 0.90 a
C2M	3.79 ± 0.31 a	1.65 ± 0.34 a	22.90 ± 4.70 a	6.29 ± 1.86 a	7.80 ± 0.10 a	1.36 ± 0.07 a
C3M	3.22 ± 1.56 abc	1.40 ± 0.68 abc	22.37 ± 3.06 a	2.88 ± 2.55 a	7.90 ± 0.18 a	1.71 ± 1.05 a
C1U	2.49 ± 0.42 bc	0.97 ± 0.18 bc	22.11 ± 4.67 a	1.91 ± 0.95 a	7.83 ± 0.06 a	2.35 ± 0.17 a
C2U	2.72 ± 0.30 abc	1.18 ± 0.13 abc	21.70 ± 1.79 a	1.58 ± 0.38 a	7.80 ± 0.10 a	2.45 ± 0.44 a
C3U	3.38 ± 0.52 ab	1.47 ± 0.23 ab	22.37 ± 1.33 a	2.25 ± 0.68 a	7.90 ± 0.06 a	2.65 ± 0.31 a
TEST F/P	3.53 0.00291 **	3.54 0.00291 **	0.96 0.48* ns	2.45 0.0256 *	1.45 0.203 ns	1.098 0.392 ns

Table 5(b)

Treatments	OM (%)	OC (%)	CEC (meq per 100 g)	C/N (ratio)	pH	EC (dS m^{-1})
T	0.61 ± 0.39 d	0.56 ± 0.69 a	19.31 ± 0.66 a	0.76 ± 0.48 b	7.85 ± 0.089a	2.32 ± 0.22 a
F	2.36 ± 0.46 b	1.03 ± 0.19 ac	22.50 ± 2.06 bc	2.06 ± 1.65 ab	7.91 ± 0.62 a	1.40 ± 0.80 a
C1	2.62 ± 0.08 ab	1.12 ± 0.03 ab	20.24 ± 2.19 ab	0.92 ± 0.07 ab	7.88± 0.23a	1.14 ± 0.56 a
C2	3.08 ± 0.32 bc	1.34 ± 0.14 bc	22.24 ± 4.19 a	1.30 ± 0.45 ab	7.94 ± 0.13 a	1.20 ± 0.64 a
C3	2.73 ± 0.25 ab	1.22 ± 0.10 ab	21.30 ± 2.24 b	2.51 ± 2.31 ab	8.16 ± 0.47 a	0.58 ± 0.10 a
C1M	2.56 ± 0.21 ab	1.11 ± 0.09 ab	20.11 ± 1.15 bc	2.59 ± 2.06 ac	8.06 ± 0.33 a	1.73 ± 1.33a
C2M	3.12 ± 0.51 bc	1.35 ± 0.22 bc	18.90 ± 3.78 b	3.27 ± 1.32 bc	7.79 ± 0.10 a	1.62 ± 1.08 a
C3M	3.57 ± 0.87 ac	1.55 ± 0.38 bc	22.64 ± 3.30 ab	2.77 ± 0.77 bc	7.95 ± 0.28 a	1.52 ± 1.12 a
C1U	3.36 ± 0.38 bc	1.46 ± 0.16 bc	21.30 ± 4.77ab	4.14 ± 1.58 bc	7.94 ± 0.19 a	1.55 ± 1.00 a
C2U	3.22 ± 0.39 bc	1.40 ± 0.17 bc	23.17 ± 2.32 ab	4.66 ± 1.58 bc	7.98 ± 0.31 a	1.59 ± 1.04 a
C3U	4.00 ± 0.22 c	1.74 ± 0.09 b	26.90 ± 3.30 a	4.22 ± 2.79 bc	8.04 ± 0.30 a	1.47 ± 0.99 a
TEST F/P	17.16 0.0000***	5.180.00015***	2.23 0.0406 *	2.98 0.00882 **	0.664 0.74 ns	0.91 0.536 ns

Legend: *** $p < 0.001$; ** $p < 0.01$; * $p < 0.05$; n.s = no significant. Means followed by the same letter in a column do not differ significantly according to the *test* Tuckey ($p > 0.05$). OM: organic matter; OC: organic carbon; CEC; cation exchange capacity; C/N: the carbon/nitrogen ratio; pH: hydrogen potential; EC = electrical conductivity.

Table 6. (a) and (b). Results of the ANOVA for the Effect of different date palm compost modalities on Soil chemical properties two depths: 0–20 cm and 20–40 cm

Table 6(a)

Treatments	TN (%)	P (ppm)	K (meq per 100 g)	Ca (meq per 100 g)	Mg (meq per 100 g)	Na (meq per 100 g)	CT (%)	CA (%)
T	0.29 ± 0.18	57.67 ± 16.46	0.75 ± 0.08 c	15.64±3.00	2.65 ± 1.31 ab	0.87 ± 0.08 b	34.69 ± 0.80 ac	15.34 ± 0.40 ac
F	0.57 ± 0.18	70.00 ± 28.11	1.30 ± 0.40 abc	13.75 ± 3.55	2.31 ± 1.40 ab	1.48 ± 0.28 bd	34.75 ± 1.34 ab	15.38 ± 0.69 ab
C1	0.59 ± 0.53	55.75 ± 9.81	0.93 ± 0.15 bc	12.62 ± 0.57	2.08 ± 1.25 ab	1.04 ± 0.32ab	35.09 ± 0.22 ab	15.54 ± 0.11 ab
C2	0.66 ± 0.20	78.09 ± 11.77	0.94 ± 0.11 bc	14.07± 1.42	2.47 ± 1.16 ab	1.79 ± 0.24 acd	35.02 ± 0.96 ab	15.51 ± 0.48 ab
C3	1.04 ± 0.44	85.17± 23.77	1.01± 0.20 bc	14.30 ±2.53	1.76 ± 1.00 ab	1.79 ± 0.06 acd	34.02 ± 0.76 a	15.01 ± 0.38 a
C1M	0.48 ± 0.26	78.34 ± 20.32	0.93 ± 0.18 bc	12.96 ±1.19	1.66 ± 1.36 ab	1.14 ± 0.32 bc	35.76 ± 0.35 bc	15.88 ± 0.17 bc
C2M	0.28 ± 0.08	76.92 ± 6.99	1.25 ± 0.40 abc	12.94 ± 138	3.38± 1.05 bc	0.92 ± 0.67 b	36.43 ± 0.22 b	16.21 ± 0.11 b
C3M	0.71 ± 0.62	79.80 ± 18.87	1.47 ± 0.66 abc	12.51 ±0.40	3.78 ± 1.05 bc	2.23 ± 0.28 d	36.09 ± 0.34 bc	16.05 ± 0.85 bc
C1U	0.61 ± 0.29	70.17 ± 8.91	0.76 ± 0.14 c	12.97± 1.20	6.06 ± 1.18 c	1.38 ± 0.32 bc	35.75 ± 0.15 bc	15.88 ± 0.07 bc
C2U	0.78 ± 0.20	87.21 ± 20.99	1.83 ± 0.14 ab	11.97 ± 0.54	4.22 ± 0.38 ac	1.86 ± 0.25 cd	35.76 ± 0.35 bc	15.88 ± 0.17 bc
C3U	0.71 ± 0.27	55.38 ± 39.39	1.96 ± 0.84 a	13.50±0.33	1.43 ± 0.87 b	1.82 ± 0.15 cd	36.23 ± 1.06 bc	16.11 ± 0.52 bc
TEST F/P	1.641 0.138 ns	1.79 0.101 ns	4.61 0.00039***	1.316 0.263 ns	5.96 0.000***	8.260.000 ***	4.52 0.0000 ***	4.52 0.0000 ***

Table 6(b)

Treatments	TN (%)	P (ppm)	K (meq per 100 g)	Ca (meq per 100 g)	Mg (meq per100 g)	Na (meq per 100 g)	CT (%)	CA (%)
T	0.36 ± 0.06 b	53.25 ± 5.97	0.25 ± 0.02 a	12.34 ± 0.34 ab	4.97 ± 1.17 ab	2.15 ±0.41 b	46.11 ± 0.60 ab	21.05 ± 0.29 ab
F	0.71 ± 0.44 ab	86.83 ± 23.79	0.69 ± 0.16 ab	14.26 ± 0.35 b	2.04 ± 1.38 ab	1.72 ± 0.29 b	45.17 ± 0.80 ab	21.60 ± 0.38 ab
C1	1.24 ± 0.07 a	78.58 ± 13.63	0.66 ± 0.04 ab	13.29 ± 0.45 ab	3.44 ± 1.35 ab	0.89± 0.23 a	46.79 ± 1.22 ab	21.39 ± 0.61 ab
C2	1.13 ± 0.41 a	80.62 ± 23.58	0.73 ± 0.22 ad	10.83 ± 0.53 a	5.65 ± 1.45 ab	1.77 ± 0.24 b	45.17 ± 0.90 ab	20.58 ± 0.45 ab
C3	0.74 ± 0.43 ab	89.46 ± 8.56	0.63 ± 0.13 ab	12.47 ± 0.20 ab	1.08 ± 0.81 ab	2.13 ± 0.51 b	43.89 ± 0.58 bc	19.94 ± 0.29 bc
C1M	0.68 ± 0.45 ab	79.96 ± 18.33	0.58 ± 0.21 ac	11.22 ± 0.47 a	3.58 ± 2.02 ab	1.63 ± 0.21 b	41.76 ± 3.39 c	18.88 ± 1.70 c
C2M	0.50 ± 0.30 ab	75.17 ± 9.88	0.72 ± 0.23 ab	13.02 ± 1.26 ab	2.16 ± 1.18 ab	1.53 ± 0.09 b	44.57 ± 1.16 bc	20.28 ± 0.58 bc
C3M	0.57 ± 0.14 ab	89.71 ± 17.45	1.31 ± 0.37 d	14.03 ± 2.61 b	2.08 ± 0.45 ab	1.94 ± 0.36 b	48.41 ± 1.86 a	22.20 ± 0.93 a
C1U	0.37 ± 0.11 b	73.42 ± 19.25	0.98 ± 0.18 bcd	12.24 ± 1.89 ab	2.45 ± 1.06 ab	1.96 ± 0.16 b	45.59 ± 1.05 ab	20.79 ± 0.52 ab
C2U	0.32 ± 0.08 b	74.04 ± 18.31	1.21 ± 0.40 bd	13.44 ± 0.68 ab	1.53 ± 0.65 ab	1.77 ± 0.16 b	45.17 ± 0.44 ab	20.58 ± 0.22 ab
C3U	0.60 ± 0.38 ab	72.55 ± 17.58	1.19 ± 0.32 bd	11.86 ± 0.91 ab	1.73 ± 1.09 a	1.50± 0.23 ab	44.92 ± 0.32 bc	20.46 ± 0.16 bc
TEST F/P	3.78 0.00182**	1.45 0.204 ns	7.175 0.0000***	3.67 0.00226**	6.89 0.0000***	5.87 0.00000***	5.72 0.0000***	5.72 0.0000 ***

Legend: *** $p < 0.001$; ** $p < 0.01$; * $p < 0.05$; ns = no significant. Means followed by the same letter in a column do not differ significantly according to the test. ($p > 0.05$). TN: total nitrogen; P: available phosphorus; K: exchangeable potassium; Ca: exchangeable calcium; Mg: Exchangeable magnesium; Na: exchangeable sodium; CT: Total Calcium Carbonate; CA: active Calcium Carbonate.

Organic carbon (OC) followed a similar pattern, with the highest concentrations recorded under treatment C2M (1.65 ± 0.34%) and C3U (1.74 ± 0.09%) These results confirm the important role of compost in enhancing soil structure and promoting soil carbon sequestration, which is in good agreement with findings reported by Ameziane et al. (2019), Spaccini & Piccolo (2020), Chen et al. (2023), and Li et al. (2023).

The CEC values reached 18.77 ± 5.58 meq per 100 g in the surface layer (0–20 cm) under treatment C1 and 26.90 ± 3.30 meq per 100 g in the subsurface layer (20–40 cm) under treatment C3U. These results indicate enhanced cation retention capacity in the subsurface soil, which improves the soil's ability to retain essential nutrients and reduce leaching losses, thereby maintaining nutrients available for crop uptake. These findings are consistent with observations reported by Asaye et al. (2022).

The C/N ratio (carbon/nitrogen) ultimately varies greatly between treatments (from 6.29, C2M to 1.58, C2U) representing a balance between organic matter build-up and N-enrichment necessary to support the subsequent gradual mineralisation (Smith et al., 2024). These results underline the importance of the balanced management of the applied organic nutrients and mineral fertiliser in calcareous soils of semi-arid regions to maintain the sustainability of nutrient balance (Krištaponytė., 2005).

Effect of different date palm compost modalities on soil chemical properties

The data from analysis of variance in Table 6(a) and 6(b) the soil chemical properties as in the case of the botanical characteristics of soil, the influence of the combined effects of the fertilisation date palm compost, mineral+fertilisers varies greatly. The cation exchangeable ions (Na, Mg and K) also reveal a highly significant change (K no amendments (0.25 ± 0.02 meq per 100 g). The improvement in cations availability observed in the present study can chiefly be attributed to the results reported by Singh et al. (2021), who shows the importance of organic amendments in nutrient mobilization in semi-arid calcareous soils. The highest concentration of total N is reported in the only-compost treatment (C1: 1.24 ± 0.07%; C2: 1.13 ± 0.41%) while the presence of urea exerted a lesser effect (C1U: 0.37 ± 0.11%; C2U: 0.32 ± 0.08%), due to possible interaction between mineral and organic sources in the deep N process (Marzi et al., 2020).

There were no significant differences in available phosphorus between treatments ($p > 0.05$), with values ranging from 53.25 ± 5.97 ppm (control) to 89.71 ± 17.45 ppm (C3M). This lack of response to phosphorus reflects the specific constraints of calcareous soils, where precipitation with calcium limits phosphorus availability (Leytem & Mikkelsen, 2005).

Relationships analysis of the effects of date palm compost

Correlation matrix analysis, Principal Component Analysis (PCA), Ascending Hierarchical Classification (AHC) and linear regression, made it possible to carry out an overall study, synthesis, grouping and modelling of the complex effects of various applications of date palm compost on soil parameters.

The advantages of integrated fertilisation can be explained by the complementary nature of the two sources: compost improves soil structure and biological activity by increasing organic matter (Ameziane et al., 2019) while mineral fertiliser quickly meets crop needs through the immediate release of nitrogen or phosphorus (Saini et al., 2025).

This combination makes it possible to circumvent certain classic limitations of calcareous soils, in particular the low natural availability of phosphorus due to precipitation with calcium (Teng et al., 2020; Jalali & Jalali, 2022).

The correlation matrices (Fig. 2) corroborate these observations, showing a strong relationship (r = 1.00) between organic matter and organic carbon, and notable positive correlations between potassium, C/N and organic matter, both at shallow depths (0–20 cm) and deep depths (20–40 cm). Research has been carried out in Morocco and the Mediterranean Basin, showing the positive effects of the application of compost from date palm on organic matter, organic carbon and K+ exchangeability in calcareous soils, thus confirming the good conjunction of organic fertility and mineral nutrition (Ou-Zine et al., 2021; Badawi, 2022; Kavvadias et al., 2024).

The integrated treatments (C1M, C2M) showed a clear advantage in terms of root nutrition and subsurface fertility, where the effects are particularly marked for potassium, magnesium, electrical conductivity and organic matter at a depth of 20–40 cm.

The compost has C/N ratio close to equitability (12.54, Table 2) compared to uncomposted residues, which biases towards the high mineralization rates (Lazicki et al., 2020). However, the strong negative relationship between total nitrogen (NT) and pH (r = −0.64) alters the traditional model of nitrogen limitation in alkaline soils in which calcareous soils normally impose a 30–40% decrease mineralisation efficiency (Zarabi & Jalali, 2013).

The high organic matter (58% OM) contained in the compost affects the relationship K–organic matter (r = 0.89) at depth (20–40 cm) suggesting the potential of stable organo-mineral complexes due to phenolic compounds that occur in date palm tissues (Abid et al., 2020).

Detailed analysis of the correlation matrix, obtained by merging depths (0–20 cm) and (20–40 cm) (Fig. 6) and calculating averages per treatment, reveals strong statistical links between most of the major soil fertility parameters. Correlation coefficients frequently exceed 0.90 between organic matter (OM), total nitrogen (TN), organic carbon (OC), potassium (K), cation exchange capacity (CEC), calcium (Ca), magnesium (Mg) and the R(C/N) ratio. This means that an increase in organic matter, obtained through the addition of organic residues, compost or sheep manure, is systematically accompanied by an improvement in the availability of major nutrients and the soil's ability to retain them. For example, the OM–TN correlation (r = 0.96) shows that enriching the soil with organic matter directly increases total nitrogen, while the OM–OC correlation (r = 0.98) illustrates the structural relationship between these two components.

The strong correlations between CEC, calcium, magnesium and the soil R(C/N) ratio (CEC–Ca r = 0.93; Mg–Ca r = 0.97) indicate that improving soil exchange capacity, promoted by organic inputs, enhances the availability of essential cations and soil structural stability. Phosphorus (P) also shows high correlations with CEC and organic matter (P–CEC r = 0.71; P–OM r = 0.70), suggesting that integrated fertilisation, combining organic matter and mineral fertilisers, improves phosphorus availability while enhancing overall fertility.

Sodium (Na) and pH show weaker or insignificant correlations with other parameters, indicating that they evolve relatively independently and require specific monitoring, particularly to prevent the risks of salinisation or acidification.

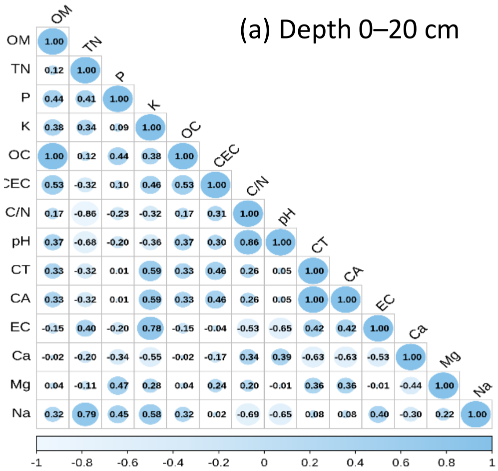

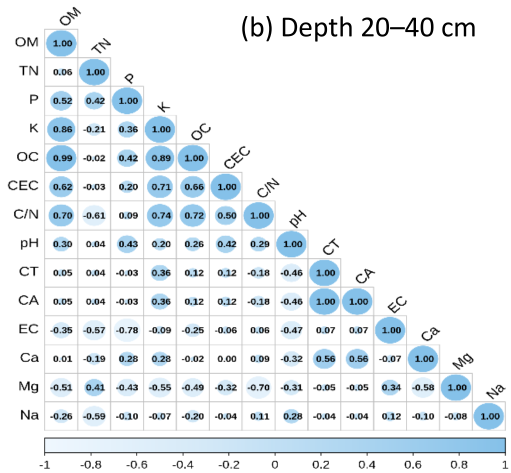

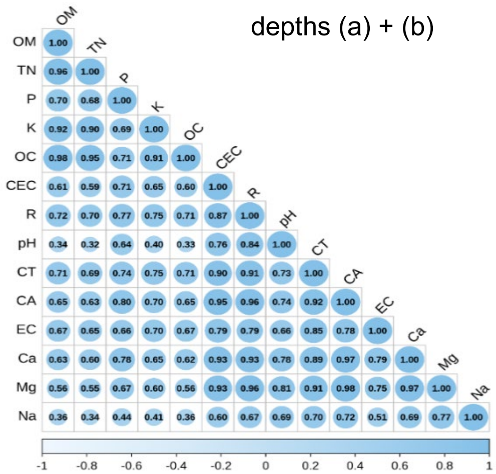

Figure 6. Correlation matrix depths (0–20 cm) and (20–40 cm), depth (a), depth (b) and depth (a+b).

Research rigorously confirms that integrated fertilisation, combining organic and mineral inputs, simultaneously and consistently improves most soil chemical properties, particularly in semi-arid regions (Wang et al., 2025). The increase in organic matter plays a central role, promoting the retention and availability of essential nutrients, while improving organic carbon, total nitrogen, available phosphorus, cation exchange capacity and soil pH (Ejigu et al., 2021).

This combined management not only sustainably increases soil productivity and resilience, but also limits the risks of sodium-related imbalances or acidification by buffering pH variations and improving soil structure (Wang et al., 2025).

The beneficial effects of integrated fertilisation are observed on various types of soil (tropical, clayey, sandy, degraded, etc.) and in different climatic contexts, confirming its universal effectiveness for sustainable and productive agriculture, even in areas with severe environmental constraints (Urmi et al., 2022).

Principal component analysis (Fig. 7, a) reveals a clear discrimination between fertilisation treatments, with 50.9% of variance explained (PC1: 31%, PC2: 19.9%).

With respect to the C3, C3M, and C3U treatments showing segregations in the optimal quadrant of the factorial space, we believe they exhibit quite stable relationships with the major fertility components: electrical conductivity (EC), total calcium carbonate (TCC), total nitrogen (TN) and organic matter (OM). They are clearly highly efficient for improving the fertility of alkaline soils (Urmi et al., 2022).

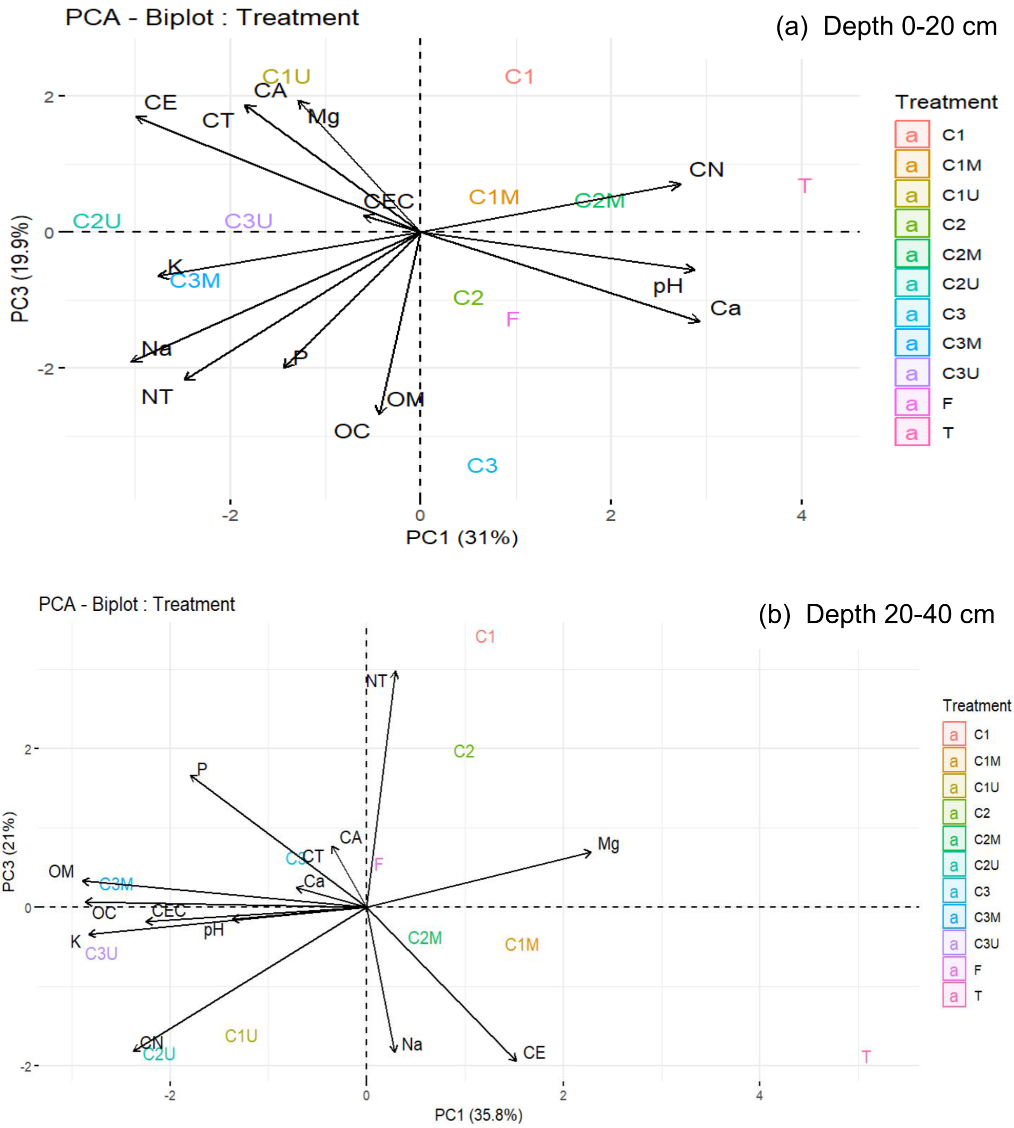

Figure 7. Principal component analysis of depth 0–20 cm(a) and depth 20–40 cm (b).

In contrast, T and F control and manure-only treatments are arranged in a low-productivity area, which provides evidence that adapted fertilisation strategy are necessary. Low rates (C1, C1M, C1U) are not effective at all and intermediate (C2, C2M) rates show intermediate effectiveness.

That potassium is greatly limited in the former soils, is still-better demonstrated by the fact that applications of potassium do not increase yield in the presence of organic matter, even though such practice may facilitate potassium release. Potassium supply is often significantly enhanced when organic matter content exceeds a threshold level, and the supply of potassium is promoted by increasing organic matter, even though to a lesser extent than that observed for N (Zhao et al., 2016). However, low doses and/or single manure application cannot ensure a proper restoration of soil fertility, indicating the need for an intelligent analytical and integrated strategy in soil maintenance.

The principal component analysis of the 20–40 cm depth (Fig. 7, b) shows good discrimination of the fertilisation treatments accounting for 53.4% (PC1 = 35.8% and PC2 = 17.6%) of the variation which is even higher compared to the depth 0–20 cm. The biplot revealed that treatment-C3M, treatment-C3U, treatment-C2U and treatment-C2M stand further apart from the other groups based on their related positions with the soil variables. The treatments C3M and C3U representers the lower left quadrant where a high influence of the C/N and CEC are observed, where CEC and C/N ratio explained the most variation. Treatment C2U, immediately adjacent these groups, also shows significant impact on C/N ratio, which is associated with high potassium concentration. Last, the treatment C2M, which also had a high C/N ratio, is a specific treatment for sodium (Na). It is thus the high C/N ratio, CEC, potassium and sodium value itself in combination, which particularly distinguished these four treatments, and the variation in treatment could largely be attributed to these variables in the multivariate analysis.

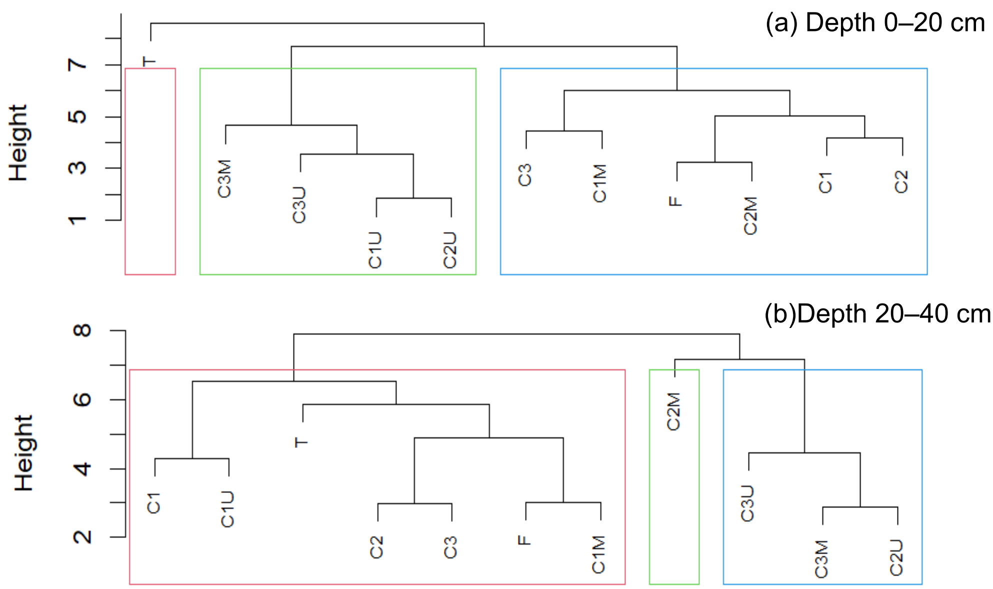

Figure 8. Ascending Hierarchical Classification of depth 0–20cm(a) and depth 20–40cm (b).

The ascending hierarchical classification (Fig. 8) shows that integrated (organic and mineral) fertilisation systems are the best for recovery the fertility of calcareous soils intended for cereal crops. Using this approach, treatments were categorised into three broad groups: (1) high-rate applications (C3M, C3U) – where this achieved the best performance across agronomy parameters; (2) intermediate rates of fertilisation – mainly increasing availability of Mg and deep layer fertility; and (3) control and low-rate applications – where little overall performance was observed on such parameters across all four agronomy response indicators. These groupings corroborate the results of previous research (Zhang et al., 2022; Kumari et al., 2024) highlighting that application of organic amendment in combination with mineral fertilizer allows favourable mineralization scheduling for nutrient release and increased soil fertility (Okhumata, 2022; Oyetunji et al., 2022).

When considering the multivariate approach, linear regression analysis (Fig. 9) in combination disentangled indirect influences between organic matter and the main soil fertility variables. Date palm compost and mineral fertiliser inputs in the depth 0–20 cm exhibited a perfect positive relationship with organic matter for organic carbon ($R^2 = 1.0$). This organic matter increase matches the positive changes in carbon quantity at the depth 0–20 cm, a major driver of soil structure and productivity, as stressed by Ou-Zine et al. (2021), El Janati et al. (2023), and Kumari et al. (2024).

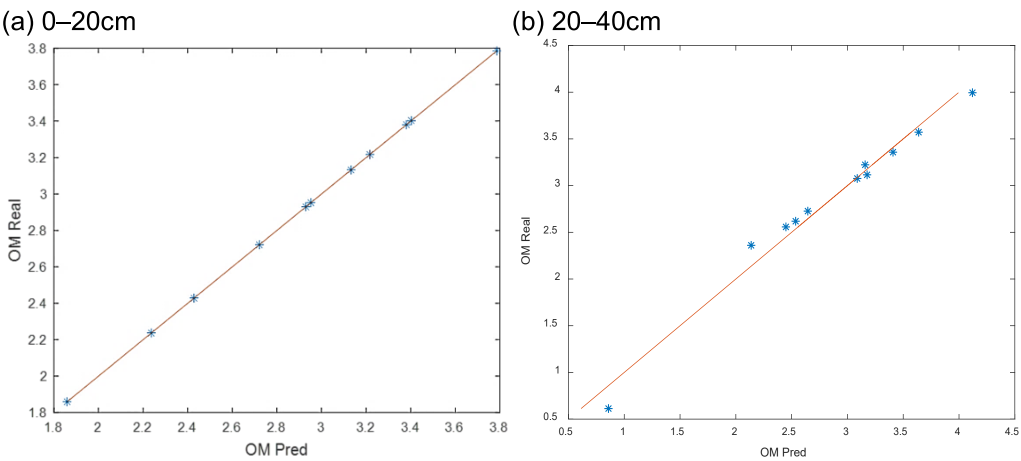

OM = 2.2987•OC
$R^2 = 1$

OM = –0.4663–0.1392•K + 3.0318•OC – 0.0172•CEC–0.0125•C/N
$R^2 = 0.98$

Figure 9. (a) soil organic matter as a function of organic carbon $R^2 = 1$; (b) organic matter as a function of exchangeable potassium, cation exchange capacity and C/N ratio. $R^2 = 0.98$.

In the depth 20–40 cm, the model showed that carbon amount continues to be a primary determinant of organic matter content, but that its influence on organic matter dynamics is also controlled by other chemical conditions particularly with respect to major cation dynamics (K; CEC) and C/N ratio. Indeed, there is a relationship between CEC and organic matter, which has been demonstrated in the literature (Nouar et al., 2019) These findings suggest that depth 0–20 cm management alone is not enough to improve fertility; proper and reasonable management of the depth 20–40 cm, where root systems developed, is also required as explicitly stated by Li et al. (2023).

This method of modelling provides important advantages for the agricultural and land management community. Adjusting the rates of compost and mineral fertilisers to the soil conditions, for each layer, is important for a sustainable recovery of the organic matter and improving the stability and flexibility of the soil. This is an important factor to sustain cereal systems under a semi-arid environment found by (Zhao et al. (2016).

The results align with recent studies reporting increased soil carbon stocks in calcareous soils of semi-arid regions under Integrated Nutrient Management (INM) (Singh et al., 2021; Li et al., 2023; Kumari et al., 2024). Mixed fertility approaches address environmental constraints by combining organic matter inputs from compost, which improve soil structure, water retention, and stimulate microbial activity, with mineral fertilisers that provide immediate nutrient supply, particularly nitrogen and phosphorus. In calcareous soils, high pH restricts phosphorus availability, reflected by the lack of significant difference in available phosphorus between the 0–20 cm and 20–40 cm soil layers, indicating complex phosphorus dynamics. Phosphorus fixation, mainly through reactions with calcium and magnesium, can reduce plant-available phosphorus by over 80% (Adnan et al., 2025). Precipitation and adsorption processes in these soils diminish the effectiveness of phosphorus amendments from both organic and mineral sources (Hinsinger, 2001). The combined application of date palm compost and monoammonium phosphate (MAP) markedly enhances organic matter content, organic carbon, and cation exchange capacity (CEC) by increasing soil organic matter stocks and promoting the formation of organo-mineral complexes with soil calcium carbonates (Ben Mbarek et al., 2019; Abid et al., 2020; Islam et al., 2022; Kavvadias et al., 2024). Compost also stimulates microbial activity, notably Actinobacteria and saprotrophic fungi, accelerating organic matter decomposition and nutrient release (Islam et al., 2022; Ghouili et al., 2023; Zhao et al., 2025). Microbial biomass is subsequently stabilised through mineral association, enhancing carbon retention and CEC (Islam et al., 2022; Zhao et al., 2025). The increase in organic matter density raises the number of negative charges on soil particle surfaces, improving retention of cations such as Ca^{2+}, Mg^{2+}, and K^{+} (Ben Mbarek et al., 2019; Abid et al., 2020; Kavvadias et al., 2024). Stability of soil organic matter in calcareous contexts results from the formation of organo-mineral complexes, precipitation of organic compounds with calcium, and accumulation of microbial necromass, which slows mineralisation and favours long-term carbon storage (Islam et al., 2022; Zhao et al., 2025). However, phosphorus availability remains limited due to precipitation of MAP-derived phosphorus as poorly soluble calcium phosphates, temporary microbial immobilisation, and the high buffering capacity of calcareous soils that restricts phosphorus solubilisation even in presence of organic acids from compost (Abid et al., 2020; Ghouili et al., 2023; Kavvadias et al., 2024; Zhao et al., 2025).

CONCLUSION

The results of this study indicate that integrated fertilisation practices (C3U, C3M, C2U), involving the application of date palm frond compost combined with mineral fertilisers (urea 46% and MAP) as a basal input for cereals, are both effective and environmentally sustainable for improving the fertility of calcareous soils. Among these treatments, C3M was identified as the most effective, demonstrating that integrated date palm compost fertilisation is particularly well-suited to the region’s calcareous soils.

This approach significantly enhanced key soil fertility parameters, including organic matter (OM), organic carbon (OC), cation exchange capacity (CEC), the C/N ratio, and particularly potassium (K) content. These findings provide valuable insights into the efficiency of integrated fertilisation under semi-arid calcareous soil conditions.

However, experimental observations were limited to a single agricultural year and one study site, which may not adequately capture spatial and temporal variability. The research was additionally constrained by limited water availability, reducing irrigation capacity and thus influencing crop performance. These conditions reflect the broader challenges typical of semi-arid agroecosystems. Nevertheless, the study incorporated participatory research involving local farmers to ensure practical relevance and the co-production of knowledge. Further multi-annual and multi-site investigations are therefore recommended to validate and enhance the robustness and transferability of these findings.

ACKNOWLEDGEMENTS. We would like to thank Ms Asma Belouanes, Manager of the Rendement Plus laboratory-Batna.

REFERENCES

Abd El-Aziz, M.A., Abd Elghany, S.H., Elbagory, M., El-Gamal, B.A., AbdEl-Khalek, A.A., AbdEL-Azeem, S.M., Omara, A.E.-D. & Khalifa, T.H. 2025. Enhancing soil health and crop performance under saline-sodic calcareous soil: A comparative study of nano-sulfur and mineral sulfur combined with compost application. *Agronomy* **15**(3), 510. https://doi.org/10.3390/agronomy15030510

Abid, W. & Ammar, E. 2022. Date Palm (*Phoenix dactylifera* L.) Wastes Valorisation: A Circular Economy Approach. In M.F. Ramadan & M.A. Farag (Eds.), Mediterranean Fruits Bio-wastes (pp. 403–430). *Springer International Publishing*. https://doi.org/10.1007/978-3-030-84436-3

Abid, W., Mahmoud, I.B., Masmoudi, S., Triki, M.A., Mounier, S. & Ammar, E. 2020. Physico-chemical and spectroscopic quality assessment of compost from date palm (Phoenix dactylifera L.) waste valorisation. *Journal of Environmental Management* **264**, 110492. https://doi.org/10.1016/j.jenvman.2020.110492

Adnan, M., Fahad, Shah, Saleem, Muhammad Hamzah, & Lal, R. 2025. Sustainable phosphorus management in calcareous soils: Problems and prospects. *Journal of Plant Nutrition* **1–48**(13), 2179–220022. https://doi.org/10.1080/01904167.2025.2477269

Al-Suhaibani, N., Selim, M., Alderfasi, A. & El-Hendawy, S. 2020. Comparative Performance of Integrated Nutrient Management between Composted Agricultural Wastes, Chemical Fertilizers, and Biofertilizers in Improving Soil Quantitative and Qualitative Properties and Crop Yields under Arid Conditions. *Agronomy* **10**(10), Article 10. https://doi.org/10.3390/agronomy10101503

Ameziane, H., Nounah, A., Khamar, M. & Zouahri, A. 2019. Use of olive pomace as an amendment to improve physico-chemical parameters of soil fertility. *Agronomy Research* **17**(6), 2158–2171. https://doi.org/10.15159/AR.19.212

Ameziane, H., Nounah, A., Khamar, M. & Zouahri, A. 2020. Composting olive pomace: evolution of organic matter and compost quality. *Agronomy Research* **18**(1), 5–17. https://doi.org/10.15159/AR.20.004

Amirouche, M., Smadhi, D., Zella, L. & Bachir, H. 2021. Rainfall Trends in Semi-Arid Cereal Regions of Algeria. *Al-Qadisiyah Journal for Agriculture Sciences* **11**(1), 36–44. https://doi.org/10.33794/qjas.2021.129187.1000

Arroussi, A., Tahri, A., Kalloum, S., Abdelli, N. & Bouziane, N. 2022. Valorization of lignocellulosic material from date palm waste (Phoenix dactylefera L. Elhmira cultivar) by composting as organic fertilizer. *U.P.B. Scientific Bulletin, Series B, Chemistry and Materials Science* **84**(1), 59–72. https://www.researchgate.net/publication/359083454

Asaye, Z., Kim, D.-G., Yimer, F., Prost, K., Obsa, O., Tadesse, M., Gebrehiwot, M. & Brüggemann, N. 2022. Effects of Combined Application of Compost and Mineral Fertilizer on Soil Carbon and Nutrient Content, Yield, and Agronomic Nitrogen Use Efficiency in Maize-Potato Cropping Systems in Southern Ethiopia. *Land* **11**(6), Article 6. https://doi.org/10.3390/land11060784

Ashraf, Z. & Hamidi-Esfahani, Z. 2011. Date and Date Processing: A Review. *Food Reviews International* **27**(2), 101–133. https://doi.org/10.1080/87559129.2010.535231e06074. https://doi.org/10.1016/j.heliyon.2021.e06074

Aydi, S., Sassi Aydi, S., Rahmani, R., Bouaziz, F., Souchard, J.P., Merah, O. & Abdelly, C. 2023. Date-Palm Compost as Soilless Substrate Improves Plant Growth, Photosynthesis, Yield and Phytochemical Quality of Greenhouse Melon (Cucumis melo L.). *Agronomy* **13**, 212. https:// doi.org/10.3390/agronomy13010212

Badagliacca, G., Testa, G., La Malfa, S.G., Cafaro, V., Lo Presti, E. & Monti, M. 2024. Organic fertilisers and bio-waste for sustainable soil management to support crops and control greenhouse gas emissions in Mediterranean agroecosystems: A review. *Horticulturae* **10(**5), 427. https://doi.org/10.3390/horticulturae10050427

Badawi, M.A. 2022. Co-Composting Date Palm Tree Wastes and its Effects on Soil Fertility. *Key Engineering Materials* **925**, 73–83. https://doi.org/10.4028/p-h3cj16

Ben Mbarek, H., Mahmoud, I., Chaker, R., Rigane, H., Maktouf, S., Arous, A., Soua, N., Khlifi, M. & Gargouri, K. 2019. Change of soil quality based on humic acid with date palm compost incorporation. *International Journal of Recycling of Organic Waste in Agriculture* **1–8**(3). https://doi.org/10.1007/s40093-019-0254-x

Benabderrahim, M.A., Elfalleh, W., Belayadi, H. & Haddad, M. 2017. Effect of date palm waste compost on forage alfalfa growth, yield, seed yield and minerals uptake. *International Journal of Recycling of Organic Waste in Agriculture* **7**, 19. doi: 10.1007/s40093-017-0182-6

Bhatia, T. & Sindhu, S.S. 2024. Sustainable management of organic agricultural waste: Circular strategies, technologies and prospects for soil fertility improvement. *Discover Agriculture* **4**, Article 130. https://doi.org/10.1007/s44279-024-00147-7

Bontpart, T., Weiss, A., Vile, D., Gérard, F., Lacombe, B., Reichheld, J.-P. & Mari, S. 2024. Growing on calcareous soils and facing climate change. *Trends in Plant Science* **29**(12), 1319–1330. https://doi.org/10.1016/j.tplants.2024.03.013

Brownrigg, S., McLaughlin, M.J., McBeath, T. &Vadakattu, G. 2022. Effect of acidifying amendments on P availability in calcareous soils. *Nutrient Cycling in Agroecosystems* **124**(2), 247–262. https://doi.org/10.1007/s10705-022-10241-1

Chen, Z., Wei, Y., Zhang, Z., Wang, G. & Li, J. 2023. Organic carbon sequestration in Chinese croplands under compost application and its contribution to carbon neutrality. *Environmental Science and Pollution Research* **30**(4), 9022–9035. https://doi.org/10.1007/s11356-022-21254-2

Devkota, K.P., Devkota, M., Rezaei, M. & Oosterbaan, R. 2022. Managing salinity for sustainable agricultural production in salt-affected soils of irrigated drylands. *Agricultural Systems* **198**, 103390. https://doi.org/10.1016/j.agsy.2022.103390

Dignac, M.F., Derrien, D., Barré, P., Barot, S., Cécillon, L., Chenu, C., Chevallier, T., Freschet, G.T., Garnier, P., Guenet, B., Hedde, M., Klumpp, K., Lashermes, G., Maron, P.A., Nunan, N., Roumet, C. & Basile-Doelsch, I. 2017. Increasing soil carbon storage: mechanisms, effects of agricultural practices and proxies. A review. *Agronomy for Sustainable Development* **37**(2), 14. https://doi.org/10.1007/s13593-017-0421-2

Ding, Z., Kheir, A.M.S., Ali, M.G.M., Ali, O.A.M., Abdelaal, A.I.N., Lin, X., Zhou, Z., Wang, B. & Liu, B. 2020. The integrated effect of salinity, organic amendments, phosphorus fertilizers, and deficit irrigation on soil properties, phosphorus fractionation and wheat productivity. *Scientific Reports* **10**, 2736. doi: 10.1038/s41598-020-59650-8

DSA. 2023. Climatic report of Batna region, 2021-2023. Directorate of Agricultural Services of Batna Province, Algeria.

Ejigu, D., Pushpalatha, R., Jayaprakash, S.K., Gangadharan, B., Himanshu, S.K., & Gopakumar, S. 2025. Integrated Fertilizers for Sustainable Wheat Production to Improve Food Security – A Comprehensive Review. *Journal of Plant Nutrition and Soil Science* **188**(1), 5–16. https://doi.org/10.1002/jpln.202400213

Ejigu, W., Selassie, Y.G., Elias, E. & Damte, M. 2021. Integrated fertilizer application improves soil properties and maize (Zea mays L.) yield on Nitisols in Northwestern Ethiopia. *Heliyon* **7**(1).

El Janati, M., Robin, P., Akkal-Corfini, N., Bouaziz, A., Sabri, A., Chikhaoui, M., Thomas, Z., & Oukarroum, A. 2023. Composting date palm residues promotes circular agriculture in oases. *Biomass Conversion and Biorefinery* **13**(16), 14859–14872. doi: 10.1007/s13399-022-03387-z

Estefan, G., Sommer, R. & Ryan, J. 2013. *Methods of Soil, Plant, and Water Analysis: A manual for the West Asia and North Africa region* (3rd ed.). Beirut, Lebanon: International Center for Agricultural Research in the Dry Areas (ICARDA). https://hdl.handle.net/20.500.11766/7512

Faiad, A., Alsmari, M., Ahmed, M., Bouazizi, M., Alzahrani, B. & Alrobei, H. 2022. Date Palm Tree Waste Recycling: *Treatment and Processing for Potential Engineering Applications. Sustainability* **14**, 1134. https://doi.org/10.3390/su14031134

Ghouili, E., Abid, G., Hogue, R., Jeanne, T., D'Astous-Pagé, J., Sassi, K., Hidri, Y., M'hamed, H., Somenahally, A., Xue, Q., Jebara, M., Ouertani, R., Riahi, J., De Oliveira, A. & Muhovski, Y. 2023. Date Palm Waste Compost Application Increases Soil Microbial Community Diversity in a Cropping Barley (Hordeum vulgare L.) Field. *Biology* **12**. https://doi.org/10.3390/biology12040546.

Ghouili, E., Hidri, Y., M'Hamed, H.C., Somenahally, A., Xue, Q., Znaïdi, I.E.A., Jebara, M., Ouertani, R.N., Muhovski, Y., Riahi, J., Abid, G. & Sassi, K. 2022. Date palm waste compost promotes plant growth and nutrient transporter genes expression in barley (Hordeum vulgare L.). *South African Journal of Botany* **149**, 247–257. https://doi.org/10.1016/j.sajb.2022.06.018

Gómez-Muñoz, B., Hatch, D.J., Bol, R. & García-Ruiz, R. 2012. The compost of olive mill pomace: From a waste to a resource - Environmental benefits of its application in olive oil groves. In *Sustainable development* (pp. 459–482). InTech. https://doi.org/10.5772/8244

Habchi, A., Kalloum, S. & Bradai, L. 2022. Follow the degradation of organic matter during composting of date palm (phoenix dactylifera L) waste by physicochemical properties, UV-visible and FT-IR analysis. *International Journal of Environmental Analytical Chemistry*, **102**(12), 2895–2912. https://doi.org/10.1080/03067319.2020.1761347

Hakimi, F., Sebbar, A., Bouamri, R., Sidikou, A.A.H., El Janati, M. & Bouaziz, A. 2024. Effects of Compost and Compost Tea on Soil Properties and Nutrient Uptake of the Moroccan Date Palm Cultivar "Mejhoul" under Organic Cultivation. *Journal of Ecological Engineering* **25**, 224–240. https://doi.org/10.12911/22998993/188334

Hinsinger, P. 2001. Bioavailability of soil inorganic P in the rhizosphere as affected by root-induced chemical changes: A review. *Plant and Soil* **237**(2), 173–195. https://doi.org/10.1023/A:1013351617532

Islam, M., Singh, B. & Dijkstra, F. 2022. Stabilisation of soil organic matter: interactions between clay and microbes. *Biogeochemistry* **160**, 145–158. doi: 10.1007/s10533-022-00956-2

Istifadah, N., Firman, A. & Desiana, M. 2020. Effectiveness of compost and microbial-enriched compost to suppress powdery mildew and early blight diseases in tomato. *Journal of Animal and Plant Sciences* **30**, 377–383. https://doi.org/10.36899/JAPS.2020.2.0031

Jalali, M. & Jalali, M. 2022. Effect of Low-Molecular-Weight Organic Acids on the Release of Phosphorus from Amended Calcareous Soils: Experimental and Modeling. *Journal of Soil Science and Plant Nutrition* **22**(4), 4179–4193. https://doi.org/10.1007/s42729-022-01017-1

Kavvadias, V., Le Guyader, E., El Mazlouzi, M., Gommeaux, M., Boumaraf, B., Moussa, M., Lamine, H., Sbih, M., Zoghlami, I.R., Guimeur, K., Tirichine, A., Adelfettah, A., Marin, B. & Morvan, X. 2024. Using date palm residues to improve soil properties: The case of compost and biochar. *Soil Systems* **8**(3), 69.https://doi.org/10.3390/soilsystems8030069

Krištaponytė, I. 2005. Effect of fertilisation systems on the balance of plant nutrients and soil agrochemical properties. *Agronomy Research* **3**, 45–54.

Kumari, M., Prakash, D., Sheoran, S., Yadav, P.K., Ankit, Yadav, H.K., Apurva, Gupta, R.K., El-Hendawy, S. & Mattar, M.A. 2024. Long-Term Manuring and Fertilization Influence on Soil Properties and Wheat Productivity in Semi-Arid Regions. *Agronomy* **14**. https://doi.org/10.3390/agronomy14102383

Kumari, V. & Purakayastha, D.T. 2020. Effect of protracted fertilization and manuring on changeable pools of soil organic matter in four different soil types with wheat-based cropping systems of India. *International Journal of Chemical Studies* **8**(2), 430–436. https://doi.org/10.22271/chemi.2020.v8.i2g.8804

Lanno, M., Silm, M., Shanskiy, M., Kisand, A., Orupld, K. & Kriipsalu, M. 2020. Open windrow composting of fish waste in Estonia. *Agronomy Research* **18**(4), 2465–2477. https://doi.org/10.15159/AR.20.194

Lazicki, P., Geisseler, D. & Lloyd, M. 2020. Nitrogen mineralization from organic amendments is variable but predictable. *Journal of Environmental Quality* **49**(2), 483–495. https://doi.org/10.1002/jeq2.20030

Leytem, A.B. & Mikkelsen, R.L. 2005. The nature of phosphorus in calcareous soils. *Better Crops* **89**(2), 11–13.

Li, H., Lehmann, A., Rongstock, R., Xu, Y., Kunze, E., Meidl, P. & Rillig, M.C. 2025. Diversity of organic amendments increases soil functions and plant growth. *Plants People Planet* **7**(1), 80–86. https://doi.org/10.1002/ppp3.10588

Li, S., Wei, W. & Liu, S. 2023. Long-Term Organic Amendments Combined with Nitrogen Fertilization Regulates Soil Organic Carbon Sequestration in Calcareous Soil. *Agronomy* **13**, 291. https://doi.org/10.3390/agronomy13020291

Manzoor, M., Ma, L., Ni, K. & Ruan, J. 2024. Influence of Organic and Inorganic Fertilizers on Tea Growth and Quality and Soil Properties of Tea Orchards Top Rhizosphere Soil. *Plants* **13(2**), 207. https://doi.org/10.3390/plants13020207

Marschner, P. & Rengel, Z. 2023. Nutrient availability in soils. In Marschner's Mineral Nutrition of Plants (pp. 315-330). *Academic Press*. https://doi.org/10.1016/B978-0-12-819773-8.00003-4

Marzi, M., Shahbazi, K., Kharazi, N. & Rezaei, M. 2020. The Influence of Organic Amendment Source on Carbon and Nitrogen Mineralization in Different Soils. *Journal of Soil Science and Plant Nutrition* **20**(1), 177–191. https://doi.org/10.1007/s42729-019-00116-w

Mathieu, C. & Pieltain, F. 2003. *Analyse chimique des sols: méthodes choisies* (388 pp.). Paris : Tec & Doc, Lavoisier. ISBN 978-2-7430-0620-4

Mattila, T.J. & Rajala, J. 2021. Estimating cation exchange capacity from agronomic soil tests: Comparing Mehlich-3 and ammonium acetate sum of cations. *Soil Science Society of America Journal* **86**(1), 47–50. https://doi.org/10.1002/saj2.20340

Moinet, G.Y., Cieraad, E., Hunt, J.E., Fraser, A., Turnbull, M.H. & Whitehead, D. 2020. Soil heterotrophic respiration is insensitive to changes in soil water content but related to microbial access to organic matter. *Geoderma* **274**, 114437. doi: 10.1016/j.geoderma.2020.114437

NASA Langley Research Center. 2025. Prediction Of Worldwide Energy Resources (POWER) Data Access Viewer. NASA Earth Science Directorate Applied Science Program. Retrieved October 15, 2025, from https://power.larc.nasa.gov/

Nouar, S., Baha, M., Latati, M., Djebbar, R. & Reguieg, L. 2019. Short-term effect of sawdust biochar and bovine manure on the physiological behavior of turnip (Brassica rapa L.) grown in open fields in the Algiers region. *Agronomy Research* **17**(6), 2373–2385. https://doi.org/10.15159/AR.19.210

Okhumata, D. 2022. Comparative Effects of Mineral Fertilizer, Compost and Compost – Mineral Fertilizer on Biological, Chemical and Physical Properties of Soil. *Journal of Wastes and Biomass Management* **4**, 73–77. https://doi.org/10.26480/jwbm.02.2022.73.77

Ou-Zine, M., Symanczik, S., Rachidi, F., Fagroud, M., Aziz, L., Abidar, A., Mäder, P., Achbani, E.H., Haggoud, A., Abdellaoui, M. & Bouamri, R. 2021. Effect of Organic Amendment on Soil Fertility, Mineral Nutrition, and Yield of Majhoul Date Palm Cultivar in Drâa-Tafilalet Region, Morocco. *Soil Sci Plant Nutr* **21**, 1745–1758. doi: 10.1007/s42729-021-00476-2

Oyetunji, O., Bolan, N. & Hancock, G.A. 2022. A comprehensive review on enhancing nutrient use efficiency and productivity of broadacre (arable) crops with the combined utilization of compost and fertilizers. *Journal of Environmental Management* **317**, 115395. https://doi:10.1016/j.jenvman.2022.115395

Qadir, M., Quillérou, E., Nangia, V., Murtaza, G., Singh, M., Thomas, R.J., Drechsel, P. & Noble, A.D. 2014. Economics of salt-induced land degradation and restoration. *Natural Resources Forum* **38**(4), 282–295. https://doi.org/10.1111/1477-8947.12054

Rabot, E., Wiesmeier, M., Schlüter, S. & Vogel, H.J. 2018. Soil structure as an indicator of soil functions: A review. *Geoderma* **314**, 122–137. doi: 10.1016/j.geoderma.2017.11.009

Saber, M.A., El-Khayat, R.M., El-Shahat, R.M. & Badawi, M.A. 2024. Effect of bio and organic fertilizers on yield and quality of date palm *Phoenix dactylifera*, cv Sakkoti fruit grown in Aswan Governorate and their contents of iron and zinc. *African Journal of Biological Sciences* **6**(2), 2552–2568. https://doi.org/10.48047/AFJBS.6.2.2024.2552-2568

Saini, N., Yadav, H.S., Saini, S., Sharma, A. & Saini, N. 2025. Advances in Integrated Nutrient Management Practices for Cereal Crops: A Comprehensive Review. *International Journal of Plant & Soil Science* **37**(1), 375–383. https://doi.org/10.9734/ijpss/2025/v37i15279

Siebielec, G., Siebielec, S. & Lipski, D. 2020. Long-term impact of sewage sludge, digestate and mineral fertilizers on plant yield and soil biological activity. *Agronomy* **10**, 1429. https://doi.org/10.3390/agronomy10091429

Singh, S.P., Dutta, S.K., Jha, S., Prasad, S.S., Chaudhary, S.K., Sahi, V. & Majumdar, K. 2021. Nutrient management in calcareous soil improves rice-maize sustainable yield index, performance indicators. *Journal of Plant Nutrition* **44**(11), 1571–1586. https://doi.org/10.1080/01904167.2020.1867740

Smadhi, D., Zella, L. & Bachir, H. 2017. Droughts in semi-arid cereal regions of Algeria. *Journal of Fundamental and Applied Sciences* **9**(2), 1063–1073 https://doi.org/10.4314/jfas.v9i2.29

Smith, B.C., Rogan, T.A., Redding, M.R. & Rabbi, S.M.F. 2024. Carbon-to-nitrogen stoichiometry of organic amendments regulates microbial biomass growth and nitrogen mineralization in soil. *Soil Use and Management* **40**(4), e13116. doi: 10.1111/sum.13116

Spaccini, R. & Piccolo, A. 2020. Amendments with humified compost effectively sequester organic carbon in agricultural soils. *Land Degradation & Development* **31**(10), 1206–1216. https://doi.org/10.1002/ldr.3524

Šařec, P., Látal, O., Novák, P., Holátko, J., Novák, V., Dokulilová, T. & Brtnický, M. 2020. Changes in Soil Properties and Possibilities of Reducing Environmental Risks Due to the Application of Biological Activators in Conditions of Very Heavy Soils. *Agronomy Research* **18**(4), 2581–2591.https://doi.org/10.15159/AR.20.196

Teng, Z., Zhu, J., Shao, W., Zhang, K., Li, M. & Whelan, M. J. 2020. Increasing plant availability of legacy phosphorus in calcareous soils using some phosphorus activators. *Journal of Environmental Management* **256**, 109952. https://doi.org/10.1016/j.jenvman.2019.109952

Tucker, B. 1954. The determination of exchangeable calcium and magnesium in carbonate soils.. *Crop & Pasture Science* **5**, 706–715. https://doi.org/10.1071/AR9540706.

Urmi, T.A., Rahman, M.M., Islam, M.M., Islam, M.A., Jahan, N.A. Mia, M.A.B. Akhter, S. Siddiqui, M.H. & Kalaji, H.M. 2022. Integrated Nutrient Management for Rice Yield, Soil Fertility, and Carbon Sequestration. *Plants* **11**, 138. doi: 10.3390/plants 11010138.

Wang, N., Zhang, T., Li, Y., Cong, A., Lian, J. & Feng, K. 2025. Integrated application of fertilization increased maize (Zea mays L.) yield by improving soil quality, particularly under limited water conditions in a semi-arid sandy area. *Agricultural Water Management* **309**, 109334. https://doi.org/10.1016/j.agwat.2025.109334

Withers, P.J., Rodrigues, M., Soltangheisi, A., de Carvalho, T.S., Guilherme, L.R., Benites, V.M., Gatiboni, L.C., de Sousa, D.M., Nunes, R.S., Rosolem, C.A., Andreote, F.D., de Oliveira, A., Jr., Coutinho, E.L. & Pavinato, P.S. 2019. Transitions to sustainable management of phosphorus in Brazilian agriculture. *Scientific Reports* **8**(1), 2537. doi: 10.1038/s41598-018-20887-z

Zarabi, M. & Jalali, M. 2013. Nitrogen mineralization in two calcareous soils treated with raw organic amendments. *Clean Technologies and Environmental Policy* **15**(2), 317–331. https://doi.org/10.1007/s10098-012-0526-x

Zhang, C., Zhao, Z., Li, F. & Zhang, J. 2022. Effects of Organic and Inorganic Fertilization on Soil Organic Carbon and Enzymatic Activities. *Agronomy* **12**, 3125. doi: 10.3390/ Aagronomy12123125

Zhao, J., Ni, T., Li, J., Lu, Q., Fang, Z., Huang, Q., Zhang, R., Li, R., Shen, B. & Shen, Q. 2016. Effects of organic–inorganic compound fertilizer with reduced chemical fertilizer application on crop yields, soil biological activity and bacterial community structure in a rice-wheat cropping system. *Applied Soil Ecology* **99**, 1–12. doi: 10.1016/j.apsoil.2015.11.00

Zhao, Q., Bell, S., Kukkadapu, R., Richardson, J., Cliff, J., Bowden, M., Leichty, S. & Hofmockel, K. 2025. Accumulation of Soil Microbial Necromass Controlled by Microbe-Mineral Interactions. *Environmental science & technology*. doi: 10.1021/acs.est.5c01482

Agronomy Research **24**(S1), 41–53, 2026
https://doi.org/10.15159/AR.25.108

Productive and feeding performance of dairy cows fed sugarcane bagasse ammoniated with urea and cottonseed

A.S. Ribeiro*, A.J.V. Pires, D.C. Santos, M.L.P. Albuquerque, F.F. Silva, I.C. Dutra, S.S. Amorim, P.C.S. Galvao, M.L.S. Santos, M.V. Amaral, P.P.P. Publio and G.R.S. Oliveira

State University of Southwest of Bahia, BR45700-000, Itapetinga, Bahia, Brazil
*Correspondence: amanda.s.ri@hotmail.com

Received: September 25th, 2025; Accepted: December 1st, 2025; Published: December 9th, 2025

Abstract. The objective was to evaluate the use of ammoniated sugarcane bagasse (ASB) and cottonseed (CS) in the diet for lactating cows and their effects on intake, nutrient digestibility, dairy performance, microbial synthesis and ingestive behavior. The experiment was carried out at Bela Vista Farm (Encruzilhada-BA) and at the Forage and Pasture Laboratory of UESB (Itapetinga-BA), using eight multiparous ½ Holstein/Zebu crossbred cows with an average lactation of 20 kg day^{-1} and body weight of 454.7 ± 23.6 kg. The cows were distributed in two 4×4 Latin squares, in a 2×2 factorial scheme, evaluating ammoniated sugarcane bagasse (30% or 40%) associated or not with cottonseed (0% or 18%). The experiment had four periods of 21 days, 17 of adaptation and 4 of collection, totaling 84 days. The interaction between the proportions of ASB and CS was not significant for any of the variables evaluated. The inclusion of 30% sugarcane bagasse obtained from sugarcane bagasse resulted in higher intakes of dry matter (DM), crude protein (CP), ether extract (EE), non-fibrous carbohydrates (NFC), and total digestible nutrients (TDN), without influencing the consumption of neutral detergent fiber corrected for ash and protein. Higher intake ($P < 0.05$) of DM, CP, NFC, and TDN was observed in the diet without sugarcane bagasse, and in the diet with sugarcane bagasse, EE intake was higher ($P < 0.05$). The ASB content and the inclusion of CS influenced digestibility at 40% ASB, and with CS, they provided lower digestibility. Furthermore, individual factors did not affect these variables ($P < 0.05$). Feed efficiency and percentage of total solids in milk were higher for diets with 40% ASB. The use of 40% ASB with CS is recommended.

Key words: feeding behaviour, forage alternatives, milk composition, rumen fermentation, sustainability.

INTRODUCTION

Dairy farming plays an essential role in food security by providing high-value nutritional products. However, in the Brazilian semiarid region, this activity is mostly carried out by small-scale farms that face significant challenges due to irregular rainfall and high temperatures. These factors reduce forage availability throughout the year, compromise herd performance, and increase the need for low-cost feed alternatives (Lima et al., 2021).

Sugarcane bagasse is one of the main by-products of the sugar and alcohol agroindustry, with Brazil being the largest producer of sugarcane in the world, Producing an average of 678.7 million tons per year (Silva et al., 2025). Although it is a roughage with low nutritional value, characterized by high fiber and low protein content, its wide availability and low cost make it a strategic option for supplementation. Ammoniation with urea has been used to improve its nutritional value by increasing fiber digestibility and voluntary intake by ruminants (Publio et al., 2025).

Another relevant by-product is cottonseed, widely available in Brazil. This feedstuff has high protein and energy content and does not require prior processing, which allows it to partially replace conventional ingredients in the diets of dairy cows. Its inclusion may contribute to the nutritional balance of diets and enhance productive efficiency in systems with limited resources (Costa et al., 2011).

The use of by-products such as sugarcane bagasse enriched with urea and cottonseed is a strategic alternative to mitigate costs, utilize agro-industrial residues, and improve feeding efficiency in dairy cows in semiarid regions. However, it is necessary to evaluate the effects of this association on intake, digestibility, milk production, and feeding behavior of the animals (Sun et al., 2022).

This experiment was designed to evaluate the productive and feeding performance of dairy cows fed sugarcane bagasse ammoniated with urea, either with or without cottonseed.

MATERIALS AND METHODS

The experiment was carried out in two stages: the field trial at Fazenda Bela Vista, in Encruzilhada-BA, and the laboratory analyses at the Forage and Pasture Laboratory of the State University of Southwest Bahia (UESB), Itapetinga-BA campus. Eight multiparous crossbred ½ Holstein × Zebu cows, averaging 20 kg of milk day^{-1}, 454.7 ± 23.6 kg live weight, in mid-lactation were used.

The animals were assigned to two 4×4 Latin squares in a 2×2 factorial arrangement, consisting of ammoniated sugarcane bagasse at two inclusion levels (30 and 40%) associated or not with cottonseed (18% of the diet). Cows were housed in individual pens (8 m²), covered, with concrete floors, and equipped with individual feeders and waterers. The study was conducted over 84 days, with four 21-day experimental periods, comprising 17 days for adaptation and 4 days for data collection, conducted from February to May 2023.

The experiment was designed in a 2×2 factorial scheme and limited to a restricted number of animals (*n* = 8), reflecting budgetary limitations for acquiring infrastructure and herds, given the restrictions on government resources allocated to research. However, the use of two 4×4 Latin squares was required to maximize statistical power and improve the use of available resources, allowing each animal to receive all four diets throughout the four experimental periods.

Diets were formulated according to NRC (2001) to meet the nutritional requirements of cows producing 20 kg of milk day^{-1}. The forage-to-concentrate ratio was 30:70 for diets with 30% sugarcane bagasse and 40:60 for diets with 40%, and all diets were isonitrogenous. Diets were offered ad libitum twice daily (07:00 and 15:00 h), allowing approximately 10% orts.

Table 1. Chemical analysis of the ingredients in the experimental diets

Item	Ingredients				
	Raw sugarcane bagasse	Ammoniated bagasse (8% urea)	Ground corn	Soybean meal	Cottonseed
Dry matter (%)	59.4	42.5	80.6	84.1	88.2
Crude protein[1]	1.3	20.0	9.9	52.5	28.9
Ether extract[1]	1.5	3.4	6.7	1.5	20.2
NDFap[1]	80.2	62.7	19.4	23.8	49.4
NDFi[1]	59.5	40.8	3.9	0.9	20.1
Gray [1]	1.7	4.6	2.1	6.2	4.2
Lignin[1]	22.9	10.4	1.4	0.7	7.4
NFC[1]	16.7	9.2	73.2	30.1	7.9
TDN[2]	37.0	45.7	84.5	83.3	81.5

[1]Values in percentage of dry matter; NDFcp – neutral detergent fiber corrected for ash and protein; NDFi – indigestible neutral detergent fiber; NFC – non-fiber carbohydrates; TDN – total digestible nutrients; [2]estimated according to NRC (2001).

Offered feed, residual feed, and fecal samples were collected throughout the sampling periods for chemical analysis, as described by Detmann et al. (2022). Dry matter (DM), ash, crude protein (CP), ether extract (EE), neutral detergent fiber (NDF), neutral detergent fiber corrected for ash and protein (NDFap), acid detergent fiber (ADF), lignin, and indigestible NDF (iNDF) were determined. Total carbohydrates (Sniffen et al., 1992), non-fiber carbohydrates (Detmann et al., 2012), and total digestible nutrients (NRC, 2001) were calculated using specific equations. Nutrient intake was estimated from chemical composition, and fecal excretion was determined using iNDF as an internal marker.

Table 2. Percentage composition of experimental diets

Ingredients	Diets 1	Diets 2	Diets 3	Diets 4
	30% Ammoniated bagasse		40% Ammoniated bagasse	
	0% CS	18% CS	0% CS	18% CS
Ammoniated bagasse	30.00	30.00	40.00	40.00
Cottonseed	0.00	18.00	0.00	18.00
Corn	56.00	43.00	46.00	33.00
Soybean	11.00	6.00	11.00	6.00
Mineral mixture	3.00	3.00	3.00	3.00
Total	100.00	100.00	100.00	100.00
Chemical composition of diets				
Dry matter (%)	74.28	75.11	70.57	71.03
Crude protein[1]	14.18	14.99	14.68	14.85
Ether extract[1]	4.26	5.98	3.66	5.23
NDF_{ap}[1]	23.93	27.94	27.99	31.20
NDFi[1]	13.14	15.25	16.94	18.85
Gray [1]	5.75	5.68	6.48	6.29
Lignin[1]	3.45	4.15	4.37	4.96
NFC[1]	51.87	45.42	47.20	42.01
TDN[2]	65.53	66.93	64.66	63.14

[1]Values in percentage of dry matter; 2estimated according to NRC (2001).

The excretion of total purine derivatives (TPD) was estimated by the sum of the amounts of allantoin and uric acid excreted in the urine and allantoin in the milk. The amount of absorbed microbial purines ($mmol^{-1}$) was estimated from the excretion of total purines ($mmol^{-1}$), using the equation proposed by Verbic et al. (1990): AP = (TPD – 0.385× BW0.75) / 0.85, where: AP = absorbed purines (mmol day^{-1}) TPD = total purine derivatives (mmol day^{-1}) 0.85 = recovery of absorbed purines as DP in the urine 0.385 = endogenous excretion of DP in the urine (mmol) per unit of metabolicsize. Microbial nitrogen (g NM day^{-1}) was estimated from the amount of purines absorbed (mmol day^{-1}) according to the equation by Chen & Gomes (1992): NM (g day^{-1}) = (70×PA)/ (0.83×0.116 ×1,000). Where: 70 = purine nitrogen content (mg $mmol^{-1}$) 0.83 = intestinal digestibility of microbial purines 0.116 = purine-N:total-N ratio in bacteria.

Microbial synthesis efficiency was calculated as follows: ESPBmic = [(NM× 6.25)]/ITDN.

Milk yield was recorded daily from the 17th to the 21st day of each experimental period. Individual milk samples were collected for analysis of protein, fat, lactose, total solids, solids-not-fat, casein, somatic cell count (SCC), and milk urea nitrogen (MUN) at the Dairy Cattle Laboratory (ESALQ/USP). Composite samples were also stored for allantoin determination, according to Broderick & Clayton (1997).

Table 3. List of abbreviations

ASB	Ammoniated Sugarcane Bagasse
CS	Ammoniated Sugarcane Bagasse
DMI	Dry Matter Intake
DM	Dry Matter
ITDN	Intake Total Digestible Nutrients
CP	Crude Protein
EE	Ether Extract
NDF	Neutral Detergent Fiber
NDFap	Neutral Detergent Fiber corrected for ash and protein
ADF	Acid Detergent Fiber
iNDF	Indigestible Neutral Detergent Fiber
NFC	Non-Fiber Carbohydrates
TDN	Total Digestible Nutrients
BW	Body Weight
MW	Metabolic Weight
SEM	Standard Error of the Mean
TPD	Total Purine Derivatives
AP	Absorbed Purines
NM	Microbial Nitrogen
ESPBmic	Microbial Protein Synthesis Efficiency
SCC	Somatic Cell Count
MUN	Milk Urea Nitrogen
MP	Milk Production
PFCM	Production of Fat-Corrected Milk
DDE	Defatted Dry Extract
FE	Feed Efficiency
NRC	National Research Council
DMI	Dry Matter Intake
CPI	Crude Protein Intake
EEI	Ether Extract Intake
NDFapI	NDF corrected for ash and protein Intake
NFCI	Non-Fiber Carbohydrates Intake
TDNI	Total Digestible Nutrients Intake

Feeding behavior was evaluated on the 21st day of each period by continuous visual observation over 24 hours at 10-minute intervals, recording feeding, rumination, and idling activities (Mezzalira et al., 2011). The efficiencies of feeding and rumination were assessed based on Bürger et al. (2000).

Data were subjected to analysis of variance using the *F*-test at a 5% probability level with the SAS® Studio software (2024).

Table 3 presents the abbreviations used in the results and discussion.

RESULTS AND DISCUSSION

No statistically significant interaction was found between the proportions of ammoniated sugarcane bagasse (ASB) and cottonseed (CS) on nutrient intake ($P > 0.05$) (Table 4). The inclusion of 30% ASB resulted in higher intakes of DMI, CPI, EEI, NFCI, and TDNI ($P < 0.05$). The NDF ap was not influenced ($P > 0.05$).

Higher intakes of DMI, CPI, NFCI, and TDNI were observed in the diet without CS compared to the diet with CS. Ether extract intake was higher in the diet with CS inclusion ($P < 0.05$).

For the intake variables related to body weight (BW%) and metabolic weight (MW%), the inclusion of 30% ASB and the diet without CS resulted in higher dry matter intake. NDF ap intake (BW%) was influenced by ASB, with the diet with 30% ASB showing higher intake.

Dry matter and nutrient intake decreased with increasing ASB percentage in diets to 40% bagasse, which is possibly related to the increase in iNDF and lignin in diets containing 40% (Table 4).

Table 4. Dry matter intake and nutrients in the diet of crossbred cows fed ammoniated sugarcane bagasse (ASB) with or without cottonseed (CS)

Item	ASB		CS		SEM[1]	*P*-value		
	30	40	0	18		ASB	CS	ASB×CS
Intake (kg day^{-1})								
Dry matter	18.38	16.94	18.21	16.41	0.65	0.001	0.008	0.360
Crude protein	2.96	2.53	2.87	2.63	0.08	0.002	0.035	0.868
Ether extract	1.04	0.75	0.80	0.99	0.07	0.007	0.043	0.830
NDFap[2]	5.21	4.95	5.08	5.07	0.16	0.147	0.998	0.634
NFC[3]	9.98	7.62	9.94	7.66	0.36	0.001	0.001	0.302
TDN[4]	13.47	10.86	12.96	11.36	0.39	0.001	0.007	0.965
Intake (% body weight)								
DM[6]	3.96	3.32	3.93	3.45	0.08	0.001	0.001	0.998
NDFap	1.04	0.99	1.01	1.01	0.02	0.021	0.975	0.151
Intake (% metabolic weight)								
DM	0.192	0.157	0.186	0.163	4.36	0.001	0.002	0.872

[1]SEM: standard error of the mean; [2]Neutral Detergent Fiber corrected for ash and protein; [3]Non-fiber carbohydrates; [4]Total digestible nutrients; [6]Dry matter; ASB = sugarcane bagasse; CS = cottonseed.

Recent research in Brazil has shown greater intake of crossbred cows compared to the NRC (Da Silva et al. 2024; Jesus et al., 2020), since the NRC uses data only from Holstein cows, raised in different conditions to the animals in this study, which are ½ Holstein/Zebu crossbred cows. This difference can be attributed to several factors, such as the breed of animals, climatic conditions and food management, which can influence intake in isolation or in combination.

In studies, Almeida et al. (2018), evaluating non-ammonized sugarcane bagasse as a roughage in lactating cows with four different levels of sugarcane bagasse (45, 50, 55 and 60%) and a control diet, reported that DM intakes (14.6, 13.9, 12.9, 11.3) respectively, decreased linearly as a function of bagasse inclusion.

The inclusion of CS affected ($P < 0.05$) the intake of crude protein (CP) due to the DM intake and the diets being isonitrogenous. Animals that received diets without CS showed higher CP intake (Table 4).

EE intake was higher for cows fed CS ($P < 0.05$) than for cows fed the diet without CS. As in the present study, Nogueira et al. (2019), evaluating dry matter intake, nutrient digestibility, and feeding behavior of cows fed CS (30% DM of the diet) and vitamin E, observed that the addition of cottonseed to the diets, regardless of the inclusion of vitamin E, increased EE intake by 306%. In the present study, the EE concentration in the experimental diet increased with the inclusion of CS (18% DM of the diet), increasing EE intake by 123%.

This increase in EE concentration occurs due to the chemical composition of CS, which presents a high amount of this component (20.2%) (Table 1), in diets with inclusion of CS as a replacement, mainly for soybean meal, a food that has quantities of EE (1.5%) (Table 1), favored the increase in the energy density of the diet. This also influenced dry matter intake, in which cows fed a diet with CS of higher energy density obtained lower intake (DMI = 17.41 kg day^{-1}) compared to cows fed a diet without CS (DMI = 19.91 kg day^{-1} (Table 4).

ASB was expected to limit intake due to its NDF content and potential filling effect. It is well established that ruminant DMI is limited by physical distension of the gastrointestinal tract (Molavian et al., 2020). The filling effect of the diet may be influenced by the quantity and degradation kinetics of NDFap, as reported by Grant & Cotanch (2012).

However, this was not what occurred in the present study, since ammoniated bagasse was used, in which ammoniation with urea probably caused the breaking of the esterified bonds within the cell wall, as proven by the reduction of iNDF from 59.5 to 40.8% DM, of lignin from 22.9 to 10.4% DM and an increase in TDN from 37.0 to 45.7 (Table 1). Providing higher intake than expected for the two percentages of bagasse.

The average intake of NDF accp was 1.01% of BW, a value within the limit suggested by Mertens (1997), of 1.2% of BW for lactating cows, since, above this value, it would be limiting for DM intake, when its voluntary intake is highly related to the NDF content in the diets.

In research, Da Silva et al. (2024), evaluating the intake of dairy cows fed 40% ASB in the diet, found a maximum NDF intake of 1.30% BW, above that recommended by Mertens (1997) to avoid limiting intake due to fiber content, and a dry matter intake of 3.9% BW. The authors reported that even with the high level of fiber intake, there was no limitation on DM intake. In the present study, levels of 30 and 40% ASB were used, which demonstrated that these percentages did not limit the animals' intake.

Table 5 presents the values referring to the digestibility coefficients, there was no significant interaction between the proportions of ASB and CS ($P > 0.05$). The ASB content and the inclusion of CS influenced the digestibility of crude protein in which the percentage of 40% sugarcane bagasse and with CS provided lower digestibility ($P < 0.05$).

This probably occurred because the protein in whole cottonseed is located mainly inside the seed, surrounded by the husk and mixed with fat, which delays its release into the rumen (Mullenix et al., 2022), and the diet with 40% bagasse has a higher portion of roughage and a lower portion of concentrate, with sugarcane bagasse having a low protein content and relatively low quality.

In the 30% ASB diet, there is a lower roughage to higher concentrate ratio, which contributes to greater protein digestibility. In diets without CS, the protein source used is soybean meal, which has greater digestibility than the CS protein, contributing to its increase.

Table 5. Digestibility coefficient of dry matter and nutrients in the diet of crossbred cows fed ammoniated sugarcane bagasse (ASB) associated or not with cottonseed (CS)

Item	ASB		CS		SEM[1]	*P*-value		
	30	40	0	18		ASB	CS	ASB×CS
Dry matter	45.87	46.1	45.65	46.32	0.92	0.816	0.489	0.673
Crude protein	64.91	60.34	66.84	58.42	0.82	0.001	0.001	0.266
Ether extract	63.15	61.63	59.73	65.05	0.66	0.062	0.001	0.369
NDFap[3]	34.18	37.89	36.59	35.48	3.08	0.272	0.731	0.331
NFC[4]	83.38	83.29	81.03	85.63	0.40	0.832	0.001	0.631
TDN[5]	66.23	63.9	65.09	65.04	0.70	0.016	0.936	0.081

[1]SEM: standard error of the mean; [2]Probability; [3]Neutral Detergent Fiber corrected for ash and protein; [4]Non-fiber carbohydrates; [5]Total digestible nutrients; ASB = sugarcane bagasse, CS = cottonseed.

It was observed that the inclusion of CS provided higher digestibility coefficients for the ether extract and non-fibrous carbohydrates, this occurred due to the bromatological characteristics of CS, which has 20% EE with high digestibility.

The diet with 30% ASB inclusion had a higher total digestible nutrient (TDN) content. This was likely because ASB has a high NDF value, and at 40% inclusion, there is a higher roughage:concentrate ratio, which contributes to lower dietary digestibility, compared to the diet with 30% ASB inclusion, which has a lower amount of dietary fiber and a higher concentrate ratio, which has greater digestibility.

Nogueira et al. (2019) reported that the inclusion of 30% CS in the diet of Holstein cows improved the EE digestibility coefficients by 14% and decreased the NFC digestibility coefficients by 9.0%. For the dry matter and NDF digestibility coefficients, the ASB percentage and CS inclusion factors did not influence the digestibility of the diets.

Table 6 presents the values of microbial protein synthesis and microbial efficiency. There was no significant interaction between the ASB proportion and CS inclusion factors for the microbial production and microbial efficiency variables ($P > 0.05$). The factors did not individually influence the evaluated variables.

Table 6. Microbial protein synthesis and microbial efficiency of crossbred cows fed ammoniated sugarcane bagasse (ASB) associated or not with cottonseed (CS)

Item	ASB		CS		SEM[1]	*P*-value		
	30	40	0	18		ASB	CS	ASB×CS
Microbial production (g day^{-1})								
Microbial CP	1,548.7	1,456.1	1,396.3	1,608.5	225.74	0.696	0.383	0.945
Microbial efficiency								
g CP kg^{-1} TDN	115.6	133.1	110.8	137.8	18.36	0.381	0.195	0.903

[1] SEM: standard error of the mean; ASB = sugarcane bagasse; CS = cottonseed.

Microbial protein synthesis averaged 1,502.4 g day^{-1} and was not influenced by the diets ($P > 0.05$). Because the diets were calculated to be isonitrogenous and maintained the same NFC proportion, they likely contributed to this result. This NFC balance, together with the release of ammonia into the ruminal fluid resulting from the degradation of nitrogen compounds when animals consumed diets with an average of 14.7% crude protein (Table 2), possibly suggests that the diets promoted the synchronization of protein and energy degradation and possibly provided ammonia nitrogen for use by the ruminal microbiota in microbial synthesis, since the synthesis of microbial protein in ruminants relies directly on the availability of carbohydrates and nitrogen in the rumen (NRC, 2001).

According to Valadares Filho et al. (2010), the efficiency of microbial synthesis is 120 g CP kg^{-1} TDN as a reference for tropical conditions. In this present study, the diets provided promoted an average microbial efficiency of 124.3 g CP kg^{-1} TDN, a value close to that recommended by Valadares Filho et al. (2010).

According to Bünemann et al. (2020), a low ruminal pH can reduce fiber digestion and, therefore, decrease microbial efficiency, which is defined as microbial protein synthesized by fermented organic matter. A decrease in fiber digestion can prevent a uniform energy supply throughout the day, which is necessary for optimal microbial growth. This did not occur because the fiber content used likely provided ideal conditions for the rumen and its microbial population.

The addition of CS did not influence ($P > 0.05$) the microbial efficiency (g CP kg^{-1} TDN), despite CS being rich in ether extract that can generally interfere with the synthesis of microbial protein due to a possible toxic effect on microorganisms (Doreau & Ferlay, 1995). However, intake of this EE likely did not affect microbial growth in the rumen. The exact mechanism of lipid toxicity on these microorganisms is still unclear, but it is suggested that it may be related to the barrier that lipids create around feed particles, impairing microbial colonization and degradation (Van Soest, 1994).

Table 7 presents the values related to the production and composition of milk from crossbred cows fed ammoniated ASB associated or not with CS. There was no significant interaction between the factors percentage of ASB and inclusion of CS for the milk production and composition variables ($P > 0.05$).

The percentage of ASB influenced the variables of total solids and feed efficiency, in which the proportion of 40% of ASB provided higher averages with 13.14 and 0.99, respectively. For feed efficiency, there was an influence of the inclusion of CS ($P < 0.05$), where cows fed diets with cottonseed obtained greater feed efficiency with a value of 0.96.

It was expected that diets with 30% ASB would obtain greater feed efficiency, because it had a higher roughage: concentrate ratio and would provide a greater quantity of nutrients than the diet with 40% bagasse. However, the diet with a concentrate: roughage ratio of 60:40 was sufficient to meet the maintenance and production needs of the cows, since they are crossbred cows with an average production of 20 kg of milk, their genetics did not allow greater production even with a diet with better quality nutrients. Visibly, the cows began to gain weight and increase their body condition score as the experimental period progressed, so these nutrients, in addition to meeting maintenance and production requirements, also contributed to the increase in body weight.

Dry matter intake (DMI) is the starting point for nutrient intake, particularly protein and energy, and is therefore crucial for animal performance. Although cows consumed less DM and nutrients in the 40% diets, this did not affect milk production, and milk intake was higher than estimated (DMI = 14.4 kg day^{-1}).

There was no influence of the diets on milk production, corrected milk production and fat content ($P > 0.05$), possibly indicating that the supply of nutrients to the animal, and especially to the mammary gland, was not limited in any of the diets provided.

Mohamed et al. (1988) reported that supplementation with whole oilseeds, such as cottonseed, can maintain or increase milk fat percentage. This is because, despite containing high levels of oil, the fat present in these seeds is encapsulated. This encapsulation allows for slow release in the rumen, and some of the fat escapes to be utilized in the intestine. This means that the fat from oilseeds is released gradually, which may contribute to maintaining or increasing fat levels in the animals' milk.

The results of the physicochemical analyses of the milk, as presented in Table 7, met the requirements established by Normative Instruction No. 77 (BRASIL, 2018). This regulation establishes the minimum levels of fat 3.0%, protein 2.9%, lactose 4.3% and defatted dry extract in the milk 8.4%. This suggests that the milk produced by cows receiving diets with ASB and CS inclusion, under the same conditions, does not present significant changes in its physicochemical characteristics.

Table 7. Milk production and composition of crossbred cows fed ammoniated sugarcane bagasse (ASB) with or without cottonseed (CS)

Item	ASB		CS		SEM[1]	*P*-value		
	30	40	0	18		ASB	CS	ASB×CS
MP(kg day^{-1})	19.01	19.31	18.99	19.32	0.48	0.553	0.553	0.366
PFCM (kg day^{-1})	18.07	18.88	18.62	18.35	0.64	0.250	0.673	0.892
Fat	3.58	3.81	3.83	3.55	0.12	0.110	0.063	0.258
Protein	3.69	3.75	3.71	3.73	0.07	0.397	0.868	0.061
Lactose	4.47	4.54	4.45	4.55	0.03	0.114	0.073	0.069
Total Solids	12.71	13.14	13.03	12.83	0.07	0.001	0.057	0.081
DDE[3]	9.16	9.33	9.19	9.29	0.07	0.065	0.229	0.084
FE[4]	0.78	0.99	0.82	0.92	0.04	0.004	0.040	0.092

[1]Standard error of the mean; [2]Probability; [1]in percentage; MP = milk production; PFCM = production of fat-corrected milk; [3]DDE= defatted dry extract; [4]FE= feed efficiency (kg of milk kg^{-1} of dry matter consumed). ASB = sugarcane bagasse, CS = cottonseed.

In this study, the average values for fat, protein, lactose, and defatted dry extract were 3.7, 3.7, 4.5, and 9.2, respectively. Therefore, this milk is considered within the normal standards established by law and can be used by dairy industries to produce various dairy products. This result indicates that CS supplementation does not compromise the quality of the milk produced.

Costa (2017), evaluating the different levels of inclusion of whole cottonseed (0, 6, 12, 18 and 24%) in the total diet of dairy cows, found similar results for milk composition, reporting that there was no difference in milk composition; however, milk production was affected by the inclusion of CS, presenting a quadratic effect.

Table 8 presents the values relating to the analysis of feeding behavior of crossbred cows, of crossbred cows fed with ASB associated or not with CS.

There was no significant interaction between the ASB percentage and CS inclusion factors ($P < 0.05$). However, the factors increased the time spent on the chewing variable in minutes g^{-1} of DM and minutes g^{-1} of NDF in diets with a 40% ASB inclusion percentage, with averages of 48.93 minutes g^{-1} of DM and 163.57 minutes g^{-1} of NDF. And for CS inclusion, there was a greater time spent in diets with CS, with 47.46 minutes g^{-1} of DM.

According to Mendes et al. (2010), one of the main elements that directly influences behavioral activities is the levels of neutral detergent fiber present in the diet, especially rumination. According to Van Soest (1994), this behavior is affected by the physical and chemical properties of the diet and is proportional to the cell wall content of the roughage. Despite the high amount of ASB used, the percentages of 30 and 40% did not influence feeding, rumination, or idleness ($P > 0.05$).

Table 8. Feeding behavior of crossbred cows fed ammoniated sugarcane bagasse associated or not with cottonseed

Item	ASB		CS		SEM[1]	*P*-value		
	30	40	0	18		ASB	CS	ASB×CS
Food								
min day^{-1}	323.7	358.7	342.5	340.0	33.6	0.33	0.94	0.33
min kg^{-1} DM	16.2	23.7	18.2	21.7	3.1	0.54	0.32	0.43
min kg^{-1} NDF cp^{-1}	62.6	78.7	69.5	71.8	9.5	0.14	0.81	0.36
%/day	22.4	24.9	23.7	23.6	2.3	0.33	0.94	0.33
Rumination								
min day^{-1}	425.0	416.2	398.7	442.5	44.7	0.85	0.36	0.57
min kg^{-1} DM	21.6	25.1	21.0	25.7	2.9	0.27	0.16	0.62
min kg^{-1} NDF cp^{-1}	82.6	84.7	80.1	87.2	9.6	0.83	0.49	0.64
% day^{-1}	29.5	28.9	27.6	30.7	3.1	0.85	0.36	0.57
Leisure								
min day^{-1}	691.2	665.0	698.7	657.5	35.9	0.49	0.29	0.81
% day^{-1}	48.0	46.1	48.5	45.6	2.4	0.49	0.29	0.81
Chew								
n $cake^{-1}$	48.1	44.8	47.3	45.5	3.2	0.34	0.60	0.26
s $cake^{-1}$	55.0	51.5	55.1	51.4	3.2	0.33	0.30	0.26
N day^{-1}	22203.0	21847.6	20463.9	23586.6	2474.8	0.89	0.25	0.56
min day^{-1}	748.7	775.0	741.2	782.5	35.9	0.49	0.29	0.81
min kg^{-1}DM	37.8	48.9	39.3	47.4	1.4	0.00	0.00	0.48
min kg^{-1}NDF cp^{-1}	145.2	163.5	149.7	159.0	4.4	0.00	0.08	0.33

[1] Standard error of the mean, ASB = sugarcane bagasse, CS = cottonseed.

The ASB percentage influenced the time spent chewing, with cows fed 40% ASB in the diets spending 48.93 min g^{-1} DM and 163.57 min g^{-1} NDF/pwt. This was expected due to the amount of NDF in this diet. The same occurred when cows were fed diets with CS for the chewing variable, where cows spent more time with 47.46 min g^{-1} DM.

These results can be explained by the similarity in the nutritional composition of the diets and in the composition of the ammoniated bagasse, which due to its chemical characteristics, mainly in relation to the fibrous fraction that had a significant reduction in the content of NDFap, NDFi and lignin, causing changes in the behavioral parameters evaluated, presenting averages of 341.2 (min day^{-1}) for feeding and 420.6 (min day^{-1}) for rumination.

The lack of differences in the variables evaluated indicates that ASB, when ammoniated, had improved digestibility, resulting in shorter rumination times compared to conventional feeding and idle periods. Consequently, this improvement in digestibility did not cause significant differences in the cattle's chewing activity.

These results can be explained by the similarity in the nutritional composition of the diets and in the composition of the ammoniated bagasse, which, due to its chemical characteristics, mainly in relation to the fibrous fraction, had a significant reduction in the content of NDFap, NDFi and lignin, causing changes in the behavioral parameters evaluated, presenting averages of 341.2 (min day^{-1}) for feeding and 420.6 (min day^{-1}) for rumination.

The variables evaluated indicate that ASB, when ammoniated, had improved digestibility, resulting in shorter rumination times compared to conventional feeding and idle periods. Consequently, this improved digestibility did not cause significant differences in the cattle's chewing activity.

Mendes et al. (2010) reported that one of the main factors influencing cattle behavioral activities is related to the percentage of neutral detergent fiber (NDF) present in their diets. Specifically, they highlight the impact of NDF content on the animals' rumination, a behavior fundamental for efficient fiber degradation.

As noted by Van Soest (1994), rumination is influenced by the physical and chemical properties of the diet, being proportional to the cell wall content of the roughage present in it. This means that diets with a higher NDF content require more chewing time for their degradation, thus stimulating rumination. Therefore, the composition of diets, especially fiber content, plays a crucial role not only in cattle nutrition but also in their natural behaviors, directly influencing their well-being and overall health.

CONCLUSIONS

The use of diets containing 40% ammoniated sugarcane bagasse (ASB) with the inclusion of cottonseed (CS) is recommended for lactating Holstein × Zebu crossbred cows, compared to the 30% ASB diet. Although the study was limited to a 2×2 design and a restricted number of animals due to resource constraints, the combination of 40% ASB with CS optimized feed efficiency and milk quality.

REFERENCES

Almeida, G.A.P., De Andrade, F.M., De Lima, S.J., Chagas, J.C.C., Véras, A.S.C., De Barros, L.J.A. & De Almeida, G.L.P. 2018. Sugarcane bagasse as exclusive roughage for dairy cows in smallholder livestock system. *Asian-Australasian Journal of Animal Sciences* **31**(3), 379.

Brazil. 2018. Laws, decrees, etc. Normative Instruction No. 76 of November 26, 2018 of the Secretariat of Agricultural Defense of the Ministry of Agriculture, Livestock and Supply. *Official Gazette* (Federative Republic of Brazil) Brasília, Published on: 11/30/2018, Edition: 230, Section: 1, Page: 9.

Broderick, G.A. & Clayton, M.K. 1997. A statistical of animal and nutrition factors influencing concentrations of milk urea nitrogen. *Journal of Dairy Science* **80**(11), 2964–2971.

Bünemann, K., Johannes, M., Schmitz, R., Hartwiger, J., Von Soosten, D., Hüther, L. & Dänicke, S. 2020. Effects of different concentrate feed proportions on ruminal ph parameters, duodenal nutrient flows and efficiency of microbial crude protein synthesis in dairy cows during early lactation. *Animals* **10(**2), 267.

Bürger, P.J., Pereira, J.C., Queiroz, A.C., Coelho Da Silva, J.F., Valadares Filho, S.D.C., Cecon, P.R. & Casali, A.D.P. 2000. Ingestive behavior in Holstein calves fed diets with different concentrate levels. *Brazilian Journal of Animal Science* **29**, 23642.

Chen, X.B. & Gomes, M.J. 1992. Estimation of microbial protein supply to sheep and cattle based on urinary excretion of purine derivatives - an overview of technical details. *International Feed Research Unit - Bucksburnd: Rowett Research Institute* **21**.

Costa, D.A., Carneiro, J.C., Lopes, F.C.F., Gama, M.A.S., Saliba, E.O.S. & Rebouças, G.M.N. 2011. Production and composition of milk from cows fed a diet containing different levels of cottonseed. *Semina: Ciência Agrárias*, Londrina, **32**, 2001–2010.

Costa, Edvaldo Nascimento. 2017. *Cottonseed in diets of lactating cows*. Itapetinga, BA: UESB, 80p. Thesis. (Doctorate in Animal Science, Area of Concentration in Ruminant Production). (in Portuguese).

Da Silva, R.M., Pires, A.J.V., Da Silva, F.F., De Sousa Nogueira, M., De Santana, Jr., H.A. & Dos Santos Alves, G. 2024. Effect of replacing ground corn with cactus pear Nopalea cochenillifera (L.) on feed intake and digestibility, water intake, milk production and composition in Holstein× Gyr cows. *Tropical Animal Health and Production* **56**(8), 341.

Detmann, E., Silva, L.F.C., Rocha, G.C., Palma, M.N.R. & Rodrigues, J.P.P. 2022. Methods for Food Analysis – INCT. *Animal Science* **18**, 350 (in Portuguese).

Detmann, E., Souza, M.A., Valadares Filho, S.C., Queiroz, A.C., Berchielli, T.T., Saliba, E.O.S., Cabral, L.S., Pina, D.S., Ladeira, M.M. & Azevedo, J.A.G. 2012. Methods for Food Analysis - INCT - *Animal Science*. 1st ed. Visconde do Rio Branco: Suprema, 214 (in Portuguese).

Doreau, M. & Ferlay, A. 1995. Effect of dietary lipids on the ruminal metabolism in the rumen: A review. *Livestock Production Science* **43**, 97–110.

Grant, R.J. & Cotanch, K.W. 2012. Higher forage diets: dynamics of passage, digestion, and cow productive responses. *In Proc. Cornell Nutr. Conf.* Feed Manufac. October 16-18. Syracuse, NY, 45–57.

Jesus, Marly Rosa. 2020. *Ammoniated sugarcane bagasse associated with forage cactus in diets for dairy cows.* Thesis (Doctorate in Animal Science). Itapetinga, BA: UESB (in Portuguese).

Lima, M.V.G., Pires, A.J.V., Da Silva, F.F., Teixeira, F.A., De Carvalho Silva Castro Nogueira, B.R., Rocha, L.C., Da Silva, G.P., Andrade, W.R. & De Carvalho, G.G.P. 2021. Intake, digestibility, milk yield and composition, and ingestive behavior of cows supplemented with byproducts from biodiesel industry. *Tropical Animal Health end Production* **53**, 1–11.

Mendes, C.Q., Turino, V.C., Susin, I., Pires, A.V., Morais, J.B. & Gentil, R.S. 2010. Ingestive behavior of lambs and nutrient digestibility of diets containing a high proportion of concentrate and different sources of neutral detergent fiber. *Brazilian Journal of Animal Science* **39**(3), 594–600.

Mertens, D.R. 1997. Creating a system for meeting the fiber requirements of dairy cows. *Jornal of Dairy Science* **80**(7), 1463–1481.
Mezzalira, J.C., Carvalho, P.C.F., Fonseca L.,Bremm, C., Reffatti, M.V., Poli, C.H.E.C. & Trindade, J.K.D. 2011. Methodological aspects of ingestive behavior of grazing cattle. *Brazilian Journal of Animal Science* **40**, 111420.
Mohamed, O.E., Satter, L.D., Grummer, R.R. & Ehle, F.R. 1988. Influence of dietary cottonseed and soybean on milk production and composition. *Journal of Dairy Science* **71**, 2677–2688.
Molavian, M., Ghorbani, G.R., Rafiee, H. & Beauchemin, K.A. 2020. Substitution of wheat straw with sugarcane bagasse in low-forage diets fed to mid-lactation dairy cows: Milk production, digestibility, and chewing behavior. *Journal of dairy science* **103**(9), 8034–8047.
Mullenix, M.K., Stewart Jr, R.L., Jacobs, J.L. & Davis, D.L. 2022. Invited Review: Using whole cottonseed and cotton harvest residue in southeastern US beef cattle diets: Quality, intake, and changes in feed characteristics. *Applied Animal Science* **38**, (5), 447–455.
National Research Council. 2001. Nutrients requirements of the dairy cattle. Washington, D.C: *National Academy Press*, **7**, 381.
Nogueira, R.G.S., Perna, F., Pereira, A.S.C. & Rodrigues, P.H.M. 2019. Nutrient digestibility and changes in feeding behavior of cattle fed cottonseed and vitamin E. *Agricultural Science* **76**,112–122.
Publio, P.P.P., Pires, A.J.V., Dutra, I.C., Sousa, M.P., Figueiredo, G.C., Santos, H.O., Oliveira, G.R.S., Ferreira, E.P.L., Santos, A.F., Cardoso, P.H.S., Teixeira, F.A. & Albuquerque, M.L.P. 2025. Ammoniated sugarcane bagasse associated with cottonseed in sheep diets. *Agronomy Research* **23**(S2), 882–903.
SAS on Demand for Academics 2024 https://www.sas.com/en_us/software/on-demand-foracademics.html.
Silva, N.V., Pires, A.J.V., Dutra, I.C., Silva, H.S., Santos, B.E.F., Nogueira, M.S., Cruz, N.T., Silva, A.P.G., Teixeira, L.S., Oliveira, G.R.S., Dutra, G.C. & Teixeira, L.S. 2025. The quality and fermentation of the total diet containing BRS capiaçu or sugarcane with or without urea. *Agronomy Research* **23(**S2), 935–947.
Sniffen, C.J.,O'connor, D.J.,Van Soest, P.J.,Fox, D.G. & Russell, J.B. 1992. A net carbohydrate and protein system for evaluating cattle diets: carbohydrate and protein availability. *Journal of Animal Science* **70**(12), 3562–3577.
Sun, X., Su, Y, Hao, Y., Zhang, J., Yue, X., Wang, W., Ma, Z., Chu, K., Wang, S., Wang, Y.E. & Li, S. 2022. Effect on the Digestibility, Productivity, Fat Profile, and Milk Gossypol Levels in Lactating Dairy Cows. *Frontiers in Nutrition* **9**, 801712.
Valadares Filho, S.C., Marcondes, M.I., Chizzotti, M.L. & Paulino, P.V.R. 2010. *Nutritional requirements of purebred and crossbred zebu cattle* - BR-CORTE. Viçosa, MG: UFV, Suprema Gráfica Ltda., **2**, 193.
Van Soest, P.J. 1994. *Nutritional ecology of the ruminant.* 2.ed. Ithaca: Cornell University Press, 476 pp.
Verbic, J., Chen, X.B., MacLeod, N.A. & Orskov, E.R. 1990. Excretion of purine derivatives by ruminants. Effect of microbial nucleic acid infusion on purine derivative excretion by steers. *Journal of Agricultural Science* **114**(3), 243–248.

Agronomy Research **24**(S1), 54–73, 2026
https://doi.org/10.15159/AR.25.110

Global systematic review of cassava production and meta-analysis of the effects of fertilization on yield

K. Promnikorn[1], P. Saengnuan[2], P. Kittipadakul[3] and E. Kraichak[1,*]

[1]Kasetsart University, Faculty of Science, Department of Botany, Ngamwongwan Rd. 50, TH10900 Bangkok, Thailand
[2]Mahidol University International College, Department of Biological Science, Phutthamonthon Sai 4 Rd. 999, TH73170 Nakhon Pathom, Thailand
[3]Kasetsart University, Faculty of Agriculture, Department of Agronomy, Ngamwongwan Rd. 50, TH10900 Bangkok, Thailand
[*]Correspondence: ekaphan.k@ku.th

Received: October 9th, 2025; Accepted: November 19th, 2025; Published: December 30th, 2025

Abstract. Cassava plays a significant role in global food security as a staple food crop for billions of people in developing countries. However, the systematic summary of recent studies on cassava production has not been thoroughly compiled. This study aimed to identify key aspects of cassava production, with a particular focus on the effects of fertilization, through a systematic review and meta-analysis. A search of the Scopus database from 1970 to 2022 identified 229 studies on cassava production, of which 83 met the inclusion criteria and were categorized into eight main topics: soil, pest and disease control, genetics and biotechnology, crop management, land, post-harvest and physiology, modeling, and environmental factors. The meta-analysis of studies regarding fertilizer application ($n = 7$) revealed a modest overall effect of fertilization on cassava yield (effect size = 0.75, 95% *CI*: 0.53–0.96), with micronutrients and macronutrients showing more significant effects compared to organic fertilizers. Additionally, the study found that regional differences influenced fertilization effectiveness, with South America and Southeast Asia showing higher positive responses to fertilization compared to Africa, likely due to varying soil fertility and nutrient limitations. Soil texture also significantly impacted fertilizer efficiency, with silt loam showing the highest fertilizer response. However, the results are based on a limited number of studies, highlighting a critical gap in agricultural research: the lack of comprehensive statistical reporting. This limitation hampers the ability to conduct more robust meta-analyses. Future research should focus on improving statistical reporting practices and exploring region-specific fertilizer strategies to enhance cassava yield sustainably.

Key words: forest plot, fresh root yield, on-field, random effect model, standard mean difference (SMD).

INTRODUCTION

Cassava (*Manihot esculenta* Crantz) is a vital staple crop for millions in tropical and subtropical regions, valued for its resilience to drought and poor soils, and its critical role in food security and industrial applications (IAEA, 2018). Global cassava production has shown steady growth over the past decade, rising from approximately 275 million tonnes in 2012 to over 327 million tonnes in 2022 (FAOSTAT, 2023). Africa remains the leading cassava-producing region, accounting for about 60% of total global output, followed by Southeast Asia (26%) and South America (9%) (FAOSTAT, 2023). This upward trend underscores the crop's growing importance in enhancing food security and supporting livelihoods in developing regions.

Despite cassava's adaptability, yields remain suboptimal in many regions, primarily due to declining soil fertility and limited fertilizer use – challenges compounded by economic constraints faced by smallholder farmers (Howeler, 1991; Senkoro et al., 2018). The persistent yield gap, where actual yields fall far below potential, underscores the urgent need for research into agronomic practices, particularly fertilization strategies that can sustainably boost productivity (Howeler, 1991; Senkoro et al., 2018; Okoth Omondi & Yermiyahu, 2021). Although cassava can grow without fertilizer, reliance on natural soil fertility often leads to nutrient mining and long-term soil degradation, particularly in smallholder systems across Africa, Asia, and South America (Cadavid et al., 1998; Howeler, 2014).

Recent research on cassava production has increasingly focused on optimizing fertilizer management, understanding varietal responses, and improving soil health. Studies consistently demonstrate that cassava responds positively to nitrogen (N), phosphorus (P), and potassium (K) fertilization (Howeler, 1991; Wilson & Ovid, 1994; Senkoro et al., 2018; Chua et al., 2020; Okoth Omondi & Yermiyahu, 2021; Sinta & Dansa, 2023). Optimal rates and combinations of NPK fertilizers have been shown to increase root yield, starch content, and economic returns (Wilson & Ovid, 1994; Senkoro et al., 2018; Katuromunda et al., 2021; Sinta & Dansa, 2023).

Furthermore, integrated fertilization strategies combining organic and inorganic fertilizers have shown significant promise. Both organic amendments (such as poultry manure, compost) and mineral fertilizers, as well as their combinations, can substantially enhance cassava growth, yield, and soil fertility (Nassy et al., 2020; Katuromunda et al., 2021; Ikeh et al., 2023). These integrated approaches not only boost yields but also improve soil organic matter, nutrient availability, and microbial diversity across diverse genotypes and environments, supporting sustainable production systems (Nassy et al., 2020; Ikeh et al., 2023). Additionally, the timing and method of fertilizer application, along with interactions with planting density and crop age, are recognized as important factors influencing cassava productivity (Yabuta et al., 2021; Enesi et al., 2022).

However, the literature on cassava fertilization presents conflicting results. Studies report both substantial yield increases and minimal or no benefits from fertilizer application, with outcomes often depending on the genotypes, types of fertilizer, and environmental conditions (Pimentel et al., 2021). Responses to fertilization can vary significantly by location, variety, and soil type, underscoring the need for site-specific recommendations (Wilson & Ovid, 1994; Katuromunda et al., 2021; Enesi et al., 2022). This variability makes it difficult for farmers, extension agents, and policymakers to make evidence-based decisions about fertilization strategies. Furthermore, the economic implications of fertilizer use are particularly important for smallholder farmers with limited resources, requiring careful evaluation of cost-effectiveness across different contexts.

Systematic reviews and meta-analyses provide robust tools for synthesizing empirical evidence across diverse studies, employing transparent and repeatable methodologies (Koricheva et al., 2013). In agriculture, they have been instrumental in evaluating practices such as conservation agriculture (Pittelkow et al., 2015), the impacts of organic farming (Tuck et al., 2014), the effects of climate change (Challinor et al., 2014), and yield stability (de Ponti et al., 2012). However, no comprehensive synthesis has been conducted specifically to evaluate the effects of fertilization on cassava productivity. This research gap is particularly concerning given that cassava production systems are highly diverse, spanning different continents, soil types, and management practices, making individual studies insufficient for generating broadly applicable recommendations.

To address this gap, this study conducted a systematic review and meta-analysis of cassava production research published between 1970 and 2022. The objectives were to: (1) identify key areas of research focus on cassava production, (2) assess the effects of different fertilizer types on cassava yield, and (3) highlight existing knowledge gaps that warrant further investigation. By statistically aggregating results from eligible studies, this analysis provides evidence-based insights into fertilizer effectiveness and supports the development of region-specific recommendations to enhance cassava yield sustainably.

MATERIALS AND METHODS

Search strategy

A systematic review on cassava production was conducted following the 'Preferred Reporting Items for Systematic Reviews and Meta-Analyses' (PRISMA) framework (Fig. 1; Tugwell & Tovey, 2021). The Scopus database was queried using the search string: (TITLE-ABS-KEY ('cassava production') AND TITLE-ABS-KEY (yield OR biomass OR tuber OR root OR 'storage root' OR 'root weight')) AND (LIMIT-TO (DOCTYPE, 'ar') OR LIMIT-TO (DOCTYPE, 'cp')). The search fields were restricted to abstract, key words, and title, while the document type was limited to published articles or conference proceedings. The search was performed on March 16, 2022, encompassing publications from 1970 to 2022.

Study screening and selection

After searching studies according to the search strategy in Scopus, the abstracts of all retrieved studies were subsequently screened using AbstractR (Wallace et al., 2012). Initially, studies were included if productivity traits, such as fresh/dry root yield or biomass, related to cassava production were mentioned in the abstracts. Studies were excluded if (i) they were review articles or (ii) the abstracts indicated the topics of economics, food science, and energy. The studies that passed the abstract screening were further selected based on the following eligibility criteria: (i) full text availability in English; (ii) field-level experimental design; (iii) provision of information on control and treatments; and (iv) at least fresh root yield reported as the outcome data on cassava productivity. The studies meeting these criteria were then categorized into the following topics: soil, pest & disease control, genetic & biotechnology, crop management, land, post-harvest & physiology, modeling, and environmental factors to identify recent topics of research on cassava production.

Data extraction

After categorizing topics of studies and ranking them by the number of studies, the most frequently studied topic on cassava production was selected for meta-analysis. The productivity trait focused primarily on studies that presented data on fresh root yield. To be included in the analyses, studies had to report three main statistics for both control and treatment groups: mean ($\overline{X}$), standard deviation (*SD*) or standard error (*SE*), and sample sizes (replications). In some cases, studies reported only within-study SD instead of within-group *SD*; the within-study *SD* was used when all groups had equal sample sizes. Additionally, if studies did not report all *SD*s, the *SE* was recalculated to *SD* (Eq. 1). When data was represented in a bar graph, the image was digitized using the PlotDigitizer Free Online App (https://plotdigitizer.com) to extract values. The means, *SD*s, and sample sizes for both control and treatment groups of all studies were prepared in Microsoft Excel (version 16.89)

Data analysis and reporting

To perform a meta-analysis, all means, *SD*s, and sample sizes of each group in each study were calculated to a standardized mean difference (*SMD*) by Hedges'd method (Eq. 2; Hedges, 1981), being the mean difference between control and treatment weighted by pooled SD (Eq. 3). In this study, the *SMD* was used to quantify the magnitude of differences between the control group and each of the treatment groups, and it was used as an effect size to compare the results of different studies that focused on the same topic on a common scale. The *SMD* was calculated using the function 'metacont' in the R package 'meta' (version 4.3.2).

$$SE = \sqrt{n} \cdot SD \quad (1)$$

$$SMD = \left(\overline{X}_T - \overline{X}_C\right) / S_{pooled} \quad (2)$$

$$S_{pooled} = \sqrt{(n_T - 1)SD_T^2 + (n_T - 1)SD_C^2 \; / \; (n_T - 1) + (n_C - 1)} \quad (3)$$

where SE – the standard error; SD – the standard deviation; n – the sample size; SMD – the standardized mean difference; $\overline{X}_T$ – the mean of the treatment group; $\overline{X}_C$ – the mean of the control group; S_{pooled} – the pooled *SD*; n_T – the sample size of the treatment group; n_C – the sample size of the control group.

We generated an estimate of the overall mean effect size using both fixed-effect and random-effect models using the 'metacont' function in the R package 'meta' (version 4.3.2). Heterogeneity of effect sizes was assessed using the I^2 and τ^2 statistics (Copes & Ojiambo, 2021).

To visualize the results from the meta-analysis, a forest plot was used to represent the *SMD*s of each study with a 95% confidence interval (*CI*). The forest plot was generated using the function 'forestplot' in the R package 'meta' (version 4.3.2)

RESULTS

Distribution of topics in cassava yield research

Search results

The search in Scopus retrieved 229 studies on cassava production that were published between 1970 and 2022. From abstract screening, 83 studies met the inclusion criteria, including being research articles, having an English full-text access, related to cassava production, and reporting productivity traits (Fig. 1).

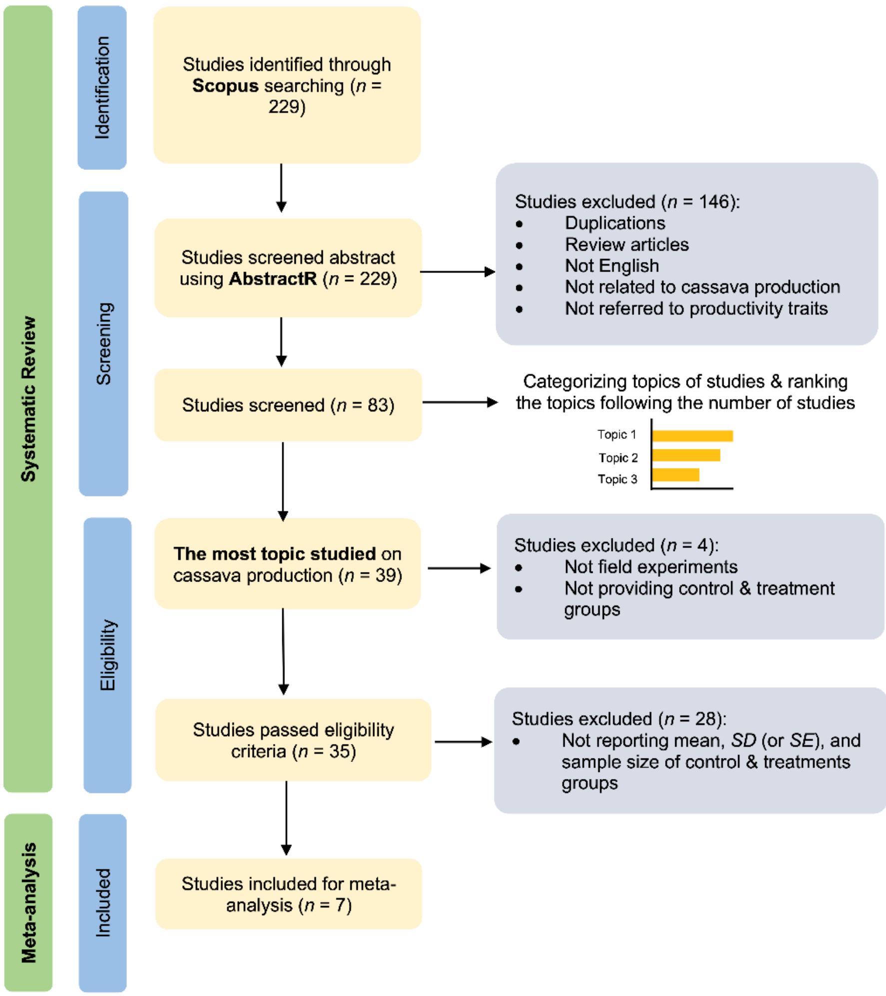

Figure 1. Identification, screening, and inclusion of the publications on cassava production using the Preferred Reporting Items for Systematic Reviews and Meta-analysis.

Geographical distribution of the included studies

The regions with the most studies (*n* = 42 out of 83 studies) were Africa, followed by Southeast Asia (*n* = 20), South America (*n* = 16), Asia (*n* = 4), and Australia (*n* = 2), respectively. Four countries with the highest number of studies were Nigeria (*n* = 19), Thailand (*n* = 11), Indonesia (*n* = 7), and Colombia (*n* = 7; Fig. 2).

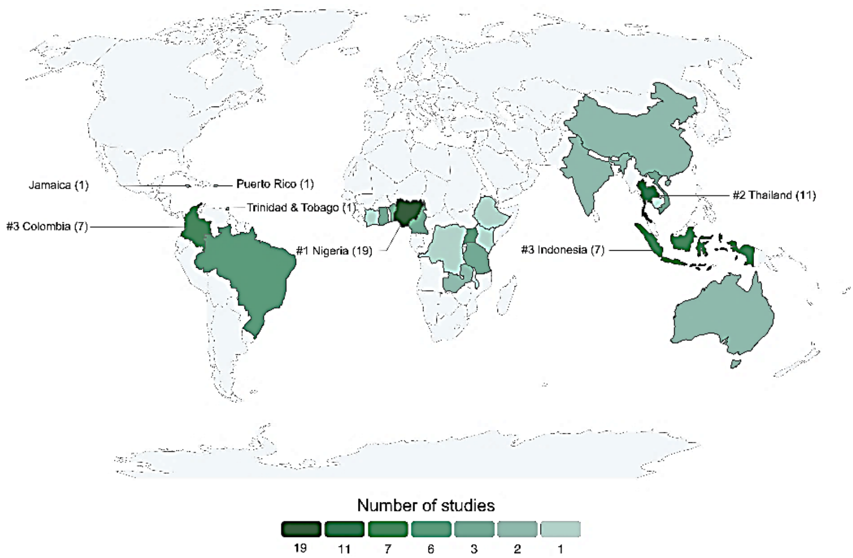

Figure 2. Countries with studies on cassava production meeting the inclusion criteria for systematic review. The #1, #2, and #3 symbols indicate the top three countries by the number of studies. Numbers in brackets refer to the number of studies.

Categorized topics of the included studies

The 83 abstract-screened studies could be identified based on different topics with individual studies potentially encompassing multiple topics, including soil (n = 39 out of 83 studies); pest & disease control (n = 24); genetics & biotechnology (n = 17); crop management (n = 13); land (n = 5); post-harvest & physiology (n = 4); modeling (n = 3); and environmental factors (n = 3), respectively. The soil topic had the most recent studies on cassava production, particularly fertilization (Fig. 3).

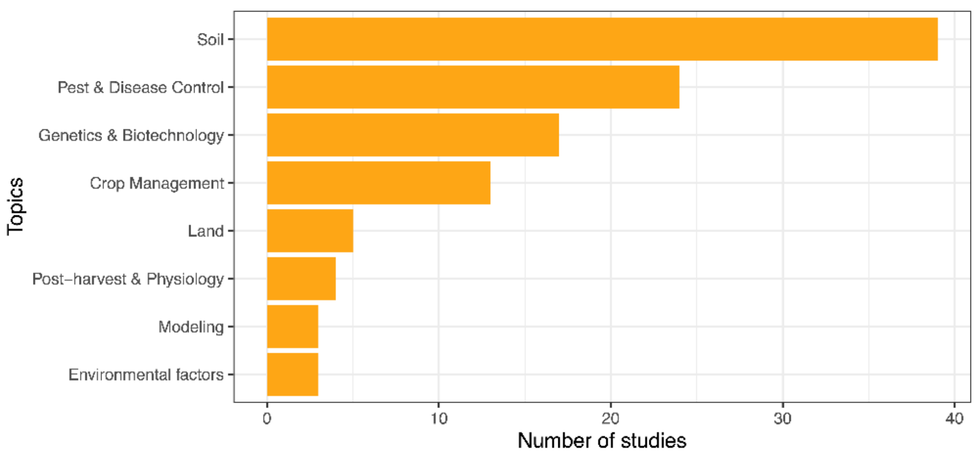

Figure 3. Main topics of 83 cassava production studies meeting the inclusion criteria for systematic review, with individual studies potentially encompassing multiple topics.

Within the fertilization topic, seven studies reported sample sizes and statistical data, including means, *SD*, and *SE*, which allowed us to perform a meta-analysis of fertilization on cassava production. Moreover, the studies were conducted a subgroup analysis based on fertilizer types, dividing the studies into three groups (macronutrients, organics, micronutrients); planting regions, dividing the studies into three groups (Africa, Southeast Asia, South America); and soil textures, dividing the studies into five groups (sandy loam, silt loam, clay, loamy sand, clay loam) (Table 1).

Table 1. Soil studies on cassava production for each categorical grouping in the meta-analysis

Categories		No. of studies	Authors
All studies (n = 7)			
Fertilizer types	Macronutrients	6	Cadavid et al. (1998); Aliyu et al. (2019) Odedina et al. (2012); Kaweewong et al. (2013) Carsky & Toukourou, (2005); Pypers et al. (2012)
	Organics	1	Odedina et al. (2012)
	Micronutrients	1	Marchi et al. (2020)
Planting regions	Africa	5	Cadavid et al. (1998); Aliyu et al. (2019) Carsky & Toukourou (2005) Odedina et al. (2012); Pypers et al. (2012)
	Southeast Asia	1	Kaweewong et al. (2013)
	South America	1	Marchi et al. (2020)
Soil textures	Sandy loam	5	Cadavid et al. (1998); Odedina et al. (2012) Carsky & Toukourou (2005) Pypers et al. (2012); Kaweewong et al. (2013)
	Silt loam	1	Aliyu et al. (2019)
	Clay	1	Kaweewong et al. (2013)
	Loamy sand	1	Kaweewong et al. (2013)
	Clay loam	1	Marchi et al. (2020)

Meta-analysis of fertilization on cassava yield

Overall effect

The meta-analysis of all studies (N = 7 studies, 67 treatments) provided an overall effect size of 0.75 (95% *CI*: 0.53, 0.96) based on the random-effects model. Effect sizes across all studies ranged widely, with 95% CIs spanning from – 1.70 to 20.68. Notably, the majority of treatments across all studies had 95% *CI*s that included zero. However, 6 out of 67 treatments, all involving phosphate addition, showed 95% *CI*s entirely above zero. Interestingly, the test for heterogeneity of effect sizes across all studies was not significant ($I^2 = 0\%$, $\tau^2 < 0.0001$, $p = 0.9603$) (Fig. 4). This lack of heterogeneity suggests that all studies share a common underlying effect size, despite the variability observed in individual treatment outcomes.

These findings highlight the generally positive impact of the treatments, particularly those involving phosphate addition. However, the wide range of confidence intervals and the prevalence of intervals including zero underscore the need for cautious interpretation of results across different contexts and treatment types.

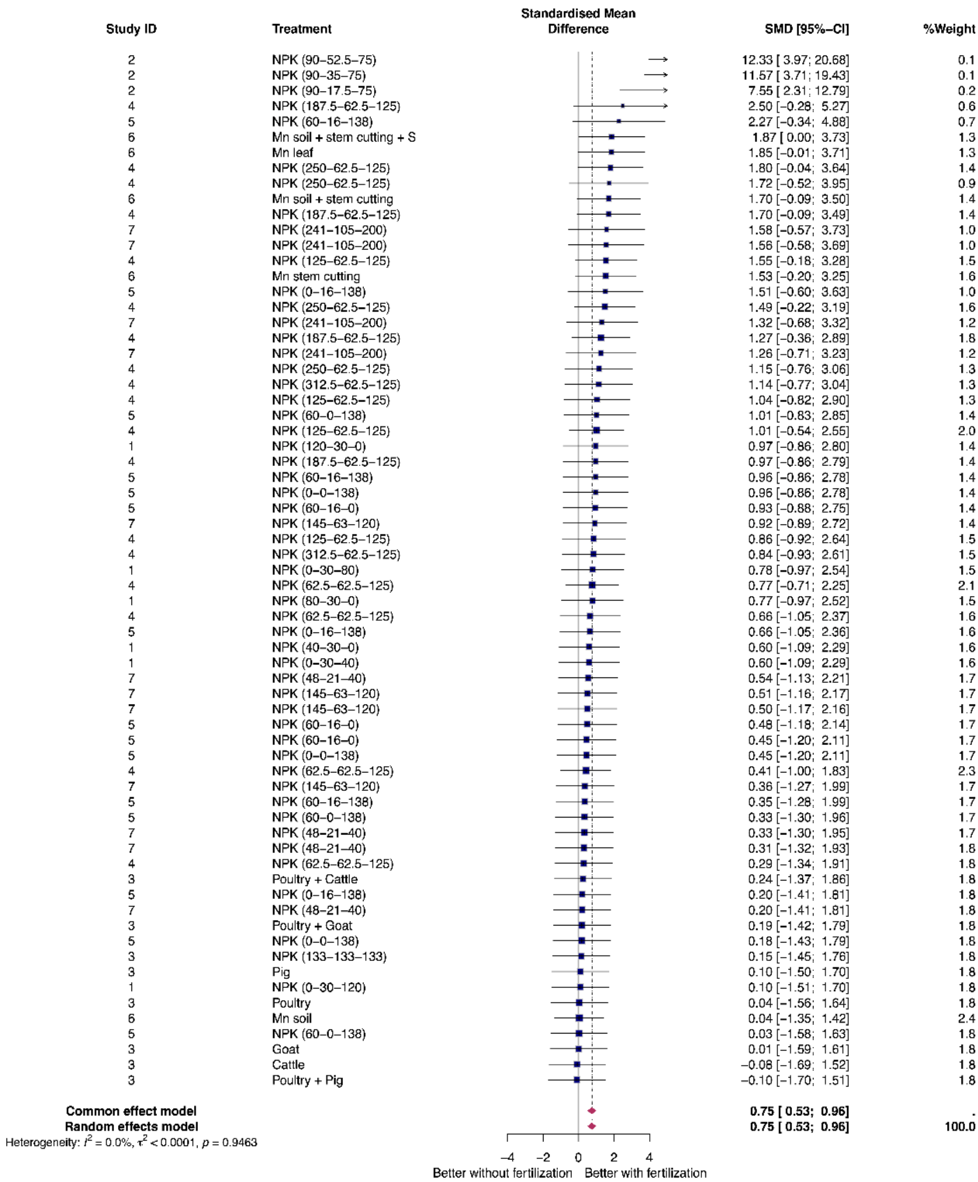

Figure 4. Forest plot showing the magnitude of effect sizes derived from standardized mean differences across studies evaluating fertilization efficiency on cassava fresh root. The blue boxes represent the estimated true effect for each study, with horizontal lines indicating their 95% confidence intervals. The pink diamond at the bottom shows the overall pooled effect from all included studies.

Subgroup effects

These studies were further utilized for subgroup analyses, categorizing the data into three distinct groups: fertilizer types, planting regions, and soil textures (Table 1). The results of the subgroup analyses were as follows.

Fertilizer types. Analysis of the effect sizes revealed varying impacts across different fertilizer types. Micronutrients (N = 1 study, five treatments) showed an effect size of 1.26 (95% *CI*: 0.42, 2.10), with low heterogeneity ($I^2 = 3\%$, $\tau^2 = 0.1634$, $p = 0.39$). Macronutrients (N = 6 studies, 55 treatments) demonstrated a larger effect at 0.81 (95% *CI*: 0.57, 1.05), exhibiting no heterogeneity ($I^2 = 0\%$, $\tau^2 < 0.0001$, $p = 0.96$). However, organics (N = 1 study, seven treatments) exhibited a smaller effect of 0.05 (95% *CI*: − 0.55, 0.66), with perfect homogeneity ($I^2 = 0\%$, $\tau^2 = 0$, $p = 1.00$). Notably, only the organic fertilizers' confidence interval spanned zero. The consistently low heterogeneity within subgroups corroborates the suggestion of a common effect size shared among fertilizer types (Table 2; Fig. 5).

Table 2. Effect sizes of fertilizations on cassava production (fresh root weight) by subgroups

Subgroups	N	n_t	SMD (95% CI)	Heterogeneity		
				I^2	τ^2	*P-value*
Fertilizer type						
Micronutrients	1	5	1.26 (0.42, 2.10)	3%	0.1634	0.39
Macronutrients	6	55	0.81 (0.57, 1.05)	0%	< 0.0001	0.96
Organic	1	7	0.05 (-0.55, 0.66)	0%	0.0000	1.00
Planting region						
South America	1	5	1.26 (0.42, 2.10)	3%	0.1634	0.39
Southeast Asia	1	18	1.08 (0.66, 1.49)	0%	0.0000	1.00
Africa	5	48	0.55 (0.28, 0.82)	0%	< 0.0001	0.85
Soil texture						
Silt loam	1	3	9.54 (5.68, 13.41)	0%	0.0000	0.54
Clay loam	1	5	1.26 (0.42, 2.10)	3%	0.1634	0.39
Loamy sand	1	4	1.19 (0.38, 1.99)	0%	0.0000	0.85
Clay	1	4	1.15 (0.34, 1.96)	0%	0.0000	0.62
Sandy loam	5	55	0.55 (0.32, 0.78)	0%	0.0000	1.00
OVERALL	7	67	0.75 (0.53, 0.96)	0%	< 0.0001	0.95

N – the number of studies; n_t – the number of treatments; *SMD* – standardized mean difference; 95% *CI* – 95% confidence interval.

Planting regions. Regional analysis unveiled varying degrees of impact. South America (N = 1 study, five treatments) showed the highest effect size at 1.26 (95% *CI*: 0.42, 2.10), with low heterogeneity ($I^2 = 3\%$, $\tau^2 = 0.1634$, $p = 0.39$). Southeast Asia (N = 1 study, 18 treatments) followed at 1.08 (95% *CI*: 0.66, 1.49), displaying no heterogeneity ($I^2 = 0\%$, $\tau^2 = 0$, $p = 0.93$). Africa ($n = 5$ studies, 48 treatments) displayed a more modest effect of 0.55 (95% *CI*: 0.28, 0.82), also with no heterogeneity ($I^2 = 0\%$, $\tau^2 < 0.0001$, $p = 0.85$). Importantly, all regions' confidence intervals excluded zero. The consistently low or absent within-group heterogeneity further supports the indication of a shared effect size across planting regions (Table 2; Fig. 6)

Soil textures. Soil texture analysis provided diverse results. Silt loam ($n = 1$ study, three treatments) exhibited an exceptionally high effect size of 9.54 (95% *CI*: 5.68, 13.41), with no heterogeneity ($I^2 = 0\%$, $\tau^2 = 0$, $p = 0.54$). Clay loam (N = 1 study, five treatments) and loamy sand (N = 1 study, four treatments) showed similar effects at 1.26 (95% *CI*: 0.42, 2.10) and 1.19 (95% *CI*: 0.38, 1.99), respectively. Clay loam displayed low heterogeneity ($I^2 = 3\%$, $\tau^2 = 0.1634$, $p = 0.39$), while loamy sand showed no heterogeneity ($I^2 = 0\%$, $\tau^2 = 0$, $p = 0.85$). Clay (N = 1 study, four treatments) demonstrated a lower effect of 1.15 (95% *CI*: 0.34, 1.96), with no heterogeneity ($I^2 = 0\%$, $\tau^2 = 0$, $p = 0.62$). All soil textures' confidence intervals wereabove zero. The consistently low or absent within-group heterogeneity across all soil textures reinforces the suggestion of a common effect size shared among soil types. (Table 2; Fig. 7)

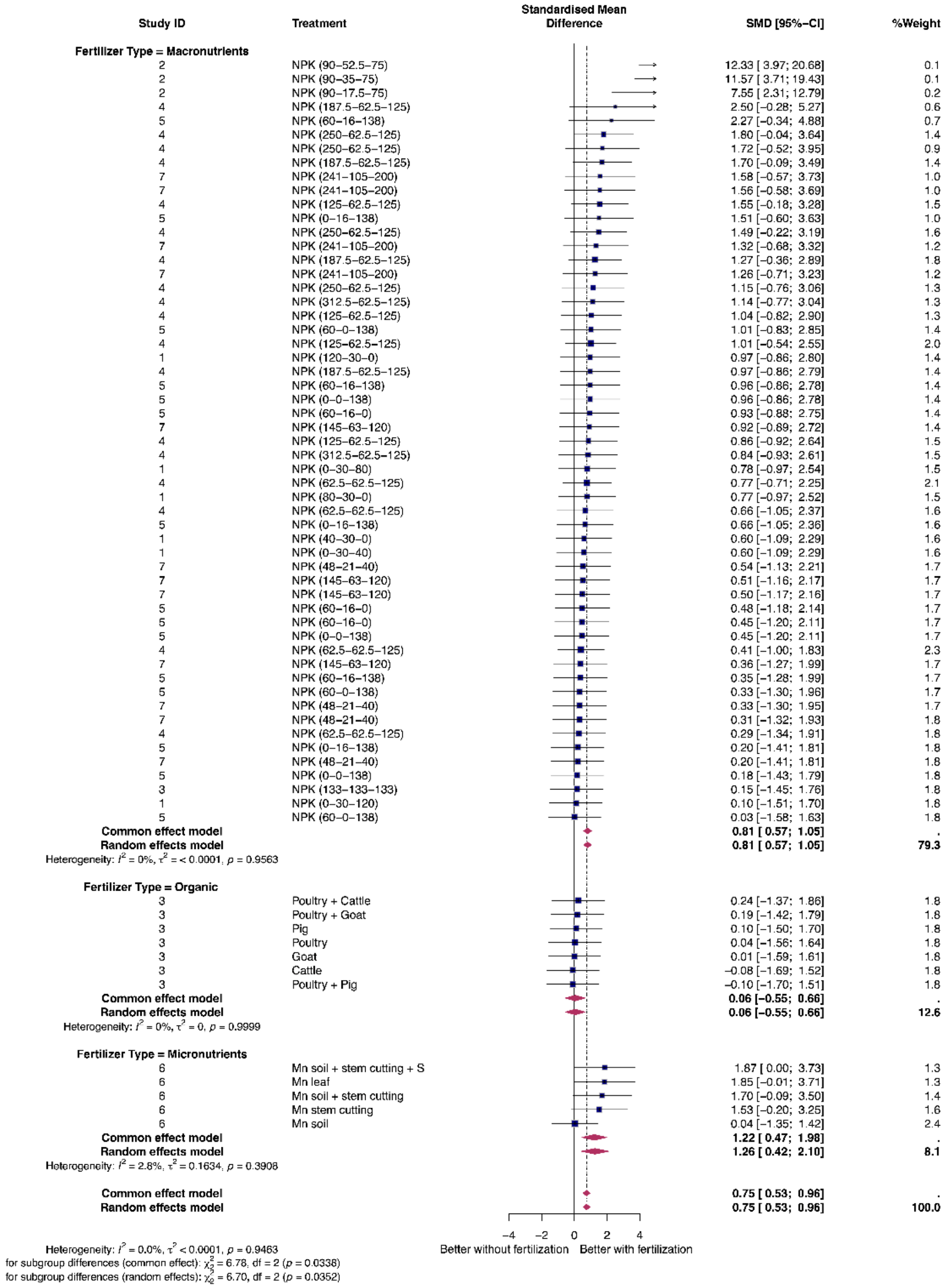

Figure 5. Forest plot of fertilization studies in cassava production, sup-grouped by fertilizer types.

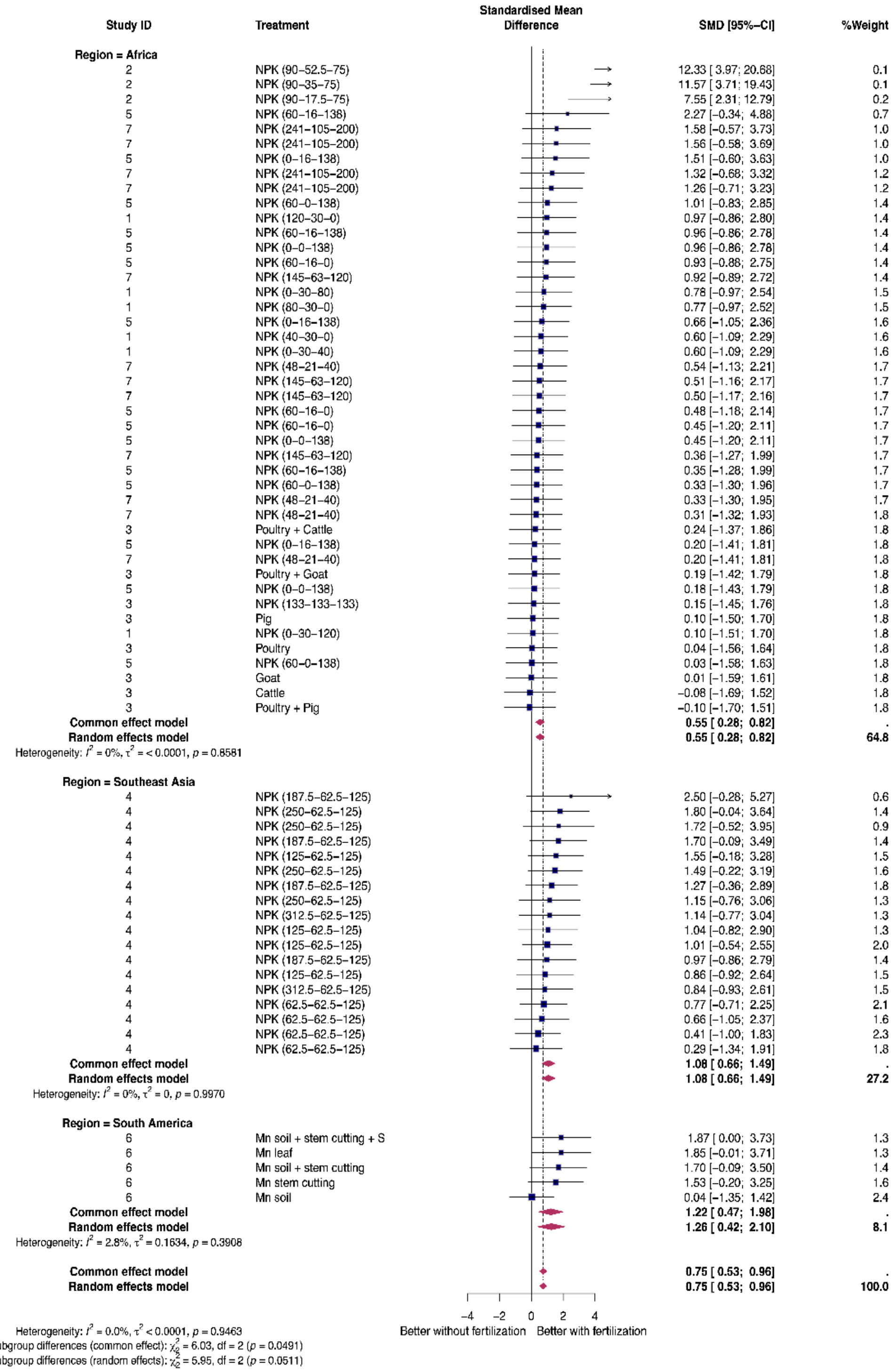

Figure 6. Forest plot of fertilization studies in cassava production, sup-grouped by continental regions.

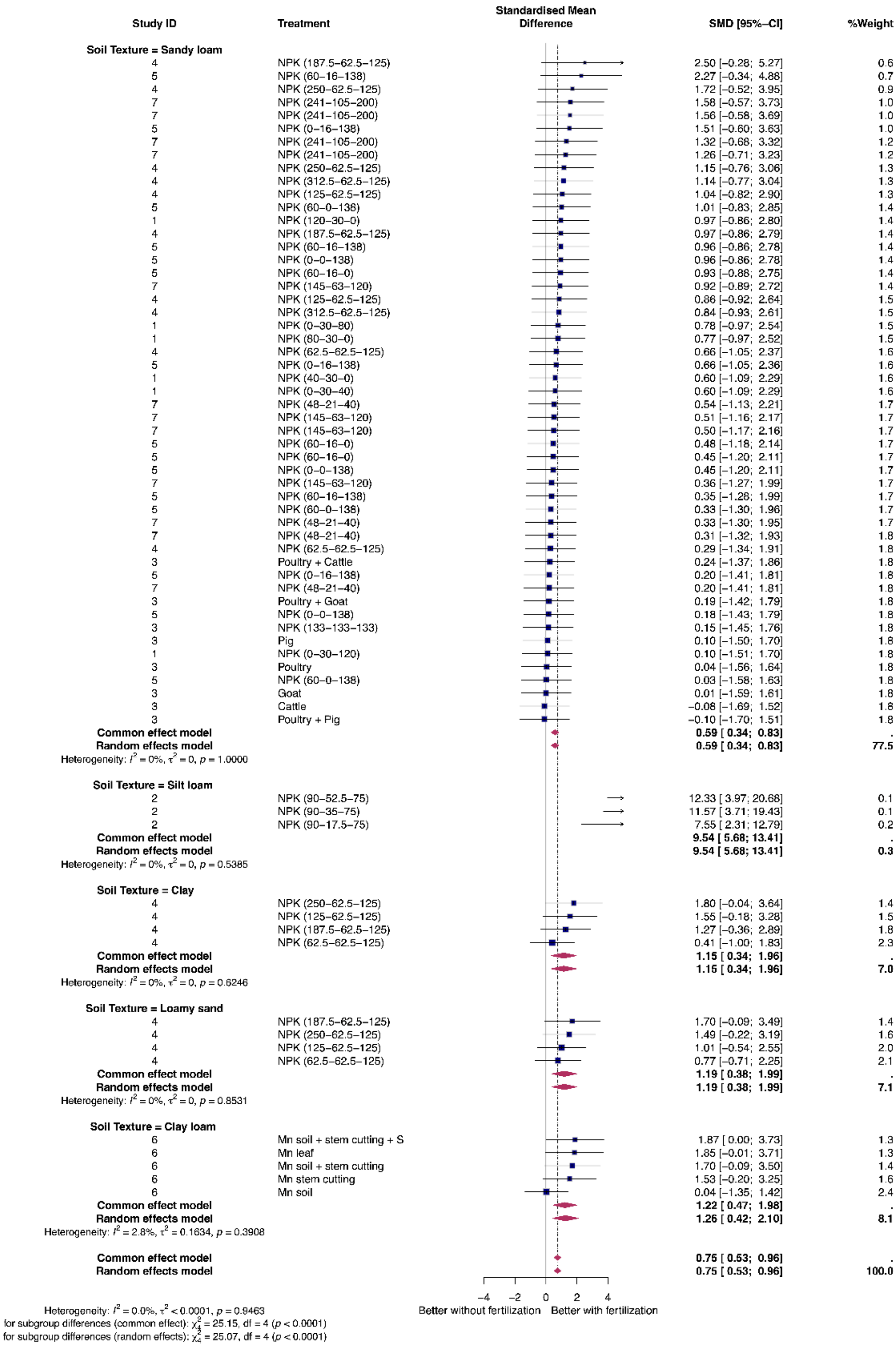

Figure 7. Forest plot of fertilization studies in cassava production, sup-grouped by soil textures.

DISCUSSION

Our systematic review screened 85 studies on cassava production, of which 39 (46%) examined fertilizer application effects on yield. Only seven of these fertilization studies met our inclusion criteria for meta-analysis. Given that cassava is a crop harvested from underground and the majority of cassava cultivation occurs in African regions with low soil fertility, it is reasonable that research has focused on soil contexts, particularly applying fertilization to improve soil fertility. To evaluate the effectiveness of fertilization across comparable studies, we performed a meta-analysis examining its impact on cassava yield.

Our meta-analysis revealed that an overall moderately positive effect of fertilizer application on cassava yield, with heterogeneity approaching zero at a statistically significant level (Fig. 4). The existing studies consistently demonstrate that fertilizer application enhances cassava yield in a similar manner across different research contexts, such as varying fertilizer types, soil textures, and planting regions.

Effectiveness of different fertilizer types on cassava yield

Our subgroup analyses by fertilizer types revealed significant differences in the effectiveness of various fertilizer types on cassava yield, as reflected by their distinct effect size. Micronutrients demonstrated the highest effect size, followed by macronutrients and organic fertilizers, showing the lowest effect (Table 2).

Micronutrients. Fertilization with micronutrients showed a notably greater positive influence on cassava yield compared to macronutrients and organic fertilizers. However, this finding should be interpreted cautiously as it was based on a single study on Manganese with relatively few treatments ($N = 5$) and samples ($n = 20$), whereas macronutrient data were derived from six studies with substantially more treatments ($n = 55$) and samples ($n = 356$). The limited data for micronutrients might have influenced the magnitude of the observed effect.

Despite the limited sample size in our meta-analysis, emerging research supports the potential of micronutrient fertilization for substantial yield improvements. Specifically, manganese fertilization through foliar spraying or treating stem cuttings with manganese solutions before planting effectively increased fresh root yield, shoot yield, and the number of roots by 516%, 227%, and 319% respectively, compared to control treatments (Marchi et al., 2020). These findings suggest that micronutrient deficiencies, particularly manganese, may be significant but underrecognized constraints to cassava productivity, especially in intensively cultivated areas where soil micronutrient depletion or limited bioavailability is more likely to occur (Howeler, 2001; Marchi et al., 2020).

Macronutrients. Chemical fertilizers containing macronutrients (both NPK combinations and individual nutrients) demonstrated a greater positive influence on cassava yield compared to organic fertilizers. This superior performance can be attributed to the precise nutrient composition of chemical fertilizers. Commercial fertilizers contain exact ratios of nutrients, typically expressed as percentages of N, P, and K, allowing farmers to supply just the right amounts needed by cassava plants. Additionally, these fertilizers are sold in dry form, maximizing their nutrient concentration while minimizing water content, which enhances their effectiveness (Howeler & Maung Aye, 2014).

Multi-location trials across Africa and Asia consistently reported significant yield gains with NPK application, with increases ranging depending on application rates (Carsky & Toukourou, 2005; Kaweewong et al., 2013; Aliyu et al., 2019). Nitrogen fertilizer enhances overall plant growth, increases the efficiency of photosynthesis, and boosts the leaf area index (LAI), leading to higher yields, with fresh root yields (Kaweewong et al., 2013).

Phosphorus is often a limiting nutrient in savanna soils, and its improved acquisition is crucial for increasing crop yields (Aliyu et al., 2019). Withholding phosphorus from a complete fertilizer regime resulted in significant yield reductions (Carsky & Toukourou, 2005). In low phosphorus conditions, co-application of phosphorus fertilizer with arbuscular mycorrhizal fungal (AMF) inoculants can reduce phosphorus fertilizer requirements while maintaining statistically similar root fresh yields to full phosphorus application (Aliyu et al., 2019).

Potassium deficiency is often the main limiting factor when cassava is grown continuously without potassium fertilizer, with withholding potassium leading to significant yield reductions (Howeler, 2001; Carsky & Toukourou, 2005). This wide range in response rates underscores the importance of site-specific nutrient management, as the magnitude of yield response depends heavily on initial soil fertility status and the specific nutrients limiting production in each location.

Organics. In contrast, organic fertilizers showed the lowest effect size with a confidence interval that included zero (– 0.04, 0.57), suggesting their impact might not be statistically significant in some contexts. Several factors can explain this limited effectiveness. According to Howeler & Maung Aye (2014), while manure provides valuable secondary nutrients and improves soil structure and water-holding capacity, it contains relatively small amounts of the macronutrients (N, P, K) that crops need in larger quantities. Furthermore, the nutrient composition of organic fertilizers cannot be tailored to the specific requirements of cassava and varies considerably depending on their source, animal feed, and storage methods. This variability likely contributed to their less consistent performance compared to chemical fertilizers in enhancing cassava yield.

However, it is important to note that organic fertilizers provide benefits beyond immediate yield increases. Research indicates that organic amendments such as poultry or cattle manure and compost improve soil organic carbon content and contribute to long-term soil health maintenance (Cadavid et al., 1998; Odedina et al., 2012; Pypers et al., 2012). Single applications of organic manure significantly increased soil Na, K, Mg, and CEC, available P, Zn, and organic matter compared to control treatments (Odedina et al., 2012). The addition of organic and organo-mineral fertilizers increased cassava tuber weight and biomass production (Odedina et al., 2012).

While their immediate effect on cassava yield may be lower than that of chemical fertilizers, organic inputs play a crucial role in sustainable production systems by enhancing soil physical and biological properties over time. Mulch applications significantly reduced soil temperatures, increased soil organic carbon, and improved levels of K, P, Ca, and Mg in the soil while maintaining soil pH near its initial value (Cadavid et al., 1998).

Relationship between soil texture and fertilizer efficiency

Soil texture plays a fundamental role in determining fertilizer efficiency for cassava cultivation, with different soil types exhibiting markedly distinct responses to nutrient applications. The subgroup analyses revealed striking variations in fertilizer responsiveness across soil textures, with silt loam demonstrating an exceptionally high fertilizer response, substantially exceeding the responses observed in clay loam, loamy sand, clay, and sandy loam soils (Table 2). This remarkable variation underscores the critical importance of soil physical properties in governing fertilizer use efficiency for cassava production. The differential responses across soil textures can be attributed to three interconnected mechanisms (physical, chemical, and biological processes) that collectively influence nutrient availability and plant uptake.

Physical properties and nutrient retention. Soil texture directly affects pore size distribution, water retention, and drainage characteristics, which in turn influence nutrient mobility and accessibility (Chaem-Ngern et al., 2020; Xie et al., 2020). Silt loam soils, with silt as the dominant component, possess an optimal balance of small pores that effectively retain water and nutrients while maintaining adequate drainage and aeration for root development (Wang et al., 2022). This dual advantage enables silt loam to combine the benefits of both fine and coarse-textured soils. Cassava performs optimally in well-structured, loose soils that promote oxygen availability, prevent root rot, and enhance overall productivity (Fasinmirin & Reichert, 2011). In contrast, sandy and loamy sand soils, characterized by low cation exchange capacity (CEC) and poor nutrient retention capacity, experience significant leaching losses of applied fertilizers, particularly potassium (K) and nitrogen (N), resulting in reduced fertilizer use efficiency and lower cassava yields compared to finer-textured soils (Chaem-Ngern et al., 2020; Xie et al., 2020).

Chemical properties and cation exchange. The chemical composition of soil texture classes fundamentally determines their capacity to retain and supply nutrients to plants. Silt loam soils benefit from moderate clay and organic matter content, which confers high cation exchange capacity, ensuring that applied NPK fertilizers remain plant-available rather than being lost through leaching processes (Wang et al., 2022). The superior nutrient retention in finer-textured soils such as sandy clay loam and loam enables more effective utilization of fertilizer inputs compared to coarse-textured soils (Pongsivapai et al., 2016; Xie et al., 2020). Conversely, heavy clay soils, while possessing high nutrient retention capacity, may hold water too tightly and impede root penetration or restrict oxygen supply, potentially limiting nutrient uptake efficiency (Fasinmirin & Reichert, 2011).

Biological interactions and root development. Well-structured loam soils create favorable conditions for vigorous root system development and support beneficial symbiotic relationships with microorganisms, particularly mycorrhizal fungi, which enhance nutrient uptake capacity (Wang et al., 2022). The biological activity in these soils further contributes to nutrient cycling and availability. In contrast, coarse sandy soils not only allow rapid nutrient leaching but also provide less favorable conditions for beneficial microbial associations, further reducing fertilizer efficiency.

This comprehensive understanding of soil texture-fertilizer interactions provides a foundation for developing site-specific nutrient management strategies that optimize both fertilizer efficiency and cassava productivity while considering the inherent limitations and advantages of different soil types.

Regional variation in fertilizer response

Geographical and environmental differences between planting regions significantly impact the efficiency of fertilizer use in increasing cassava yields. The subgroup analyses revealed notable disparities in the effectiveness of fertilizer application on cassava yield. The strongest effect was observed in South America, followed by Southeast Asia, with Africa showing a relatively lower effect size. Despite these differences, heterogeneity remained minimal, indicating consistent responses within each region (Table 2). These differences were likely due to contrasting soil fertility levels, dominant nutrient limitations, and management practices across regions.

In South America, cassava was primarily cultivated on acidic and nutrient-depleted soils such as Ultisols, Alfisols, and Oxisols, which were often severely deficient in phosphorus (Pellet & El-Sharkawy, 1993; Howeler, 2012). This marked nutrient limitation likely contributed to the high responsiveness of cassava to fertilization in this region, particularly when phosphorus was applied. Moreover, cassava was commonly integrated into mixed farming systems when fertilizer use may be prioritized when resources were available, further enhancing the observed effect size. Despite cassava's adaptability to marginal soils, studies suggested that without external inputs, yield remained suboptimal, which created a greater relative gain when fertilizers were introduced (Henry & Hershey, 2001; Howeler, 2012)

In Southeast Asia, the soils, mainly Ultisols, Inceptisols, and Alfisols, were relatively more fertile compared to South America, and phosphorus deficiency was less widespread (Howeler, 2012). Nevertheless, cassava showed a strong yield response to nitrogen and potassium in this region, especially in intensively cultivated areas of China and Vietnam (Howeler, 2012). The higher effect size in Southeast Asia can be attributed to regionally targeted fertilizer regimes that address specific nutrient demands, coupled with more developed infrastructure and extension services that support the adoption of fertilizers.

Conversely, in Africa, particularly in West Africa, cassava was grown across diverse soil types with significant variability in fertility. Continuous cultivation without adequate replenishment had led to widespread potassium deficiency, which was considered the primary limiting nutrient in many cassava-growing areas (Howeler, 2012; Ezui et al., 2016). Despite the observed deficiency, the effect size of fertilization in Africa was the lowest among the regions. The lowest effect size might reflect suboptimal fertilizer application rates, limited access to appropriate nutrient formulations, and economic constraints faced by smallholder farmers, which reduced the effectiveness of fertilizer use in practice (Fermont et al., 2009; Howeler, 2012; Ezui et al., 2016).

Additionally, Africa accounted for the majority of included studies (48 out of 67 treatments), which may introduce a distributional bias in the overall effect size, as underperformance in this region can disproportionately influence the pooled average. In contrast, fewer studies from South America and Southeast Asia, despite showing higher responsiveness, may not fully capture the potential of well-managed fertilization practice in those contexts.

Geographical conditions may indeed affect cassava yield through several combined factors. However, the large effect size observed in South America may not definitively demonstrate that this region has superior fertilizer response compared to the other regions, given that the effect size is derived from a limited number of studies. However, South America continues to represent a region where cassava demonstrates substantial responsiveness to fertilization interventions, likely due to the specific soil-plant-environment interactions that have evolved in these acidic, nutrient-depleted soils.

CONCLUSION

This systematic review and meta-analysis indicated that research on cassava production has predominantly focused on nutrient management interventions to improve yields. The aggregated evidence suggests that fertilizer application provides only modest overall yield gains, with minimal effect sizes for organic inputs. By contrast, inorganic fertilizers, especially those supplying phosphorus, tended to have clearer positive impacts on cassava yields. However, these yield responses varied markedly across soil types and regions, implying that local soil fertility and environmental conditions strongly modulate fertilization outcomes.

A critical limitation of this study is that only seven studies met our inclusion criteria for meta-analysis. This small sample size reflects both the scarcity of standardized cassava fertilization research and our rigorous selection requirements for cross-study comparison. Consequently, our findings should be interpreted with appropriate caution, particularly when extrapolating to regions or conditions underrepresented in the available literature. While our robust methodological approach helps ensure the reliability of our conclusions, the limited evidence base inherently constrains the statistical power and generalizability of our results.

This meta-analysis identified a major obstacle in the lack of standardized statistical reporting in agricultural studies. Few studies reported complete statistical details (means, standard deviations, and sample sizes), hindering robust cross-study comparisons and the ability to conduct a fully comprehensive meta-analysis. Despite the observed benefits of targeted fertilization, particularly phosphorus supplementation, the evidence base remains constrained by inconsistent data reporting and context-dependent results. To address these issues, we recommend that future research adopt standardized statistical reporting practices and explore region-specific fertilizer management approaches. Such improvements would enhance data synthesis and guide more effective fertilization recommendations tailored to local conditions in cassava production.

ACKNOWLEDGEMENTS. We would like to thank the Biodiversity, Ecology, and Evolution research (BEER) Lab at the Department of Botany, Kasetsart University, for supporting facilities and research space.

REFERENCES

Aliyu, I.A., Yusuf, A.A., Uyovbisere, E.O., Masso, C. & Sanders, I.R. 2019. Effect of co-application of phosphorus fertilizer and in vitro-produced mycorrhizal fungal inoculants on yield and leaf nutrient concentration of cassava. PLoS One **14**, e0218969.

Cadavid, L.F., El-Sharkawy, M.A., Acosta, A. & Sánchez, T. 1998. Long-term effects of mulch, fertilization and tillage on cassava grown in sandy soils in northern Colombia. *Field Crops Res* **57**, 45–56. https://doi.org/10.1016/S0378-4290(97)00114-7

Carsky, R.J. & Toukourou, M.A. 2005. Identification of nutrients limiting cassava yield maintenance on a sedimentary soil in southern Benin, West Africa. *Nutr Cycl Agroecosyst* **71**, 151–162. https://doi.org/10.1007/s10705-004-1803-9

Chaem-Ngern, C., Anusontpornperm, S., Thanachit, S. & Kheoruenromne, I. 2020. Response of Cassava, Huay Bong 80 Variety, Grown in an Ustic Quartzipsamment, to Chicken Manure and Potassium Fertilizer. *Commun Soil Sci Plant Anal* **51**, 2765–2777. https://doi.org/10.1080/00103624.2020.1849260

Challinor, A.J., Watson, J., Lobell, D.B., Howden, S.M., Smith, D.R. & Chhetri, N. 2014. A meta-analysis of crop yield under climate change and adaptation. *Nat Clim Chang* **4**, 287–291. https://doi.org/10.1038/nclimate2153

Chua, M.F., Youbee, L., Oudthachit, S., Khanthavong, P., Veneklaas, E.J. & Malik, A.I. 2020. Potassium Fertilisation Is Required to Sustain Cassava Yield and Soil Fertility. *Agronomy* **10**, 1103. https://doi.org/10.3390/agronomy10081103

Copes, W.E. & Ojiambo, P.S. 2021. Efficacy of Hypochlorite in Disinfesting Nonfungal Plant Pathogens in Agricultural and Horticultural Plant Production: A Meta-Analysis. *Plant Dis* **105**, 4084–4094. https://doi.org/10.1094/PDIS-09-20-2046-RE

de Ponti, T., Rijk, B. & van Ittersum, M.K. 2012. The crop yield gap between organic and conventional agriculture. *Agric Syst* **108**, 1–9. https://doi.org/10.1016/j.agsy.2011.12.004

Enesi, R.O., Hauser, S., Pypers, P., Kreye, C., Tariku, M. & Six, J. 2022. Understanding changes in cassava root dry matter yield by different planting dates, crop ages at harvest, fertilizer application and varieties. *European Journal of Agronomy* **133**, 126448. doi: 10.1016/j.eja.2021.126448

Ezui, K.S., Franke, A.C., Mando, A., Ahiabor, B.D.K., Tetteh, F.M., Sogbedji, J. & Janssen, B.H., Giller, K.E. 2016. Fertiliser requirements for balanced nutrition of cassava across eight locations in West Africa. *Field Crops Res* **185**, 69–78. doi: 10.1016/j.fcr.2015.10.005

FAOSTAT, 2023. Crops and livestock products [WWW Document]. URL https://www.fao.org/faostat/en/#data/QCL (accessed 5.21.23).

Fasinmirin, J.T. & Reichert, J.M. 2011. Conservation tillage for cassava (*Manihot esculenta* crantz) production in the tropics. *Soil Tillage Res* **113**, 1–10. doi: 10.1016/j.still.2011.01.008

Fermont, A.M., van Asten, P.J.A., Tittonell, P., van Wijk, M.T. & Giller, K.E. 2009. Closing the cassava yield gap: An analysis from smallholder farms in East Africa. *Field Crops Res* **112**, 24–36. https://doi.org/10.1016/j.fcr.2009.01.009

Hedges, L.V. 1981. Distribution Theory for Glass's Estimator of Effect size and Related Estimators. *Journal of Educational Statistics* **6**, 107–128. doi: 10.3102/10769986006002107

Henry, G. & Hershey, C. 2001. Cassava in South America and the Caribbean. In *Cassava: Biology, Production and Utilization*. CABI Publishing, UK, 17–40. doi: 10.1079/9780851995243.0017

Howeler, R. 2014. *Sustainable soil and crop management of cassava in Asia: a reference manual*. CIAT Publication No. 389. Cali, CO: Centro Internacional de Agricultura Tropical (CIAT), 280 pp.

Howeler, R. 2012. Short-and long-term N, P and K requirements of cassava. In Howeler, R. (ed.), *The Cassava Handbook: A Reference Manual Based on the Asian Regional Cassava Training Course, Held in Thailand*. Centro Internacional de Agricultura Tropical (CIAT), Bangkok, pp. 429–545.

Howeler, R. & Maung Aye, T. 2014. *Sustainable management of cassava in Asia: from research to practice*. International Center for Tropical Agriculture (CIAT), The Nippon Foundation, Vietnam, 168 pp.

Howeler, R.H. 2001. Cassava mineral nutrition and fertilization. In *Cassava: Biology, Production and Utilization*. CABI Publishing, UK, 115–147. doi: 10.1079/9780851995243.0115

Howeler, R.H. 1991. Long-term effect of cassava cultivation on soil productivity. Field Crops Res **26**, 1–18. https://doi.org/10.1016/0378-4290(91)90053-X

IAEA, 2018. Cassava production guidelines for food security and adaptation to climate change in Asia and Africa. International Atomic Energy Agency, Vienna.

Ikeh, A.O., Ndaeyo, N.U. & Ikeh, C.E. 2023. Effects of integrated fertilization on soil sustainability and cassava (*Manihot esculenta* Crantz) yield in an ultisol. Journal of Current Opinion in Crop Science **4**, 89–102. https://doi.org/10.62773/jcocs.v4i2.197

Katuromunda, S., Ekwaro, B. & Wanaku, B. 2021. Yield Performance of Newly Developed Cassava Varieties in Response to Inorganic Fertilizers. *Mod Appl Sci* **15**, 60. https://doi.org/10.5539/mas.v15n4p60

Kaweewong, J., Kongkieaw, T., Tawornprek, S., Yampracha, S. & Yost, R. 2013. Nitrogen requirements of cassava in selected soils of Thailand. *Journal of Agriculture and Rural Development in the Tropics and Subtropics* **144**, 13–19.

Koricheva, J., Gurevitch, J. & Mengersen, K. 2013. *Handbook of meta-analysis in ecology and evolution*. Princeton University Press.

Marchi, G., Fialho, J. de F., Rein, T.A., Santos Junior, J. de D.G. dos, Vieira, E.A., Sousa-Silva, J.C., Malaquias, J.V. & Silva, D.R.G. 2020. Manganese fertilization for sweet cassava production under organic management system. *Pesqui Agropecu Trop* **50**. https://doi.org/10.1590/1983-40632020v5066133

Nassy, M.L.M., Hauser, S., Egwekhide, M., Batawila, K., Kulakow, P. & Abberton, M. 2020. Leaf and roots yields responses of three improved cassava (*Manihot esculenta* Crantz) varieties to organo-mineral fertilizers and leaf harvest in the South-West Nigeria. *Int J Biol Chem Sci* **14**, 1432–1447. https://doi.org/10.4314/ijbcs.v14i4.21

Odedina, J., Ojeniyi, S. & Odedina, S. 2012. Integrated nutrient management for sustainable cassava production in South Western Nigeria. *Arch Agron Soil Sci* **58**, 132–140. https://doi.org/10.1080/03650340.2012.695865

Okoth Omondi, J. & Yermiyahu, U. 2021. Improvement in Cassava Yield per Area by Fertilizer Application, In *Cassava - Biology, Production, and Use*. IntechOpen. https://doi.org/10.5772/intechopen.97366

Pellet, D. & El-Sharkawy, M.A. 1993. Cassava varietal response to phosphorus fertilization. I. Yield, biomass and gas exchange. *Field Crops Res* **35**, 1–11. doi: 10.1016/0378-4290(93)90131-6

Pimentel, M.L., Reis, I.M.S., Castro, J.S. de, Portela, V.S., Romano, M.L.P.C., Vildoso, C.I.A., Gasparin, E. & Sia, E.F. de. 2021. Cassava yield indicators and total organic carbon in tropical soils under different fertilization treatments. *Aust J Crop Sci.* 1325–1331. https://doi.org/10.21475/ajcs.21.15.10.p3291

Pittelkow, C.M., Liang, X., Linquist, B.A., van Groenigen, K.J., Lee, J., Lundy, M.E., van Gestel, N., Six, J., Venterea, R.T. & van Kessel, C. 2015. Productivity limits and potentials of the principles of conservation agriculture. *Nature* **517**, 365–368. doi: 10.1038/nature13809

Pongsivapai, P., Thongjoo, C., Romkaew, J. & Inboonchuay, T. 2016. Effect of Fertilizer Management in Combination with Soil Conditioner on Yield of Cassava Cultivated on Coarse-Textured Soil in Thailand. *Mod Appl Sci* **10**, 239. doi: 10.5539/mas.v10n11p239

Pypers, P., Bimponda, W., Lodi-Lama, J., Lele, B., Mulumba, R., Kachaka, C., Boeckx, P., Merckx, R. & Vanlauwe, B. 2012. Combining Mineral Fertilizer and Green Manure for Increased, Profitable Cassava Production. *Agron J* **104**, 178–187. doi: 10.2134/agronj2011.0219

Senkoro, C.J., Tetteh, F.M., Kibunja, C.N., Ndungu-Magiroi, K.W., Quansah, G.W., Marandu, A.E., Ley, G.J., Mwangi, T.J. & Wortmann, C.S. 2018. Cassava Yield and Economic Response to Fertilizer in Tanzania, Kenya and Ghana. *Agron J* **110**, 1600–1606. https://doi.org/10.2134/agronj2018.01.0019

Sinta, Z. & Dansa, Y. 2023. Yield and quality response of cassava (*Manihot esculenta* Crantz) to nitrogen and potassium fertilizer rates at Arba Minch, Southern Ethiopia. *J Plant Nutr* **46**, 3557–3568. https://doi.org/10.1080/01904167.2023.2209109

Tuck, S.L., Winqvist, C., Mota, F., Ahnström, J., Turnbull, L.A. & Bengtsson, J. 2014. Land-use intensity and the effects of organic farming on biodiversity: a hierarchical meta-analysis. *Journal of Applied Ecology* **51**, 746–755. https://doi.org/10.1111/1365-2664.12219

Tugwell, P. & Tovey, D. 2021. PRISMA 2020. *J Clin Epidemiol* **134**, 5–6. https://doi.org/10.1016/j.jclinepi.2021.04.008

Wallace, B.C., Small, K., Brodley, C.E., Lau, J. & Trikalinos, T.A. 2012. Deploying an interactive machine learning system in an evidence-based practice center. In *Proceedings of the 2nd ACM SIGHIT International Health Informatics Symposium*. ACM, New York, NY, USA, pp. 819–824. https://doi.org/10.1145/2110363.2110464

Wang, L., He, Z., Zhao, W., Wang, C. & Ma, D. 2022. Fine Soil Texture Is Conducive to Crop Productivity and Nitrogen Retention in Irrigated Cropland in a Desert-Oasis Ecotone, Northwest China. *Agronomy* **12**, 1509. https://doi.org/10.3390/agronomy12071509

Wilson, H. & Ovid, A. 1994. Influence of fertilizers on cassava production under rainfed conditions. *J Plant Nutr* **17**, 1127–1135. https://doi.org/10.1080/01904169409364793

Xie, X., Machikowa, T. & Wonprasaid, S. 2020. Fertigation based on a nutrient balance model for cassava production in two different textured soils. *Plant Prod Sci* **23**, 407–416. https://doi.org/10.1080/1343943X.2020.1743189

Yabuta, S., Fukuta, T., Tamaru, S., Goto, K., Nakao, Y., Khanthavong, P., Ssenyonga, P. & Sakagami, J.I. 2021. The Productivity of Cassava (*Manihot esculenta* Crantz) in Kagoshima, Japan, Which Belongs to the Temperate Zone. *Agronomy* **11**, 2021. https://doi.org/10.3390/agronomy11102021

Agronomy Research **24**(S1), 74–95, 2026
https://doi.org/10.15159/AR.26.003

Effects of different spacing and polybag sizes on growth of oil palm (*Elaeis guineensis* Jacq.) seedlings in the main nursery

A.M. Afandi, A.S. Halimatul*, N.S. Amanina, Z.Z. Norliyana, O.A. Meilina, R. Mohd Shahrin, A.M. Nik Khairol and A.M.M. Hasnul

Malaysian Palm Oil Board, 6, Persiaran Institusi, Bandar Baru Bangi, MY43000 Kajang, Selangor, Malaysia
*Correspondence: halimatul.saadiah@mpob.gov.my

Received: July 28th, 2025; Accepted: December 21st, 2025; Published: January 12th, 2026

Abstract. The significance of regulating spacing and polybag size in the primary oil palm nursery lies in ensuring an optimal growth environment for uniform and healthy seedlings. However, current recommendations provide limited quantitative evidence on how reduced spacing and smaller polybags influence seedling performance, leaving gap in a practical nursery management guideline. Therefore, an experiment was carried out in the oil palm main nursery to evaluate different spacing design and polybag sizes up to 14 months after planting (MAP). The spacing arrangement of seedlings significantly affected their growth performance compared to polybag sizes. Spacing below 0.75 m produced tall and etiolated seedlings, with height increasingly by 19.60% at 8 MAP and up to 32.00%at 12 to 14 MAP, accompanied by excessively elongated rachis length which made them unsuitable for field planting and problematic for nursery handling. In contrast, using smaller polybag size of 30 cm × 38 cm (12" × 15") resulted in only minor growth differences compared to the standard polybag, with no negative effect on seedling performance or nutrient content up to 12 MAP. There are specific needs for optimum seedling performance unrestricted by growth competition, minimal risk of etiolation, good survival rate, easy nursery maintenance, and reduced maintenance costs for higher profits. Based on current research findings, seedlings considered appropriate for field planting at 10 to 12 MAP must meet some specific criteria; including a bole diameter ranging between 49 to 64 mm, a total frond production between 11 to 15 per seedling, rachis length of frond 3 between 58 to 93 cm, seedling height within the range of 118 to 179 cm, and a petiole cross-section between 1.48 to 2.10 cm^2. These findings support the importance of maintaining acceptable spacing while supporting the use of smaller polybags to reduce costs without compromising seedling quality.

Key words: oil palm nursery, oil palm seedling, polybag sizes, polybag spacing.

INTRODUCTION

Oil palm (*Elaeis guineensis* Jacq.) remains one of the world's most productive source of vegetable oil and vital commodity for the food, biofuel, and oleochemical industries. In Malaysia, a major producing country, the crop's economic contribution is substantial, with export earnings reaching RM 109.39 billion in 2024, highlighting its critical role in the national and global agricultural economy (Parveez et al., 2025). Oil palm's high oil yield per unit area makes it essential for meeting the growing global demand for fats and oils. Therefore, optimising its cultivation from the earliest nursery stages is crucial for maintaining productivity and supporting long-term industry competitiveness.

Oil palm nursery is the initiating link in the palm oil supply chain and the foundation for every successful oil palm plantation (Mutert et al., 1999; Mohd Rais, 2021). The production of superior and healthy oil palm seedlings has the potential for sustaining large oil yields for 25 years or more (Mutert et al., 1999; Mohd Rais, 2021). Good nursery management during seedling cultivation with proper planning and handling should be maintained at the highest standard to ensure healthy, vigorous, and uniform oil palm seedlings (Hassan et al., 2023). Furthermore, reducing the high rate of seedling mortality also keeps production costs low and increases profit (Mutert et al., 1999; Mohd Rais, 2021).

In 2007, MPOB introduced the MPOB Code of Practice (CoP) to emphasize the significance of high-quality planting materials and sound agricultural techniques in oil palm plantations (Bernama, 2017). This comprehensive Code outlines essential elements necessary for meeting the requirements of various activities and ensuring compliance with standards to meet user needs. The CoP comprises seven distinct guidelines tailored to different stages along the palm oil supply chain, including nurseries, estates, smallholders, mills, refineries, and bulking installations for handling palm and palm kernel oil. Notably, the Code of Good Nursery Practice for Oil Palm Nurseries (CoPN) was specifically introduced in July 2012 to address nursery-related practices (Ahmad et al., 2022). The CoPN provides guidelines that cover the aspects of growing oil palm planting materials in the nursery, from the point of germinated seeds or ramets received, until they are ready for field planting (MPOB, 2016; Mohd Rais, 2021).

The importance of polybag spacing and size at the main nursery of oil palm often depends on facilitating optimal growth conditions for seedlings. Proper spacing minimizes light competition between palms, allows for easy access for maintenance tasks such as weeding and manuring, and ensures uniform growth (Mutert et al., 1999; Laksono et al., 2019). The recommended polybag spacing changes according to the age of seedlings at field planting, with different triangular spacing values for various age ranges. The CoPN clearly stated that the polybag used shall be a perforated black polythene bag with 500 gauges (0.125 mm) of thickness and size shall not be less than 38 cm × 45 cm (15" × 18") (MPOB, 2016; Mohd Rais, 2021). A smaller polybag measuring less than 30 cm × 38 cm (12" × 15") may be used for seedlings or ramets that are kept in the polybag not more than 11 months after the sowing germinated seeds or ramets (MPOB, 2016).

Appropriate arrangement of polybags is highly determined by the size of polybag used. Polybag size of 38 cm × 45 cm (15" × 18") shall be arranged in not less than 0.9 m × 0.9 m × 0.9 m measured center to center to achieve an equilateral triangular spacing (MPOB, 2016; Mohd Rais, 2021). For the same objective, polybag size of 30 cm × 38 cm (12" × 15"), shall be arranged at not less than 0.75 m × 0.75 m × 0.75 m measured center to center and these two-design allowed approximately 14,000 and 20,000 seedlings per hectare, respectively (MPOB, 2016; Mohd Rais, 2021). Previous studies have shown that the growth of seedlings aged between 10 and 12 months in the main nursery showed satisfactory growth and in return, produces the highest fresh fruit bunch FFB in the field (Afandi, 2011; Afandi et al., 2019).

An experiment was conducted by Akpo et al. (2014b) to evaluate the effects of polybag sizes (small; 25 cm × 30 cm, medium; 31 cm × 31 cm and large; 40 cm × 40 cm), substrate type (forest soil, household waste substrate, arable soil and arable soil with manure) and fertilizer supply (no fertilization, split dose and full dose) on seedlings (Akpo et al., 2014b). Although substrate and fertiliser supply impacts were largely consistent over time (Fang et al., 2022), the effects of polybag size increased, eventually outpacing substrate, fertilizer, and the interaction effects approximately two months onwards. The number of leaves increased linearly with time, the height and collar diameter of seedlings increased exponentially. Data analysis with different growth models showed that polybag size had the most significant impact on seedling growth rates, followed by the substrate (Akpo et al., 2014b; Salisu et al., 2018). However, most previous studies evaluated polybag size independently or under experimental conditions that differ from current large-scale nursery operations, limiting their direct applicability to present nursery management.

Polybag size has a profound effect on oil palm seedling growth (Poorter et al., 2012; Salisu et al., 2018). In small polybags, applying 10 g of fertilizer once each month had fatal consequences on seedling's survival. Medium polybags filled with arable soil and animal manure, without any fertilizer, promoted good seedling development. This method seemed to be the best balance between quality and production cost, although large polybags produced the best seedlings. The interaction of the three factors (bag size, substrate and fertilizer) was not significant for seedling allometric variables (seedling height, leaf number, most developed leaf length and root-collar diameter) (Akpo et al. 2014a).

Observation comparison of DxP planting material (PM) under normal nursery practices between a previous study by Afandi (2011) and the current study showed that there was an improvement in the quality of oil palm seedlings over time (Afandi, 2011). Therefore, it is possibility that smaller polybag sizes and closer arrangements of polybags may be considered for use in the main nursery. The production of high-quality seedlings during the main nursery stage is crucial for ensuring growth, successful field establishment, and long-term yield potential (Siti Atikah et al., 2019). These seedlings are more capable of withstanding transplanting stress and maintaining vigorous growth under filed conditions. The use of closer spacing might optimize the available space without compromising seedlings allowing higher plant density and better land use efficiency, compared to the conventional spacing (Applied Agricultural Resources Sdn Bhd., 2020). Understanding the influence of these factors on early seedling growth is crucial for improving nursery productivity.

This study was conducted to determine the effects of different seedling spacings and polybags sizes on the growth performance, dry matter production, and overall vigour of oil palm seedling at the main nursery stage. By quantifying these key growth responses, the study aims to identify the most efficient spacing arrangement and polybag size that support healthy seedling development and can contribute to improvements in current nursery practices. The results presented in this work may provide a new perspective on standard nursery practices, thereby strengthening the MPOB CoP 1001: 2015 – Code of Good Nursery Practice for Oil Palm Nurseries (Second edition) (MPOB, 2016).

Previous studies have investigated the effects of polybag size, substrate type, and fertilisation on oil palm seedling growth (Afandi, 2011; Poorter t al., 2012; Akpo et al., 2014a, 2014b; Salisu et al., 2018). While polybag size consistently influenced seedling height, collar diameter, and leaf development, most studies were conducted under small-scale or experimental conditions, limiting their applicability to contemporary large-scale nursery practices. Additionally, interactions between polybag size and spacing have not been reassessed under latest operational standards, leaving a gap in optimizing land use efficiency and seedling quality.

MATERIALS AND METHODS

Study site

The trial was carried out at Tapak Semaian Hong Seng Sdn. Bhd., Jalan Muar, Yong Peng, Johor. Inland mineral topsoil was used as the growing medium, following standard practice in main nurseries (Gillbanks, 2003). The soil was sieved through a 5 mm mesh to remove stones, large clods (> 1 cm), and other debris before being filled into large polybags and lined up in a triangular pattern. Uniform three-month-old seedlings were selected from pre-nursery before transferring into the polybags (Keni et al., 2023). Seedling maintenance followed standard practices recommended by the MPOB (MPOB, 2016). Throughout the study, seedlings were watered twice daily with approximately 500 mL of water per seedling using the overhead sprinkler irrigation. Sprinklers are commonly used in nurseries to maintain soil moisture, a critical factor in effective crop irrigation management (Jobbágy et al., 2016). The seedling treatments plots were arranged symmetrically at each sprinkler point to ensure same amount of daily watering (Figs 1–2). Fertilisation was carried out monthly using a balanced NPK compound fertilizer at rates recommended for main nursery. Pest and disease monitoring was performed weekly. Any infestations were managed using approved nursery level measures.

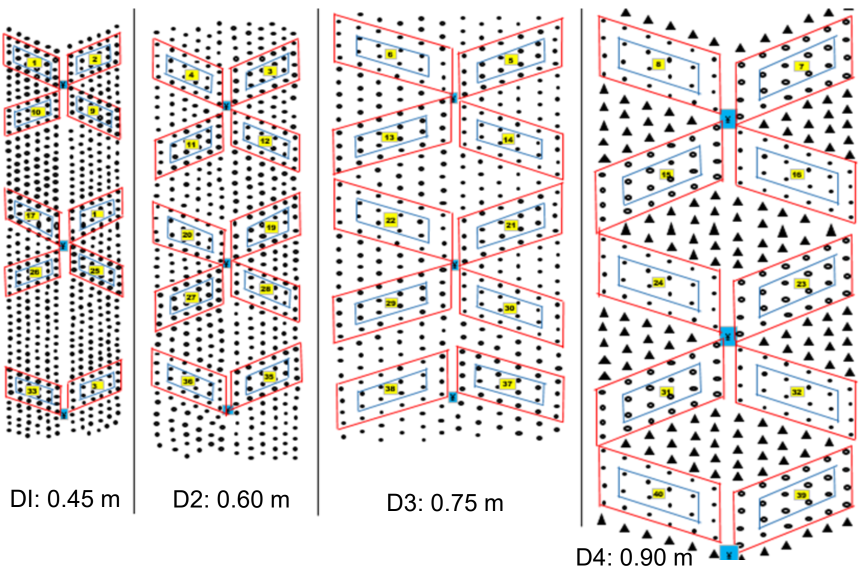

Figure 1. Plot arrangement at the main nursery with seedlings plots arranged symmetrically on each sprinkler point.

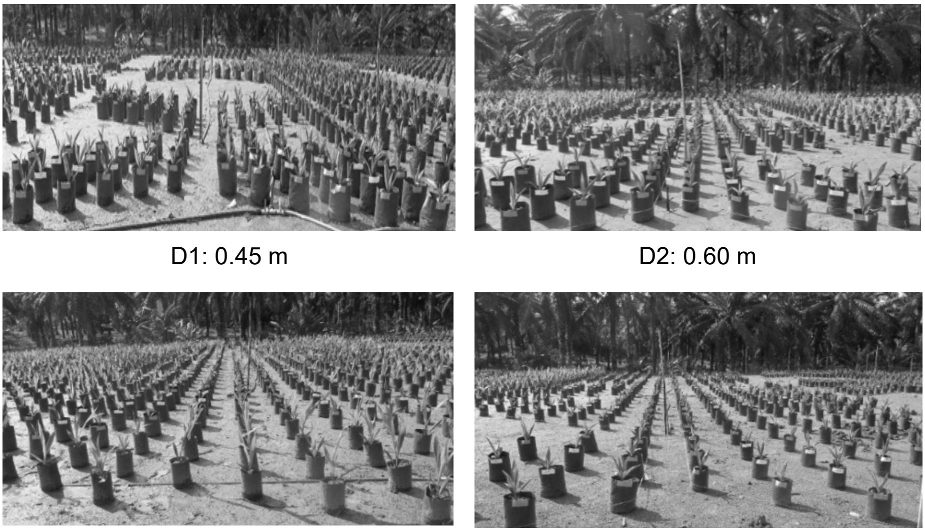

Figure 2. An overview of the arrangement of seedlings in triangular polybag spacing at trial site.

Experimental details

Commercial DxP materials of *Elaeis guineensis* Jacq were used for this trial. The experiment was conducted using a randomized complete block design (RCBD) with five replications to minimize environmental variation within the nursery. Blocking was based on uniformity of light exposure and slope direction across the nursery area to control for potential micro-environmental effects. Each treatment combination was randomly assigned within each block to ensure unbiased placement.

Treatments followed a 4×2 factorial structure, consisting of four polybags spacing (D1, D2, D3, and D4) arranged in a triangular planting pattern and two polybag sizes (S1 and S2), as shown in Table 1. Each experimental plot contained eight recording seedlings per treatment per replicate, resulting in a total of 320 seedlings (4 spacing × 2 sizes × 5 replicates × 8 seedlings). The study duration was 14 months. Growth performance of oil palm seedlings was evaluated based on fresh weight of plant and media, vegetative growth parameters, nutrient content, dry matter production, and field observation.

Table 1. Treatments on polybag spacing and size

Treatment	Polybag spacing and size
	Polybag spacing (Triangular polybag spacing) (D)
D1	0.45 m × 0.45 m × 0.45 m
D2	0.60 m × 0.60 m × 0.60 m
D3	0.75 m × 0.75 m × 0.75 m
D4	0.90 m × 0.90 m × 0.90 m
	Polybag size (S)
S1	38 cm × 45 cm (15" × 18")
S2	30 cm × 38 cm (12" × 15")

Note: D4 and S1 are the current standard practices for the main nursery for up to 12 months while D3 and S2 was up to 11 months (MPOB, 2016).

The selected spacing distances (0.45 m, 0.90 m) and polybag sizes (30 × 38 cm, 38 × 45 cm) were chosen to create a gradient from restrictive to optimal growth conditions, reflecting common commercial nursery practices. Spacing directly affects light interception and competition, influencing seedling architecture and the risk of etiolation (Corley & Tinker, 2016; Oomen, 2023). Similarly, polybag size constrains root development, nutrient uptake, and biomass accumulation, with smaller volumes known to limit later growth stages (Poorter et al., 2012; Afandi, 2011). This combination provides a scientifically supported range to evaluate their combined effects on oil palm seedling performance.

Fresh weight of seedling and soil media

The fresh weight of seedling and soil media was determined at the age of 14 MAP for standard density (D4) only to evaluate the differences in weight for ease in handling during seedling transfer from nursery to field planting.

Vegetative growth measurements

Total green fronds (frond seedling^{-1}), frond length (cm), palm height (cm), bole diameter (mm) and petiole cross-section of frond 2 (PCS, cm^2) were taken at 8 months, 10 months, 12 and 14 months from planting (MAP) as described by Zuraidah et al. (2017). The fresh weight of seedlings and media were determined at the ages of 10, 12 and 14 MAP to evaluate the differences in weight for ease of handling during seedling transfer from nursery to field planting. Plant growth analysis, involving destructive sampling of four plants per treatment was carried out at 10, 12, and 14 MAP. The oil palm seedlings were separated into rachis, leaflets, bole, and roots. To accelerate the drying process, samples were cut into smaller pieces, and dried at 60 °C for 48 hours, until constant weight was achieved, before being weighed for dry weight determination (Militello et al., 2018).

Foliar analysis

The interpretation of the changes in the chemical composition of leaves was carried out to analyze the content of Nitrogen (N), Phosphorus (P), Potassium (K), Calcium (Ca) and Magnesium (Mg). Dried samples of rachis, leaflets, roots, and stems were dried and ground. Approximately 1 g of oven-dried plant tissue sample was weighed, placed into a silica basin and subsequently heated at 500 °C in a muffle furnace for 4 hours. The sample was then mixed with 10 mL of 20% nitric acid, covered with a watch glass and digested in a steam bath for 1 hour. Once the digestion process was completed, the sample was filtered through an Albert 502 filter paper into a 100 mL volumetric flask. Then, Ca and Mg were determined using an atomic absorption spectrophotometer (Perkin Elmer 3100, USA). Phosphorus was determined colourimetrically with a spectrophotometer (Genesys 20, USA) using the vanadomolybdate yellow method. Plant K content was determined by a flame photometer (Sherwood 410, UK). In contrast, plant N content was determined by wet digestion using concentrated H_2SO_4 in the presence of a catalyst to convert the organic N to the ammonium form. The solution releases free ammonia following NaOH alkaline distillation. The distillate was collected in boric acid and diluted with HCl and with a mixed indicator (pH 4.5) and NH4 determined by titration until the red colour was obtained.

Analysis of data

All data were analysed using SAS statistical software (version 9.4; SAS Institute Inc., Cary, NC, USA) to evaluate the effects of polybag spacing (D1-D4), polybag size (S1-S2), and their interaction on the growth performance of seedlings. The experiment followed a RCBD with five replicates. Prior to analysis, the data were tested for normality using the Shapiro-Wik test and for homogeneity of variances using Levene's test. All data were subjected to analysis of variance (ANOVA). When significant differences were detected, treatment means were compared using Duncan's Multiple Range Test (DMRT) at a 5% probability level ($P \leq 0.05$). The seedling growth performance was established with a coefficient of variation (CV) value that was adopted in research for data analysis: (1) CV value less than 7.0% would be rated as high precision; (2) value between 7.0 and 19.0% would be moderate precision; (3) value greater than 19.0% but below 25.0% would be regarded as low accuracy; and (4) value greater than 25.0% shows very low accuracy (Couto et al., 2013). Results are presented as mean ± standard error (SE).

RESULTS AND DISCUSSION

The relationship between the polybag sizes and fresh weight of oil palm seedling

The fresh weight of the seedling and the soil media is shown in Table 2. The average total fresh weight measurements, including roots and soil media, at 10 to 14 MAP were 22.99 kg (S1) and 12.23 kg per seedling (S2), respectively, with a percentage weight difference of up to 46.82%. This disparity is attributed to unrestricted growth, particularly in the root section, as observed by Poorter et al. (2012). Additionally, the S1 and S2 polybags had average soil weights of 19.95 kg and 9.51 kg, respectively, resulting in a 52.32% difference in fresh soil weight between the two.

The use of different sizes of polybags not only affected the fresh weight of seedlings but also impacts the weight of the soil media, consequently influencing the workload during seedling transfer. The lightweight soil in 30 cm × 38 cm polybags facilitates easier handling and transport of seedlings, minimizing the workload during their transfer from the nursery to the planting site in the field, as suggested by Hashim et al. (1987). The utilization of smaller polybag volumes significantly enhances nursery efficiency and economic viability by reducing labour and time requirements. Studies by Adu-Yeboah et al. (2015) and Gebisa (2024) demonstrate that smaller or medium-sized polybag allowmore seedlings to be transported per trip and lower input use, thereby substantially lowering logistic overhead for large-scale distribution. These findings indicate that reducing polybag size can enhance operational efficiency and nursery management without compromising seedling quality.

Table 2. Average fresh weight of seedling and soil media for standard density at 14 months after planting

Polybag size	Total fresh weight of seedling (kg)	Weight of soil media, (kg)	Total fresh weight of seedling and soil media (kg)
SI	3.04	19.95	22.99
S2	2.72	9.51	12.23

Note: S1 = 15" × 18" (38.10 cm × 45.72 cm); S2 = 12" × 15" (30.48 cm × 38.10 cm).

Vegetative characteristics of seedlings

The ANOVA tables of the vegetative growth components of DxP seedlings at ages 8, 10, 12 and 14 MAP are shown in Table 3. The height of seedlings is a significant parameter in evaluating their growth (Klymenko et al., 2010). The results showed that the size of the polybag used significantly influenced the seedling height as early as 8 MAP, with a significant difference ($P \leq 0.01$), and a similar effect was noted on polybag spacing. The impact of the treatment on the height of the seedlings was gradually increased up to 14 MAP. At 10 MAP, both treatments had significantly higher growth components of oil palm seedlings such as rachis length, bole diameter, relative leaf area, frond dry weight and petiole cross-section. This was due to the early establishment phase of the seedlings during which competition for resources such as light, nutrients, and space was intense, significantly impacting various growth parameters. The seedlings were still in a critical growth stage, explaining why multiple parameters are influenced by planting density (Bonneau et al., 2014; Lewis et al., 2020; Bonneau et al., 2022). However, as the seedlings reached 14 MAP, only rachis length was consistently affected by both treatments over time. This condition occurred because by this stage, the seedlings may have undergone some adjustment and acclimatization to the planting density, leading to a more specific impact on rachis length compared to other parameters (Bonneau et al., 2014; Lewis et al., 2020; Bonneau et al., 2022). During the 12 MAP, spacing treatment affected the number of total fronds, rachis length and seedling height. It only started to significantly increase frond production and relative leaf area during 14 MAP. Meanwhile, for polybag size treatment, frond dry weight and petiole cross-section showed that it was highly significant starting from 12 MAP and beyond, except for rachis length and seedling height. Also, the petiole-cross section was commonly used as a parameter to calculate frond dry weight (de Maijer, 2023).

Based on the ANOVA table, spacing was more influential and affected seedlings growth than polybag size at the age of 10 to 12 MAP. It was the seedling height and rachis length that were among the most affected. However, statistical analysis of two-way interaction demonstrated that neither spacing nor polybag size was significant for seedling allometric variables in either month. This finding contrasts with a previous study (Afandi, 2011), which reported significant interaction effects on bole diameter and petiole cross-section parameters comparing spacing and polybag size. This was due to the considerable impact of restricted space or closer planting arrangement as opposed to previous studies where the competition effect between seedlings was more substantial.

The results of treatments effect on seedling growth at 8 MAP are shown in Table 4, Figs 3 and 4, respectively. Seedlings grown under the denser planting system (D1) attained a significantly greater height (113.32 cm), a 19.6% increase over those at standard spacing (D4, 91.16 cm), likely due to competition for light and space stimulating vertical growth. However, a consistent variation was observed by other parameters. Meanwhile, the effect of using polybag size S2 showed significantly lower values on most seedling growth parameters as compared to S1. At this stage, the seedlings gave their undesirable growth due to the adverse conditions of the spacing and polybag sizes. This delay in growth could be attributed to inadequate spacing between seedlings, inappropriate polybag sizes, or other unfavourable environmental factors affecting the seedlings' development.

Table 3. ANOVA table for oil palm seedlings at 8, 10, 12 and 14 months after planting (MAP)

Variation	df	Frond production	Total frond (sdg^{-1})	Rachis length (cm)	Height (cm)	Bolediameter (mm)	Relative leaf area (cm^2)	Frond dry weight (kg)	Petiole cross section (cm^2)
8 MAP									
Spacing (D)	3	-	2.025	50.905*	1,097.447**	66.730**	-	0.001	0.063*
Size (S)	1	-	2.025	83.665*	407.809**	75.625*	-	0.0009*	0.083*
D × S	3	-	0.292	10.021	23.084	11.174	-	0.000	0.005
10 MAP									
Spacing (D)	3	1.700*	2.166*	2,131.435**	3,789.137**	172.589**	0.1182**	0.0006**	0.0642**
Size (S)	1	0.400	1.600	649.394**	1,540.081**	165.934**	0.0156*	0.0024**	0.214**
D × S	3	0.000	0.467	74.522	31.638	67.670	0.002	0.000	0.006
12 MAP									
Spacing (D)	3	0.692	4.558**	4,107.685**	12,829.553**	434.186*	0.041	0.003	0.297*
Size (S)	1	0.0250*	1.225	858.216**	1,990.074**	164.430	0.170*	0.0081**	0.731**
D × S	3	0.092	0.092	35.209	78.482	35.988	0.007	0.001	0.042
14 MAP									
Spacing (D)	3	2.091**	9.758**	6,656.168**	14,782.457**	558.394*	0.078**	0.001	0.087
Size (S)	1	0.025	2.025*	858.865**	1,932.100**	58.033	0.134**	0.0031**	0.342**
D × S	3	0.025	0.092	48.575	168.393	36.084	0.012	0.000	0.077

Note: MAP = Months after planting, figures at each column are the mean square (MSE) of the treatment. *, ** Significant at $P \leq 0.05$ and ≤ 0.01 respectively.

Table 4. The effects of polybag spacing and size on vegetative growth at 8 months after planting (MAP)

Distance	Total frond (sdg^{-1})	Rachis length (cm)	Height (cm)	Bole diameter (mm)	Frond dry weight (kg)	Petiole cross ection (cm^2)
D1	9.20a	44.92a	113.32a	34.94a	0.30a	0.89a
D2	8.60ab	39.91b	94.45b	28.98b	0.28b	0.73b
D3	8.10b	40.42b	92.04b	30.19b	0.28b	0.73b
D4	8.60ab	42.02ab	91.16b	31.88ab	0.29ab	0.83ab
LSD (0.05)	0.7625	3.2450	4.9210	3.2420	0.0128	0.1227
MSE	1.4522	26.1372	347.8626	30.0370	0.0003	0.0345
CV (%)	9.6507	8.4710	5.4955	11.2371	4.8858	16.8587
Polybag Size						
S1	8.85a	43.26a	100.94a	32.87a	0.29a	0.84a
S2	8.40a	40.37b	94.55b	30.12b	0.28b	0.75b
LSD (0.05)	0.5392	2.2950	3.4790	2.2930	0.0090	0.0867

Note: Means with the same letter within the same column were significantly different at $P \leq 0.05$.

Inadequate spacing and incorrect polybag sizes can hinder the seedlings' growth leading to undesirable outcomes such as stunted growth or poor development (Cui et al., 2020). Furthermore, field development of seedlings aged 6 and 8 MAP resulted in high mortality due to transplanting shock and pest infestation (Afandi et al., 2019).

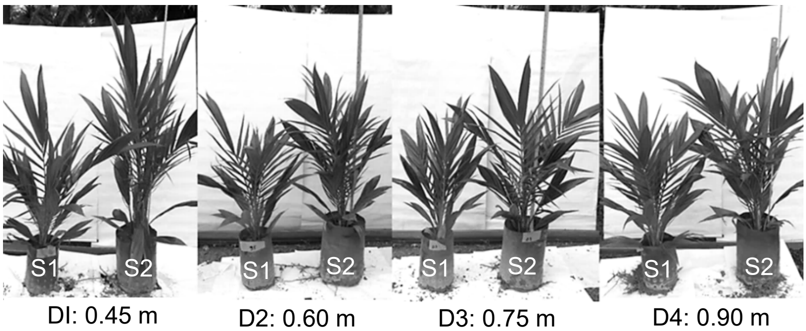

Figure 3. Comparison of seedling growth at age 8 month after planting (MAP) under different spacing and polybag size.

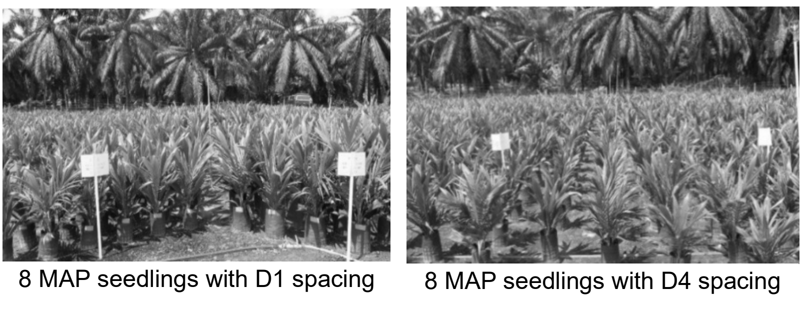

Figure 4. Growth of seedlings at age 8 month after planting (MAP) with D1 (0.45 m) spacing begins to show etiolation characteristics as compare to D4 (0.90 m).

The most appropriate seedling growth assessment was at the age of 10 to 12 MAP (Fig. 5). At this age, the seedlings were very ideal for field planting or to be sold by nursery operators. It was important to determine seedling growth parameters at of 10 MAP, as it is the minimum age of seedlings allowed for field transplanting under MPOB Code of Good Nursery Practice for Oil Palm Nurseries (MPOB, 2016).

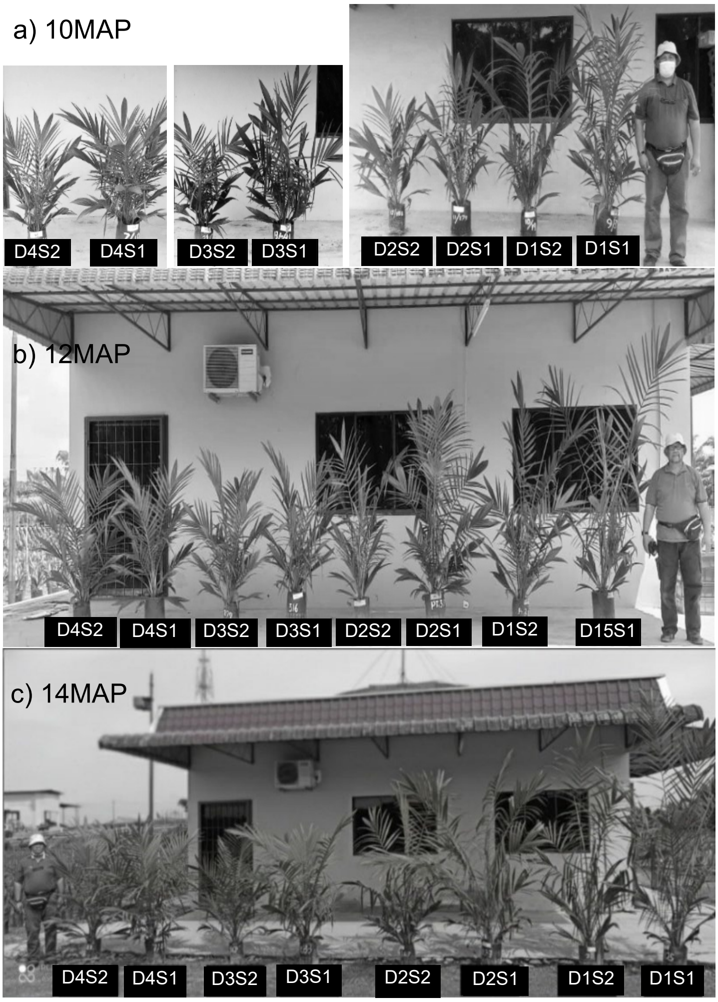

Figure 5. Comparison of seedling growth at 10, 12, and 14 months after planting (MAP) under different spacing and polybag sizes (D1S1–D4S2). Images are arranged chronologically and grouped consistently by treatment to facilitate visual comparison of height, canopy development, and overall seedling performance.

The results of the study in Tables 5, 6 and 7 showed that all parameters have a CV value below 19%, and were highly accurate in the total frond, height, frond dry weight and petiole cross-section. This suggests that there was an influence of spacing and polybag size on growth of the seedlings. Furthermore, Afandi et al. (2019) clarified that there was no significant difference in the cumulative mean of FFB yield as well as its components at 10 MAP and 12 MAP treatments over eight years, which in return found 10 MAP gave a comparable FFB yield similar to the 12 MAP seedlings (Afandi et al., 2019).

Table 5. The effects of polybag spacing and size on vegetative growth at 10 months after planting (MAP)

Distance	Frond production	Total frond (sdg^{-1})	Rachis length (cm)	Height (cm)	Bole diameter (mm)	Relative leaf area (cm^2)	Frond dry weight (kg)	Petiole cross section (cm^2)
D1	3.90b	12.00a	91.77a	165.74a	55.74a	0.55a	0.38a	1.72a
D2	4.70a	12.30a	66.42b	147.38b	46.22c	0.53a	0.37b	1.57b
D3	4.50ab	11.90ab	61.91b	126.78c	48.88bc	0.36b	0.36b	1.54b
D4	3.90b	11.20b	60.65b	124.22c	52.44ab	0.36b	0.37b	1.58b
LSD $_{(0.05)}$	0.6121	0.7138	9.1380	7.9870	4.9560	0.0587	0.0090	0.0906
MSE	0.6363	1.8272	704.7183	1,251.6541	101.2846	0.0353	0.0005	0.0518
CV (%)	15.7212	6.5754	14.2119	6.1821	10.6458	14.2289	2.6803	6.1766
Polybag Size								
S1	4.35a	12.05a	74.22a	147.23a	52.86a	0.47a	0.38a	1.67a
S2	4.15a	11.65a	66.16b	134.82b	48.78b	0.43a	0.36b	1.53b
LSD $_{(0.05)}$	0.4328	0.5047	6.4610	5.6480	3.5050	0.0415	0.0064	0.0640

Note: Means with the same letter within the same column were significantly different at $P \leq 0.05$.

It can be concluded that the rachis length and height values were significantly higher in D1 and D2 as compared to D3 and D4 at 10 and 12 MAP (Tables 5 and 6). Spacing had a significant influence on the behaviour of plants such as affecting the plants' architecture, development, weight and quality (Makhadmeh et al., 2017).

Table 6. The effects of polybag spacing and size on vegetative growth at 12 months after planting (MAP)

Distance	Frond production	Total frond (sdg^{-1})	Rachis length (cm)	Height (cm)	Bole diameter (mm)	Relative leafarea (cm^2)	Frond dry weight (kg)	Petiole cross section (cm^2)
D1	3.00ab	13.70b	130.98a	242.46a	65.66b	0.87a	0.46a	2.46a
D2	2.90b	13.00c	101.93b	196.85b	60.30b	0.72a	0.45ab	2.35ab
D3	3.10ab	14.30ab	88.07c	169.70c	65.49b	0.76a	0.43b	2.14b
D4	3.50a	14.50a	87.91c	163.92c	76.02a	0.81a	0.47a	2.54a
LSD $_{(0.05)}$	0.4819	0.6749	6.8070	9.6400	6.4410	0.1389	0.0286	0.2837
MSE	0.2386	2.1068	1,259.7168	3,904.3797	168.3696	0.0426	0.0019	0.1864
CV (%)	16.8353	5.3101	7.2686	5.4447	10.5146	19.2167	6.9588	13.0584
Polybag Size								
S1	3.10a	14.05a	106.85a	200.29a	68.89a	0.85a	0.46a	2.51a
S2	3.15a	13.70a	97.59b	186.18b	64.84a	0.72b	0.43b	2.24b
LSD $_{(0.05)}$	0.3408	0.4773	0.8130	0.8130	4.5540	0.0982	0.0202	0.2006

Note: Means with the same letter within the same column were significantly different at $P \leq 0.05$.

High planting density may increase the intensity of the competition. The rachis length and height correlated with increasing plant density per unit area and is mainly caused by competition due to limited light in crowded spacing. The elongation of the rachis, relative to overall growth, suggested that the oil palm seedlings were experiencing stress, which was likely induced by light competition (Corley & Tinker, 2016; Oomen, 2023).

However, instead of etiolation, seedlings in D1 and D2 spacing also showed relatively wide internodes of the leaflets. These features are not appropriate to characterise the seedlings as normal growth. In the normal spacing of D4, the average rachis length was only between 60.65 to 87.91 cm at and 12 MAP, while D1 showed the longest rachis length of 91.77 to 130.98 cm at the same time point. The tallest seedling was also recorded in D1 at 242.46 cm, which was 32% higher than in normal seedlings at 12 and 14 MAP (Tables 6 and 7). This indicates that the narrow spacing causes the seedlings to grow tall and etiolate as well as to have a rachis that elongates rapidly because of light competition (Fig. 5). During the 12 MAP and 14 MAP, when the spacing was adequate as seen in D3 and D4, the bole diameter increased due to the lower competition provided by larger spacing. The seedlings growth parameter with significantly higher value was found to be in seedlings grown in S1 polybag as compared to S2 but the difference was less than 8%. The results showed that the growth was not highly significant at 12 MAP when planted at D4 and D3 and S1 and S2. The differences were 6.67 and 6.88% respectively, and these differences were relatively small and acceptable. Based on these findings, therefore, oil palm seedlings can be maintained at the main nursery for up to 12 MAP by using S2 polybag size.

Table 7. The effects of polybag spacing and size on vegetative growth at 14 month after planting (MAP)

Distance	Frond production	Total frond (sdg^{-1})	Rachis length (cm)	Height (cm)	Diameter (mm)	Relative leaf area (cm^2)	Frond dry weight (kg)	Petiole cross section (cm^2)
D1	2.00b	14.00b	174.25a	283.35a	62.51b	1.06b	0.45b	2.42b
D2	2.30b	15.90a	142.67b	246.50b	76.94a	1.19a	0.45b	2.44ab
D3	3.00a	16.10a	119.38c	210.19c	77.25a	1.06b	0.47a	2.61a
D4	2.80a	15.90a	120.13c	198.26d	66.39b	0.98c	0.47a	2.57ab
LSD $_{(0.05)}$	0.3121	0.6254	5.8820	10.5000	6.6440	0.0689	0.0168	0.1735
MSE	0.6113	3.3568	1,992.7045	4,338.3905	177.0263	0.0404	0.0008	0.0840
CV (%)	13.4928	4.4116	4.6162	4.8882	10.2487	7.0256	3.9841	7.5447
Polybag size								
S1	2.50a	15.70a	143.74a	241.53a	71.98a	1.13a	0.47a	2.60a
S2	2.55a	15.25b	134.47b	227.63b	69.57a	1.01b	0.45b	2.42b
LSD $_{(0.05)}$	0.2207	0.4422	4.1600	7.4280	4.6980	0.0488	0.0119	0.1227

Note: Means with the same letter within the same column were significantly different at $P \leq 0.05$.

Recent studies showed that D1 and D2 cause seedlings to quickly compete for space and light even when planted using standard polybag sizes (S1). This condition will cause distorted growth as well as complicating seedlings maintenance work at main nurseries such as fertilizing, pest and disease control, census and culling (Fig. 6). Meanwhile, spacing at D3 and D4 using both polybags S1 and S2 still showed normal growth at each stage of seedling age. Data on the height from the combination treatment of D1S1, D1S2, D2S1 and D2S2 showed between 188.10 to 249.98 cm at 12 MAP as compared to the standard plot which was between 160.72 and 178.69 cm, and there was a difference of 20%. Taller seedlings would complicate the transportation, and field planting and are vulnerable to wind damage during planting. Therefore, planting spacing of less than 0.75 cm is not recommended. Larger polybags produce bigger and heavier seedlings, which increase the logistic burden during transport and field planting. Therefore, a more manageable seedling size is preferable from a practical and operational standpoint (Akpo et al., 2014a; Anaba et al., 2020).

Figure 6. Narrow spacing arrangement of 0.45 m and 0.60 m.

Dry weight of oil palm seedlings

Dry weight measurements at different harvested ages are presented in Table 8 and Fig. 7. The dry weight of the seedlings in all treatments increased markedly with age. The aboveground dry weight slightly decreased when the spacing increased as in D3 and D4. However, the difference was not significant. The data obtained showed that the dry weight of the roots was not significantly affected by polybag spacing. The dry weight of the aboveground, roots, as well as total dry matter, was significantly higher in S1 than in S2. The difference was between 11.71% to 13.20% and 11.62% to 22.65% for aboveground and roots, respectively. Meanwhile, the disparity ranges from 12.81% to 14.04% on the total dry weight of the seedlings.

Table 8. The effects of polybag spacing and size on seedlings dry weight

Treatment	Above ground (g seedling^{-1})			Root (g seedling^{-1})			Total Dry matter (g seedling^{-1})		
	10 MAP	12 MAP	14 MAP	10 MAP	12 MAP	14 MAP	10 MAP	12 MAP	14 MAP
Polybag Spacing									
D1	329.08a	577.14a	900.34a	113.28a	133.08a	131.78b	442.34a	710.20a	1,035.09a
D2	336.15a	512.30a	819.65ab	116.30a	132.45a	142.11ab	452.46a	644.76a	961.74a
D3	356.94a	509.84a	771.43ab	115.71a	130.41a	152.95ab	472.65a	640.24a	924.36a
D4	370.14a	529.64a	755.86b	119.48a	137.24a	168.14a	489.60a	666.86a	923.98a
LSD $_{(0.05)}$	52.10	107.50	133.60	12.26	25.78	24.96	50.39	114.60	148.50
Polybag Size									
S1	372.68a	565.90a	863.12a	123.36a	149.86a	167.74a	496.04a	715.76a	1,030.83a
S2	323.47b	498.54a	762.02b	109.02b	116.73b	129.75b	432.49b	615.28b	891.75b
LSD $_{(0.05)}$	36.84	76.04	94.49	8.67	18.23	17.65	35.63	81.02	105.0

Note: Means with the same letter within the same column were significantly different at $P \leq 0.05$; MAP = Months after planting.

Total dry weight of seedlings increased gradually from 10 to 14 MAP cross all treatments, suggesting continuous biomass accumulation during the nursery stage (Fig. 7). Treatments D2S1, D2S2, and D3S1 produced the highest total dry weight, around 950 to1,000 g plant^{-1} at 14 MAP, while D3S2 and D4S2 recorded slightly lower values. The overall trend showed a slight decreased across treatments, indicating limited variation in growth performance. These results imply that moderate spacing combined with adequate polybag size enhances canopy expansion and root development, contributing to better seedling vitality. Furthermore, the reduced spacing of 0.75 m yielded comparable biomass to the conventional 0.9 m, confirming that nursery space can be efficiently optimized without compromising seedling growth and quality.

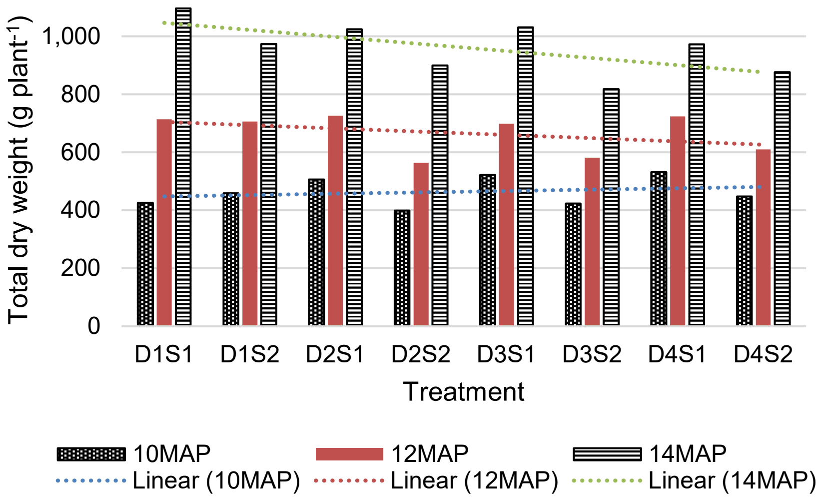

Figure 7. Comparison of total dry weight at various planting and treatments ages.

The superior performance of the larger S1 polybag is quantitatively demonstrated by a statistically significant 12.8% to 14.04% greater dry weight compared to S2. On the other hand, the non-significant effect of planting density on dry matter supports the inference that spacing can be optimized. These results collectively establish that seedling growth is principally controlled by polybag size, while nursery spacing can be efficiently reduced without compromizing biomass production.

Meanwhile, in treatments D1 and D2, the combination of closely arranged seedlings had a higher total dry weight. The primary cause for this observation was due to longer rachis and taller seedlings as discussed. The data suggest that the response to light competition, in terms of plant height and rachis length, became more pronounced with increasing competition density. According to Gruntman et al. (2017), plants showed greater height in crowded conditions compared to sparse treatments. The increase in plant height was accompanied by a corresponding increase in the total dry weight (Kalaitzoglou et al., 2019). However, a high value of total dry matter did not represent good quality seedlings. In nursery practice, oil palm seedling quality is assesed based on height, basal diameter, leaf characteristics, and shoot-root balance, rather than dry weight alone (Bhadouria et al., 2018; Wagino et al., 2018). Afandi (2011) found that seedling performance was optimal when the above-ground dry weight reached 666.20 g per plant. In contrast, the current study found that, the high total dry weight did not necessarily imply good quality of the seedling, as space and light competition led to etiolated and elongated seedling growth, resulting in an overall increase in dry weight. A previous study found that 10% of the variation in total dry matter production between polybag sizes 15" × 18" and 12" × 15" was attributed to the same spacing (Afandi, 2011). The discrepancy was only 10.4% if the same polybag size was used but required to be arranged in 0.9 m and 0.75 m spacing. These differences can be mitigated through effective agronomic practices within the expected period of one year after planting in the field.

High dry matter production can be achieved when compost is used as a growth medium compared to conventional soil media. Additionally, optimizing polybag size and implementing appropriate planting spacing arrangements also contribute to improved dry matter yield (Lord & Betitis, 2007; Afandi, 2011). The current study showed that without any restricting factors on seedling growth, the average total dry weight was 609.68 g and increased to 713.95 g when there was competition due to denser spacing.

Nutrient status

The level of nutrient content in all seedling tissue (leaf, rachis, palm base, and root) was compared with the control plot, i.e. seedlings using polybag S1 and arranged with D4 spacing. A summary of nutrient analysis results are presented in Tables 9 and 10. Data showed that N values in leaf and rachis samples were found to be higher in closely arranged seedlings (D1 and D2). This is probably due to the high N requirement to accommodate the vegetative growth i.e. height and rachis of the seedlings. Nitrogen is required especially to young oil palm to increase the net assimilation rate which leads to promoting growth (Corley & Mok, 1972; Breure, 1982; Uwumarongie-Ilori et al., 2012). Nitrogen plays a crucial role in supporting rapid plant growth through enhanced chlorophyll and protein synthesis and nitrogen availability can influence plant physiological traits and performance (Andersen et al., 2010). Therefore, maintaining a sufficient N supply is crucial during the initial five years following planting (Goh et al., 2003). Meanwhile, there was no significant difference in major nutrient content in other parts of the seedling related to the spacing arrangement, except for phosphate only at 10 MAP.

There was also no significant difference in nutrient content for all seedling components when grown using S1 and S2 (Table 11 and 12). This indicated that the lower soil media in S2 (52.32%) was still capable of supplying nutrients for the entire seedling component up to 12 MAP. These results support and recommend the retention of seedlings in 12" × 15" polybags until the age of 12 MAP in the main nursery as compared to a maximum period of 11 months contrary to the recommendation stated in MPOB Code of Practice: Code of good nursery practice for oil palm nurseries (MPOB, 2016).

Table 9. The effects of polybag spacing and size on leaf nutrient content

Treatment	Leaf (% Dry matter)											
	N		P		K		Ca		Mg		B	
Distance	10 MAP	12 MAP	10 MAP	12 MAP	10 MAP	12 MAP	10 MAP	12 MAP	10 MAP	12 MAP	10 MAP	12 MAP
D1	2.79a	2.83a	0.19a	0.19a	1.46a	1.51a	0.42a	0.38a	0.14ab	0.12b	16.70a	13.56a
D2	2.64ab	2.79ab	0.18a	0.18a	1.45a	1.57a	0.39ab	0.35a	0.13b	0.12b	17.10a	13.42a
D3	2.47b	2.70ab	0.15b	0.19a	1.39a	1.52a	0.36b	0.35a	0.13b	0.12b	16.12a	11.69a
D4	2.44b	2.59b	0.16b	0.18a	1.37a	1.51a	0.41a	0.37a	0.16a	0.15a	15.83a	11.68b
LSD $_{(0.05)}$	0.2243	0.2184	0.0226	0.0133	0.1622	0.1203	0.0417	0.0620	0.0256	0.0249	1.9820	1.320
Polybag Size												
S1	2.59a	2.72a	0.18a	0.18a	1.41a	1.50a	0.40a	0.36a	0.13a	0.13a	16.47a	12.66a
S2	2.58a	2.74a	0.16a	0.19a	1.43a	1.55a	0.39a	0.35a	0.14a	0.12a	16.41a	12.52a
LSD $_{(0.05)}$	0.1586	0.1544	0.0159	0.0094	0.1147	0.0850	0.0295	0.0438	0.0181	0.0176	1.4020	0.9336

Note: Means with the same letter within the same column were significantly different at $P \leq 0.05$; MAP = Months after planting.

Table 10. The effects of polybag spacing and size on rachis nutrient content

Treatment	Rachis (% Dry matter)											
	N		P		K		Ca		Mg		B	
Distance	10 MAP	12 MAP	10 MAP	12 MAP	10 MAP	12 MAP	10 MAP	12 MAP	10 MAP	12 MAP	10 MAP	12 MAP
D1	0.66a	0.49a	0.09a	0.09a	1.10a	1.11a	0.27a	0.17a	0.07a	0.06a	11.88a	7.10a
D2	0.48b	0.45ab	0.09a	0.10a	1.20a	1.11a	0.21b	0.19a	0.06ab	0.05a	9.27b	9.39a
D3	0.38c	0.44ab	0.11a	0.10a	1.14a	1.16a	0.14c	0.20a	0.05b	0.06a	7.68b	11.34a
D4	0.39c	0.36b	0.11a	0.10a	1.30a	1.12a	0.15c	0.20a	0.06ab	0.06a	8.58b	6.26a
LSD $_{(0.05)}$	0.0691	0.0820	0.0240	0.0199	0.2093	0.1935	0.0317	0.0337	0.0136	0.0104	1.645	4.778
Polybag Size												
S1	0.49a	0.45a	0.09b	0.09a	1.17a	1.11a	0.21a	0.20a	0.07a	0.06a	9.57a	7.92a
S2	0.46a	0.42a	0.11a	0.09a	1.21a	1.14a	0.17b	0.19a	0.06b	0.05a	9.13a	9.13a
LSD $_{(0.05)}$	0.0489	0.0580	0.0170	0.0141	0.1480	0.1368	0.0224	0.0238	0.0096	0.0073	1.1630	3.378

Note: Means with the same letter within the same column were significantly different at $P \leq 0.05$; MAP = Months after planting.

Table 11. The effects of polybag spacing and size on palm base nutrient content

Treatment	Palm base/bole (% Dry matter)											
	N		P		K		Ca		Mg		B	
Distance	10 MAP	12 MAP	10 MAP	12 MAP	10 MAP	12 MAP	10 MAP	12 MAP	10 MAP	12 MAP	10 MAP	12 MAP
D1	0.98a	0.76a	0.21a	0.15a	1.35a	1.05a	0.18a	0.19a	0.10ab	0.08a	11.94a	6.46a
D2	0.65a	0.80a	0.15b	0.16a	1.01b	1.09a	0.13b	0.18a	0.07b	0.08a	10.25a	5.86a
D3	0.73a	0.67a	0.16ab	0.15a	1.01b	1.04a	0.14b	0.17a	0.08ab	0.07a	10.50a	5.26ab
D4	0.71a	0.64a	0.18ab	0.14a	0.11ab	1.00a	0.19a	0.15a	0.11a	0.08a	7.21b	4.39b
LSD $_{(0.05)}$	0.3717	0.1628	0.0561	0.0297	0.2917	0.1879	0.0274	0.0388	0.0289	0.0151	1.9200	1.1890
Polybag Size												
S1	0.72a	0.71a	0.17a	0.14a	1.10a	1.03a	0.16a	0.17a	0.09a	0.07a	10.13a	5.56a
S2	0.82a	0.73a	0.19a	0.16a	1.14a	1.06a	0.16a	0.18a	0.09a	0.08a	9.83a	5.42a
LSD $_{(0.05)}$	0.2628	0.1151	0.0398	0.0210	0.2062	0.1329	0.0193	0.0274	0.0205	0.0106	1.3580	0.8411

Note: Means with the same letter within the same column were significantly different at $P \leq 0.05$; MAP = Months after planting.

Table 12. The effects of polybag spacing and size on root nutrient content

Treatment	Root (% Dry matter)											
	N		P		K		Ca		Mg		B	
Distance	10 MAP	12 MAP	10 MAP	12 MAP	10 MAP	12 MAP	10 MAP	12 MAP	10 MAP	12 MAP	10 MAP	12 MAP
D1	0.71a	0.72a	0.09b	0.09a	0.84a	0.71a	0.08a	0.09a	0.06a	0.06a	4.93a	5.86a
D2	0.80a	0.70a	0.12a	0.09a	0.95a	0.65a	0.08a	0.09a	0.06a	0.06a	4.28a	6.56a
D3	0.73ab	0.73a	0.10ab	0.10a	0.82a	0.78a	0.09a	0.08a	0.05a	0.06a	5.04a	6.01a
D4	0.62b	0.75a	0.09b	0.10a	0.81a	0.82a	0.08a	0.09a	0.05a	0.06a	4.58a	6.40a
LSD $_{(0.05)}$	0.1648	0.1211	0.0187	0.0167	0.2422	0.1863	0.0341	0.0136	0.0109	0.0085	1.010	2.387
Polybag Size												
S1	0.71a	0.72a	0.09b	0.08b	0.82a	0.73a	0.08a	0.09a	0.06a	0.06a	4.51a	5.79a
S2	0.72a	0.73a	0.11a	0.10a	0.89a	0.74a	0.08a	0.08a	0.05a	0.06a	4.91a	6.63a
LSD $_{(0.05)}$	0.1165	0.0856	0.0132	0.0118	0.1712	0.1317	0.0241	0.0096	0.0076	0.0060	0.7145	1.6880

Note: Means with the same letter within the same column were significantly different at $P \leq 0.05$; MAP = Months after planting.

Seedling performance

Relative comparisons were made to compare the performance of previous seedlings (Afandi, 2011) with those used in this trial based on five growing parameters, namely total frond production, rachis length, height, bole diameter and petiole cross-section. A comparison was made with seedlings planted on the control plot using a polybag size of 15" × 18" with an arrangement distance of 0.9 m. This relative comparison indicates that the quality of the DxP oil palm seedlings used in the current study is superior to that of the previous batch of seedlings. The results of the present study shows that total frond production (14.05 sdg^{-1}), rachis length (130 cm), plant height (242 cm), bole diameter (68.89 mm), and petiole cross-sectional area (2.51 cm^2) were significantly greater than the values reported by Afandi (2011), who documented 13.44 sdg^{-1}, 72 cm, 152 cm, 67.21 mm, and 1.10 cm^2, respectively. These differences indicate a markedly improved vegetative performance relative to previously published findings. The mean difference was 35% and 24.90%, respectively, at 10 MAP and 12 MAP. The parameters of the rachis length, height and petiole cross-section contribute to this percentage. While total dry weight production at 12 MAP showed the same pattern, i.e. the seedlings used in the current study produced better total dry weight with differences of 19.68%, 27.28% and 21.44% for above-ground, root and total dry weight, respectively. This is indicative of a significant improvement in the quality of the current generation of planting materials over time.

This study addresses a key research gap by providing quantitative evidence on the effect of spacing and polybag size influence oil palm seedling growth up to 14 MAP. The results highlight the novelty of identifying the biological limits of seedling density, where spacing below 0.75 m leads to abnormal elongation and showing that the smaller polybag size remains adequate up to 12 MAP. These findings offer clear scientific implications by strengthening the physiological basis for nursery recommendations and supporting more cost-efficient management practices.

CONCLUSION

The results of the current study suggest that the arrangement of polybags of oil palm seedlings less than 0.75 m × 0.75 m × 0.75 m (30" × 30" × 30") produces tall, etiolated seedlings and is therefore not recommended for nursery practice. Spacing below 0.75 m increased seedling height by 19.60% at 8 MAP and up to 32.00% at 12 to 14 MAP. Accompanied by excessive rachis elongation, making the seedlings unsuitable for field planting and difficult to manage during routine nursery operations. The seedlings should be arranged in a triangular polybag spacing of 0.75 m (2.5') to 0.9 m (3.0'), resulting no adverse effect on growth. This assessment was made based on the seedling growth, dry weight production, nutrient content as well as routine nursery management. The use of the smaller S2 polybag; 30 cm × 38 cm (12" × 15"), resulted in only minor differences relative to the standard size, with no negative impact on seedling quality or nutrient status when maintained at the main nursery until 12 MAP.

RECOMMENDATIONS

The results of the current study also showed that the key factor affecting the overall performance of seedlings was the spacing arrangement in the main nursery instead of the polybag size used. Based on the present study, the recommended standard recorded by the DxP seedlings used suitable for field planting at age 10 to 12 MAP are as follows:

i. Bole diameter: 49 to 64 mm,
ii. Total number of frond production: 11 to 15 seedling^{-1},
iii. Rachis length of frond 3: 58 to 93 cm,
iv. The seedlings heights: 118 to 179 cm,
v. Petiole cross-section: 1.48 to 2.10 cm^2.

However, it should be noted that these measurements may vary depending on the specific oil palm planting materials and clones used.

These findings provide practical guidance for nursery operators, indicating that optimal spacing and appropriate polybag size can maintain adequate nutrient supply without compromising seedling quality. Future research should further examine how nutrient use efficiency changes under different management conditions to refine nursery recommendations.

ACKNOWLEDGEMENTS. The authors would like to thank the Director-General of MPOB for granting permission to publish this article. We would also like to acknowledge the support and guidance of the Director of the Biology and Sustainability Research Division, Mr Tan Kim Tun, President of MOPNA, the representatives of MOPNA and the staff of the Agronomy and Geospatial Technology Unit. An appreciation goes to Tapak Semaian Hong Seng Sdn Bhd for the provision of a study area.

REFERENCES

Adu-Yeboah, P., Amoah, F.M., Dwapanyin, A.O., Opoku-Ameyaw, K., Opoku-Agyeman, M.O., Acheampong, K., Dadzie, M.A., Yeboah, J. & Owusu-Ansah, F. 2015. Effects of polybag size and seedling age at transplanting on field establishment of cashew (*Anacardium occidentale*) in northern Ghana. *American Journal of Experimental Agriculture* **7**(5), 308–314. https://doi.org/10.9734/AJEA/2015/16122

Afandi, A.M. 2011. The effects of spacing and polybag size on growth and dry matter production of oil palm seedlings. *MPOB 156th VIVA Committee Meeting*, VIVA No. 534/2011(03).

Afandi, A.M., Zuraidah, Y., Nur-Zuhaili, H.A.Z.A., Khairuman, H., Zulkifli, H., Abd Fatah, I., Irman-Fareez, K., Andi, M.A. & Siti-Rashidah, M. 2019. Seedling age at field planting affecting the oil palm performance. *OPB* **79**, 1–8.

Ahmad, S.M., Saari, I.S., Arshad, F., Ismail, A., Salleh, K.M. & Rahami, M.S. 2022. Factors influencing the level of acceptance of code of good nursery practice (CoPN) among oil palm nursery operators. *Journal of Sustainability Science and Management* **17**(1), 177–186. https://doi.org/10.46754/jssm.2022.01.011

Akpo, E., Stomph, T.J., Kossou, D.K., Omore, A.O. & Struik, P.C. 2014a. Effects of nursery management practices on morphological quality attributes of tree seedlings: The case of oil palm. *Forest Ecology and Management* **324**, 28–36. doi: 10.1016/j.foreco.2014.03.045

Akpo, E., Stomph, T.J., Kossou, D.K. & Struik, P.C. 2014b. Growth dynamics of tree nursery seedlings: the case of oil palm. *Scientia Horticulturae* **175**, 251–257. doi: 10.1016/j.scienta.2014.06.020

Anaba, B.D., Yemefack, M., Abossolo-Angue, M., Ntsomboh-Ntsefong, G., Bilong, E.G., Ebongue, G.F.N. & Bell, J.M. 2020. Soil texture and watering impact on pot recovery of soil-stripped oil palm (*Elaeis guineensis* Jacq.) seedlings. *Heliyon*, **6**(10), e05310. https://doi.org/10.1016/j.heliyon.2020.e05310

Andersen, K.M., Corre, M.D., Turner, B.L. & Dalling, J.W. 2010. Plant–soil associations in a lower montane tropical forest: physiological acclimation and herbivore-mediated responses to nitrogen addition. *Functional Ecology* **24**(6), 1171–1180.

Applied Agricultural Resources Sdn. Bhd. 2020. Nursery: Set-up. https://aarsb.com.my/nursery-set-up

Bernama. 2017. Codes of Practice for Palm Oil Industry to Take Effect 2008. http://bepi.mpob.gov.my/news/detail.php?id=4194

Bhadouria, R., Srivastava, P., Singh, S., Singh, R., Raghubanshi, A.S. & Singh, J.S. 2018. Effects of Effects of light, nutrient and grass competition on growth of seedlings of four tropical tree species. *Indian Forester* **144**(1), 54–65. doi: 10.36808/if/2018/v144i1/121306

Bonneau, X. & Impens, R. 2022. Experimental determination of the optimum oil palm planting density in Western Africa. *OCL* **29**, 30. https://doi.org/10.1051/ocl/2022019

Bonneau, X., Vandessel, P., Buabeng, M. & Erhahuyi, C. 2014. Early impact of oil palm planting density on vegetative and oil yield variables in West Africa. doi: 10.1051/ocl/2014009

Breure, C.J. 1982. Factors affecting yield and growth of oil palm teneras in West New Britain. In: Pushparajah, E. & Chew, P.S. (eds), *The Oil Palm in Agriculture in the Eighties – Volume I*. ISP, Kuala Lumpur, 109–130.

Corley, R.H.V. & Mok, C.K. 1972. Effects of nitrogen, phosphorus, potassium and magnesium on growth of the oil palm. *Experimental Agriculture* **8**(4), 347–353. doi: 10.1017/S0014479700005470

Corley, R.H.V. & Tinker, P.B. 2016. *The Oil Palm* (5th ed.). World Agriculture Series. Wiley Blackwell, Oxford, UK. 290–328. https://doi.org/10.1002/9781118953297

Couto, M.F., Peternelli, L.A. & Barbosa, M.H.P. 2013. Classification of coefficients of variation for sugarcane crops. *Ciência Rural* **43**, 957–961. doi: 10.1590/S0103-84782013000600003

Cui, J., Lamade, E. & Tcherkez, G. 2020. Seed germination in oil palm (Elaeis guineensis Jacq.): a review of metabolic pathways and control mechanisms. *International Journal of Molecular Sciences* **21**(12), 4227. https://doi.org/10.3390/ijms21124227

de Maijer, D. 2023. Evaluation of intercropping watermelon and immature oil palm: implications for vegetative growth, fruit weight and yield. *MSc Thesis*, Wageningen University, 46 pp.

Fang, Y., Nunez, G., Fisher, P. & Munoz, P.R. 2022. Effect of container size, substrate composition and genotype on growth and fruit quality of young southern highbush blueberry. *Scientia Horticulturae* **302**, 111149. doi: 10.1016/j.scienta.2022.111149

Gebisa, L.A. 2024. Cost of Productions and Partial Budget Analysis of Coffee (Coffea arabica L.) Seedling Across Various Pot Sizes and Biochar-Based Media Preparations. *American Journal of Bioscience and Bioengineering*, **12**(5), 76–82. Doi: 10.11648/j.bio.20241205.11

Gillbanks, R.A. 2003. Standard agronomic procedures and practices. In: Fairhurst, T. & Härdter, R. (eds), *Oil Palm: Management for Large and Sustainable Yields*. PPI/PPIC & IPI, Singapore, 115–150.

Gruntman, M., Groß, D., Májeková, M. & Tielbörger, K. 2017. Decision-making in plants under competition. *Nature Communications* **8**, 2235. doi: 10.1038/s41467-017-02147-2

Goh, K.J., Härdter, R. & Fairhurst, T. 2003. Fertilizing for maximum returns. In: Fairhurst, T. & Härdter, R. (eds), *Oil Palm: Management for Large and Sustainable Yields*. PPI, PPIC & IPI, Singapore, 279–306.

Hassan, H., Yahya, A., El Pebrian, D. & Su, A.S.M. 2023. Development and field evaluation of a seedling polybag soil filling machine for oil palm nursery. *Journal of Oil Palm Research* **35**(1), 100–110.

Hashim, M.T., Yeow, K.H. & Poon, Y.C. 1987. Recent development in nursery practice – potting media. In: *Proceedings of the 1987 International Palm/Oil Palm Conferences*, PORIM, Kuala Lumpur, 369–371.

Jobbágy, J., Krištof, K. & Findura, P. 2016. Soil compaction caused by irrigation machinery. *Research in Agricultural Engineering* **60**(Special issue), 1–8.

Kalaitzoglou, P., Van Ieperen, W., Harbinson, J., Van der Meer, M., Weerheim, K., Nicole, C. & Marcelis, L.F. 2019. Effects of far-red light on tomato growth and production. *Frontiers in Plant Science* **10**, 373. https://doi.org/10.3389/fpls.2019.00322

Keni, M.F., Zainuddin, N. & Masri, M.M.M. 2023. Improving growth performance of oil palm seedlings using mixtures of organic and chemical fertilisers. *Journal of Oil Palm Research* **35**(1), 147–156.

Klymenko, O., Klymenko, M., Kartyzhova, L. & Alechenkova, Z. 2010. Cultivation of sweet cherry seedlings using phosphate-mobilizing microorganisms. *Agronomy Research* **8**, 633–636.

Laksono, N.D., Setiawati, U., Nur, F., Rahmaningsih, M., Anwar, Y., Rusfiandi, H., Sembiring, E.H., Forster, B.P., Subbarao, A.S. & Zahara, H. 2019. *Nursery Practices in Oil Palm: A Manual.* CABI, Volume **17**.

Lewis, K., Rumpang, E., Kho, L.K., McCalmont, J., Teh, Y.A., Gallego-Sala, A. & Hill, T.C. 2020. Assessment of oil palm aboveground biomass on tropical peat. *Scientific Reports* **10**, 2230. https://doi.org/10.1038/s41598-020-58982-9

Lord, S. & Betitis, S. 2007. The role of EFB compost and its effect in New Britain Palm Oil Ltd nurseries. In: *Proceedings of PIPOC 2007 International Palm Oil Congress*, Kuala Lumpur.

Makhadmeh, I.M., Al-Tawaha, A., Edaroyati, P., Al-Karaki, G., Tawaha, A.R.A. & Hassan, S.A. 2017. Effects of different growth media and planting densities on lettuce in soilless systems. *Research on Crops* **18**(2), 294–298.

Militello, M., Sortino, G., Talluto, G. & Gugliuzza, G. 2018. Split water application for water reduction in *Callistemon Citrinus* pot plant. *Agronomy Research* **16**(5), 2097–2109.

Mohd Rais, M.B. 2021. Pelaksanaan Mandatori CoPN. *Warta Sawit* **79**(3), 5–7.

MPOB. 2016. *MPOB Code of Practice (MPOB CoP 1001:2015): Code of Good Nursery Practice for Oil Palm Nurseries.* 2nd ed. MPOB Publication.

Mutert, E., Esquívez, A.S., de los Santos, A.O. & Cervantes, E.O. 1999. The oil palm nursery: foundation for high production. *Better Crops International* **13**(1), 39.

Oomen, D. 2023. *Establishment intercropping: effects of watermelon, banana, cassava and maize on oil palm performance*. MSc Thesis, Wageningen University & Research, 57 pp.

Parveez, G.K.A., Ghazali, R., Hassan, N.A.M., Zairun, M.A., Othman, A., Kannan, P., Sin, T.S., Tee, V.P., Idris, Z. & Moslim, R. 2025. Oil palm economic performance in Malaysia and R&D progress in 2024. *Journal of Oil Palm Research* **37**(2), 187–208. https://doi.org/10.21894/jopr.2025.0031

Poorter, H., Bühler, J., van Dusschoten, D., Climent, J. & Postma, J.A. 2012. Pot size matters: meta-analysis of rooting volume effects. *Functional Plant Biology* **39**(11), 839–850. https://doi.org/10.1071/FP12049

Salisu, M.A., Sulaiman, Z., Samad, M.Y.A. & Kolapo, O.K. 2018. Effect of container type and size on growth and root morphology of rubber. *International Journal of Science and Technology Research* 7, 21–27.

Siti Atikah, A., Nor Aini, A.S. & Rosli, R. 2019. Cost of production in the Malaysian oil palm nursery sector. *Oil Palm Industry Economic Journal* **19**(2), 18–26. https://palmoilis.mpob.gov.my/publications/OPIEJ/opiejv19n2-siti.pdf

Uwumarongie-Ilori, E.G., Sulaiman-Ilobu, B.B., Ederion, O., Imogie, A., Imoisi, B.O., Garuba, N. & Ugbah, M. 2012. Vegetative growth performance of oil palm seedlings under organic and inorganic fertilizers. *Greener Journal of Agricultural Science* **2**, 26–30.

Wagino, W., Tarigan, S.M. & Febrianto, E.B. 2018. Respon pertumbuhan kelapa sawit (Elaeis Guineensis Jacq.) varietas dyxp dumpy pada kondisi stres air di pembibitan awal. Agrotekma: *Jurnal Agroteknologi dan Ilmu Pertanian* **3**(1), 17–26. doi: 10.31289/agr.v3i1.1934

Zuraidah, Y., Masli, E., Salina, S., Hazira, H., Zulkifli, H. & Hanif, H. 2017. *Oil Palm Vegetative Measurements Manual.* MPOB, Bangi, 36 pp.

Agronomy Research **24**(S1), 96–113, 2026
https://doi.org/10.15159/AR.26.004

Phytochemical screening and evaluation of antioxidant and antimicrobial activity of *Solanum incanum*: medicinal plant from Al-Baha Region

S.G. Mohammed[1,2], H. Maaroufi Dguimi[1,*], S.H. Bashir[1,3], S.A. Tammam[4], H. Abdalgadir[1], S.M. Howladar[5] and F.O. Alzahrani[1]

[1]Al-Baha University, Faculty of Science, Department of Biology, Al-Baha, Saudi Arabia
[2]University of Khartoum, Faculty of Science, Department of Botany, Khartoum, Sudan
[3]Bahri University, Collage of applied and industrial Sciences, Department of Chemistry, Sudan
[4]Assiut University, Assiut, Faculty of Science, Department of Botany, Assiut, Egypt
[5]University of Jeddah, College of Sciences, Department of Biological Sciences, Jeddah, Saudi Arabia
[*]Correspondence: houda_maaroufi@yahoo.fr

Received: October 1st, 2025; Accepted: December 22nd, 2025; Published: January 12th, 2026

Abstract. *Solanum incanum* is a prominent medicinal plant, used to treat various ailments. The current study sought to assess the phytochemical profile, as well as the antioxidant and antimicrobial activities, of the crude methanolic extract and the corresponding chloroform, ethyl acetate, n-hexane, and aqueous fractions of the leaves, stem bark, and fruits. Leaf and fruit extracts had the largest levels of polyphenols, flavonoids, tannins, and alkaloids referring to stem-bark. Hexadecanoic acid methyl ester is a major phytochemical component revealed in different plant parts, especially in stem-bark with 31.82% level. The 9,12,15-Octadecatrienoic acid, methyl ester is also revealed in all plant parts, especially in leaf with 20.07%. Fruit and leaf ethyl acetate and water fractions showed the highest antioxidant capacity compared to stem-bark fractions. Using the agar disc diffusion method, antimicrobial activity was evaluated in vitro against four different bacterial species and one fungal species (*Candida albicana*). The ethyl acetate, n-hexane, and chloroform fractions of fruits and leaves showed strong antimicrobial activity against all microorganisms. Aqueous fraction of different plant parts was inactive or partially active against tested microorganisms. The high total content of phenols, flavonoids, tannins and alkaloids, especially in leaves and fruits, correlates positively with the highest antimicrobial and antioxidant activities detected in these parts of the plant.

Key words: GC-MS Analysis, free radical scavenging, solanaceae, phenolic compounds.

INTRODUCTION

Solanum incanum L. is part of the complex and widely distributed *S. incanum* sensu lato group, native to a broad region across Africa and the Middle East (Samuels, 2012). Its distribution spans from North Africa through the savannah regions of sub-Saharan

Africa, the Arabian Peninsula, and into parts of the Middle East and India (Ranil et al., 2017; El-Shaboury et al., 2021). In Saudi Arabia, it is a common component in the flora of the southwestern highlands. This plant is a perennial shrub, well adapted to arid and semi-arid conditions of the desert. This bushy herb is widely distributed throughout Al-Baha area. This plant species is used in traditional medicine to treat throat and chest problems (Zivanayi et al., 2023), as antiseptic for dermatomycosis, and as antihyperlipidemic (Andargie et al., 2022; Ohalete, 2023). Fruit extracts presented too, an antidiabetic activity (Satyanarayana et al., 2022).

While it has usually been harvested from the wild for traditional uses, its biological robustness and the growing interest in its bioactive compounds argue for considerable potential for cultivation. Successful cultivation would ensure a sustainable and standardized supply that is necessary for any future pharmaceutical use, as was explored with other wild species of the genus Solanum (Ranil et al., 2017). Recent phytochemical studies of Solanum species have reported the presence of flavonoids, amides, steroids, steroidal saponins, steroidal alkaloids, and lignans, (Ateshim & Tekle, 2022).

Plant phytochemicals play a vital role in drug discovery as they can be used directly as drugs, as synthetic precursors, or as lead compounds (Kim et al., 2021; Chaachouay et al., 2024). In this context, medicinal plants are a particularly valuable resource, due to their rich diversity of bioactive chemicals (Augšpole et al., 2018; Espro et al., 2021; Yazarlu et al., 2024). In *S. incanum*, the most important classes of bioactive compounds are tannins, flavonoids, alkaloids and phenolic compounds (Lezoul et al., 2020; Roy et al., 2022). Interestingly, the phytocomplex of *S. incanum,* characterized by the presence of fatty acid esters, alkaloids, and sterols, shows a very good correspondence with the bioactive profile reported for other medicinal plants of recognized pharmaceutical relevance. Among others, hexadecanoic acid methyl ester was identified by GC-MS in the sclerotia of Pleurotus tuber-regium (Oseghale et al., 2025), a mushroom with important medicinal properties, and in the leaves of *Heinsia crinita*, traditionally used in medicine (Mgbeje et al., 2016). The fatty acid esters and sterols identified in *S. incanum* are also relevant in the anticancer profile of *Melastomastrum capitatum* (Ukwubile et al., 2019) and in the wild and cultivated specimens of *Leonotis nepetifolia*, a plant with anti-inflammatory and analgesic properties (de Oliveira et al., 2015). This comparative phytochemical profile underlines the potential of *S. incanum* as a source of lead compounds for pharmaceutical development.

In humans, Reactive Oxygen Species (ROS) are generated endogenously through metabolism or exogenously by environmental stresses that can cause oxidative damage to cellular macromolecules, including lipids, proteins, and DNA (Di Meo et al., 2022). It is considered a fundamental contributor to the pathogenesis of many chronic health risks, such as cardiovascular, neurodegenerative, and inflammatory diseases. Lack of antioxidants accelerates the development of degenerative diseases, including cardiovascular diseases, cancers (Rychter et al., 2022), neurodegenerative diseases, Alzheimer's disease, (Pritam et al., 2022) and inflammatory diseases (García-Sánchez et al., 2020). Plant phytochemicals in medicinal plants could serve as a preventive medicine. *S. incanum* along with several other medicinal plants, has been reported with potential antioxidant activity (Akanmu et al., 2021; Chivodze et al., 2021).

Additinally, the antioxidant capacity conferred by polyphenolic and flavonoid content in various plants, especially medicinal plants, represents a significant potential for the salt stress mitigation (Maaroufi-Dguimi et al., 2025).

Solanum incanum has significant antibacterial activity (Chivodze et al., 2021; Karanja et al., 2021; Musyimi et al., 2021). The antimicrobial activity of *S. incanum* has been reported in plant extracts (Vaou et al., 2021), essential oils (Ramsey et al., 2020) or isolated compounds such as alkaloids (Ti et al., 2021), flavonoids (Sok Yen et al., 2021), sesquiterpene lactones (Liu et al., 2021), diterpenes (Mohammed et al., 2022), triterpenes (Renda et al., 2022) or naphthoquinones (Ahmadi et al., 2020).

In the Al-Baha region (Fig. 1), *S. incanum* is used in traditional medicine, yet there is no scientific evidence supporting its bioactivity or biological safety. The lack of scientific information in the literature regarding the phytochemical analysis and bioactivity of different parts of this plant prompted the current study. The aim is to establish the phytochemical profile and evaluate the antioxidant and antimicrobial activities of methanolic extracts from the leaves, stem-bark and fruits.

Figure 1. Map of Kingdom of Saudi Arabia showing Al-Baha Province.

MATERIALS AND METHODS

Plant material

Solanum incanum was collected in October 2023 of five localities from Al-Baha region in south western Saudi Arabia located in the Sarawat Mountains (Fig. 1). In each locality and within the area of collection, around 10 individual mature plants were sampled for the creation of a composite sample for each part: leaves, stem-bark, and fruits. The plants that were sampled were mature, characterized by fully expanded leaves, and immature to mature fruits. Although there is variation in individual plant architecture, as noted in studies of Saudi *S. incanum* populations (AL-Rowaily et al., 2021), the general morphology of the mature plants sampled was 3–5 main stems with numerous leaves (estimated > 30–50 per plant) and fruit clusters (Fig. 2). Plant materials collected from different locations were combined and thoroughly homogenized into one composite sample for each respective plant part to ensure representativeness for chemical and biological analyses, accounting for natural intra-species variability. The pooling strategy herein adopted is a common approach in phytochemical screening in order to have a representative profile of the species from the region.

The specific collection sites were at an altitude of approximately 2,000 meters above sea level. In period collection, the region experiences a climate with temperatures ranging from 24 °C to 35 °C and an average rainfall of about 18 mm. The plants were growing in an open area with full sunlight exposure on soils with textures ranging from clay loam to loamy to sandy loam.

The plants were identified according to the key diagnostic morphological features described for the *S. incanum* complex by Samuels, 2012; Kannan et al., 2023. These features include: the presence of sharp, broad-based prickles on stems and midribs; ovate to elliptic leaves with sinuate or lobed margins covered in stellate hairs. Fruits were spherical berries, approximately 2–3 cm in diameter, exhibiting characteristic white streaks on a green background. Such a morphological profile agrees with the description of *S. incanum* from the southwestern highlands of Saudi Arabia given by El-Shaboury et al., 2021 and ALshaqhaa et al. 2023. Such a plant was taxonomically recognized and verified by Dr. Haidar Abd Al Gadir of the Biology Department, Al-Baha University, where voucher specimens (voucher number: ABUSI-1023) were deposited in the university herbarium for future reference.

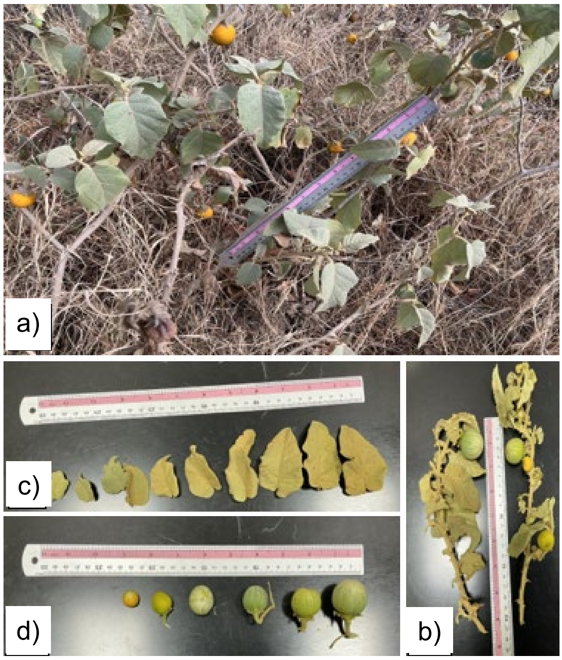

Figure 2. *S. Incanum* (a) whole plant in field (b) branch of plant (c) leaves (d) Fruits.

Determination of phytochemical components

Plant samples were shade dried and separately ground into fine powder using a mechanical grinder and then stored in airtight containers. To ensure a representative sample for chemical and biological analyses, the plant materials(leaves, stem-bark, and fruits) collected from the various locations were combined and thoroughly homogenized into a single composite sample for each respective plant part. A 15 g of powder from each plant part (leaves, stem-bark and fruits) was defatted with n-hexane then extracted three times by exhaustive maceration in 150 mL of 80% methanol for 48 hours on an shaker (150 rpm). Following filtration, the filtrates were concentrated to dryness under reduced pressure at 40 °C using a rotary evaporator (Buchi, USA). The resulting crude extract was stored in amber glass vials at 4 °C to protect it from light and degradation for pending analysis (Fig. 3).

Figure 3. Different plant parts (leaves, fruits and stem-barks) ground and their extracts.

For the quantitative assays, the total phenolic, flavonoid, tannin, and alkaloid content were determined spectrophotometrically. Each extract was analyzed in triplicate (n = 3 analytical replicates), and the results are expressed as the mean ± standard deviation (SD).

Determination of total polyphenols. The quantification of total phenolic content was performed by means of the Folin-Ciocalteu calorimetric (Cicco et al., 2019). A 200 µl of extract (0.5 mg mL^{-1}) in methanol was added with 1.5 mL diluted Folin-Ciocalteu reagent (1:10) and mixed and allowed to equilibrate for 1–2 minutes. A 2.5 mL sodium carbonate (2.0 10^{-1}) was added to the test tube and incubated at room temperature for 30 minutes. The absorbance of the generated solution was measured at 760 nm using water as a blank. The results were calculated based upon a gallic acid standard curve ($y = 0.7962x – 0.0372$, $R^2 = 0.9794$).

Determination of total flavonoids. The total flavonoid content was determined using the aluminum chloride colorimetric method (Pothitirat et al., 2009). In short, 1 mL of each extract was combined with 1 mL of the aluminum chloride solution ($2.0 \cdot 10^{-2}$). The mixture was incubated at room temperature for 10 min, and the absorbance was read at 415 nm. Quantification was based on a standard curve for quercetin ($y = 1.4712x – 0.2389$, $R^2 = 0.9887$).

Determination of tannins. The tannin content was assessed through the vanillin-HCl method (Rebaya et al., 2014), by mixing 12.5 µl of the extract with a solution of 1% vanillin (w/v) at a volume of 750 µl, and adding 375 µl of 8% HCl (v/v). After 15 minutes of incubation at room temperature, the absorbance was read at 500 nm. Catechin standard curve = ($y = 2.2648x + -0.2069$; $R^2 = 0.9934$).

Determination of total alkaloids. According to the procedure given by Shamsa et al. in 2008, total alkaloid content was determined for each suspension. To prepare the samples, 1 mg of each respective plant extract was dissolved in 2N HCl and filtered. From the filtrate, 1 mL was taken with 5 mL of phosphate buffer (pH 4.7), to which 5 mL of bromocresol green (BCG) solution was added at the same time (final concentration was 10-4 M). For the extracts, dilution was done with chloroform (*10), and the absorbance was measured at 470 nm. Atropine was used as the standard ($y = 0.9011x – 0.1097$ $R^2 = 0.9923$).

Biological activities and Gas Chromatography-Mass Spectrometry analysis (GC-MS)

The plant powder of each part was soaked in ethanol (70%, two weeks, 3 times) at room temperature. The resulting residues were filtered, pooled and evaporated to dryness under reducing pressure at 45 °C to afford a green viscous syrup. The crude extract so obtained, was transferred on Petri plate, allowed to dry and finally weighed. The crude ethanol extract was suspended in distilled water and defatted with n-hexane. The defatted ethanol extract was further fractionated by using Chloroform, ethyl acetate and n-butanol, respectively to afford n-hexane fraction, Chloroform fraction, ethyl-acetate fraction, and water fraction. It is important to point out that the use mixture of solvents (Ethanol 70%) throughout all extraction process to assure the extraction of all polar and non-polar compounds.

Gas chromatography-mass spectrometry analysis. An analysis using GC-MS was performed on a Shimadzu GCMS-QP2010-Ultra, featuring an Rtx-5ms capillary column (30 m × 0.25 mm × 0.25 µm). Helium was used as the carrier gas, with a flow rate of 1.61 mL min^{-1}. A 1 µl sample was injected in split mode (injector temperature: 300 °C). The temperature program was as follows in the GC oven: 60 °C (held for 0 min), ramped up to 300 °C at 10 °C min^{-1}, and held for 3 min (total run time: 26 min). The MS interface was maintained at 250 °C and the ion source was kept at a temperature of 200 °C. Mass spectra were obtained throughout the entire scan range of m/z 40–500. Compounds were identified from mass spectral and retention index values from the NIST (National Institute of Standards and Technology) mass spectral library. GC-MS analysis was performed on a single injection per composite sample for the qualitative identification of constituents. The relative abundances reported are based on the peak area percentage of the total ion count from a single run and should be interpreted as indicative.

Antimicrobial assay. The antimicrobial potential of the plant extracts was examined through the agar disc diffusion method, as previously described by the Clinical and Laboratory Standards Institute (CLSI; formerly National Committee for Clinical Laboratory Standards (NCCLS), 2006). To obtain bacterial suspensions, the density of bacterial cell suspensions was adjusted to 10^8 CFU mL^{-1} (0.5 McFarland standard) using a sterile saline. A 100 µl sample of each suspension was evenly spread on the surface of Mueller-Hinton Agar (MHA) plates and allowed to dry in a sterile cabinet for 5 min. Following this, discs of sterile filter paper (6 mm diameter) were placed onto the inoculated agar and impregnated with 20 µl of the extract's solution. The plates were inverted and incubated at 37 °C for 24 hours. The same methodology was used for the control plates inoculated with pathogen strains resistant to the extracts. Following incubation the diameters of inhibition zones were measured. Antimicrobial activity was interpreted according to the following criteria: inactive (< 9 mm), partially active (9–12 mm), active (13–18 mm), and very active (> 18 mm; Mukhtar & Ghori, 2012).

Antioxidant activity. To assess antioxidant potentials, the DPPH (2, 2-diphenyl-1-picrylhydrazyl) free radical scavenging test is used. DPPH radical scavenging was carried out using the method established by Shimada et al., 1992. Using a 96 well plate, test samples were allowed to react with stable free radical (DPPH) at 37 °C for 30 minutes. DPPH concentration was held constant at 300 µM. Test samples were prepared in dimethyl sulfoxide (DMSO), while DPPH was dissolved in ethanol. After the incubation period, the decrease in absorbance was measured at 517 nm using a multiplate reader spectrophotometer. The % radical scavenging activity of samples was calculated as compared to the control group which was treated with DMSO. All tests and analyses were performed in triplicate.

Statistical analysis

All quantitative experiments were performed with at least three independent replicates ($n \geq 3$). Data are presented as the mean ± standard deviation (SD). At the probability level < 0.05, significant differences between the means of the various treatments were determined using ANOVA analysis and Tukey's *HSD* tests. SPSS software version 20.1 (IBM version 20.0.2004) was used.

RESULTS AND DISCUSSION

Total polyphenols content

Alkaloids, phenols, tannins, and flavonoids have been found in various plant parts of *S. incanum*, according to a number of recent studies (Akanmu et al., 2021; Karanja et al., 2021; Musyimi et al., 2021). The content of phytochemical components in different plant parts was illustrated in Table 1. Results showed a higher content of polyphenols in all plant parts referring to flavonoid, tannin and alkaloid levels. As summarized in Table 1, the leaves consistently contained the highest levels of all quantified phytochemicals, polyphenols, flavonoids, tannins, and alkaloids, followed by the fruits. The stem-bark exhibited significantly lower concentrations of these bioactive compounds compared to the other plant parts.

Table 1. Total polyphenol, flavonoid, tannin and alkaloid contents in different parts of *Solanum incanum***.** Columns with different letters (a, b, c) for each variable differ significantly according to Tukey's test ($p < 0.05$)

Plant part	Poyphenols (mg GAE per g DW)	Flavonoids (mg QE per g DW)	Tannins (mg CE per g DW)	Alkaloids (mg AE per g DW)
Leaves	9.0 ± 0.01^{a}	7.6 ± 0.12^{a}	3.6 ± 0.08^{a}	4.6 ± 0.04^{a}
Stem-bark	3.3 ± 0.02^{c}	1.8 ± 0.00^{c}	1.6 ± 0.02^{b}	2.2 ± 0.03^{c}
Fruits	7.6 ± 0.05^{b}	5.8 ± 0.05^{b}	3.0 ± 0.06^{a}	3.1 ± 0.01^{b}

As reported in Table 1 and according to Chivodze et al., qualitative phytochemical analysis showed that various plant parts of *S. incanum* contained phenols, flavonoids, coumarins, and condensed tannins. These diverse phytochemical types have important medicinal uses and could help researchers create new medications against various disorders (Saboon et al., 2019). Furthermore, the environment, climate, and plant organ all had a significant impact on the biochemical components, particularly polyphenolics and flavonoids (Ivanova et al., 2022).

Gas chromatography-mass spectrometry analysis (GC-MS) in hexane fraction in different plant parts

Table 2 listed the 19 compounds that were present in leaves. The two main compounds found in the leaf hexane fraction were 9, 12, 15-Octadecatrienoic acid, methyl ester (20.07%), and hexadecanoic acid, methyl ester (26.84%). In leaf hexane fraction, the 9, 12-Octadecadienoic acid (Z, Z)-, methyl ester and squalene levels were about 12.09%. Some trace compounds were also reported. Eleven compounds were identified via volatile metabolites in the fruit hexane fraction (Table 3). The predominant component was 9-Octadecenoic acid (Z)-, methyl ester (48.78%), followed by Hexadecanoic acid, methyl ester (18.92%). Table 4 displayed the identification of 20 compounds within the stem-bark n-hexane fraction. The predominant compound was Hexadecanoic acid methyl ester, which constituted 31.82% of the total fraction. Additionally, the 9, 12-Octadecadienoic acid (Z, Z)-methyl ester was present at a significant level of 29.08%. Other compounds were found in smaller quantities.

Table 2. GC-MS Analysis showing the chemical constituents in leaf extract of n-hexane fraction

Peak No.	Compound	Retention time (RT)	Relative abundance (%)	Formula	Major mass spectral data m/z
5	Hexadecanoic acid, methyl ester	16.387	26.84	$C_{17}H_{34}O_2$	41, 57, 74, 87, 143
11	9,12,15-Octadecatrienoic acid, methyl ester	18.216	20.07	$C_{19}H_{32}O_2$	41, 55, 67, 79, 95, 108
9	9,12-Octadecadienoic acid (Z,Z)-, methyl ester	18.139	12.09	$C_{19}H_{34}O_2$	41, 55, 67, 81, 95, 109
19	Squalene	24.329	12	$C_{30}H_{50}$	41, 69, 81, 95
13	Methyl stearate	18.404	6.46	$C_{19}H_{38}O_2$	41, 43, 57, 74, 87, 298
12	Phytol	18.324	5.51	$C_{20}H_{40}O$	41, 57, 71, 95, 123
10	9-Octadecenoic acid (Z)-, methyl ester	18.182	4.69	$C_{19}H_{36}O_2$	41, 55, 69,74, 97, 98
18	Gamma-Sitosterol	23.982	4.53	$C_{29}H_{50}O$	41, 43, 57, 81, 95, 107, 145, 161, 213, 303, 414
4	4-Hexadecen-6-yne (Z)-	16.159	1.4	$C_{16}H_{28}$	41, 43, 67, 79, 93, 107
17	Stigmasterol	22.84	1.39	$C_{29}H_{48}O$	41, 55, 69, 83, 91, 105, 119, 133, 145, 159, 412
1	Methyl tetradecanoate	14.175	1.01	$C_{15}H_{30}O_2$	41, 57, 74, 87
8	Heptadecanoic acid, methyl ester	17.418	0.85	$C_{18}H_{36}O_2$	41, 57, 74, 87
14	Eicosanoic acid, methyl ester	20.26	0.85	$C_{21}H_{42}O_2$	41, 43, 57, 74, 87, 143
16	Docosanoic acid, methyl ester	21.961	0.67	$C_{23}H_{46}O_2$	41, 43, 57, 74, 87, 143
15	Phenol, 2-2'methylenebis[6-(1,1-dimethylethyl)-4-methyl-Cresol	21.285	0.45	$C_{23}H_{32}O_2$	57, 149, 164, 177, 340
6	Hexadecanoic acid, 14-methyl-, methyl ester	17.134	0.44	$C_{18}H_{36}O_2$	27, 41, 57, 74, 87
3	2-Pentadecanone,6,10,14-trimethyl-Hexahydrofarnesyl acetone	15.542	0.37	$C_{18}H_{36}O$	41, 43, 58, 71, 85
2	Pentadecanoic acid, methyl ester	15.307	0.18	$C_{16}H_{32}O_2$	41, 57, 74, 87
7	Cis-10-Heptadecenoic acid, methyl ester	17.206	0.18	$C_{18}H_{34}O_2$	27, 41, 55, 69, 97, 98

GC-MS analysis of different plant parts was illustrated in Table 2, 3 and 4. Results showed two major compounds in all plant parts of hexane fraction, with different level. The 9, 12, 15-Octadecatrienoic acid, methyl ester was revealed in all plant parts, but the highest level was identified in fruit extract (48.78%). The hexadecanoic acid, methyl ester presented a major compound in all plant parts, but the highest level was revealed in stem-bark fraction (31.82%). Usually, these bioactive substances were associated with possible antibacterial and antioxidant properties. Recently, Shaaban et al 2021 reported that hexadecanoic acid methyl ester had effective antibacterial activity against multidrug-resistant bacteria. Another study reported that seed oil from *Lepidium sativum* exhibited broad-spectrum antimicrobial activity and showed antioxidant and anti-inflammatory activities (Alqahtani et al., 2019). *Lepidium sativum* seed oil was found to contain both hexadecanoic acid methyl ester and 9,12-Octadecadienoic acid methyl ester (Alqahtani et al., 2019).

Table 3. GC-MS analysis showing the chemical constituents in fruit extract of n-hexane fraction

Peak No.	Compound	Retention time (RT)	Relative abundance (%)	Formula	Major mass spectral data m/z
6	9-12-Octadecadienoic acid (Z,Z)-, methyl ester	18.141	48.78	$C_{19}H_{34}O_2$	41, 55, 67, 81, 95, 294
2	Hexadecanoic acid, methyl ester	16.387	18.92	$C_{17}H_{34}O_2$	41, 57, 74, 87, 143
9	Methyl stearate	18.402	9.26	$C_{19}H_{38}O_2$	41, 43, 57, 74, 87, 298
7	9-Octadecenoic acid (Z)-, methyl ester	18.181	7.78	$C_{19}H_{36}O_2$	41, 55, 69, 74, 97, 98
8	9,12,15-Octadecatrienoic acid, (Z,Z,Z)- methyl ester	18.214	6.29	$C_{18}H_{30}O_2$	55, 67, 79, 95, 108
10	11,14-Eicosadienoic acid, methyl ester	18.628	4.71	$C_{21}H_{38}O_2$	41, 55, 67, 81, 95, 109
3	n-Hexadecanoic acid	16.851	2.24	$C_{16}H_{32}O_2$	43, 60, 73, 85, 129
11	Eicosanoic acid, methyl ester	20.251	1.05	$C_{21}H_{42}O_2$	41, 43, 57, 74, 87, 326
5	Heptadecanoic acid, methyl ester	17.416	0.61	$C_{18}H_{36}O_2$	41, 57, 74, 87, 143
1	9-Hexadecenoic acid, methyl ester, (Z)	16.19	0.23	$C_{17}H_{32}O_2$	41, 55, 69, 74, 96
4	Hexadecanoic acid, 14-methyl-, methyl ester	17.039	0.13	$C_{18}H_{36}O_2$	41, 57, 74, 87, 284

In the leaves of pink flowered *c. roseus*, GC-MS analysis reported the presence of 9,12,15-Octadecatrienoic acid, methyl ester. Additionally, pink-flowered *C. roseus* exhibited higher levels of total flavonoid and phenolic content, which were linked to significant antioxidant activity (Rani & Kapoor, 2019). Recently, Ilozue et al., 2024 reported on the GC-MS profiling of wo herbal mixtures marketed for the treatment of Staphylococcus infection and typhoid and malaria. The study revealed the presence of 9-Octadecenoic acid (Z)-, methyl ester, among other active compounds. The presence of this compound, along other active compounds, helps to explain the various pharmacological activities of these herbal drugs.

GC-MS analysis of leaf extract of *Catharanthus roseus* and *Moringa oleifera* revealed the presence of 9-Octadecenoic acid (Z)-, methyl ester. The presence of this compound, along with other active compounds, has been associated with important antioxidant and antimicrobial activity (Syeda & Riazunnisa, 2020).

Additionally, GC-MS analysis has indicated a rich profile of fatty acid methyl esters in *S. incanum,* dominated by Hexadecanoic acid methyl ester (palmitic acid) and different octadecadienoic/trienoic acid methyl esters (linoleic/ linolenic acids) in all analyzed parts of the plant. Comparison of these results with other medicinal plants, and specifically with the Lepidium genus, adds to the potential bioactivity of the studied extracts. Accordingly, the main compounds identified in *S. incanum*, have a close similarity to the various Lepidium species reported for their pharmacological activities. For example, Hexadecanoic acid, methyl ester, which is a major component in the *S. incanum* stem-bark (31.82%), leaves (26.84%), and fruits (18.92%), has been reported as a major compound in *Lepidium sativum* seed oils by Getahun et al. (2020) and Akash & Singh (2017), and Kumar et al. (2020). This is commonly known for its antimicrobial and anti-inflammatory activities (Shaaban et al., 2021; Alqahtani et al., 2019). Also, linoleic acid was a dominant constituent in *S. incanum* stem-bark (29.08%) and leaves

(12.09%). This compound is also a major component of the *L. sativum* seed oil, as proved in different studies (Getahun et al., 2020; Kumar et al., 2020). 9,12,15-Octadecatrienoic acid, methyl ester (linolenic acid), dominant in *S. incanum* leaves at 20.07% and fruits at 6.29%, is also reported in *L. sativum* (Kumar et al., 2020).

Table 4. GC-MS analysis showing the chemical constituents in stem-bark extract of n-hexane fraction

Peak No.	Compound	Retention time (RT)	Relative abundance (%)	Formula	Major mass spectral data m/z
8	Hexadecanoic acid methyl ester	16.39	31.82	$C_{17}H_{34}O_2$	41, 57, 74, 87, 143
11	9,12-Octadecadienoic acid (Z,Z)-, methyl ester	18.142	29.08	$C_{19}H_{34}O_2$	41, 55, 67, 81, 95
13	9,12,15-Octadecatrienoic acid, methyl ester	18.221	12.23	$C_{19}H_{32}O_2$	79, 67, 95, 93, 108
15	Methyl stearate	18.406	7.85	$C_{19}H_{38}O_2$	41, 43, 57, 74, 87, 143
20	Gamma-Sitosterol	23.981	4.63	$C_{29}H_{50}O$	41, 43, 57, 81, 95, 107, 145, 213, 303, 414
14	Phytol	18.325	2.57	$C_{20}H_{40}O$	41, 43, 57, 71, 123
12	9-Octadecenoic acid (Z)-, methyl ester	18.17	1.93	$C_{19}H_{36}O_2$	41, 55, 69, 74, 97, 98
16	Eicosanoic acid, methyl ester	20.26	1.56	$C_{21}H_{42}O_2$	41, 43, 57, 74, 87, 143
17	Phenol, 2,2'-methylenebis[6-(1,1-dimethyl)-4-methyl-cresol	21.285	1.53	$C_{23}H_{32}O_2$	41, 57, 91, 121, 149, 161, 177, 340
19	Stigmasterol	22.841	1.39	$C_{29}H_{48}O$	55, 69, 83, 97, 255, 412
1	Methyl tetradecanoate	14.18	0.95	$C_{15}H_{30}O_2$	41, 55, 57, 74, 87
10	n-Nonadecanol-1	18.029	0.84	$C_{19}H_{40}O$	41, 55, 83, 97, 111
9	Heptadecanoic acid methyl ester	17.422	0.81	$C_{18}H_{36}O_2$	41, 57, 74, 87, 143
3	5-Octadecenoic acid, methyl ester	15.145	0.55	$C_{19}H_{36}O_2$	41, 67, 74, 96, 98
4	Pentadecanoic acid, methyl ester	15.31	0.45	$C_{16}H_{32}O_2$	41, 57, 74, 87
18	Docosanoic acid methyl ester	21.96	0.44	$C_{23}H_{46}O_2$	41, 43, 57, 74, 87, 143
5	2-Pentadecanone, 6,10,14-trimethylpentadecane	15.544	0.39	$C_{18}H_{36}O$	41, 43, 58, 71, 85
6	Pentadecane	16.077	0.33	$C_{15}H_{32}$	41, 43, 57, 71, 85
7	9-Hexadecenoic acid, methyl ester, (Z)-methyl palmitoleate	16.195	0.33	$C_{17}H_{32}O_2$	55, 69, 87, 98
2	Tetradecane	14.986	0.31	$C_{14}H_{30}$	41, 43, 57, 71, 85

Compounds in *S. incanum*, like Methyl stearate and Pentadecanoic acid, methyl ester, have also been recorded in *Lepidium cartilagineum* (Dávid et al., 2024). This comparative analysis underlines the fact that the high concentration of shared bioactive fatty acid esters between *S. incanum* and well-documented Lepidium species suggests a significant antioxidant and antimicrobial activities. Thus, the presence of such compounds known to contribute to the therapeutic effects of established medicinal plants reinforces the potential of S. *incanum* as a valuable source of natural bioactive agents.

Antimicrobial activity of different plant parts

In this study, the antimicrobial activity of four selected fractions of *Solanum incanum* was assayed *in vitro* by agar disc diffusion method against four bacterial species

(*E. coli, Pseudomonas aeruginosa, Bacillus subtilis* and *Staphylococcus aureus*) and one fungus (C*andida. albicana*). The Fig. 4 showed results of antimicrobial activity of different fractions of each plant part (leaves, fruits and stem-bark). The chloroform, ethyl acetate, and n-hexane fractions of the leaves exhibited the broadest spectrum of inhibitory activity, with mean inhibition zones ranging from 14 to 18 mm against all tested bacterial strains and *C. albicans*, indicating strong antimicrobial potential. The three fractions of fruits (chloroform, ethyl acetate and n-hexane) had good activity against all microorganisms with inhibition zone ranged between 15–18 mm. Aqueous fraction of fruit was inactive against *Bacillus subtilis*, *Escherichia coli* and *Pseudomonas aeruginosa*. Stem-bark aqueous fraction was partially active against *Staphylococcus aureus* and *Candida albicans.* The ethyl acetate and n-hexane fractions of stem-bark were active against all tested microorganisms. Chloroform fraction exhibited good activity against *Staphylococcus aureus* and C*andida albicana* only. The aqueous fraction of the strain was partially active against *Staphylococcus aureus* and *Candida albicans* and not active against the other microorganisms tested.

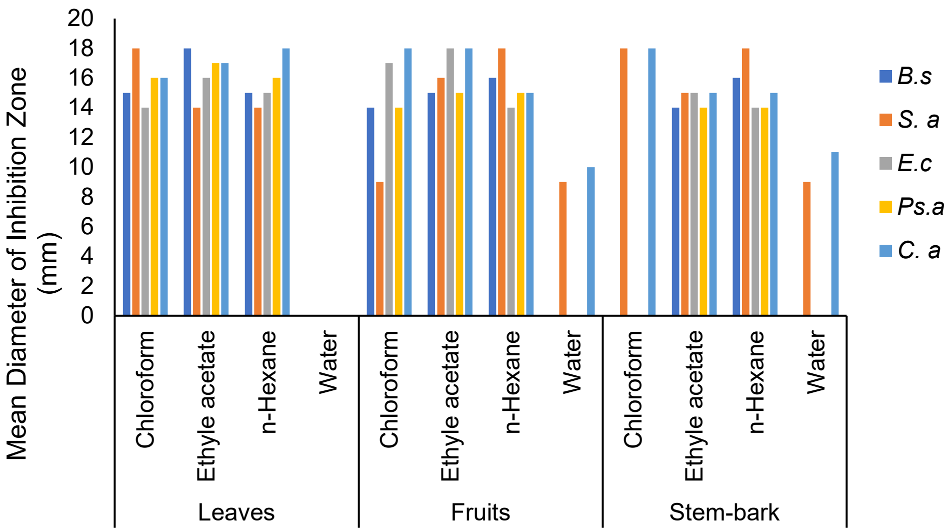

Figure 4. Antimicrobial activity of *Solanum incanum* against standard microorganisms.
(E. c.: Escherichia coli ATCC 25922; P. a.: Pseudomonas aeruginosa ATCC 27853; S. a.: Staphylococcus aureus ATCC 25923; B. s.: Bacillus subtilis ATCC 2836; C.a: Candida albicans). Mean diameter of growth inhibition zone in (mm) (conc. 2 mg/disc).

The current study found that ethyl acetate and n-hexane fractions of stem-bark were active against all microorganisms tested. Only *Staphylococcus aureus* and *Candida albicana* were susceptible to the chloroform fraction. The aqueous fraction of stem-bark was partially active against *Staphylococcus aureus* and *Candida albicans* but inactive against the other microorganisms tested. The significant inhibition zones produced by the ethyl acetate and n-hexane fractions, particularly from fruits and leaves, suggest the presence of potent antimicrobial compounds. While the disc diffusion method effectively identifies bioactive extracts, future research is essential to determine the

Minimum Inhibitory Concentration (MIC) and Minimum Bactericidal Concentration (MBC) of these promising fractions to fully quantify their antibacterial and antifungal efficacy.

Solanum incanum has been shown in several studies to have antimicrobial activity (Karanja et al., 2021). Microbial activity in *Solanum incanum* varied according to plant part and extract fraction. In 2017, Sahle & Okbatinsae discovered anti-fungal and antibacterial activity in ethyl acetate, ethanol, chloroform, petroleum ether, and water fruit extracts. Ethyl acetate, ethanol, and chloroform fruit extracts outperformed aqueous extracts. In the present study, the aqueous fraction was less effective than the chloroform, ethyl acetate, and n-hexane fractions in leaves, stem-bark, and fruits. While in stem-bark and fruits, the aqueous fraction was partially active against *Staphylococcus aureus* and *Candida albicans*. The efficacy of fruit extracts is consistent with previous reports; for instance, Karanja et al. (2021) demonstrated their activity against plant pathogens, while Indhumathi & Mohandass (2014) reported potent antimicrobial activity in a crude ethanol extract. The crude ethanol extract showed the highest antibacterial activity (26 mm) against *Staphylococcus aureus* and also showed good antibacterial activity (10–25 mm) against all pathogenic bacteria.

The hydroacetone extract was also reported to be very efficient for the prevention and treatment of microbial diseases in poultry (Séré et al., 2022). Furthermore, Karanja et al reported that *S. incanum* had remarkable antimicrobial activity (Karanja et al., 2021). Additionally, Ateshim et al. found that the chloroform extract from *S. incanum* roots revealed important antibacterial activity against *S. aureus* (Ateshim, & Tekle, 2022). In a study by Jepkoech & Gakunga, methanolic extracts from *S. incanum* fruits displayed greater antibacterial activity compared to aqueous extracts against *S. aureus* (Jepkoech & Gakunga, 2017). In 2021, Musyimi et al. reported that seed ethanoic extract was the most effective for antimicrobial activity against *E. coli* and *S. aureus*. Furthermore, in 2024, Melliti et al., reported that stem and leaf methanolic extract of tunisian *Pancratium maritimum* was rich in alkaloids and showed excellent antibacterial and antifungal potentials within its alkaloid fractions (Melliti et al., 2024).

Antioxidant activity

DPPH was used to measure the antioxidant activity of different fractions. Strong antioxidant activity was demonstrated by various fractions of ethanolic extracts of leaves, stem bark, and fruits. Among all tested fractions, the ethyl acetate fractions of fruits (89 ± 0.01%) and leaves (86 ± 0.07%) exhibited the highest antioxidant activity (Fig. 5). The aqueous fraction of fruits (83 ± 0.01) and leaves (85 ± 0.01) also showed significant antioxidant activity. Whereas, the stem-bark's n-hexane fraction had the lowest antioxidant activity (09 ± 0.0). The ethyl acetate fraction of fruits and leaves showed the best antioxidant activity, which can be attributed to the higher content of polyphenolic compounds detected in leaves and fruits (Table 1). Škrovánková et al found a strong positive correlation between free polyphenols levels and antioxidant capacity in pseudocereals such as amaranth, buckwheat, and quinoa (Škrovánková et al., 2020). Additionally, Chivodze et al., demonstrated that ethyl acetate fraction of leaves exhibited a high reducing antioxidant capacity, which was associated with the presence of high level of polyphenols in leaves (Chivodze et al., 2021). Leaf and fruit extracts contained high levels of flavonoids (Table 1).

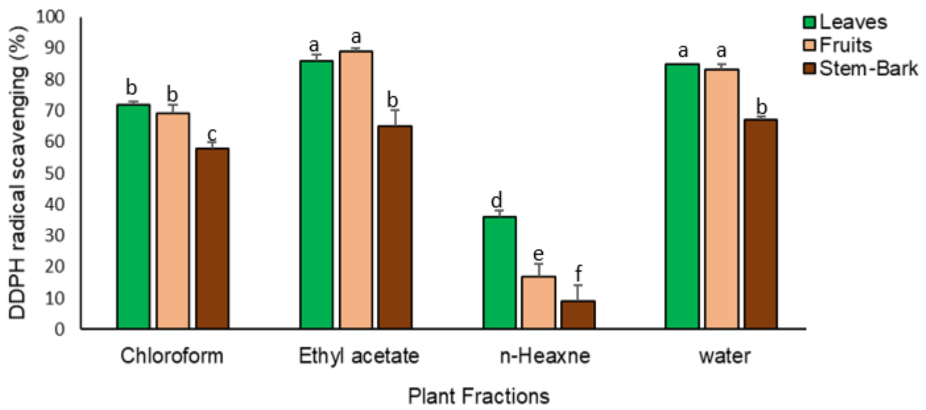

Figure 5. *In vitro* antioxidant activity of different *Solanum incanum* fractions measured by DPPH radical scavenging assay. Data are presented as mean % scavenging ± standard deviation (n = 3). Different lowercase letters above the bars indicate statistically significant differences among the fractions as determined by ANOVA followed by Tukey's HSD test ($p < 0.05$).

To quantitatively establish the relationship between phytochemical composition and antioxidant efficacy, a Pearson correlation analysis was done. The resulting matrix, shown in Table 5, indicates an extremely strong positive correlation between the total phenolic content and the antioxidant activity across most fractions, especially for the chloroform and water fractions, with r = 0.999 and 0.991, respectively.

Table 5. Pearson correlation matrix (r-values) between the antioxidant activity of solvent fractions and the phytochemical content of *Solanum incanum* extracts

Variable	AOX-CHF	AOX-EA	AOX-HEX	AOX-W	POLY	FLAV	TANN
AOX-EA	0.949						
AOX-HEX	0.853	0.645					
AOX-W	0.995	0.977	0.794				
POLY	0.999	0.938	0.869	0.991			
FLAV	0.995	0.912	0.902	0.979	0.998		
TANN	0.996	0.916	0.897	0.981	0.998	1.000	
ALK	0.895	0.710	0.996	0.844	0.909	0.936	0.932

Abbreviations: AOX: Antioxidant activity; CHF: Chloroform fraction; EA: Ethyl acetate fraction; HEX: n-Hexane fraction; W: Water fraction; POLY: Total polyphenols; FLAV: Total flavonoids; TANN: Total tannins; ALK: Total alkaloids. Values of |r| > 0.87 indicate a very strong positive correlation ($p < 0.05$).

Similarly, flavonoid and tannin content showed very strong associations, establishing that these polyphenolic compounds are the major contributors to the radical scavenging activity of *S. incanum*. The sole notable exception was the n-hexane fraction, whose antioxidant activity was less strongly linked with polyphenols but very strongly associated with alkaloid content (r = 0.996), suggesting a solvent-dependent bioactivity of non-polar alkaloids as dominant antioxidants in the n-hexane fraction, while polyphenols were dominant in more polar fractions.

Flavonoids are phenolic substances derived from a variety of vascular plants that act as antioxidants and antimicrobials (Hassanpour & Doroudi, 2023). Akanmu et al. 2021 reported that aqueous and methanolic extracts from the fruits of *S. incanum* had significant DPPH radical scavenging activity, especially the aqueous extract. Current study revealed too, that leaf and fruit extracts had the highest tannin content referring to stem-bark (Table 1). The high level of alkaloids in fruits and leaves could be related too to the high antioxidant capacity in these plant parts (Table 1). Antasionasti et al. suggested that antioxidant activity is strongly influenced by the tannin, total flavonoid, and total phenolic contents (Antasionasti et al., 2021).

CONCLUSIONS

Current results indicated that methanolic extracts of various plant parts of *S. incanum* collected from the Al-Baha region are rich in polyphenols, flavonoids tannins and alkaloids, especially leaves and fruits. In addition, GC-MS analysis revealed the presence of two major compounds across all plant parts: the 9, 12, 15-Octadecatrienoic acid, methyl and the hexadecanoic acid, methyl ester. The presence of these compounds, along with other active constituents, explains the diverse pharmacological activities of the studied plant. Interestingly enough, high levels of total phenolic, flavonoid, tannin, and alkaloid content, especially in the leaves and fruits correspond to the significant antimicrobial and antioxidant activities observed in these parts. In general, the strong inhibitory activity observed against several pathogens positions the leaf and fruit extracts, especially in ethyl acetate and n-hexane fractions, as prime candidates for further isolation of active compounds and determination of their MIC)/ MBC values.

REFERENCES

Ahmadi, E.S., Tajbakhsh, A., Iranshahy, M., Asili, J., Kretschmer, N., Shakeri, A. & Sahebkar, A. 2020. Naphthoquinone derivatives isolated from plants: recent advances in biological activity. *Mini reviews in medicinal chemistry* **20**(19), 2019–2035. https://doi.org/10.2174/1389557520666200818212020

Akanmu, A.O., Sodipo, O.A., Sandabe, U.K., Shamaki, B.U., Balogun, S.T. & Akinwunmi, K.F. 2021. Proximate and elemental analyses, phytochemical screening and antioxidant activities of aqueous and ethanol extracts of solanum incanum linn. fruits. *Bulletin of Pharmaceutical Sciences Assiut University* **44**(1), 49–62. doi: 10.21608/bfsa.2021.174130

Akash, S.S. & Singh, S.K. 2017. Phytoconstituents estimation of Lepidium sativum L. seed extract using GC-MS spectroscopy. *World J. Pharm. Res.* **7**, 1360–1367. doi: 10.20959/wjpr20181-10538

Alqahtani, F.Y., Aleanizy, F.S., Mahmoud, A.Z., Farshori, N.N., Alfaraj, R., Al-Sheddi, E.S. & Alsarra, I.A. 2019. Chemical composition and antimicrobial, antioxidant, and anti-inflammatory activities of Lepidium sativum seed oil. *Saudi journal of biological sciences* **26**(5), 1089–1092. https://doi.org/10.1016/j.sjbs.2018.05.007

AL-Rowaily, S.L., Alghamdi, A.O., Alghamdi, S.S. & Al-Barty, A.M. 2021. Assessment of morphological and molecular variability of some *Solanum melongena* L. cultivars and wild *Solanum incanum* L. in Saudi Arabia. *BIOLOGIA FUTURA* **72**(2), 187–199. https://doi.org/10.1007/s42977-020-00052-2

ALshaqhaa, M., Alwhibi, M., Afzal, M. & Alshaharni, M.O. 2023. Morphological and molecular barcoding characterization of four invasive species of Solanaceae in the Southern region of Saudi Arabia. *Biomedical Sciences and Clinical Research* **2**(3), 275–285.

Andargie, Y., Sisay, W., Molla, M. & Tessema, G. 2022. Evaluation of antidiabetic and antihyperlipidemic activity of 80% methanolic extract of the root of Solanum incanum linnaeus (solanaceae) in mice. *Evidence-Based Complementary and Alternative Medicine* **2022**(1), 4454881. https://doi.org/10.1155/2022/4454881

Antasionasti, I., Datu, O.S., Lestari, U.S., Abdullah, S.S. & Jayanto, I. 2021. Correlation analysis of antioxidant activities with tannin, total flavonoid, and total phenolic contents of nutmeg (myristica fragrans houtt) fruit precipitated by egg white. *Borneo Journal of Pharmacy* **4**(4), 301–310. https://doi.org/10.3390/antiox10101530.

Ateshim, B. & Tekle, F. 2022. Evaluation of antimicrobial activity and phytochemical screening of *Silene macrosolen* and *Solanum incanum*: a common medicinal plant in Eritrea. *J. Bacteriol Mycol Open Access* **10**(1), 15–20.

Augšpole, I., Dūma, M. & Ozola, B. 2018. Bioactive compounds in herbal infusions. *Agronomy Research* **16**(S2), 1322–1330. http://dx.doi.org/10.15159/ar.18.013.

Chaachouay, N. & Zidane, L. 2024. Plant-derived natural products: a source for drug discovery and development. *Drugs and Drug Candidates* **3**(1), 184–207. doi: 10.3390/ddc3010011

Chivodze, R.S., Sulemane, A.I., Magaia, I., Saete, V.N., Rugunate, S.C., Zimila, H.E. & Munyemana, F. 2022. Phytochemical screening and Evaluation of Antioxidant and Antimicrobial Activity of Solanum linnaeanum Extracts. *Tropical Journal of Natural Product Research (TJNPR)* **6**(2), 194–201. doi: 10.26538/tjnpr/v6i2.5.

Cicco, N., Lanorte, M.T., Paraggio, M., Viggiano, M. & Lattanzio, V. 2009. A reproducible, rapid and inexpensive Folin–Ciocalteu micro-method in determining phenolics of plant methanol extracts. *Microchemical journal* **91**(1), 107–110. doi: 10.1016/j.microc.2008.08.011

Dávid, C.Z., Cui, Z., Veres, K., Kincses, A., Kúsz, N., Barta, A., ... & Vasas, A. 2024. Phytochemical and pharmacological investigation of the non-volatile compounds of Lepidium cartilagineum (JC Mayer) Thell. and determination of the essential oil composition of its flowers and fruits. *Fitoterapia* **179**, 106236. doi: 10.1016/j.fitote.2024.106236

de Oliveira, A.P., Guimaratilde, L., Turatti, I.C.C., Lopes, N.P. & da Silva Almeida, J.R.G. 2015. GC-MS analysis of esterified fatty acids obtained from leaves of wild and cultivated specimens of Leonotis nepetifolia. *Journal of Medicinal Plants Research* **9**(16), 525–530. doi: 10.5897/JMPR2014.5550

Di Meo, S., Venditti, P., Victor, V.M. & Napolitano, G. 2022. Harmful and beneficial role of El-Shaboury, G.A., Al-Wadi, H.M. & Badr, A. 2021. Biodiversity of some *Solanum* species from southwestern Saudi Arabia's highlands. *Botany Letters* **168**(2), 246–255. https://doi.org/10.1080/23818107.2020.1846614

Espro, C., Paone, E., Mauriello, F., Gotti, R., Uliassi, E., Bolognesi, M.L., ... & Luque, R. 2021. Sustainable production of pharmaceutical, nutraceutical and bioactive compounds from biomass and waste. *Chemical Society Reviews* **50**(20), 11191–11207.

García-Sánchez, A., Miranda-Díaz, A.G. & Cardona-Muñoz, E.G. 2020. The role of oxidative stress in physiopathology and pharmacological treatment with pro-and antioxidant properties in chronic diseases. *Oxidative medicine and cellular longevity* **2020**(1), 2082145. https://doi.org/10.1155/2020/2082145

Getahun, T., Sharma, V. & Gupta, N. 2020. Chemical composition, antibacterial and antioxidant activities of oils obtained by different extraction methods from *Lepidium sativum* L. seeds. *Industrial Crops and Products* **156**, 112876. doi: 10.1016/j.indcrop.2020.112876

Hassanpour, S.H. & Doroudi, A. 2023. Review of the antioxidant potential of flavonoids as a subgroup of polyphenols and partial substitute for synthetic antioxidants. *Avicenna journal of phytomedicine* **13**(4), 354.

Ilozue, N.M., Okoye, P.A. & Ekpunobi, U.E. 2024. Phytochemical Evaluation, GC-MS Profiling and Antimicrobial Activity of Two Herbal Mixtures Marketed in Anambra State. *South Asian Research Journal of Natural Products* **7**(3), 184–196. Retrieved from https://journalsarjnp.com/index.php/SARJNP/article/view/152

Indhumathi, T. & Mohandass, S.J.I.J.C.M.A.S. 2014. Efficacy of ethanolic extract of *Solanum incanum* fruit extract for its antimicrobial activity. http://www.ijcmas.com/vol6/T.Indhumathi%20and%20S.Mohandass.pdf.

Ivanova, I., Serdyuk, M., Malkina, V., Tonkha, O., Tsyz, O., Mazur, B., ... & Havryliuk, O. 2022. Cultivar features of polyphenolic compounds and ascorbic acid accumulation in the cherry fruits (Prunus cerasus L.) in the Southern Steppe of Ukraine. doi: 10.15159/AR.22.065

Jepkoech, K.E. & Gakunga, N.J. 2017. Antimicrobial activity and phytochemical screening of Solanum incanum fruit extract against clinical samples of Staphylococcus aureus collecting from Nakuru Provincial General Hospital Laboratory, Kenya. *International Research Journal of Medicine and Biomedical Sciences*. https://doi.org/10.15739/irjmbs.17.001

Kannan, N., Gopi, D.K., Shanmugam, S.K., Narayana, S.K.K. & Shamsudin, A.K. 2023. Comparative macro-microscopic studies of three wild *Solanum* species (*S. melongena* L., *S. incanum* L. and *S. virginianum* L.). *Journal of Research in Siddha Medicine* **6**(1), 1–10. https://doi.org/10.4103/jrsm.jrsm_9_23

Karanja, L.N., K'Owino, I.O., Wangila, P.T. & Ramkat, R.C. 2021. Phytochemical Composition and Antibacterial Activity of Fruit Extract of Solanum incanum L. against Ralstonia solanacearum. https://doi.org/10.9734/ajacr/2021/v9i430218

Kim, H.W., Wang, M., Leber, C.A., Nothias, L.F., Reher, R., ... & Cottrell, G.W. 2021. NPClassifier: a deep neural network-based structural classification tool for natural products. *Journal of natural products* **84**(11), 2795–2807. doi: 10.1021/acs.jnatprod.1c00399

Kumar, V., Tomar, V., Ranade, S.A., Yadav, H.K. & Srivastava, M. 2020. Phytochemical, antioxidant investigations and fatty acid composition of *Lepidium sativum* seeds. *J. Environ Biol*. **41**(1), 59–65.

Lezoul, N.E.H., Belkadi, M., Habibi, F. & Guillén, F. 2020. Extraction processes with several solvents on total bioactive compounds in different organs of three medicinal plants. *Molecules* **25**(20), 4672. https://doi.org/10.3390/molecules25204672

Liu, X., Bian, L., Duan, X., Zhuang, X., Sui, Y. & Yang, L. 2021. Alantolactone: A sesquiterpene lactone with diverse pharmacological effects. *Chemical biology & drug design* **98**(6), 1131–1145. https://doi.org/10.1111/cbdd.13972

Maaroufi-Dguimi, H., Mohammed, S.G., Hajaji, A.N. & Abdalgadir, H. 2025. Efficiency of seed priming and co-treatment strategies in salt effect mitigation using Nicotiana glauca leaf extract on tomato seedlings (Solanum lycopersicum L.). *Agronomy Research* **23**(S2), 701–722, 2025 https://doi.org/10.15159/AR.25.014

Melliti, M., Musa, E.M., Skhiri, F. & Edziri, H. 2024. HPLC Analysis, Antioxidant, Antimicrobialactivities of Alcaloids and Methanolic Extract of Pancratium maritimum Growing in Djerba. *Archives of Pharmacy Practice* **15**(3–2024), 43–48. https://doi.org/10.51847/TnMvSYHLoO

Mgbeje, B.I., Asenye, E.M., Iwara, I.A. & Ebong, P.E. 2016. Evaluation of phytochemical composition of n-hexane fractions of Heinsia crinita crude leave extracts using gas chromatography-mass spectroscopy (GC-MS). World J. *World Journal of Pharmacy and Pharmaceutical Sciences* **5**(9), 98–107. DOI: 10.20959/wjpps20169-7326

Mohammed, A., Tajuddeen, N., Ibrahim, M.A., Isah, M.B., Aliyu, A.B. & Islam, M.S. 2022. Potential of diterpenes as antidiabetic agents: Evidence from clinical and pre-clinical studies. *Pharmacological Research* **179**, 106158. doi: 10.1016/j.phrs.2022.106158

Mukhtar, S. & Ghori, I. 2012. Antibacterial activity of aqueous and ethanolic extracts of garlic, cinnamon and turmeric against Escherichia coli ATCC 25922 and Bacillus subtilis DSM 3256. *International Journal of applied biology and pharmaceutical Technology* **3**(2), 131–136.

Musyimi, D.M., Ashioya, T.A., Opande, G. & Emitaro, W.O. 2021. Antibacterial Activity of Crude Extracts of *Solanum incanum* against *Escherichia coli* and *Staphylococcus aureus*. https://repository.maseno.ac.ke/handle/123456789/4831

Ohalete, C.N. 2023. Phytochemical and antifungal properties of anara (Solanum incanum) leaf on dermatophytes. *Journal of Agriculture and Food Sciences* **21**(2), 180–193.

Oseghale, E.I., Agoreyo, B.O. & Nkollo, M.I. 2025. GC-MS Analysis of Methanolic and N-Hexane Extracts of Freshly Harvested Sclerotia of King Tuber Mushroom (Pleurotus Tuber-Regium (Fr.) Sing.). *Journal of Drug Discovery and Health Sciences* **2**(02), 60–68. https://doi.org/10.21590/jddhs.02.02.01

Pothitirat, W., Chomnawang, M.T., Supabphol, R. & Gritsanapan, W. 2009. Comparison of bioactive compounds content, free radical scavenging and anti-acne inducing bacteria activities of extracts from the mangosteen fruit rind at two stages of maturity. *Fitoterapia* **80**(7), 442–447. https://doi.org/10.1016/j.fitote.2009.06.005

Pritam, P., Deka, R., Bhardwaj, A., Srivastava, R., Kumar, D., Jha, A.K., ... & Jha, S.K. 2022. Antioxidants in Alzheimer's disease: Current therapeutic significance and future prospects. *Biology* **11**(2), 212.https://doi.org/10.3390/biology11020212

Ramsey, J.T., Shropshire, B.C., Nagy, T.R., Chambers, K.D., Li, Y. & Korach, K.S. 2020. Focus: Plant-based medicine and pharmacology: Essential oils and health. *The Yale journal of biology and medicine* **93**(2), 291. https://pmc.ncbi.nlm.nih.gov/articles/PMC7309671/

Rani, J. & Kapoor, M. 2019. Gas chromatography-mass spectrometric analysis and identification of bioactive constituents of Catharanthus roseus and its antioxidant activity. *Gas* **12**(3), 461–465. http://dx.doi.org/10.22159/ajpcr.2019.v12i3

Ranil, R.H.G., Prohens, J., Aubriot, X., Niran, H.M.L., Plazas, M., Fonseka, R.M., Vilanova, S. & Knapp, S. 2017. *Solanum insanum* L. (subgenus *Leptostemonum* Bitter, Solanaceae), the neglected wild progenitor of eggplant (*S. melongena* L.): a review of taxonomy, characteristics and uses aimed at its enhancement for improved eggplant breeding. *Genetic Resources and Crop Evolution* **64**(7), 1707–1722. doi: 10.1007/s10722-016-0467-z

Rebaya, A., Belghith, S.I., Baghdikian, B., Leddet, V.M., Mabrouki, F., Olivier, E., ... & Ayadi, M.T. 2015. Total phenolic, total flavonoid, tannin content, and antioxidant capacity of Halimium halimifolium (Cistaceae). *Journal of applied pharmaceutical science* **5**(1), 052–057. doi: 10.7324/JAPS.2015.50110

Renda, G., Gökkaya, İ. & Şöhretoğlu, D. 2022. Immunomodulatory properties of triterpenes. *Phytochemistry Reviews* **21**(2), 537–563. doi: 10.1007/s11101-021-09785-x

Roy, A., Khan, A., Ahmad, I., Alghamdi, S., Rajab, B.S., Babalghith, A.O., ... & Islam, M.R. 2022. Flavonoids a bioactive compound from medicinal plants and its therapeutic applications. *BioMed research international* **2022**(1), 5445291. doi: 10.1155/2022/5445291

Rychter, A.M., Hryhorowicz, S., Słomski, R., Dobrowolska, A. & Krela-Kaźmierczak, I. 2022. Antioxidant effects of vitamin E and risk of cardiovascular disease in women with obesity–a narrative review. *Clinical Nutrition* **41**(7), 1557–1565. doi: 10.1016/j.clnu.2022.04.032

Saboon, Chaudhari, S.K., Arshad, S., Amjad, M.S. & Akhtar, M.S. 2019. Natural compounds extracted from medicinal plants and their applications. *Natural Bio-active Compounds: Production and Applications* **1**, 193–207. doi: 0.1007/978-981-13-7154-7_7

Sahle, T. & Okbatinsae, G. 2017. Phytochemical investigation and antimicrobial activity of the fruit extract of Solanum incanum grown in Eritrea. *Ornamental and Medicinal Plants* **1**(1), 15–25. http://www.iaees.org/publications/journals/omp/rss.xml

Samuels, J. 2012. *Solanum incanum* s.l. (Solanaceae): taxonomic relationships between *S. incanum*, *S. campylacanthum*, *S. panduriforme* and *S. lichtensteinii*. *Kew Bulletin* **67**(3), 401–411. https://doi.org/10.1007/s12225-012-9373-5

Satyanarayana, N., Chinni, S.V., Gobinath, R., Sunitha, P., Uma Sankar, A. & Muthuvenkatachalam, B.S. 2022. Antidiabetic activity of Solanum torvum fruit extract in streptozotocin-induced diabetic rats. *Frontiers in nutrition* **9**, 987552. https://doi.org/10.3389/fnut.2022.987552

Séré, M., Konaté, K., Santara, B., Sanou, D.O. & Belem, A.M. 2022. Study of the antibacterial capacity of extracts of Solanum incanum L., (Solanaceae) traditionally used for the management of avian cholera in rural areas of Burkina Faso. *World Journal of Advanced Research and Reviews* **13**(01), 047–057. https://doi.org/10.30574/wjarr.2022.13.1.0717

Shaaban, M.T., Ghaly, M.F. & Fahmi, S.M. 2021. Antibacterial activities of hexadecanoic acid methyl ester and green-synthesized silver nanoparticles against multidrug-resistant bacteria. *Journal of basic microbiology* **61**(6), 557–568. doi: 10.1002/jobm.202100061

Shamsa, F., Monsef, H., Ghamooshi, R. & Verdian-Rizi, M. 2008. Spectrophotometric determination of total alkaloids in some Iranian medicinal plants. *The Thai Journal of Pharmaceutical Sciences* **32**(1), 17–20. doi: 10.56808/3027-7922.2196

Shimada, K., Fujikawa, K., Yahara, K. & Nakamura, T. 1992. Antioxidative properties of xanthan on the autoxidation of soybean oil in cyclodextrin emulsion. *Journal of agricultural and food chemistry* **40**(6), 945–948.

Sies, H., Belousov, V.V., Chandel, N.S., Davies, M.J., Jones, D.P., Mann, G.E., ... & Winterbourn, C. 2022. Defining roles of specific reactive oxygen species (ROS) in cell biology and physiology. *Nature reviews Molecular cell biology* **23**(7), 499–515. https://doi.org/10.1038/s41580-022-00456-z

Sok Yen, F., Shu Qin, C., Tan Shi Xuan, S., Jia Ying, P., Yi Le, H., Darmarajan, T., ... & Salvamani, S. 2021. Hypoglycemic effects of plant flavonoids: a review. *Evidence-Based Complementary and Alternative Medicine* **2021**(1), 2057333. doi: 10.1155/2021/2057333

Syeda, A.M. & Riazunnisa, K. 2020. Data on GC-MS analysis, in vitro anti-oxidant and anti-microbial activity of the Catharanthus roseus and Moringa oleifera leaf extracts. *Data in brief* **29**, 105258. https://doi.org/10.1016/j.dib.2020.105258

Škrovánková, S., Válková, D. & Mlček, J. 2020. Polyphenols and antioxidant activity in pseudocereals and their products. *Potravinarstvo Slovak Journal of Food Sciences*. https://doi.org/10.5219/1341

Ti, H., Zhuang, Z., Yu, Q. & Wang, S. 2021. Progress of plant medicine derived extracts and alkaloids on modulating viral infections and inflammation. *Drug design, development and therapy*, 1385–1408. https://doi.org/10.2147/DDDT.S299120

Ukwubile, C.A., Ahmed, A., Katsayal, U.A., Ya'u, J. & Mejida, S. 2019. GC–MS analysis of bioactive compounds from Melastomastrum capitatum (Vahl) Fern. leaf methanol extract: An anticancer plant. *Scientific African* **3**, e00059. doi: 10.1016/j.sciaf.2019.e00059

Vaou, N., Stavropoulou, E., Voidarou, C., Tsigalou, C. & Bezirtzoglou, E. 2021. Towards advances in medicinal plant antimicrobial activity: A review study on challenges and future perspectives. *Microorganisms* **9**(10), 2041. doi: 10.3390/microorganisms9102041

Yazarlu, O., Iranshahi, M., Kashani, H.R.K., Reshadat, S., Habtemariam, S., Iranshahy, M. & Hasanpour, M. 2021. Perspective on the application of medicinal plants and natural products in wound healing: A mechanistic review. *Pharmacological research* **174**, 105841. https://doi.org/10.1016/j.phrs.2021.105841

Zivanayi, W., Venables, L., Van de Venter, M., Rasana, N. & Hlangothi, B. 2023. Evaluating biological ethnopharmaceutical activities of fruit and root extracts of Solanum incanum L. *African Journal of Food, Agriculture, Nutrition and Development* **23**(7), 24136–24156. doi: 10.22004/ag.econ.340730.

Agronomy Research **24**(S1), 114–125, 2026
https://doi.org/10.15159/AR.26.005

Impact of combining fungicide use with calcium fertiliser for managing maize downy mildew

Suriani[1], H. Mirsam[1], Endriani[1,*], D. Meithasari[1] and E.L. Ariyanti[2]

[1]Research Center for Food Crops, Research Organization for Agriculture and Food, National Research and Innovation Agency (BRIN), Cibinong Science Center, Jl. Raya Jakarta-Bogor, Bogor, 16915, West Java, Indonesia
[2]Department of Plant Protection, Faculty of Agriculture, Universitas Islam Makassar, Jl. Perintis Kemerdekaan No.KM.9, RW.No.29, Tamalanrea Indah, Kec. Tamalanrea, Kota Makassar, Sulawesi Selatan 90245
[*]Correspondence: eendriani674@gmail.com/ endr012@brin.go.id

Received: October 16th, 2025; Accepted: December 22nd, 2025; Published: January 22th, 2026

Abstract. Downy mildew is one of the most destructive diseases of maize worldwide. Disease prevention needs to be done at an early stage of plant growth. Maize is most susceptible to downy mildew between 10 and 45 days after sowing (DAS). This study aims to determine the effectiveness of applying fungicides in the early stages of plant growth combined with the addition of calcium nutrients. The research was conducted in Maros Regency, South Sulawesi, Indonesia, using a randomized block design two factor design. The first factor was five levels of fungicide application frequency, while the second included four fertiliser elements. The downy mildew inoculum source plants were planted and inoculated with *Peronosclerospora spp.* one month before planting the test genotypes. The results showed that repeated fungicide sprays in the early stages of plant growth effectively suppressed the downy mildew infection by 19.30%. Meanwhile, the first fertilisation at 10 DAS with nitrogen, phosphorus, and calcium (NPCa) was the most effective in suppressing downy mildew compared to other fertilisation packages. The treatment combination of three repeated fungicide applications (10, 15, and 20 DAS) with NPCa fertilisation can reduce the incidence of downy mildew by up to 33.23%. However, this combination resulted in lower yields compared to NPK fertilisation. Consequently, further research is required to explore the most effective method for applying potassium and calcium fertilisers.

Key words: downy mildew, preventive, fungicide, calcium fertilizer.

INTRODUCTION

Maize is one of the world's most important food crops, besides rice and wheat. Corn is cultivated globally across diverse agro-climatic zones, such as Bangladesh (Biswas et al., 2023), Mexico (Kennett et al., 2020), and Indonesia (Herawati et al., 2023). In Indonesia, increased maize production continues to fulfil food and animal feed needs. In continuous maize production, biotic and abiotic environmental factors can be yield-limiting. One of the biotic factors frequently reported as a significant constraint on maize productivity globally is downy mildew disease, caused by *Peronosclerospora* spp.

Peronosclerospora species found in Indonesia are *P. phillippinensis, P. maydis*, *P. sorghi*, and *P. neglecta* sp. nov., which spread in different regions (Muis et al., 2023). The pathogens are obligate parasites, and the primary vector for their spore dispersal is wind. Spore germination and the infection process of *Peronosclerospora* spp. require high humidity of 80–100% and temperatures of 18–30 °C (Lukman et al., 2016; Kalqutny & Pakki, 2020). Symptoms of downy mildew on maize are chlorotic streaks on the leaves running parallel to the leaf blade. The lower and upper surfaces of the leaves are covered with white clusters of spores. Systemic infections stunt plants and cause them to fail to produce (Lukman et al., 2016; Janruang & Unartngam, 2018). Disease incidence varies between maize cultivars (Widiantini et al., 2015). Susceptible cultivars are infected early in their growth. The disease is usually visible in plants 10 to 14 days after sowing (Mirsam et al., 2021). Pakki (2017) reported that planting susceptible cultivars without fungicide application can cause plant damage up to 100%. In addition to plant genetic factors, the availability of inoculum through continuous cultivation of maize in an area causes disease outbreaks (Prasetyo et al., 2021).

Maize downy mildew can be controlled by preventive treatments. Seed treatment with systemic fungicides, such as metalaxyl, effectively controls downy mildew. However, genetic mutations of pathogens to resist metalaxyl fungicides have rendered the method ineffective. In 2019, Pakki & Djaenuddin reported that seed treatment with metalaxyl fungicide up to a dose of 7 g kg^{-1} seed was ineffective in controlling downy mildew. Therefore, additional preventive measures, such as using fungicides during the initial phases of plant development, are necessary (Gupta et al., 2014). Ganesh et al. (2024) reported that spraying fungicides on ridge gourd before and immediately after the appearance of downy mildew symptoms can reduce disease severity by up to 74.35%. Similarly, downy mildew in basil decreased by 80% after two to four applications of calcium oxide, followed by azoxystrobin and reduced plant density (Gilardi et al., 2020). These findings are supported by Dudchenko et al. (2025), who found that repeated applications of the fungicide Acanto Plus SC significantly reduced downy mildew in sunflowers in Ukraine. Disease incidence in fungicide-treated plants was limited to 3.2%, compared with 28.9% in untreated control plants.

Control of maize downy mildew needs to be carried out through integrated management. Crop resistance to downy mildew can be increased by combining fungicide with the addition of certain nutrients, such as calcium. The application of calcium (Ca^{2+}) in crops contributes to maintaining tissue firmness and cell turgor, thereby reducing the incidence of diseases and preventing physiological disorders (Jain et al., 2019). Spraying propineb-based fungicides at 2,100 g ha^{-1} is more effective in suppressing downy mildew than several other fungicides on onions (Araújo & Resende, 2020). The effect of calcium fertiliser combined with fungicide in suppressing plant diseases has been reported by Percival & Graham (2021), who demonstrated that the application of the fungicide Penconazole together with calcium fertiliser reduced the severity of guignardia leaf blotch. Spraying fungicide penconazole combined with calcium chloride three times yielded a disease incidence level that did not differ significantly from that obtained with six applications of the fungicide alone.

Bezvikonnyi et al. (2020) reported other research about demonstrating that combining fungicide with micronutrients can suppress plant disease. They conducted a study from 2015 to 2017 at the Podillya State Agricultural and Technical University Training Center experimental field in Ukraine. They found that fertilising beet with micronutrient fertilisers with the Impact fungicides reduces the prevalence of leaf disease. The effectiveness of this treatment was evidenced by an increase in leaf area and photosynthetic capacity compared with the other treatments, with the photosynthetic potential reaching 2.37 million m^2 days per ha.

In this study, we conducted an experiment focused on the control of downy mildew in maize. The foliar application of systemic fungicides at the early stages of plant growth was combined with a calcium-nutrient fertiliser.

MATERIALS AND METHODS

Planting and inoculation of inoculum source plants

The research was conducted at the Indonesian Cereals Research Institute, Ministry of Agriculture, Maros District, South Sulawesi. The planting of inoculum sources followed the method of Mirsam et al. (2021). Maize seeds of the Anoman variety were planted in three rows around the perimeter of the test plots with a spacing of 50×20 cm. The preparation of the pathogen suspension was done by taking downy mildew-infected plants at 17.00 PM by cutting the leaves starting from the base and then putting them in a plastic bag. Once collected, the leaves to be used as inoculum sources were washed under running water to remove old conidia and dirt on the leaf surface. The bases of the leaves were then soaked in sugar water at a concentration of 2% in a container under dark conditions to stimulate spore formation (sporulation). At 03:00 AM, spores were harvested by rinsing the leaves covered with white spores in a container of water. This suspension is sprayed onto the inoculum source plants.

Planting the test material

Maize variety Nasa 29 was used in this study. The test material was planted when the inoculum source plants exhibited 60–70% downy mildew infection. Maize seeds were planted in test blocks with a length of 5 m and spacing of 70×20 cm. One seed was planted per hole.

Fungicide and fertiliser application

This study was conducted using a Factorial Randomised Block Design (RBD) with two factors. The first factor involved repeated applications of a synthetic fungicide containing the active ingredients fluopicolide (6%) and propineb (66.7%) at a rate of 2 kg ha^{-1}. The five applications were F1-No fungicide spraying; F2-Fungicide spraying when the plants were 10 DAS; F3-Fungicide spraying when the plants were 10 and 15 DAS; F4-Fungicide spraying when the plants were 10, 15 and 20 DAS; and F5-Fungicide spraying when the plants were 10, 15, 20 and 25 DAS. The second factor was the application of fertiliser elements, which consists of 4 levels, namely P1-Fertilisation with N + P + K + Ca; P2-Fertilisation with N + P + K; P3-Fertilisation with N + P + Ca; and P4-Fertilisation with N + P. Overall, there are 20 treatment combinations, each of which is repeated 3 times. The first fertilisation was done when the plants were 10 DAS using the type of fertiliser elements (N from urea; P_2O_5 from SP36; K_2O from KCL; Ca) based on each treatment. The doses used in the first fertiliser were urea at 200 kg ha^{-1}, SP36 250 kg ha^{-1}, KCL 166.7 kg ha^{-1} and Calcium 6.2 kg ha^{-1}. Furthermore, the second fertilisation at the age of 30 DAS entirely used urea 200 kg ha^{-1}. Fertilisation is done by digging the soil at a distance of 5–10 cm from the corn stalks, then the fertiliser is inserted and covered again with soil.

Effect of repeated fungicide applications combined with several types of fertiliser elements on the downy mildew incidence

Observation of downy mildew intensity

Downy mildew incidence was observed at 14, 21, 28, and 35 DAS using the following formula (Formula 1):

$$\mathrm{DI} = \frac{\mathrm{A}}{\mathrm{B}} \cdot 100\% \qquad (1)$$

where DI, Disease Incidence (%); A, Number of plants infected with downy mildew; and B, number of plants observed in each treatment.

Analysis of the area under the disease development curve (AUDPC*)*

The AUDPC is calculated from the downy mildew disease intensity recorded over a defined observation period. Development. The AUDPC can describe the level of disease development in a certain time span. The AUDPC is calculated using the following equation (Mehmood & Khan, 2016):

$$\mathrm{AUDPC} = \sum_{i=1}^{n-1} \left(\frac{X_i + X_{i+1}}{2}\right)(t_{i+1} - t_i) \qquad (2)$$

where n, number of observations; x, downy mildew incidence; and $(t_{i+1} - t_i)$, time interval between observations.

Effect of repeated fungicide applications combined with several types of fertiliser elements on the plant growth and production aspects

At 60 days after sowing (DAS), plant height was measured from the soil surface to the base of the panicle using a measuring tape. Observations of yield and 1,000-seed weight were made at harvest by collecting the entire plant in each treatment. Seed production (t/ha) was calculated using the following equation:

$$\text{Yield (ton. ha}^{-1}) = \frac{10{,}000}{\text{plot size}} \cdot \frac{100 - Mo}{100 - 15} \cdot \frac{EW}{1{,}000} \cdot SP \qquad (3)$$

where *Mo*, harvest moisture content (%); Plot size, harvest area (m^2); *EW*, ear weight per plot (kg); and *SP*, shelling percentage (Azrai et al., 2023).

Data analysis

Observed data on downy mildew incidence, plant height, yield, and 1,000-seed weight were statistically analysed using ANOVA. The analysis was followed by the Least Significant Difference (*LSD*) test at the 5% level (α 0.05).

RESULTS AND DISCUSSION

Effect of repeated fungicide applications combined with several types of fertiliser elements on the downy mildew incidence

Downy mildew symptoms were not found during the first observation at 14 days after sowing (DAS). However, in the subsequent observation, disease symptoms were detected with varying levels of incidence across treatments. In the second observation at 21 DAS, we detected the onset of disease infection, with varying incidence levels among the treatments. The number of plants infected with downy mildew continued to increase until the plants were 35 DAS. Plants without fungicide treatment were infected by 53.27%, significantly higher than plants applied with fungicides with 4 different application frequency levels (Fig. 1, a).

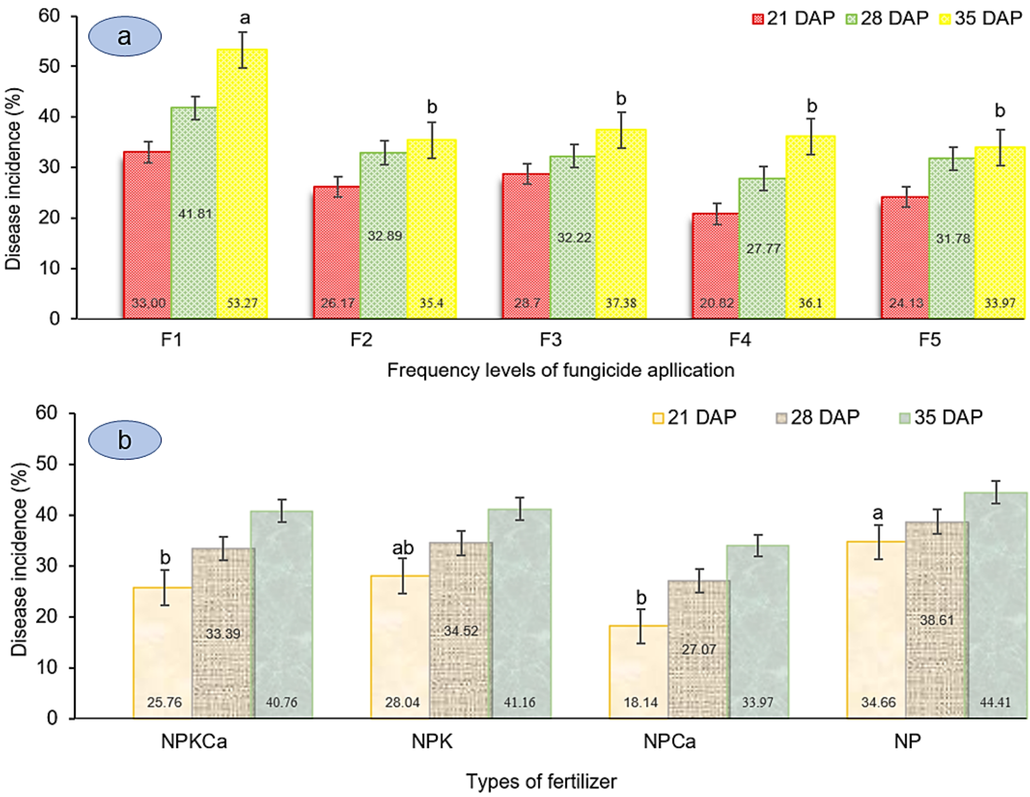

Figure 1. The incidence of maize downy mildew for fungicide treatment applied at five frequencies of application (a) and four types of fertilisation (b), observed at 21, 28, and 35 days after sowing (DAS). F1: no fungicide application; F2: Fungicide application at 10 DAS; F3: Fungicide application at 10 and 15 DAS; F4: Fungicide application at 10, 15, and 20 DAS; F5: Fungicide application at 10, 15, 20, and 25 DAS. Bar charts showing one observation time followed by the same letter are not significantly different based on the 5% *LSD* test.

The fertiliser element treatment significantly affected downy mildew incidence at 21 DAS (Fig. 1, b). Plants treated with calcium-containing fertilisers (P1 and P3) showed lower disease incidence than those receiving only nitrogen and phosphorus. However, at 28 and 35 DAS, downy mildew incidence did not differ significantly among treatments. The lowest disease incidence occurred in treatment P3 (NPCa fertilisation) at 33.97%. Fig. 2 illustrates the symptoms and signs of downy mildew disease.

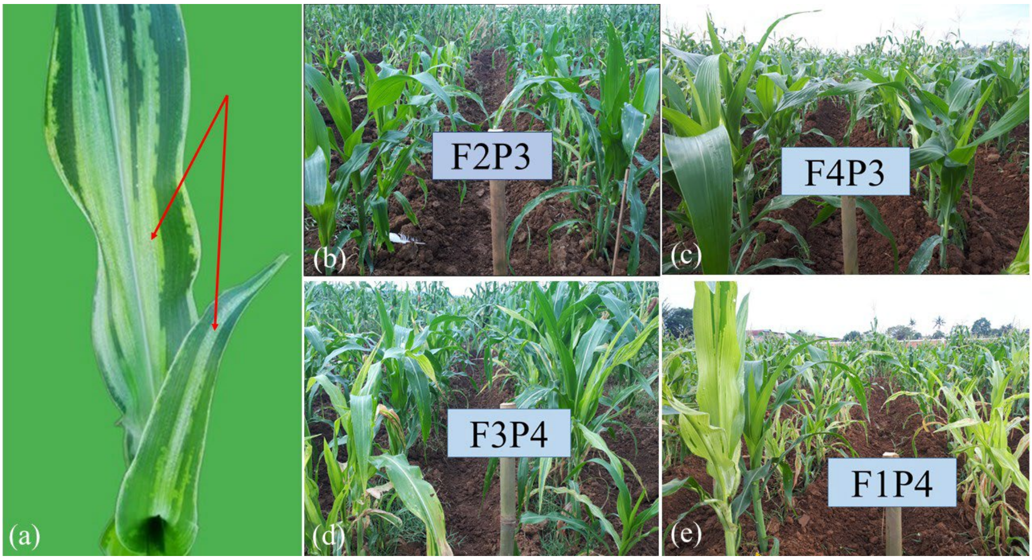

Figure 2. Symptoms of maize downy mildew appear as leaf chlorosis and white conidial growth on the leaf surface (a); Downy mildew infections under various treatments were the fungicide spraying treatment at 10 DAS combined with elemental NPKCa fertilisation (b), the fungicide spraying treatment at 10, 15, and 20 DAS combined with elemental NPKCa fertilisation (c), the fungicide spraying treatment at 10 and 15 DAS combined with elemental NP fertilisation (d), and no fungicide spraying treatment combined with elemental NP fertilisation (e).

The factor of fungicide application through the leaves showed a significant effect on reducing downy mildew disease incidence. At 35 DAS, plants that received four fungicide applications showed a 19.30% reduction in disease incidence relative to the untreated control. Preventive pesticide applications need to be done to prevent the development of *Peronosclerospora* spp. McGrath (2020) reported that fungicide applications initiated one day after sowing and repeated at seven-day intervals were highly effective, reducing downy mildew infection in basil by 87%. The applied fungicide is certain to adhere to the leaf surface, especially the lower leaf surface, so that it can inhibit or damage conidia (Kreuser & Broderick, 2017; Ons et al., 2020). While the factor of the type of fertiliser used shows the application of NPCa fertiliser has a downy mildew incidence of 10.44% lower than the disease incidence that occurs in plants fertilised with nitrogen and phosphorus elements. This shows that calcium in plants plays an important role in suppressing pathogen infection. Calcium is a structural component of the cell wall and other plant membranes that maintain the integrity and function of the cell wall (El Habbasha & Ibrahim, 2015; Lorenzetti et al., 2021). Calcium contributes to disease resistance by strengthening plant cell membrane stability and activating antioxidant enzyme systems (Yan et al., 2024).

The effect of 20 combinations of fungicide and calcium fertiliser on downy mildew incidence did not show significant differences between treatments at 21 and 28 DAS. The F4P3 combination consistently had the lowest disease incidence at both observation times, at 8.89% and 22.24%, respectively. The difference in disease incidence was significant when the plants were 35 DAS. The combination of F5P3, F4P3, F2P3 showed the lowest incidence, at 28.83, 29.11, and 30.73%, respectively (Table 1).

Table 1. Downy mildew incidence in maize as affected by different pesticide spraying frequencies and types of elemental fertilisers

Treatment	Disease incidence (%)				AUDPC	Resistance criteria
	14 DAS	21 DAS	28 DAS	35 DAS		
F1P1	0.00	37.60	42.54	58.55 ab	765.92	Susceptible
F1P2	0.00	29.14	40.33	54.31 abc	676.36	Susceptible
F1P3	0.00	25.46	36.12	49.27 abcd	603.48	Susceptible
F1P4	0.00	39.79	43.24	62.06 a	798.41	Very Susceptible
F2P1	0.00	21.21	28.20	35.86 cdef	471.38	Moderately resistant
F2P2	0.00	25.39	33.43	35.19 def	534.89	Moderately resistant
F2P3	0.00	17.76	24.87	30.73 ef	405.94	Moderately resistant
F2P4	0.00	40.33	45.06	39.82 cdef	737.09	Moderately resistant
F3P1	0.00	25.98	30.81	37.53 cdef	603.48	Moderately resistant
F3P2	0.00	30.61	33.71	37.84 cdef	582.66	Moderately resistant
F3P3	0.00	22.46	24.24	31.90 def	438.53	Moderately resistant
F3P4	0.00	37.50	42.26	48.13 abcde	726.79	Susceptible
F4P1	0.00	19.87	25.76	33.81 def	437.74	Moderately resistant
F4P2	0.00	28.88	32.40	42.91 bcdef	579.15	Susceptible
F4P3	0.00	8.89	22.44	29.11 f	321.22	Moderately resistant
F4P4	0.00	25.63	30.46	38.58 cdef	527.65	Moderately resistant
F5P1	0.00	24.15	34.66	38.05 cdef	544.84	Moderately resistant
F5P2	0.00	26.18	32.75	35.54 def	536.93	Moderately resistant
F5P3	0.00	16.12	27.68	28.83 f	407.45	Moderately resistant
F5P4	0.00	30.06	32.02	33.46 def	551.67	Moderately resistant
LSD 5%		tn	tn	1.46		

Notes: Cell numbers followed by the same letter are not significantly different at the 5% level of the Least Significant Difference test (*LSD*) 5%.

The treatment combination that most effectively suppressed downy mildew infection was found in the treatment combination of F5P3, F4P3, F2P3. These three combinations are the use of NPCa fertiliser. While the NPKCa fertiliser treatment showed higher infection than the NPCa fertiliser treatment. It is known that potassium and calcium are elements that can increase plant resistance to pathogen infection. The combination of these two elements is expected to provide higher plant resistance, but the research found different things. There was an interaction between potassium and calcium nutrients that influenced each other so that the absorption of both elements was higher when applied alone than in combination. The relationship between two or more nutrients in plant tissues can be antagonistic or synergistic depending on the plant species, cell type, leaf age, and source organ. Therefore, determining the optimal dose of nutrients is necessary to maintain proper nutritional status in plants to support increased production (Xie et al., 2021). AUDPC analysis found that the F4P3 treatment had the lowest value of 321.22 (Fig. 3). A lower AUDPC value indicates a slower rate of disease progression and lower overall disease incidence. Therefore, the findings suggest that fungicide application in the early growth stage up to 20 DAS, in combination with calcium fertilisation, effectively reduces the incidence of downy mildew.

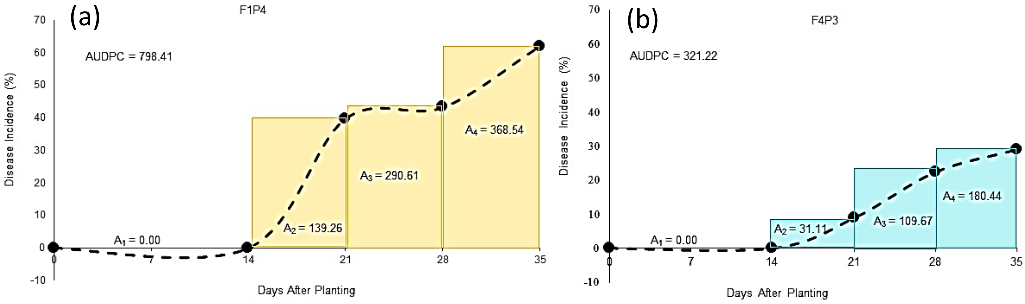

Figure 3. Maize downy mildew AUDPC graph for (a) F1P4 (no fungicide application + NP); (b) F4P3 (foliar application of fungicide at 10, 15, and 20 DAS + NPCa). A1–A4 indicate AUDPC for the first to fourth observation intervals.

Effect of repeated fungicide applications combined with several types of fertiliser elements on the plant growth and production aspects

The effect of treatments on the overall plant height of maize was not statistically significant. The highest plant height was observed in the F2P3 treatment (148.6 cm), followed by F4P1 (147.5 cm) and F4P3 (147.8 cm). In contrast, significant differences among treatments were observed in yield and the weight of 1,000 seeds (Table 2). The highest yield was recorded in treatment F5P1, reaching 6.88 ton ha^{-1}. This yield was significantly higher than those obtained from the four treatment combinations without pesticide application (F1) and from treatments involving only N and P fertilisation. The significant decrease in production, especially in the NP fertiliser treatment, was due to the low level of plant resistance to downy mildew so that the plant population was reduced. Therefore, plants require the application of macro- and micronutrient fertilisation to sustain cellular function stability and enhance their defence against pathogen infection. Rosyidah et al. (2017) reported that the use of potassium fertiliser can reduce the attack rate of bacterial wilt disease caused by *Rhizoctonia solanacearum* by 73.15%. In addition, the application of a balanced N-P-K fertiliser resulted in the highest maize yield compared to the application of NP, NK, or PK combinations (Otieno et al., 2019).

The findings of this study indicate that there are differences in effectiveness between treatments in suppressing the development of downy mildew disease and influencing plant productivity. The F4P3 treatment demonstrated the highest inhibition of downy mildew incidence. However, its crop yield was lower than the F5P1 treatment, although the difference was not statistically significant. Our findings show that calcium played an important role in lowering downy mildew incidence. As reported by previous researchers, calcium can directly affect the germination of pathogen spores (Percival & Graham, 2021). Calcium can trigger biochemical reactions that change leaf structure and function, helping the plant prevent pathogen entry (Tripathi et al., 2022). However, researchers, calcium can directly affect the germination of pathogen spores (Percival and treatments that combine potassium and calcium show lower pathogen inhibition compared to those without potassium. This reduced inhibition is likely due to the negative interaction that occurs between the two elements. Several researchers have reported that there is a cationic antagonism between calcium and potassium elements, so that high levels of one nutrient can result in reduced absorption of the other nutrient (Jēkabsone et al., 2024; He et al., 2025). Furthermore, Rhodes et al. (2018) found that potassium is more potent in reducing calcium absorption than vice versa. Although treatments with calcium elements without potassium showed the best effectiveness in suppressing corn downy mildew, production was lower. This lower yield occurs because the plants lack potassium, which plays an important role in plant physiology (Johnson et al., 2022). Therefore, future research should include additional treatment factors, such as varying calcium fertiliser application methods or other relevant agronomic practices.

Table 2. Growth and production of maize plants in repeated fungicide applications combined with several types of fertiliser elements

Treatments	Plant height (cm)	Yield (ton ha^{-1})	Seeds weight 1,000 (gr)
F1P1	126.9	4.92 bcdef	0.31 ab
F1P2	137.1	4.93 bcdef	0.33 ab
F1P3	143.3	4.44 cdef	0.30 ab
F1P4	145.1	3.89 ef	0.28 b
F2P1	144.3	5.32 abcde	0.35 ab
F2P2	128.4	5.79 abcd	0.34 ab
F2P3	148.6	5.59 abcd	0.31 ab
F2P4	127.6	4.15 def	0.28 b
F3P1	143.4	5.85 abc	0.31 ab
F3P2	143.0	5.65 abcd	0.29 b
F3P3	130.4	4.84 bcdef	0.28 b
F3P4	135.9	4.55 cdef	0.28 b
F4P1	147.5	6.47 ab	0.30 ab
F4P2	147.8	5.50 abcde	0.38 a
F4P3	147.7	6.46 ab	0.35 ab
F4P4	144.7	3.63 f	0.31 ab
F5P1	142.3	6.88 a	0.33 ab
F5P2	145.7	5.53 abcde	0.30 ab
F5P3	124.9	4.81 cdef	0.31 ab
F5P4	133.6	3.93 ef	0.29 b
LSD 5%		1.64	0.08

Notes: Cell numbers followed by the same letter are not significantly different at the 5% level of the Least Significant Difference test (*LSD*).

CONCLUSIONS

The results of the research showed that repeated fungicide spraying at the beginning of plant growth effectively reduced the incidence of downy mildew by up to 19.30%. Fungicide spraying was carried out when the plants were 10, 15, and 20 days after sowing. The treatment combination of three repeated fungicide applications (10, 15, and 20 DAS) with NPCa fertilisation can reduce the incidence of downy mildew by up to 33.23%. However, this combination resulted in lower yields compared to NPK fertilisation. Consequently, further research is required to explore the most effective method for applying potassium and calcium fertilisers.

ACKNOWLEDGEMENTS. We extend our gratitude to the Ministry of Agriculture for support funding our research through Research Funding Program of the Indonesian Cereals Research Institute.

REFERENCES

Araújo, E.R. & Resende, R.S. 2020. Propineb efficiency in controlling downy mildew of onion under field conditions. *Australasian Plant Disease Notes* **15**, 34. https://doi.org/10.1007/s13314-020-00403-x

Azrai, M., Aqil, M.M., Efendi, R., Andayani, N.N., Makkulawu, A.T., Iriany, R.N., Suarni, Yasin, M., Suwardi, Zainuddin, B., Salim, Sitaremi, T., Bahtiar, Paesal, & Suwarno, W.B. 2023. A comparative study on single and multiple trait selections of equatorial grown maize hybrids. *Frontiers in Sustainable Food Systems* **7**, 1185102. https://doi.org/10.3389/fsufs.2023.1185102

Bezvikonnyi, P., Myalkovsky, R., Muliarchuk, O. & Tarasiuk, V. 2020. Effectiveness of the combined application of micro-fertilizers and fungicides on the beet crops. *Ukrainian Journal of Ecology* **10**(6), 28–37. https://doi.org/10.15421/2020253

Biswas, R., Molla, M.M.U., Faisal-E-Alam, M., Zonayet, M. & Castanho, R.A. 2023. Profitability analysis and input use efficiency of maize cultivation in selected areas of Bangladesh. *Land* **12**, 1–23. https://doi.org/10.3390/land12010023

Dudchenko, V., Markovska, O. & Sydiakina, O. 2025. Determination of the effectiveness of fungicide protection systems as a reserve for sustainable sunflower production in south of Ukraine. *Technology Audit and Production Reserves* **1**(3), 51–57. doi: 10.15587/2706-5448.2025.323971

El Habbasha, S.F. & Ibrahim, F.M. 2015. Calcium: physiological function, deficiency and absorption. *International Journal of Chemical Technology Research* **8**(12), 196–202.

Ganesh, H.S., Yenjerappa, S.T., Aswathanarayana, D.S., Mallikarjun, K. & Kapil. 2024. Integrated disease management modules against downy mildew disease in ridge gourd. *The Pharma Innovation Journal* **13**(10), 48–52.

Gilardi, G., Garibaldi, A. & Gullino, M.L. 2020. Integrated management of downy mildew of basil. *Crop Protection* **137**, 105202. https://doi.org/10.1016/j.cropro.2020.105202

Gupta, S., Upadhyay, R.N., Kumar, S. & Razdan, V.K. 2014. Integrated disease management module for management of downy mildew of cucumber. *Indian Phytopathology* **6**(3), 268–273.

He, Y., Su, K., Wang, L., Zhou, J., Sun, S., Wang, J. & Xing, G. 2025. Modulation of potassium-to-calcium ratio in nutrient solution improves quality attributes and mineral composition of *Solanum lycopersicum* var. *cerasiforme*. *Agronomy* **15**, 1380. doi: 10.3390/agronomy15061380

Herawati, H., Riadi, M., Musa, Y., Efendi, R. & Azrai, M. 2023. Evaluation of the growth and tolerance of maize lines under aluminum stress. *Biodiversitas* **24**(3), 1417–1430. https://doi.org/10.13057/biodiv/d240311

Jain, V., Chawla, S., Choudhary, P. & Jain, S. 2019. Post-harvest calcium chloride treatments influence fruit firmness, cell wall components and cell wall hydrolyzing enzymes of Ber (*Ziziphus mauritiana* Lamk.) fruits during storage. *Journal of Food Science and Techology* **56**, 4535–4542. https://doi.org/10.1007/s13197-019-03934-z

Janruang, P. & Unartngam, J. 2018. Morphological and molecular based identification of corn downy mildew distributed in Thailand. *International Journal of Agricultural Technology* **14**(6), 848–852.

Jēkabsone, A., Karlsons, A., Osvalde, A. & Ievinsh, G. 2024. Effect of Na, K and Ca salts on growth, physiological performance, ion accumulation and mineral nutrition of *Mesembryanthemum crystallinum*. *Plants* **13**(190). https://doi.org/10.3390/plants13020190

Johnson, R., Vishwakarma, K., Hossen, M.S., Kumar, V., Shackira, A.M., Puthur, J.T., Abdi, G., Sarraf, M. & Hasanuzzaman, M. 2022. Potassium in plants: Growth regulation, signaling, and environmental stress tolerance. *Plant Physiololgy and Biochemistry* **1**(172), 56–69. https://doi.org/10.1016/j.plaphy.2022.01.001

Kalqutny, S.H. & Pakki, S. 2020. The resistance of various maize germplasms collected from several regions in Indonesia to downy mildew (*Peronosclerospora philippinensis*). *IOP Conf. Ser. Earth and Environment Science* **484**, 2–6. doi: 10.1088/17551315/484/1/012098

Kennett, D.J., Prufer, K.M., Culleton, B.J., George, R.J., Robinson, M., Trask, W.R., Buckley, G.M., Moes, E., Kate, E.J., Harper, T.K., O'Donnell, L., Ray, E.E., Hill, E.C., Alsgaard, A, Merriman, C., Merideth, C., Edgar, H.J.H., Awe, J.J. & Gutierrez, S.M. 2020. Early isotopic evidence for maize as a staple grain in the Americas. *Science Advances* **6**, eaba3245. https://doi.org/10.1126/sciadv.aba3245

Kreuser, K.E. & Broderick, K.C. 2017. Hop Downy Mildew. *Nebraska Extension Publications,* G2297. https://extensionpublications.unl.edu/assets/html/g2297/build/g2297.htm

Lukman, R., Afifuddin, A. & Lubberstedt, T. 2016. Tracing the signature of *Peronosclerospora maydis* in maize seeds. *Australasian Plant Pathology* **45**, 73–82. https://doi.org/10.1007/s13313-015-0390-3

Lorenzetti, E., Stangarlin, J.R., Carvalho, J.C., Hendges, C., Mata, T.C.D., Neto, A.J.A., Kohler, T.G., Tartaro, L., Ritter, G., Brito, O.D.C., Belmonte, C., Feroldi, L.T. & Junior, R.C. 2021. Calcium, copper, manganese and zinc and plant diseases: a review. *Australian Journal of Crop Science* **15**(05), 638–642. doi: 10.21475/ajcs.21.15.05.p2845

McGrath, M.T. 2020. Efficacy of conventional fungicides for downy mildew in field-grown sweet basil in the United States. *Plant Disease* **104**, 2967–2972. https://doi.org/10.1094/PDIS-11-19-2382-RE

Mehmood, Y. & Khan, A.A. 2016. Effectiveness of resistant germplasm and biological control agents as a sustainable management for Fusarium wilt disease on chickpea. Intl. *International Journal of Agriculture and Biology* **18**, 1–10. doi: 10.17957/IJAB/15.0158

Mirsam, H., Suriani, Rahman, A.A., Pakki, S., Azrai, M. & Prayitno, O.D. 2021. Genotipe resistance of hybrid corn varieties candidate against major corn diseases. *IOP Conf Ser: Earth. Environ Sci.* **911**, 012054. https://doi.org/10.1088/1755-1315/911/1/012054

Muis, A., Ryley, M.J., Tan, Y.P., Suharjo, R., Nonci, N., Danaatmadja, Y., Hidayat, I., Widiastuti, A., Widinugraheni, S., Shivas, R.G. & Thines, M. 2023. *Peronosclerospora neglecta* sp. nov.-a widespread and overlooked threat to corn (maize) production in the tropics. *Mycology Progress* **22**, 12. https://doi.org/10.1007/s11557-022-01862-5

Ons, L., Bylemans, D., Thevissen, K., Cammue, B.P.A. 2020. Combining biocontrol agents with chemical fungicides for integrated plant fungal disease control. *Microorganisms* **8**, 1930. https://doi.org/10.3390/microorganisms8121930

Otieno, H.M.O. 2019. Growth and yield response of maize (*Zea mays* L.) to a wide range of nutrients on ferralsols of Western Kenya. *World Scientific News* **129**, 96–106.

Pakki, S. 2017. Sustainability of superior corn varieties' resistance to downy mildew disease from the species *Peronosclerospora maydis. Jurnal Penelitian Pertanian Pangan* **1**(1), 37–44.

Pakki, S. & Djaenuddin, N. 2019. The effectiveness combination of resistant varieties and metalaxyl fungicide in controlling downy mildew disease (*Peronosclerospora maydis*) in maize plant. *Journal of Tropical Plant Pests and Diseases* **19**(1), 42–51. https://doi.org/10.23960/j.hptt.11942-51

Percival, G.C. & Graham, S. 2021. Calcium and silicon fertiliser and fungicide for pathogen management. *Arboriculture & Urban Forestry* **47**(4), 170–181. doi: 10.48044/jauf.2021.016

Prasetyo, J., Ginting, C., Akin, H.M., Suharjo, R., Niswati, A., Afandi, A., Adiwijaya, R., Sudiono, & Nurdin, M. 2021. The effect of biological agent and botanical fungicides on maize downy mildew. *Biodiversitas* **22**, 1652–1657. doi: 10.13057/biodiv/d220409

Rhodes, R., Miles, N. & Hughes, J.C. 2018. Interactions between potassium, calcium and magnesium in sugarcane grown on two contrasting soils in South Africa. *Field Crops Research* **223**, 1–11. https://doi.org/10.1016/j.fcr.2018.01.001

Rosyidah, A., Murwani, I. & Siswadi, B. 2017. Effect of the use of potassium fertiliser on the resistance and growth of tomato to bacterial wilt caused by Ralstonia solanacearum. *Journal of Environment, Agriculture and Biotechnology (IJEAB)* **2**(4), 2265–2269. http://dx.doi.org/10.22161/ijeab/2.4.89

Tripathi, R., Tewari, R., Singh, K.P., Keswani, C., Minkina, T., Srivastava, A.K., De Corato, U. & Sansinenea, E. 2022. Plant mineral nutrition and disease resistance: A significant linkage for sustainable crop protection. *Frontiers Plant Science* **13**, 883970. https://doi.org/10.3389/fpls.2022.883970

Widiantini, F., Yulia, E. & Purnama, T. 2015. Morphological variation of *Peronosclerospora maydis*, the causal agent of maize downy mildew from different locations in Java-Indonesia. *Journal of Agricultural Engineering and Biotechnology* **3**(2), 58–62. https://doi.org/10.18005/JAEB0302002

Xie, K., Cakmak, I., Wang, S., Zhang, F. & Guo, S. 2021. Synergistic and antagonistic interactions between potassium and magnesium in higher plants. *The Crop Journal* **9**(2), 249–256. https://doi.org/10.1016/j.cj.2020.10.005

Yan, L., Liu, S., Li, R., Li, Z., Piao, J. & Zhou, R. 2024. Calcium enhanced the resistance against *Phoma arachidicola* by improving cell membrane stability and regulating reactive oxygen species metabolism in peanut. *BMC Plant Biololgy* **24**, 501. https://doi.org/10.1186/s12870-024-05222-1

Agronomy Research **24**(S1), 126–146, 2026
https://doi.org/10.15159/AR.26.018

Biological responses of barley as affected by soil moisture and cationic balance in Brazil

A.B. Pereira*, R. Domingues, E.F. Caires and J.V. Mattos

State University of Ponta Grossa, Campus of Uvaranas, 4748 Carlos Cavalcanti Avenue, BR 84030-900, State of Paraná, Brazil
*Correspondence: doctorpeartree023@gmail.com

Received: December 23rd, 2025; Accepted: March 31st, 2026; Published: April 8th, 2026

Abstract. Control of water in the soil-plant-atmosphere system is vital to assure maximization of crop yield. Nutrients uptake by the plants is considerably affected by soil moisture mainly because mineral nutrients reach out for roots as a function of mass flux and diffusion. Soil cationic balance might impinge upon calcium (Ca), magnesium (Mg) and potassium (K) uptake by the plant roots. In light of the hypothesis that soil Ca:Mg ratio more suitable for agricultural crops hinges upon soil moisture, the current research aimed to study interrelationships between soil moisture status and cationic balance in soil on biological responsiveness of barley plants. The experiment was conducted in a protected environment and a randomized complete block design was used with three replicates arranged in a 4×4 factorial scheme. Soil water treatments imposed herein were defined as a function of four fractions of maximum crop evapotranspiration (ETm): 60, 80, 100, and 120% ETm along with four ratios between calcium (Ca) and magnesium (Mg): 1:1, 3:1, 6:1, and 9:1. The parameters evaluated were: plant height, number of tillers, number of ears per plant, number of grains per ear, number of grains per plant, grain weight per plant, and thousand-grain weight. Soil cationic balance did not impinge upon agronomic performance of barley crop, whereas all of response-variables evaluated were highly governed by soil water availability. Conversely, the most adequate soil Ca:Mg ratio to promote the best biological responsiveness of barley grown under a protected environment did not depend on soil moisture levels.

Key words: *Hordeum vulgare* L., soil humidity, soil Ca:Mg ratio, grain yield, soil fertility.

INTRODUCTION

Water is fundamental for the biochemical and physiological processes, playing a role as a universal solvent in order to promote transport of minerals, gases and solutes in the soil-plant-atmosphere system along with plant thermal regulation by means of crop transpiration (Costa, 2001). Water flux in the system of soil-plant-atmosphere takes place under a direct or indirect influence of atmosphere evaporative demand or reference evapotranspiration (ETo).

Uptake of mineral nutrients by the crops is highly affected by soil moisture status, once most of the macronutrients reach the roots of the plants mainly by means of mass flux and diffusion (Domingues et al., 2026). According to Barber (1974), the number of ions transported by mass flux is determined by the ion's concentration in soil solution in conjunction with crop maximum evapotranspiration (ETm or ETc).

Ca and Mg macronutrients are transported by mass flux process (Barber, 1974). Since such mineral nutrients are transported to plant roots by water, lack of water leads to reductions in mass flux of soluble nutrients in water, such as Ca and Mg (Clair & Lynch, 2010). Therefore, water deficit situations negatively affect mineral nutrition and crop growth (Marques et al., 2023).

Cationic balance prevailing in soil solution might compromise uptake of a given nutrient by the plant roots. Calcium (Ca), magnesium (Mg) and potassium (K) compete for the same sites of adsorption and absorption, as well as transportation to radicular surfaces. Excess of one particular nutrient inhibits absorption of another, culminating in nutritional deficiency symptoms in plants.

Soil cationic balance might affect agronomic performance and physiological responses of the studied agricultural crops. Under high concentration of a given specific-cation in soil solution, inhibition in absorption of other cation might be conducive to nutritional deficiency symptoms and compromise substantially biological responses of the plants. However, the impact of soil cationic balance on commercial yields turns out to be strongly driven by specie, cultivar, soil type, and prevailing microclimatic conditions of the cropping system (Domingues et al., 2026).

With the purpose of providing adequate levels of Ca and Mg in soil, several scientists recommend application of calcium sulphate and calcareous with high content in Ca (Soto et al., 2023). Nevertheless, insofar as soil Ca:Mg ratios increase Mg and K uptake is impaired by the excess of Ca absorbed by the plants (Medeiros et al., 2008). K turns out to be the macronutrient that most favours grains filling, since high levels of Ca and Mg in soil solution substantially compromise K uptake and, therefore, reduce crop yields (Lange et al., 2021). Soto et al. (2023) highlights that Ca improves soil aggregation and plays an important role in stabilization of carbon, whereas Mg reduces soil aggregation and water infiltration processes. Another main contribution factor concerning soil cationic balance as a cultural practice to be borne in mind is that it betters both nutrients availability and also biological responses of plants in such a manner as to maximize crop commercial yields and minimize costs of production in cropping systems (Chaganti et al., 2021).

Root cation exchange capacity (root CEC) is lower in monocots than in dicots, allowing them to absorb more nutrients (Asher & Ozanne, 1961). For cereals, such as maize, wheat, and rice root CEC varies from 100 to 200 mmolc kg^{-1} of dry roots, whereas for legume crops, such as soybean and common bean root CEC ranges from 400 to 800 mmolc kg^{-1} of dry roots (Fernandes & Souza, 2006). Williams & Coleman (1950) verified that root CEC of soybean was twice as much of that found for maize. Once root CEC interferes with uptake of cations and transport of Ca and Mg from soil solution to rhizosphere is regulated by mass flux mechanism, it is rather expected that soil Ca:Mg ratio more suitable for crop growth depends on crop metabolism in conjunction with root CEC and soil moisture levels (Schneider et al., 2017; Domingues et al., 2026).

Barley (*Hordeum vulgare* L.) is considered one of the most antique agricultural species in the world and is well-adapted to several environments and different latitudes (Newton et al., 2011; Dawson et al., 2015; Dellabiglia et al., 2025). Due to some special properties, barley crop might adapt to different unfavourable climatic conditions as opposed to other agricultural crops (Zargar et al., 2018). Apart from being utilized either for human or animal nutrition, barley is employed as a raw matter for beer brewing industries owing to its malt characteristics (Hong & Zhang, 2020). With a world production in 2023 of roughly 145 million tons, barley turns out to be the fourth cereal mostly grown in the world, remaining behind only rice, wheat, and maize (FAOSTAT, 2025). Under a national perspective, an estimation of commercial yields of the aforementioned winter cereal throughout the 2024 harvest was corresponding to slightly over 511-thousand tons (CONAB, 2025).

Barley crop is a target of several interference factors that preclude remarkable yields to be achieved in commercial production fields (Mulatu & Lakew, 2011). Among such factors, it is well known that soil acidity, low availability of nutrients in soil solution, insufficient drainage within soil profile, soil moisture deficits and inadequate agricultural practices are those which considerably promote abiotic stresses associated with yield gaps (Agegnehu et al., 2016; Jahromi et al., 2023). In view of such a problem, we hypothesized that soil cationic balance interferes with barley crop biological responses only under soil water deficiency conditions. In order to test this scientific hypothesis formulated by Soto et al. (2023), we stablished four different soil Ca:Mg ratios along with four distinct soil moisture levels to assess the impacts of such factors on barley agronomic performance. Thus, the current work aimed to scrutinize and comprehend existing relationships between soil humidity regimes and soil cationic balance on biological responsiveness of barley grown in a protected environment under edaphoclimatic conditions of Ponta Grossa, State of Paraná, Brazil.

MATERIAL AND METHODS

Site description and agricultural environment

The experiment was carried out in a greenhouse belonging to the State University of Ponta Grossa, Parana State, Brazil (25°5'40"S, 50°9'48"W and 956 m above sea level). The climate at the site cultivated with barley, according to the Köppen and Geiger classification, is categorized as a Cfb type (mesothermal, humid, subtropical), with mean air temperature of the coldest month below 18 °C, with fresh summers, mean air temperature of the hottest month below 22 °C and bereft of a well-defined dry season. The mean annual precipitation ranges from 1,400 to 1,600 mm, with August considered the driest month and February the rainiest one (Nitsche et al., 2019). Soil type collected from 0–20 cm-layer was a Cambisol, with soil samples seized, homogenized, and dried at atmospheric air prior to its incubation.

Experimental design, treatments, and experiment conduction

In light of cultivation of a promising genotype of barley at a commercial scale selected at Southern of Brazil, an experiment was installed and conducted under a protected environment considering a randomized complete block design with three replicates arranged in a 4×4 factorial scheme. Treatments were constituted of four levels of soil water (60, 80, 100, and 120% of maximum crop evapotranspiration – ETm) and four soil Ca:Mg ratios (1:1, 3:1, 6:1, and 9:1), which were applied to 18 kg of dry soil allotted in flexible plastic vases.

Soil water treatments were defined from the knowledge on crop water consumptive use (ETm). Therefore, distinct fractions of ETm were adopted with the aim of assessing the impact of both soil water status and soil cationic balance on response-variables, which were expressed by barley agronomic parameters.

Water treatments were adopted at the moment from which barley plants showed the second leaf entirely developed. Irrigation was applied based on gravimetric daily measurements of soil water content by means of a precision scale. Before imposition of water treatments, all vases received the same amount of irrigation water in order to assure that initial soil water supply was near or at pot capacity condition. For definition of soil Ca:Mg ratios, results of soil chemical analysis on soil samples placed in all vases were taken into consideration along with the need for addition of $CaCO_3$ and $MgCO_3$ to soil as a function of Ca:Mg ratios previously stablished.

In order to assess the effect of different Ca:Mg ratios on biological responses of barley, soil samples were subjected to incubation process before sowing. Therefore, dry soil was mixed with $CaCO_3$ (p.a.) and $MgCO_3$ (p.a.) analytical reagents to make sure that all soil cationic balance treatments stipulated in the experiment were reached.

Shortly after soil collection, drying, seizing and homogenization practices, a soil sample was collected to proceed granulometric and chemical analyses (Table 1). The purpose of the chemical analysis was to determine $CaCO_3$ and $MgCO_3$ amounts to be mixed in the soil aiming at achieving Ca:Mg ratios imposed as treatments, as well as to define precise fertilizer doses to be applied to the soil placed in the vases.

Table 1. Soil chemical and granulometric attributes before barley experiment installation under protected environment at Ponta Grossa, PR, Brazil, 2024

pH ($CaCl_2$)	H+Al	Al^{3+}	Ca^{2+}	Mg^{2+}	K^{+}	CTC $_{(pH\ 7.0)}$
	------------------------------------- $cmol_c\ dm^{-3}$ -------------------------------------					
4.5	5.61	0.5	1.4	0.4	0.06	7.47
P (Mehlich^{-1})	C-organic	Sand	Silt	Clay	Base saturation	
$mg\ dm^{-3}$	$g\ dm^{-3}$	-------------- $g\ kg^{-1}$ ----------------			%	
41.7	14	804	61	135	25	

CTC $_{(pH\ 7.0)}$ = potential cation exchange capacity; C-organic = Walkley-Black.

The $CaCO_3$ (p.a.) and $MgCO_3$ (p.a.) analytical reagents were utilized at the following proportions: a) 1:1 ratio – 13.50 g of $CaCO_3$ and 11.34 g of $MgCO_3$; b) 3:1 ratio – 20.30 g of $CaCO_3$ and 5.67 g of $MgCO_3$; c) 6:1 ratio – 23.22 g of $CaCO_3$ and 3.24 g of $MgCO_3$; d) 9:1 ratio – 24.34 g of $CaCO_3$ and 2.26 g of $MgCO_3$ for 18 kg of dry soil in each vase. Such products were incorporated into the soil and placed in the vases afterwards. All vases were irrigated for 60 days in order to maintain 80% field capacity throughout the entire incubation period to assure suitable soil water conditions for chemical reactions of correctives to take place in compliance with imposition of the water treatments.

Irrigation with deionized water was performed manually with the purpose of measuring different soil water supply levels. Variation in weight of the control-volume (soil plus plants grown in the vases) is directly proportional to the amount of water lost to the atmosphere of the protected environment under which barley was tilled. Thus, a precision scale was installed inside the experimental environment to determine the water ideal climatic demand of barley crop (ETm).

In order to guarantee a suitable water supply in the soil compatible to occurrence of maximum crop evapotranspiration (ETm), soil water content is supposed to be at or near field capacity. Under controlled environmental conditions, such a field capacity comes to being denominated as pot field (Casaroli & Lier, 2008), which is given by cessation of descending movement of gravitational water within soil profile placed in the vases.

With the purpose of determining ETm we made use of gravimetry methodology. Apart from the utilized flexible plastic vases for the experiment conduction, four more pots cultivated with barley plants were taken into consideration to measure ETm. Such recipients were irrigated up until vase capacity was reached, weighed and weighed again after a three day-period. The difference of mass for the soil-plant set between the moment vase capacity was reached and the final three day-period corresponds to the ideal water amount to be applied to each one of the vases – ETm. All of the vases were irrigated in compliance of soil moisture treatments. Such treatments were stablished as a function of four different fractions of ETm, such as 60%, 80%, 100%, and 120% ETm.

Sowing of barley was made in 48 12-L vases filled with seized dry soil on May 12th, 2023, shortly after soil incubation. Each experimental unity was depicted by one-single vase containing six plants belonging to Imperatriz cultivar. This particular genotype of barley was chosen owing to its late-growing cycle crop well-adapted to southern regions of Brazil, depicting an excellent resistance to foliar diseases in order to reduce costs with fungicide applications along with the highest productive potential that culminated in yields excelling previous commercial cultivars recommended for the region in study.

Sowing was manual with twelve seeds per vase placed beside central fertilization furrow. After emission of the first leaf, thinning was made with the purpose of maintaining six plants per vase. Fertilization was realized with 3.02 g of 3–17–00 ($N–P_2O_5–K_2O$) formulation plus 0.37 g of urea in central furrow of the soil shortly before sowing along with 0.86 g of KCl applied to soil surface followed by irrigation. Nitrogen fertilization in bands was made 15 DAE with 1.52 g of urea for each vase.

Before sowing, barley seeds were treated with Pyraclostrobin and Thiophanate-methyl fungicides and Fipronil insecticide. Throughout crop growing season, phytosanitary treatment was performed with aqueous solution fungicide Fenpropimorph in order to control net blotch (*Pyrenophora teres* Drechsler) and powdery mildew (*Blumeria graminis* f. Hordei (DC.) Speer). Visual diagnosis was carried out for identification of diseases according to Luz (1982). Control of weed infestation was manually made whenever necessary. Harvest was proceeded on October 27th, 2023, shortly after barley plants reached physiological maturation. Barley plants were cut close to the ground for assessment of crop yield components.

Biometric variables and yield components

The following barley biological parameters were evaluated herein: plant height, number of tillers, number of spikes, number of grains per spike, number of grains per plant, mass of grains per plant, thousand-grain mass.

Plant height (PH) was determined by measuring vertical distance between soil surface and insertion point of the highest spike with a ruler. Number of tillers (NT), number of spikes per plant (NSP), and number of grains per plant (NGP) were assessed by manual counting. Number of grains per spike (NGS) was calculated by ratio between number of grains produced by a given plant and number of spikes of the same plant under scrutiny.

To determine mass of grains per plant (MGP) a precision scale of the Marte make, AS 2000C model with a deviation of 0.01 g along with an error of 0.1 g was utilized. Furthermore, grain moisture was obtained by oven-drying method at 105 ± 3 °C for a 24-hour period (Brasil, 2009). From such a moisture obtained, mass of grains was adjusted to 13% of weight moisture (Eq. 1).

$$MGP = \frac{100 - PG}{100 - 13} \cdot mg \tag{1}$$

where MGP = mass of grains per plant adjusted to 13% weight moisture (%); PG = percentage of measured grain moisture (%); mg = mass of grains (g).

The thousand-grain mass (TGM) was gauged by means of Eq. 2 after correction factor applied to grain moisture.

$$TGM = \frac{MGP \cdot 1{,}000}{NG} \tag{2}$$

where NG = number of grains.

Statistical analysis

Experimental data related to barley agronomic performance and soil chemical properties were subjected to analysis of variance (ANOVA) with application of *F* test, considering a randomized complete block design with three replicates arranged in a 4×4 factorial scheme. Shortly before ANOVA with the aim of verifying normality of variances, Shapiro-Wilk test was applied to experimental data in order to confirm no need for data transformation technique.

In cases from which *F* test was significant ($P < 0.05$), experimental data were subjected to regression analysis approach to quantify the effects of four soil Ca:Mg ratios and four soil moisture levels on response-variables of barley plants grown under a protected environment in the municipality of Ponta Grossa, State of Paraná, Brazil. In light of interaction effects between soil moisture and cationic balance factors, the effects of treatments were unfolded. For the regression analyses, the choice on fitted-model was based on magnitude of coefficients of determination of the significant regressions at ($P < 0.05$). Statistical analyses were made by means of the R software (R Core Team, 2022).

RESULTS AND DISCUSSION

Prevailing climatic conditions and water applied

Measurements of daily maximum, minimal and mean air temperature regime, as well as reference evapotranspiration (ETo) were monitored under a protected environment throughout the whole barley crop growing season (Fig. 1). The mean air temperature comprised between flowering and grain filling stages was corresponding to 19.3 °C. Nevertheless, the maximum temperature measured at most of the critical phenological stages in study remained below 30 °C, which represents a thermal threshold compatible to requirements of C_3 plants (Kerbauy, 2004). The overall ETo value throughout the full-period of trial conduction was of 164.6 mm.

All vases were irrigated shortly after sowing with the purpose of maintaining soil water content compatible to pot capacity, which required an irrigation water amount corresponding to 29.0 mm. Shortly after soil water treatments stipulation, each vase received specific fractions of maximum crop evapotranspiration (ETm) in compliance with water status imposed in our experiment.

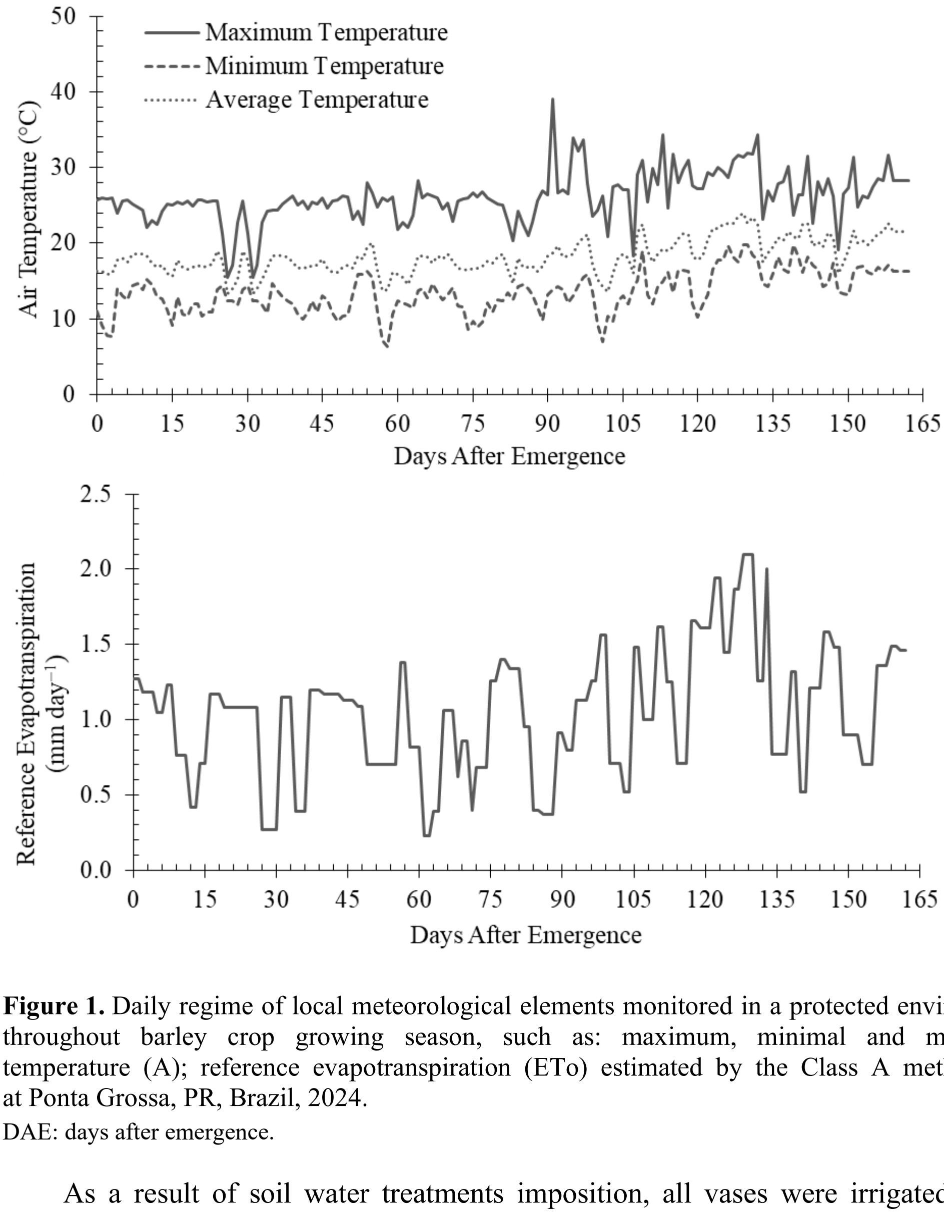

Figure 1. Daily regime of local meteorological elements monitored in a protected environment throughout barley crop growing season, such as: maximum, minimal and mean air temperature (A); reference evapotranspiration (ETo) estimated by the Class A method (B) at Ponta Grossa, PR, Brazil, 2024.

DAE: days after emergence.

As a result of soil water treatments imposition, all vases were irrigated at the following water application rates: 212.3, 176.9, 141.0, and 106.1 mm under 120%, 100%, 80%, and 60% ETm.

Plant height and number of tillers

Plant height was significantly affected by soil water supply levels (Fig. 2), but was not governed by soil Ca:Mg ratios (Fig. 3). Plant height pattern was dependent on soil water status under each soil Ca:Mg ratio treatment. At 1:1 soil Ca:Mg ratio, a quadratic behaviour described crop growth in height as a function of soil water supply, with maximum and minimal values of 56.2 and 48.0 cm under 100% and 60% ETm, respectively. A quadratic regression model for plant height varying as a function of soil water levels was also fitted for 3:1 soil Ca:Mg ratio, with a maximum threshold of 56.7 cm under 120% ETm and of 43.3 cm under 80% ETm. At 6:1 soil Ca:Mg ratio, plant height linearly increased as a function of soil water status, with maximum and minimal thresholds corresponding to 55.4 and 45.6 cm under 120% and 60% ETm, respectively. Conversely, under 9:1 soil Ca:Mg ratio, plant height was not influenced by soil water supply levels.

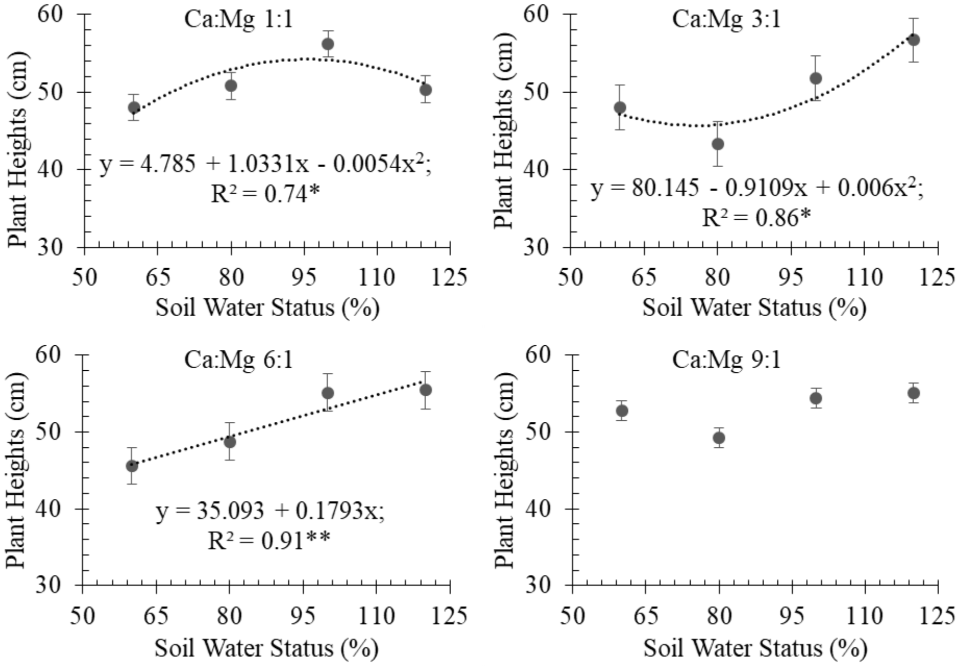

Figure 2. Barley plant height as a function of different soil water supply levels for each soil Ca:Mg ratio under protected environment at Ponta Grossa, PR, Brazil, 2024.

*: $P < 0.05$ and **: $P < 0.01$.

Plant height was significantly driven by soil water levels, however, was not conditioned by soil cationic balance. Such a response-variable presented the highest values under the wettest soil treatment. Similar to the outcomes of our current work, Sanches et al. (2015) came up with a quadratic responsiveness of different soil water levels (50%, 75%, 100%, and 125% ETm) on plant height of three barley genotypes. By examining the impact of three irrigation levels (0, 20, and 40 mm) on four barley genotypes, Mollah & Paul (2011) also detected differences in plant height under field conditions. Its mean values were of 86.1 cm, 81.8 cm, and 74.7 cm under 40 mm, 20 mm, and 0 mm, respectively. Santos et al. (2012) identified effect of water deficit imposed at the beginning of flowering over a 10-day period on wheat genotypes under protected environment. Such studies demonstrated existence of isolate effect of soil water status on agronomic performance of winter cereal crops.

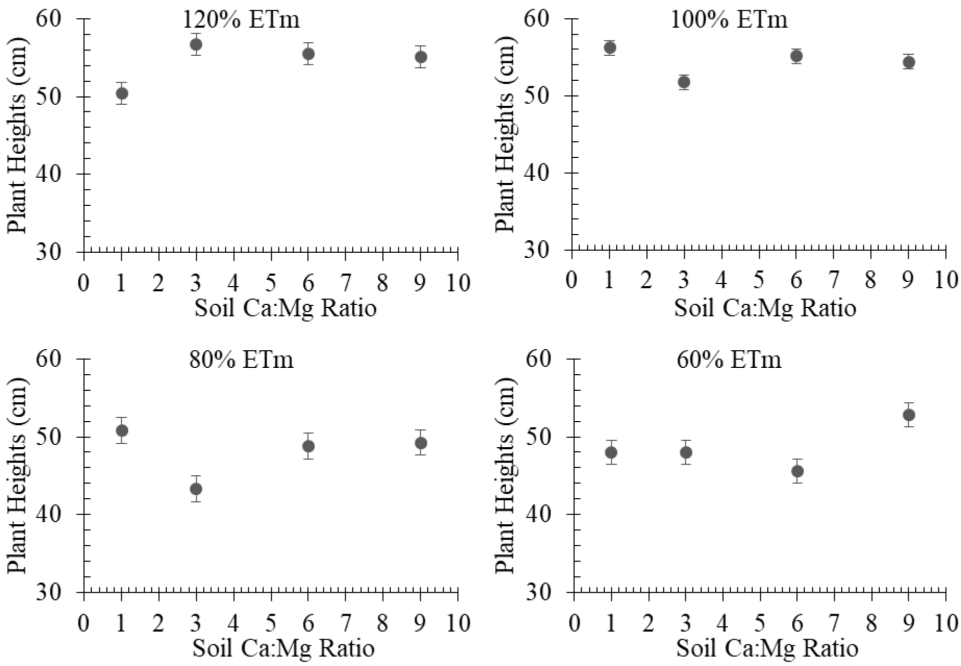

Figure 3. Barley plant height as a function of soil Ca:Mg ratios under protected environment at Ponta Grossa, PR, Brazil, 2024.
*: $P < 0.05$ and **: $P < 0.01$.

The number of tillers per plant of barley was neither significantly affected by soil Ca:Mg ratio nor by interaction effect between water supply and soil cationic balance. Such a response-variable demonstrated a linear increment in the face of rises in soil water availability (Fig. 4). The extreme values of number of tillers oscillated from 4.6 to 7.8 under water treatments of 60% and 120% ETm, respectively.

The number of tillers of barley plants was not influenced by distinct soil Ca:Mg ratios; however, it was governed by soil water status. Such a biological variable linearly increased with increments in soil water supply. A similar result was obtained by Sanches et al. (2015) in light of a linear responsiveness as a function of irrigation water amounts corresponding to 50%, 75%, 100%, and 125% ETm. Mollah & Paul (2011) also found impact of soil water status on number of tillers of barley plants, with mean thresholds of 3.6, 3.3, and 2.8 under irrigation levels of 40 mm, 20 mm, and 0 mm, respectively. The number of tillers per plant of three distinct wheat genotypes under irrigated treatments was higher as opposed to imposition of water deficit from an experiment conducted by

Santos et al. (2012). The outcomes reported by the aforementioned authors were quite similar to ours, with mean thresholds fluctuating from 11.4 to 9.6.

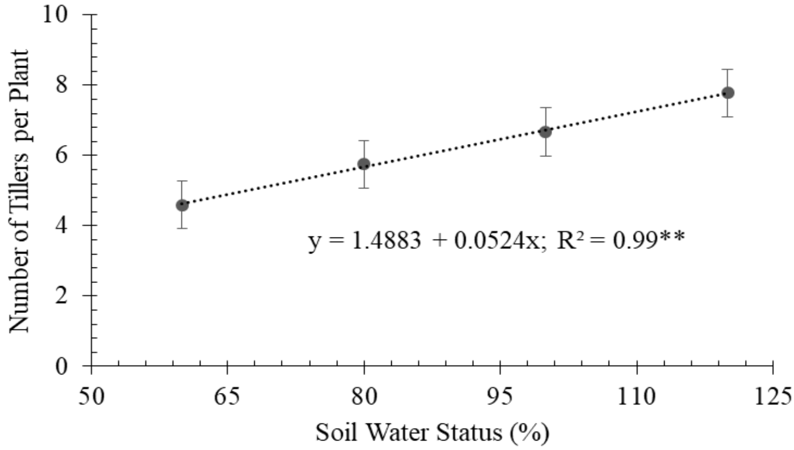

Figure 4. Number of tillers per plant as a function of soil water supply levels under protected environment at Ponta Grossa, PR, Brazil, 2024.
*: $P < 0.05$ and **: $P < 0.01$.

Effect of treatments on crop yield components

NSP was neither considerably conditioned by soil Ca:Mg ratios nor by interaction effect between water supply levels and soil cationic balance. Nevertheless, such a response-variable was impinged upon soil water status (Fig. 5). NSP linearly increased with augments in soil water supply levels. According to the fitted regression equation obtained, the highest threshold was of 5.6 under 120% ETm, whereas the lowest one was of 3.3 under 60% ETm treatment.

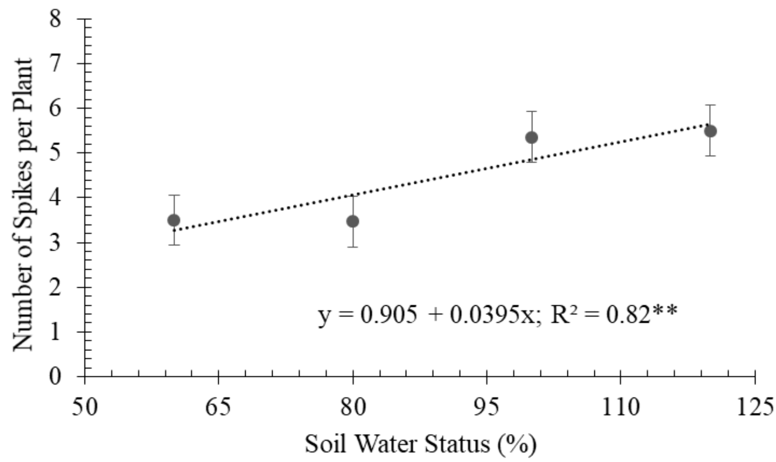

Figure 5. Number of spikes per plant as a function of soil water supply levels under protected environment at Ponta Grossa, PR, Brazil, 2024.
*: $P < 0.05$ and **: $P < 0.01$.

Soil Ca:Mg ratios did not significantly impinge upon NSP. Nevertheless, such a variable was substantially conditioned by soil water supply, being mathematically described by a linear regression model. As in our particular study, number of barley spikes per square meter of soil measured by Nagaz et al. (2008) was affected by soil water supply levels under arid climate of Mediterranean Southern Tunisia. Mean estimated values of NSP were of 219.3, 208.7, 201.0, and 189.3 under 100%, 85%, 70%, and 50% ETm, respectively.

NGP was not significantly governed by soil water supply levels, soil Ca:Mg ratios, and also by interaction effect between both factors. Its mean calculated value was corresponding to 15.2. In the same fashion as to observations for NSP, NGP was neither strongly influenced by soil cationic balance nor by interactions between water supply and soil Ca:Mg ratios; however, NGP linearly increased with rises in soil water availability (Fig. 6). Its extreme values varied from 46.5 to 89.5 under 60% and 120% ETm, respectively.

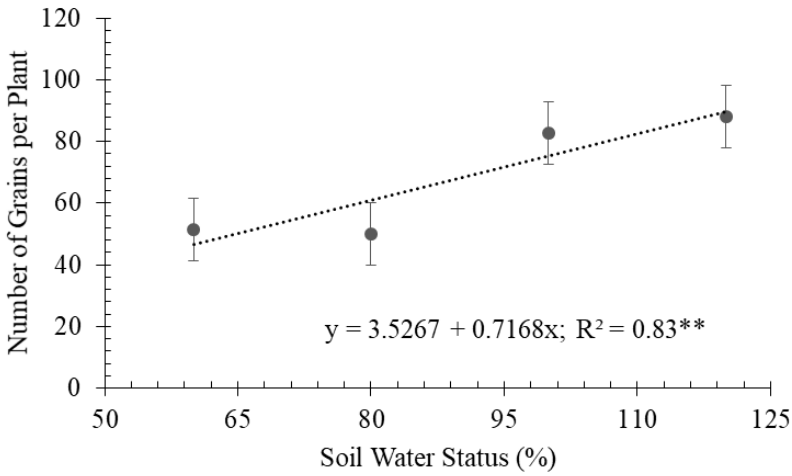

Figure 6. Number of grains per plant as a function of soil water supply levels under protected environment at Ponta Grossa, PR, Brazil, 2024.
*: $P < 0.05$ and **: $P < 0.01$.

NGS was neither determined by soil cationic balance nor by soil water status. However, Sanches et al. (2015) observed a linear increase in NGS as a function of irrigation amounts of 50%, 75%, 100%, and 125% ETm. Different from our observations, Nagaz et al. (2008) found that NGS was governed by soil water status. Mean estimated values of NGS were of 47.9, 46.0, 42.1, and 40.3 under 100%, 85%, 70%, and 50% ETm, respectively. Contrary to our outcomes, Santos et al. (2012) also detected a strong negative impact of soil water deficit on NGS of wheat plants under protected environment.

Soil Ca:Mg ratios did not substantially compromise NGP; however, such a biological variable linearly increased as a function of increments in soil water availability. Similar to our research, Mollah & Paul (2011) verified remarkable effects of soil water status on NGP, with values of 59.3, 52.7, and 46.0 under irrigation amounts corresponding to 40 mm, 20 mm, and 0 mm, respectively. Santos et al. (2012) also evidenced impact of soil water supply levels on NGP of wheat plants grown under a protected environment, with mean thresholds ranging from 629.8 under suitable soil water supply to 376.5 under water deficit condition.

MGP of barley was neither significantly affected by soil Ca:Mg ratios nor by interaction between soil water supply levels and cationic balance, suffering a linear increment as a function of increasing soil water status (Fig. 7). MGP extreme thresholds were of 4.9 g and 2.3 g under the influence of 120% and 60% ETm treatments, respectively.

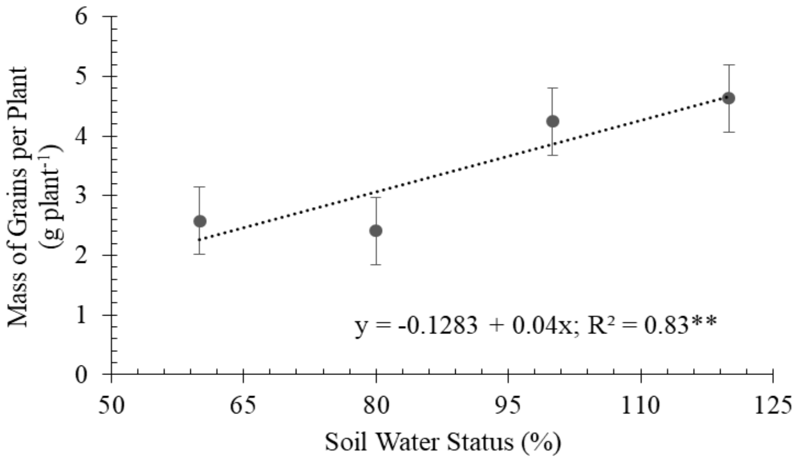

Figure 7. Mass of grains per plant as a function of soil water status under protected environment at Ponta Grossa, PR, Brazil, 2024.
*: $P < 0.05$ and **: $P < 0.01$.

MGP was not influenced by soil Ca:Mg ratios, but a linear augment in such a response-variable as a function of soil water status was verified herein. Similarly, crop yield obtained by Sanches et al. (2015) was also conditioned by soil water supply, being described by a quadratic regression model in light of cultivation of three distinct barley cultivars. As in our work, barley grain commercial yields assessed by Mollah & Paul (2011) were determined by three different soil water regimes. Yields were equivalent to 2.1, 1.9, and 1.7 Mg ha^{-1} under irrigation amounts of 40 mm, 20 mm, 0 mm, respectively. Sanches et al. (2015) also detected reductions in MGP of wheat owing to lack of water at the beginning of flowering. Mean estimated values of MGP were of 5.5 g under suitable soil water supply and 2.2 g under water deficit conditions.

TGW of barley was neither substantially conditioned by soil cationic balance nor by interaction between soil water status and Ca:Mg ratios. Nevertheless, TGW was considerably driven by soil water supply levels. Such a response-variable was mathematically described by a linear regression model that led to maximum and minimal values corresponding to 52 g and 49 g under 120% and 60% ETm, respectively (Fig. 8).

TGW was not affected by soil cationic balance; however, soil water availability exerted a significant effect on expression of such a yield component. By scrutinizing the impact of soil water supply on TGW of three barley cultivars, Sanches et al. (2015) came up with a quadratic relationship between independent variables and response-variables for their studied genotypes. Conversely, Nagaz et al. (2008), as in our study, detected impact of irrigation treatments on TGW of barley grown in open-field conditions at Southern Tunisia. Its mean thresholds gauged by the aforementioned authors were of 48.0 g, 46.7 g, 44.4 g, and 43.2 g under water treatments of 100%, 85%, 70%, and 50% ETm, respectively. In light of evaluation of effect of water deficit on three wheat varieties cultivated under protected environment conditions, Santos et al. (2012) verified that TGW of such a winter cereal was also governed by soil water supply, with mean thresholds corresponding to 35.3 g and 24.3 g under full-irrigation treatment and water deficit imposed at the beginning of flowering, respectively.

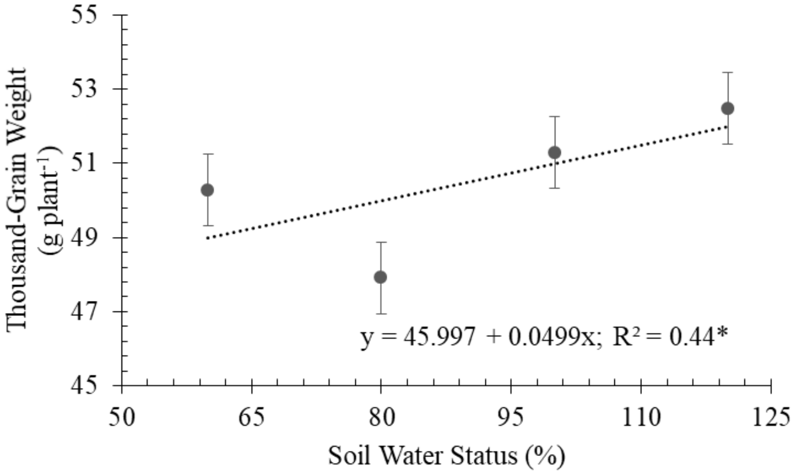

Figure 8. Thousand-grain weight as a function of soil water status under protected environment at Ponta Grossa, PR, Brazil, 2024.
*: $P < 0.05$ and **: $P < 0.01$.

Nevertheless, Medeiros et al. (2008) described a quadratic responsiveness of dry mass of aerial parts of maize plants grown under protected environment for 45 days at different soil Ca:Mg ratios. From such a particular study, the authors verified that dry mass of aerial parts of maize decreased with increments in soil Ca:Mg ratios applied (1:1, 2:1, 4:1, 8:1, 16:1, and 32:1).

Plant water status is dependent on local climatic conditions, as well as irrigation (Vasilaki et al., 2023). In general, crop productivity is a result of rate and duration of effective period of grain filling (Wijewardana et al., 2018). Thus, plants subjected to lack of water throughout such a phenological stage are a target of reductions in size and grain mass (Salinas et al., 1997). According to Shah & Paulsen (2003), lower grain yields under water deficit condition might be ascribed to reductions in photoassimilates synthetized to promote grain filling, limiting absorption of photoassimilates and diminishing duration of effective period of grain filling.

Grain yield turns out to be a consequence of expression and association of several plants' growth components (Anjum et al., 2011). Water deficit culminates in severe reductions in attributes concerning productivity of cultivated agricultural species, likely because of changes in leaf gaseous exchange properties in such a way as to limit plant tissue growth, phloem loading, translocation of assimilates, and dry matter partitioning (Farooq et al., 2009). Several metabolic processes along with activities of different enzymes that play a pivotal role in growth and crop yield are negatively affected by water deficiencies (Allen et al., 1998).

According to Medeiros et al. (2008), increments in soil saturation for Ca^{+2} might bring about nutritional unbalance owing to preferential absorption of such nutrient in detriment of Mg^{2+} and K^{+} ions. Deficiency of Mg^{2+} leads to a characteristic chlorosis between foliar nervures, firstly identified in old leaves as a result of a high mobility of this particular ion in the plants (Taiz et al., 2017). With regard to K^{+}, its deficiency is indicated by a visible symptom as a spot or marginal chlorosis, which evolves to necrosis afterwards more frequent on leaf tips, margins and between nervures. However, such effects were not observed in our study as a function of soil Ca:Mg ratios ranging from 1:1 to 9:1.

Agronomic performance of barley was not governed by soil cationic balance because the soil solution contained suitable Ca^{+2}, Mg^{+2}, and K^{+} concentrations, irrespective of those soil Ca:Mg ratios imposed in our study. Such results demonstrated that any Ca:Mg proportion applied to the soil culminated in sufficient amounts of Ca and Mg available to the plants. Supply of Ca, Mg, and K was not conditioned by soil cationic balance to the point of triggering deficiency symptoms of these macronutrients in barley crop.

Soil chemical attributes

Exchangeable Calcium content in soil was significantly affected by both water supply and soil Ca:Mg ratios. However, interaction effect between factors on exchangeable Ca content was not detected in our experiment. There was a linear reduction in exchangeable Ca content with increases in soil water availability, which fluctuated from 5.2 $cmol_c\ dm^{-3}$ under 60% ETm to 4.3 $cmol_c\ dm^{-3}$ under 120% ETm treatments (Fig. 9).

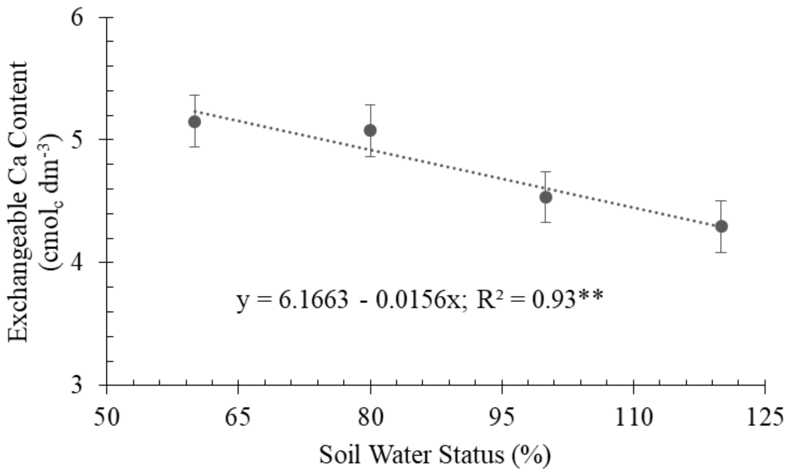

Figure 9. Exchangeable Ca content in soil after barley cultivation as a function of soil water status under protected environment at Ponta Grossa, PR, Brazil, 2024.
*: $P < 0.05$ and **: $P < 0.01$.

Regarding soil cationic balance factor, exchangeable Calcium in soil was described by a quadratic regression model, with maximum and minimal values of 5.3 and 3.7 $cmol_c\ dm^{-3}$ under 9:1 and 1:1 soil Ca:Mg ratios, respectively (Fig. 10).

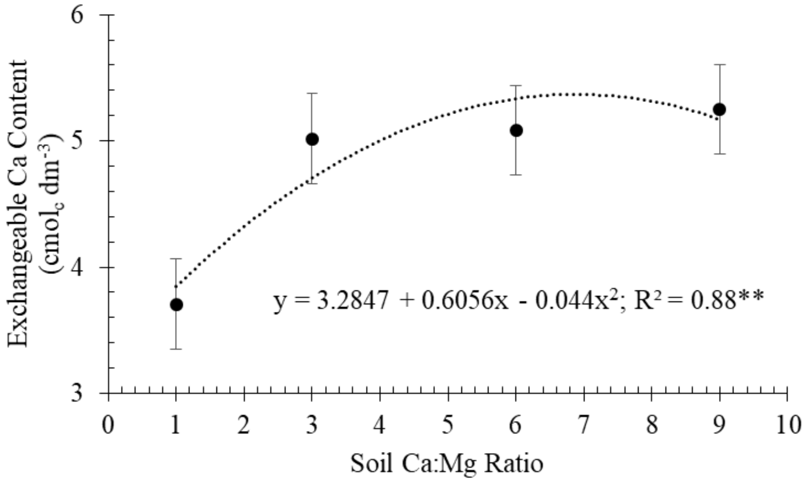

Figure 10. Exchangeable Ca content in soil after barley cultivation as a function of soil Ca:Mg ratios under protected environment at Ponta Grossa, PR, Brazil, 2024.
*: $P < 0.05$ and **: $P < 0.01$.

The increment in soil water supply was conducive to a linear reduction in exchangeable Ca content in soil under the experimental conditions of our study. The greatest soil water status is related to exchangeable Ca concentration in soil in such a manner as to increase Ca uptake in so far as soil moisture turns out be the highest. Absorption of Ca^{2+} by the roots of barley plants was governed by soil water status, demonstrating that the lowest contents of such nutrient were ascribed to the highest Ca^{2+} uptake by the roots, since such a cation gets to the roots by means of mass flux (Raij, 2011).

Increments in soil Ca:Mg ratios also significantly enhanced exchangeable Ca content in soil. This result was already expected and is extremely associated with increases in Ca in soil owing to the highest $CaCO_3$ amounts applied in detriment of the lowest $MgCO_3$ incorporated into the soil as a function of augments in Ca:Mg ratios. Similar to the outcomes reported in our research, Medeiros et al. (2008) detected a quadratic variation in exchangeable Ca contents in soil cultivated with maize as a function of soil cationic balance under protected environment throughout 45 days. Soil Ca:Mg ratios imposed in this experiment were corresponding to 1:1, 2:1, 4:1, 8:1, 16:1, and 32:1 in light of exchangeable Ca contents in soil ranging from 6.2 $cmol_c\ dm^{-3}$ under the lowest Ca:Mg ratio to 24.5 $cmol_c\ dm^{-3}$ under the highest Ca:Mg ratio. Chaganti et al. (2021) found in comparison to control treatment increments in exchangeable Ca contents in soil of 8% and 26% at Hirzel and West Badger, Ohio, USA, respectively, in the face of liming application along with magnesium sulphate throughout 2015–2020 harvest under crop rotation systems of soybean, maize, and winter cereal.

Exchangeable Mg content in soil was neither influenced by water availability nor by interaction effect between water supply levels and soil Ca:Mg ratios. Conversely, exchangeable Mg was extremely determined by soil cationic balance. A quadratic regression model described exchangeable Mg content in soil under different Ca:Mg ratios, with extreme thresholds ranging from 0.5 to 2.2 $cmol_c$ dm^{-3} under 9:1 and 1:1 Ca:Mg ratios, respectively (Fig. 11).

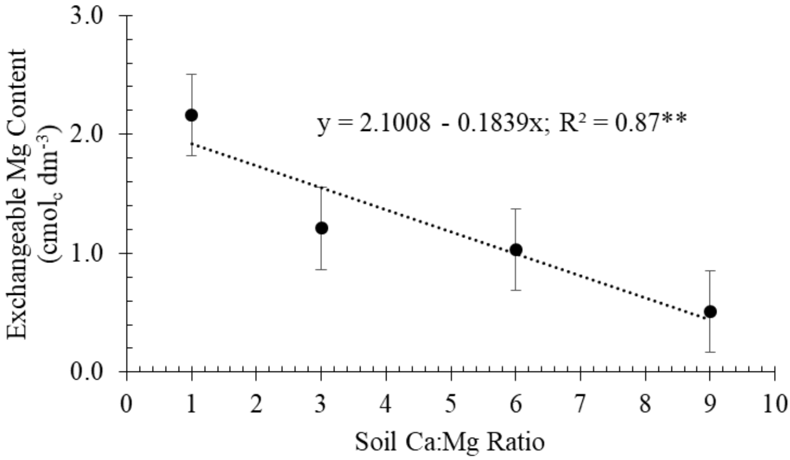

Figure 11. Exchangeable Mg content in soil after barley cultivation as a function of soil Ca:Mg ratios under protected environment at Ponta Grossa, PR, Brazil, 2024.
*: $P < 0.05$ and **: $P < 0.01$.

Similar to evidences found herein for exchangeable Ca contents in soil, a reduction in concentration of Mg in soil was a mere result of increases in $CaCO_3$ quantity in detriment of $MgCO_3$ incorporated as a function of increments in soil Ca:Mg ratios. Likely, Medeiros et al. (2008) observed that exchangeable Mg contents in soil plumbed with increases in Ca:Mg ratios in soil cultivated with maize under protected environment conditions. Their extreme thresholds obtained by the aforementioned authors were of 5.7 and 0.8 $cmol_c$ dm^{-3} under 1:1 and 32:1 soil Ca:Mg ratios, respectively. Chaganti et al. (2021) evidenced increments in exchangeable Mg contents in soil of 27% and 47% at Hirzel and West Badger, Ohio, USA, respectively, as a function of soil cationic balance in the face of liming and magnesium sulphate applications throughout 2015–2020 harvest under rotation systems with soybean, maize, and winter cereal crops.

Soil water supply did not remarkably impinge upon concentration of exchangeable K in soil after barley cultivation (Fig. 12). Furthermore, substantial effects of soil cationic balance and interaction between water supply and soil Ca:Mg ratios on exchangeable K content in soil were not evidenced in our study. Maximum and minimal exchangeable K contents in soil were of 0.27 and 0.16 $cmol_c$ dm^{-3} under 60% ETm and 120% ETm, respectively (Fig. 12).

Figs 10, 11, and 12 evidence that contents of changeable Ca, Mg, and K in soil solution shortly after cultivation of barley were above concentration thresholds recommended by literature concerning liming and soil fertilization techniques for the State of Paraná, brazil

(Pauletti & Motta, 2017). Therefore, as observed in our particular research, Soto et al. (2023) did not detect significant impacts of soil Ca:Mg ratios on soybean and maize yields throughout six harvest seasons in Ohio, USA. Distinct soil Ca:Mg ratios were obtained by the aforementioned authors by application of the following agricultural correctives: calcium sulphate, magnesium sulphate, calcium sulphate + calcitic limestone, and magnesium sulphate + dolomitic limestone. Chaganti et al. (2021) did not detect any impact of applications of calcium sulphate and magnesium sulphate on soybean, maize, and winter cereals yields throughout harvest seasons comprised from 2015 to 2020 in Hirzel and West Badger, Ohio, USA. Such a particular study demonstrated that crop commercial yields were not impinged as a function of the treatments imposed, as long as soil presented desirable levels of natural fertility to provide crops with their nutritional and physiological requirements at a given site.

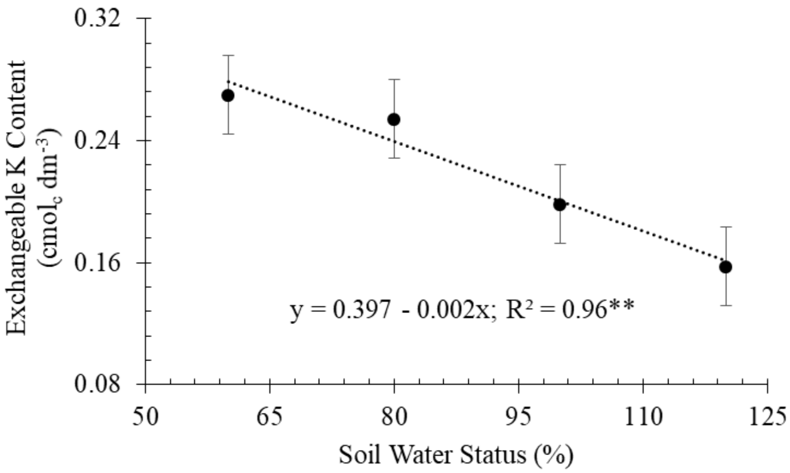

Figure 12. Exchangeable K content in soil after barley cultivation as a function of soil water status under protected environment at Ponta Grossa, PR, Brazil, 2024.
*: $P < 0.05$ and **: $P < 0.01$.

Soto et al. (2023), by conducting field experiments in the USA over 6 years, came up with the conclusion that regression analysis revealed corn yields were positively related to increasing soil pH to optimal levels but were not affected by soil Ca:Mg ratio. Conversely, soybean yields were not related to either soil Ca:Mg ratios nor soil pH. Consistent with previous studies, the aforementioned authors found that balancing soil Ca and Mg levels did not affect corn or soybean yields; however, managing soil acidity remains as a fundamental tool to improve crop yields and manage soil fertility.

The lowest exchangeable K content in soil under wettest soil moisture conditions might be related to the highest soil water availability, which favours K diffusion in soil solution along with its transportation towards rhizosphere. This can also be explained by better nutrient uptake when water is available to plants. Such a discrepancy in exchangeable K content in aerial part of barley plants between irrigated and non-irrigated treatments during periods of three, six and nine days was reported by Anjum et al. (2003).

This particular dynamic of K^+ absorption by the roots is highly driven by soil water status, revealing that the lowest exchangeable K content in soil is a consequence of a higher nutrient uptake by the plants, once the ion-root contact process from soil solution to rhizosphere predominantly takes place by means of diffusion and, at a minor magnitude, by mass flux (Raij, 2011). Both processes in turn are extremely dependent on soil water supply prevailing in agricultural production systems.

CONCLUSIONS

Barley agronomic performance was determined by soil moisture conditions. Increments in the number of tillers per plant, number of spikes per plant, number of grains per plant, mass of grains per plant, and thousand-grain mass were described by a simple linear regression model as a function of increasing soil water availability.

Barley agronomic performance was not conditioned by soil cationic balance because the soil solution contained suitable Ca^{+2}, Mg^{+2}, and K^+ concentrations, regardless of soil Ca:Mg ratios under scrutiny.

Calcium extraction by barley plants linearly augmented as a function of increasing soil water availability regimes.

Magnesium extraction by barley plants linearly plummeted with rises in soil water availability under 3:1, 6:1, and 9:1 soil Ca:Mg ratio treatments.

Soil Cationic balance did not affect extraction of calcium, magnesium, and potassium by barley plants.

Soil cationic balance did not impinge upon nutritional state of barley plants irrespective of soil moisture status.

Assessment of soil Ca:Mg ratios to maintain food security and other ecosystem services ranging from 1:1 to 9:1 does not guarantee either fertilizer or limestone use efficiency in order to substantially minimize production costs at a commercial scale in barley fields.

The most suitable soil Ca:Mg ratio for obtaining the best agricultural response of barley under a protected environment did not depend on soil moisture levels.

Additional studies are needed to further promote a better understanding on crop physiological mechanisms in light of distinct root cation exchange capacity (CEC) as a function of plant metabolism type, which certainly govern both water dynamics in the soil-plant system and also uptake efficiency of Ca, Mg, and K in agricultural production fields.

ACKNOWLEDGMENTS. This paper was financially supported by CAPES - The Coordination for The Higher Education Personnel – Finance code 001, and by CNPq – National Council for Scientific and Technological Development [Grant 304246/2021-2], Brazil. Authors are very grateful to the State University of Ponta Grossa that provided data collection for idealization and completion of the current manuscript.

REFERERENCES

Agegnehu, G., Nelson, P.N. & Bird, M.I. 2016. Crop yield, plant nutrient uptake and soil physicochemical properties under organic soil amendments and nitrogen fertilization on Nitisols. *Soil & Tillage Research* **160**, 1–13. https://doi.org/10.1016/j.still.2016.02.003

Allen Jr., L.H., Valle, R.R., Jones, J.W. & Jones, P.H. 1998. Soybean leaf water potential responses to carbon dioxide and drought. *Agronomy Journal* **90**, 375–383. https://doi.org/10.2134/agronj1998.00021962009000030010x

Anjum, F., Yaseen, M., Rasool, E., Wahid, A. & Anjum, S. 2003. Water stress in barley (*Hordeum vulgare* L.) II. Effect on chemical composition and chlorophyll contents. *Pakistan Journal of Agricultural Sciences* **40**(1–2), 45–49.

Anjum, S.A., Xie, X., Wang, L., Saleem, M.F., Man, C. & Lei, W. 2011. Morphological, physiological, and biochemical responses of plants to drought stress. *African Journal of Agricultural Research* **6**, 2026–2032. https://doi.org/10.5897/AJAR10.027

Asher, C.J. & Ozanne, P.G. 1961. The cation exchange capacity of plant roots and its relationship to the uptake of insoluble nutrients. *Australian Journal of Agricultural Research* **12**, 755–766. https://doi.org/10.1071/AR9610755

Barber, S.A. 1974. Influence of the plant root on ion movement in soil. In: CARSON, E. W. (eds.): *The plant root and its environment*. University of Virginia, Charlottesville, VA, USA, pp. 525–564.

Brasil. Ministério da Agricultura, Pecuária e Abastecimento. 2009. *Rules for Seed Analysis*. SNDA/DNPV/CLAV, Brasília, DF, Brazil, 395pp. (in Portuguese).

Casaroli, D. & Lier, Q.J. 2008. Criteria for pot capacity determination. *Revista Brasileira de Ciência do Solo* **32**(1), 59–66. https://doi.org/10.1590/S0100-06832008000100007 (in Portuguese).

Chaganti, V.N., Culman, S.W., Herms, C., Sprunger, C.D., Brock, C., Soto, A.L. & Doohan, D. 2021. Base cation saturation ratios, soil health, and yield in organic field crops. *Agronomy Journal* **113**(5), 4190–4200. https://doi.org/10.1002/agj2.20785

Clair, S.B.S. & Lynch, J.P. 2010. The opening of Pandora's Box: climate change impacts on soil fertility and crop nutrition in developing countries. *Plant and Soil* **335**(1–2), 101–115. https://doi.org/10.1007/s11104-010-0328-z

CONAB – Companhia Nacional de Abastecimento. 2025. *Brazilian Crop Monitoring: Grains – 2024/2025 Harvest – 11th Survey*. CONAB **12**(11), Brasília, DF, Brazil. https://www.gov.br/conab/pt-br/atuacao/informacoes-agropecuarias/safras (in Portuguese).

Costa, A.R. 2001. *Water relations of vascular plants*. Universidade de Évora, Évora, Portugal, 75 pp. (in Portuguese).

Dawson, I.K., Russell, J., Powell, W., Steffenson, B., Thomas, W.T.B. & Waugh, R. 2015. Barley: a translational model for adaptation to climate change. *New Phytologist* **206**(3), 913–931. https://doi.org/10.1111/nph.13266

Dellabiglia, W.J., Jorge, R.C., Rodrigues, S.A., Dal Pai, A., Sarnighausen, V.C.R. & Oliveira, V.C. 2025. Evaluation of agrometeorological parameters for the culture of hops (*Humulus lupulus* L.) in a protected environment. *Nativa* **13**(1), 70–79. https://doi.org/10.31413/nat.v13i1.17463 (in Portuguese).

Domingues, R., Mattos, J.V., Caires, E.F. & Pereira, A.B. 2026. Performance of soybean genotypes as affected by water supply levels and soil cationic balance in Brazil. *Communications in Soil Science and Plant Analysis* **57**(1), 15–31. https://doi.org/10.1080/00103624.2025.2558198 (in Portuguese).

Farooq, M., Wahid, A., Kobayashi, N., Fujita, D. & Basra, S.M.A. 2009. Plant drought stress: effects, mechanisms and management. *Agronomy for Sustainable Development* **29**, 185–212. https://doi.org/10.1007/978-90-481-2666-8_12

FAOSTAT. 2025. *Crops and livestock products*. FAO (Food and Agriculture Organization of the United Nations), Rome, Italy. https:// www.fao.org/faostat/en/#data/QCL

Fernandes, M.S. & Souza, S.R. 2006. Absorção de nutrientes [Uptake of nutrients]. In: FERNANDES, M.S. (eds.) *Nutrição mineral de plantas [Mineral nutrition of plants]*. 1.ed. Sociedade Brasileira de Ciência do Solo, Viçosa, MG, Brazil, pp. 115–153 (in Portuguese).

Hong, Y. & Zhang, G. 2020. The influence of drought stress on malt quality traits of the wild and cultivated barleys. *Journal of Integrative Agriculture* **19**(8), 2009–2015. https://doi.org/10.1016/S2095-3119(19)62794-2

Jahromi, M.N., Razzaghi, F. & Zand-Parsa, S. 2023. Strategies to increase barley production and water use efficiency by combining deficit irrigation and nitrogen fertilizer. *Irrigation Science* **41**, 261–275. https://doi.org/10.1007/s00271-022-00811-0

Kerbauy, G.B. 2004. *Plant physiology*. 1st edition, Guanabara Koogan, Rio de Janeiro, RJ, Brazil, 431 pp. (in Portuguese).

Lange, A., Cavalli, E, Pereira, C.S., Chapla, M.V. & Freddi, O.S. 2021. Calcium:magnesium ratio and chemical characteristics of soil under crop of soy and corn. *Nativa* **9**(3), 294–301. https://doi.org/10.31413/nativa.v9i3.11526 (Abstract in English).

Luz, W.C. 1982. *Diagnose das doenças da cevada no Brasil*. [Diagnosis barley diseases in Brazil]. EMBRAPA-CNPT. Extension Brochure 2, Passo Fundo, RS, Brazil, 24 pp. (in Portuguese).

Marques, D.M., Magalhães, P.C., Marriel, I.E., Gomes Junior, C.C., Silva, A.B, Reis, C.O., Souza, K.R.E.D. & Souza, T.C. 2023. Does *Azospirillum brasilense* mitigate water stress and reduce the use of nitrogen fertilizers in maize? *South African Journal of Botany* **156**, 278–285. https://doi.org/10.1016/j.sajb.2023.03.041

Medeiros, J.C., Albuquerque, J.A., Mafra, A.L., Rosa, J.D. & Gatiboni, L.C. 2008. Calcium:Magnesium ratio in amendments of soil acidity: nutrition and initial development of corn plants in a Humic Alic Cambisol. *Semina: Ciências Agrárias* **29**(4), 799–806. https://doi.org/10.5433/1679-0359.2008v29n4p799 (in Portuguese).

Mollah, M.S.I. & Paul, N.K. 2011. Responses of irrigation and fertilizers on the growth and yield of *Hordeum vulgare* L. *Bangladesh Journal of Scientific and Industrial Research* **46**(3), 369–374. https://doi.org/10.3329/bjsir.v46i3.9045

Mulatu, B. & Lakew, B. 2011. Barley research and development in Ethiopia-an overview. In: Mulatu, B. & Grando, E. (eds.): *Barley research and development in Ethiopia*. ICARDA, Addis Ababa, Ethiopia, pp. 1–18.

Nagaz, K., Toumi, I., Masmoudi, M.M. & Mechlia, N.B. 2008. Soil salinity and barley production under full and deficit irrigation with saline water. *Research Journal of Agronomy* **2**(3), 90–95.

Newton, A.C., Flavell, A.J., George, T.S., Leat, P., Mullholland, B., Ramsay, L., Revoredo-Giha, C., Russell, J., Steffenson, B.J., Swanston, J.S., Thomas, W.T.B., Waugh, R., White, P.J. & Bingham, I.J. 2011. Crops that feed the world 4. Barley: a resilient crop? Strengths and weaknesses in the context of food security. *Food Security* **3**, 141–178. https://doi.org/10.1007/s12571-011-0126-3

Nitsche, P.R., Caramori, P.H., Ricce, W.S. & Pinto, L.F.D. 2019. *Atlas climático para o Estado do Paraná* [Climatic Atlas for Paraná State]. Instituto Agronômico do Paraná, Londrina, Brazil, 210 pp. (in Portuguese).

Pauletti, V. & Motta, A.C.V. 2017. *Manual de adubação e calagem para o Estado do Paraná*. [Fertilization and Liming Manual for the State of Paraná]. Sociedade Brasileira de Ciência do Solo- Núcleo Estadual Paraná, Curitiba, PR, Brazil, 482 pp. (in Portuguese).

R Core Team. 2022. *R: A language and environment for statistical computing*. R Foundation for Statistical Computing, Vienna, Austria. https://www.R-project.org

Raij, B. 2011. *Soil fertility and nutrient management*. International Plant Nutrition Institute, Piracicaba, SP, Brazil, 420 pp. (in Portuguese).

Salinas, A., Zelener, N., Craviotto, R. & Bisaro, V. 1996. Physiological responses of different soybean cultivars to soil water stress. *Pesquisa Agropecuária Brasileira* **31**(5), 331–338 (in Spanish).

Sanches, F.M., Cunha, F.F., Santos, O.F., Souza, E.J., Leal, A.J.F. & Theodoro, G.F. 2015. Agronomic performance of barley cultivars under different irrigation depths. *Semina: Ciências Agrárias* **36**(1), 89–102. https://doi.org/10.5433/1679-0359.2015v36n1p89 (in Portuguese).

Santos, D., Guimarães, V.F., Klein, J., Fioreze, S.L. & Macedo Junior, E.K. 2012. Wheat cultivars submitted to water deficit at the beginning of flowering in greenhouse. *Revista Brasileira de Engenharia Agrícola e Ambiental* **16**(8), 836–842. http://dx.doi.org/10.1590/S1415-43662012000800004 (in Portuguese).

Schneider, H.M., Wojciechowski, T., Postma, J.A., Brown, K.M., Lücke, A., Zeisler, V., Schreiber, L. & Lynch, J.P. 2017. Root cortical senescence decreases root respiration, nutrient content and radial water and nutrient transport in barley. *Plant, Cell & Environment* **40**(8), 1392–1408. https://doi.org/10.1111/pce.12933

Shah, N.H. & Paulsen, G.M. 2003. Interaction of drought and high temperature on photosynthesis and grain-filling of wheat. *Plant Soil* **257**, 219–226. https://doi.org/10.1023/A:1026237816578

Soto, A.L., Culman, S.W., Herms, C., Sprunger, C. & Doohan, D. 2023. Managing soil acidity vs. soil Ca:Mg ratio: What is more important for crop productivity? *Crop, Forage & Turfgrass Management*, 1–10. https://doi.org/10.1002/cft2.20210

Taiz, L., Zeiger, E., Moller, I.M. & Murphy, A. 2017. *Plant physiology and development*. 6th edition, Artmed, Porto Alegre, RS, Brazil, 858 pp. (in Portuguese).

Vasilaki, C., Katsileros, A., Doulfi, D., Karamanos, A. & Economou, G. 2023. Evaluation of seven barley genotypes under water stress conditions. *Agronomy Research* **22**(1), 222–238. https://doi.org/10.15159/AR.22.083

Wijewardana, C., Reddy, K.R., Alsajri, F.A., Irby, J.T., Krutz, J. & Golden, B. 2018. Quantifying soil moisture deficit effects on soybean yield and yield component distribution patterns. *Irrigation Science* **36**, 241–255. https://doi.org/10.1007/s00271-018-0580-1

Williams, D.E. & Coleman, N.T. 1950. Cation exchange properties of plant root surfaces. *Plant and Soil* **2**(2), 243–256. https://doi.org/10.1007/BF01852352

Zargar, M., Bodner, G., Tumanyan, A., Tyutyuma, N., Plushikov, V., Pakina, E., Shcherbakova, N. & Bayat, M. 2018. Productivity of various barley (*Hordeum vulgare* L.) cultivars under semi-arid conditions in southern Russia. *Agronomy Research* **16**(5), 2242–2253. https://doi.org/10.15159/AR.18.176

Agronomy Research **24**(S1), 147–163, 2026
https://doi.org/10.15159/AR.26.022

An explainable AI-driven framework for precision agriculture: a comprehensive survey

A.D. Dhotre[1,*], S.A. Thorat[2,*], B.S. Yelure[3] and P.B. Jawade[4]

[1]Government College of Engineering, Department of Computer Science and Engineering, Karad, Maharashtra, India
[2]Government College of Engineering, Department of Information Technology, Karad, Maharashtra, India
[3]Government College of Engineering, Department of Information Technology, Kolhapur, Maharashtra, India
[4]Government College of Engineering, Department of Computer Science and Engineering, Nagpur, Maharashtra, India
*Correspondence: aakashdhotre12@gmail.com, sathorat2003@gmail.com

Received: December 30th, 2025; Accepted: March 31st, 2026; Published: April 21st, 2026

Abstract. This review focuses on crop recommendation systems and provides a thorough explanation of Explainable AI (XAI) in precision agriculture. The paper charts the development of predictive models that have been published in the literature, from straightforward, comprehensible algorithms to extremely accurate 'black box' ensemble and deep learning models, as well as their lack of transparency, which may erode farmers' confidence. In order to make these black box algorithms comprehensible and useful, the paper focuses on two XAI frameworks – LIME and SHAP – that are currently in use. The accuracy and explainability trade-off, problems with data heterogeneity, and the requirement for relevant user explanations are just a few of the significant gaps in the evidence base that are highlighted by the paper's synthesis of the research. The paper's concluding remarks provide a potential path toward integrated, reliable, and comprehensible AI systems that will enhance contemporary sustainable agriculture.

Key words: crop recommendation system, deep learning, explainable AI (XAI), LIME, machine learning, precision agriculture, SHAP, trustworthy AI.

INTRODUCTION

The global agricultural industry is at a critical point in the twenty-first century. Food production will have to be greatly rethought in light of the increasing pressures of climate change, a growing global population and sustainable use of natural resources (Hasan, 2024; Khaliq et al., 2025). As it attempts to find a balance amid these competing demands, Precision Agriculture (PA) has emerged as a significant paradigm shift that employs technology to facilitate a data-informed approach at the field level. The development of Precision Agriculture has progressed significantly over a period of time, since the 1970s, as a result of advancements in digital technology (e.g., cellular networks) and the introduction of new AI algorithms into agriculture itself.

A key driver of the paradigm shift is an increased reliance of Artificial Intelligence (AI), and more specifically, Machine Learning (ML), being the analytical 'engine' to the modern agricultural paradigm. In particular, the rise of AI-based crop recommendation systems is an exciting new development with the potential to increase agricultural productivity and profitability for farms as they will be able to recommend the most suitable crops for a particular piece of land, based on soil and climatic condition, alongside previous crop yield for that land (Doshi et al., 2018; Senapaty et al., 2024).

The development of these models in agriculture has followed a similar pattern, prioritizing prediction accuracy over other metrics like interpretability. The earliest studies leveraged relatively simple classification algorithms leveraging Decision Trees, Support Vector Machines, and Naïve Bayes, that provided some level of interpretability but were challenged by the non-linear complexity of agricultural datasets (Doshi et al., 2018; Bandara et al., 2020). The agricultural research community very quickly began to incrementally exceed predictive accuracy with ensemble algorithms such as Random Forests and Gradient Boosting, that combine multiple predictive models using deterministic or probabilistic aggregation strategies to improve predictive performance and robustness (Kulkarni et al., 2018; Shams et al., 2024). More recently, the agricultural research community has gravitated towards the application of deep learning methods or articulated techniques that use deep learning as a type of 'base algorithm framework exhibited optimal performance with complex multi-modal data, such as imagery data captured by satellite or sensor data collected in real time and is even raised the potential upper ceiling of predictive accuracy (Hasan, 2024; Malashin et al., 2024).

The ongoing push for precision, however, has resulted in an 'interpretability crisis'. As models have become more complex, the internal reasoning conducted by models has become less clear, making them into 'black boxes'. This lack of transparency introduces an enormous barrier to adoption, as farmers, quite reasonably, are likely not going to want to trust predictive recommendations and take action on them without knowledge of how the prediction occurred. To address this problem, the research field called Explainable AI (XAI) is being developed. For models in agriculture, fundamental XAI frameworks such as SHapley Additive exPlanations (SHAP) and Local Interpretable Model-agnostic Explanations (LIME) are being repurposed in a post-hoc sense to provide crucial signals on how a prediction was made (Srikanth et al., 2023; Akkem et al., 2025; Yaganteeswarudu et al., 2025).

In conclusion, developing an integrated link between these two fields is more important for the future of AI in precision agriculture than pitting one against the other. We are about to embark on a research phase where engineered XAI techniques are gradually integrated from the ground up with high-performance predictive models. The goal is to build decision-support systems that are strong, reliable, transparent, and able to produce information that farmers or users can use (Turgut et al., 2024; Martin et al., 2024; Shastri et al., 2025). By doing this, the agricultural community will be able to build a foundation of mutual respect and trust for utilizing AI's power to create a resilient, strong, and sustainable food system in the future.

The present survey considers a number of significant contributions to the expanding body of literature regarding AI-enabled Agriculture. First, it describes the many different forms of predictive models/recommendations for crops currently in use and/or under development, including everything from simple, easily understood algorithms through highly complex, accurate ‘Black Box’ approaches. Second, it provides a review of several important pieces of technology related to Explainable AI (XAI), including LIME (Local Interpretable Model-agnostic Explanations), SHAP (SHapley Additive exPlanations), and Counterfactuals, and discusses possible ways to adapt these technologies for use in developing accountability and transparency for AI used in agriculture. In addition, the survey synthesizes the literature to identify and review several critical gaps and problems regarding how we define model performance and model interpretability. In the final chapter of the work, we will introduce a new theoretical framework and research opportunities based on XAI, including how both are related to the design of connected crops recommendation systems.

The remainder of this article is clearly arranged and sequential in order to show these contributions logically. The second section outlines the rigorous survey methodology utilized to curate the literature. The third part starts with a thorough introduction to crop recommendation systems, including their technology and historical background. The fourth section then describes XAI techniques and their applications in agriculture. A critical analysis of the highlighted research possibilities, obstacles, and gaps will be provided in the fifth part. The survey's final segment will conclude with a summary of the overall contributions and the necessity of creating reliable and understandable AI to support sustainable agriculture in the future.

SURVEY METHODOLOGY

In order to obtain a thorough and precise understanding of the present-day situation, a methodical search strategy was used. Several different literature search databases, including Scopus, IEEE Xplore, Web of Science, and Google Scholar, all returned the same results when queried with similar key words. The key words were ‘precision agriculture’, ‘crop recommendations’, ‘explainable AI’, ‘machine learning’, and ‘SHAP/LIME’. The inclusion of studies in the sample involved only peer-reviewed articles or significant conference proceedings published mainly during the prior 8 years that were explicitly focused on either predictive modeling or explainability (interpretable) within an agricultural context. The process for selecting studies included initial review of titles and abstracts to eliminate papers that were not relevant to the study. After this initial process was completed, a more complete examination of the content of each selected article was performed to determine its scientific soundness as measured by the rigor of the original study, the degree of detail in the analysis and the degree to which it related to the core themes of the survey.

REVIEW OF CROP RECOMMENDATION SYSTEM

Crop recommendation systems have arisen within a clear trade-off between interpretability, forecast accuracy, and model complexity. Traditional machine learning models were used in the first generation of crop recommendation systems, which profited from these models' simplicity. Decision Trees (DT), K-Nearest Neighbors (KNN), and Naïve Bayes (NB) were appealing due to their ease of interpretation and ability to display the model's decision logic as straightforward flow-chart rules (Doshi et al., 2018; Bandara et al., 2020; Senapaty et al., 2024). However, the performance of these devices was compromised. First-generation crop recommendation models were unable to capture complex and non-linear relationships inherent in high-dimensional agricultural data, which therefore restricted the predictive power and accuracy of these first-generation models compared to models that utilized higher complexity (Kulkarni et al., 2018; Chitra et al., 2025).

To combat these limitations of accuracy, researchers have utilized more elaborate combination and advanced methods. Both Random Forests (RF) and Gradient Boosting (XGBoost), which are ensemble models with multiple base models of various forms created in succession that act as base models to stabilize predictions, quickly became the 'workhorses' of crop recommendation methods due to their consistent improvements in robustness and accuracy (Kulkarni et al., 2018; Shams et al., 2024; Chitra et al., 2025). Another recent group of model types that has yielded some promise are Deep Learning (DL) models or architectures, such as Convolutional Neural Networks (CNNs), that utilise very complicated models to draw information from complex data types such as satellite or drone imagery (Hasan, 2024; Malashin et al., 2024; Khaliq et al., 2025). These more advanced models reported improvements in predictive accuracy; however, due to the nature of the models and complexity of the underlying architecture of the model, they do provide challenges for explainability, and it can be very difficult to explain the model's recommendations.

New models and assorted data sources are moving advanced systems from improved individual crop recommendations to fully connected smart agriculture systems. The new goal is not simply to recommend an optimum crop, but a whole way in which to manage crops. For example, systems based on AI may now aggregate soil analysis and variable irrigation and fertiliser recommendations to create their own system to maximise efficiency of use (Khaliq et al., 2025). IoT devices passively tracking and monitoring farms to provide real-time updates and support adaptive decision making, coupled with historical year data with yield and market trends to support long-term strategic agricultural planning (Martin et al., 2024; Baishya & Dutta, 2025; Baraian et al., 2025). This is the multidimensional development pipeline and will be next generation, where AI technology is not only recommended optimum information, but operates with some central intelligence and a holistic approach to farm operations.

Dataset considerations and feature engineering

Table 1 displays the criteria of crop recommendation studies that employs the well-known Crop Recommendation Dataset as the starting dataset, which consists of important features such as soil nutrients (N, P, K), climate, and soil pH to develop models for recommending crops (Kulkarni et al., 2018; Kumar & Kumar, 2024; Senapaty et al., 2024). However, the area is rapidly moving beyond the traditional Crop Recommendation Dataset, in order to create more robust and complete agricultural intelligence systems. To create automated disease detection systems, for example, researchers have started experimenting with datasets that increase model capabilities, such as image datasets of plant diseases (Madharam et al., 2024; Sharma et al., 2024; Dhage et al., 2025;). When utilizing a Crop Yield Prediction Dataset, which integrates a more deliberate collection of features, such as historical yields, weather patterns, and remote sensing products to capture NDVI, there is a notable shift in agricultural intelligence from crop recommendation to forecasting and optimization (Hasan, 2024;

Malashin et al., 2024; Jagan Mohan et al., 2025). The most advanced technologies already show a clear path toward more complex and comprehensive applied systems with multidimensional, data-dense precision agriculture by using Early Crop Classification Datasets, which incorporate time-series satellite image datasets that monitor and classify crops early in the growing season (Chan et al., 2023).

Table 1. Datasets and feature types in crop recommendation

Sr. No.	Name of dataset	Features	Useful for	Used in references
1	Recommendation Crop Dataset	Soil Nutrients: Nitrogen (N), Phosphorus (P), Potassium (K); Climatic Conditions: Temperature, Humidity, Rainfall; Soil Property: pH	Identifying the optimal crop based on specific soil and environmental parameters.	Doshi et al., 2018; Kulkarni et al., 2018; Bandara et al., 2020; S & Parvathi, 2021; Musanase et al., 2023; Cartolano et al., 2024; Dey et al., 2024; Kumar & Kumar, 2024; Madharam et al., 2024; Martin et al., 2024; Senapaty et al., 2024; Shams et al., 2024; Sharma et al., 2024; Turgut et al., 2024; Akkem et al., 2025; Baishya & Dutta, 2025; Baraian et al., 2025; Chitra et al., 2025; Khaliq et al., 2025; Shastri et al., 2025; Yaganteeswarudu et al., 2025
2	Plant Disease Datasets	Images of plant leaves and stems in healthy and diseased conditions	Automated plant disease detection and classification from images	Madharam et al., 2024; Sharma et al., 2024; Dhage et al., 2025
3	Crop Yield Prediction Datasets	Past crop yield records, climatic trends, soil classification data, fertilizer application records, and remote sensing indicators (e.g., NDVI)	Forecasting agricultural output and optimising farm management for better productivity	Srikanth et al., 2023; Hasan, 2024; Malashin et al., 2024; Venugopal et al., 2024; Jagan Mohan et al., 2025
4	Early Crop Classification Datasets	Time-series satellite imagery from sources like Sentinel or Landsat	Classifying different crop types from satellite data early in the growing season for monitoring and planning	Chan et al., 2023

A review of AI approaches in crop recommendation

Table 2 provides a review of a selection of research papers that have incorporated the use of Artificial Intelligence (AI) in agriculture and in the area of crop recommendations. The studies reviewed in this article utilize various algorithms such as Random Forest Classifier (RFC) and Stochastic Gradient Descent Classifier (SGDC). Many researchers address class imbalance within the training dataset by using Synthetic Minority

Over-sampling Technique (SMOTE) which creates synthetic examples from minority classes to create a balanced dataset, thus leading to improved classifier performance (Senapaty et al., 2024). Performance of the models is evaluated with numerous metrics including Logarithmic Loss (LogLoss) which is considered a probabilistic classification performance metric and penalizes predictions that have lower confidence.

Table 2. Comparative analytics of crop recommendation systems using ML and DL

Ref.	Objective	Methodology	Novelty	Accuracy	Limitation	Future direction
Senapaty et al., 2024	Create a system to assist farmers in selecting suitable crops	Comparative analysis of ML classification models	Head-to-head comparison of standard classifiers	SGDC 100% after SMOTE	Limited to the specific dataset and geographical context	Apply XAI methods and use a larger, more diverse database
Kumar & Kumar, 2024	Create a reliable and transparent crop recommendation solution	ML model combined with an XAI framework (SHAP or LIME)	Designed with interpretability in mind for farmers.	Naïve Bayes (99.39%)	Computational overhead from XAI; explanations may be complex	Refine XAI methods to be more user-friendly for end users
Kulkarni et al., 2018	Improve accuracy in crop recommendations using ensemble modelling	Ensemble learning techniques (Bagging, Boosting, Voting)	Testing ensemble methods to maximise predictive performance	Ensemble Model 99.91%	Increased model complexity and computational cost	Test the ensemble model on more varied datasets for generalisability
Chitra et al., 2025	Improve accuracy and provide explainability through advanced ensembling	Stacked Ensemble Model combined with XAI techniques	Novel integration of stacking ensemble with interpretability methods	Weighted Stacked Ensemble (99.09%)	Very high model complexity, difficult to tune and deploy	Improve computational efficiencies and integrate other data sources
Baishya & Dutta, 2025; Sharma et al., 2024; Baraian et al., 2025; Khaliq et al., 2025	Establish a crop recommendation model for low-power systems; Create a multi-feature web-based platform; Refine recommendations through market trends; Develop an integrative system	TinyML; Integrated ML/DL models; Recommender system enhanced with trend analysis; AI-driven system combining models	Edge deployment for offline real-time results; Tri-fold web tool; Holistic approach linking soil, irrigation, and fertiliser	Optimised RFC for TinyML (98.4%); XGBoost (99.3%)	Trade-off between model accuracy and footprint; Challenges in integrating separate models; High data dependency	Improve downsized model accuracy; Adopt IoT sensors; Validate across regions and develop farmer-friendly tools

Table 2 (continued)

Jagan Mohan et al., 2025	Deploy AI and XAI for accurate crop yield forecasting	Advanced AI/DL models for yield prediction, augmented with XAI	XAI applied to the complex task of yield prediction	R2 Score: up to 0.92	Accuracy is sensitive to unpredictable factors like extreme weather	Develop lightweight models for limited-resource settings; integrate real-time data
S & Parvathi, 2021	Construct a crop recommendation system using an ANN	A feed-forward Artificial Neural Network (ANN) model.	Use of a neural network for crop recommenda tion	Logloss: 0.00034 (lower is better)	ANNs can be prone to overfitting on smaller dataset	Include seasonal crops and integrate weather and economic factors.

Many of the papers referenced also exhibit a trend of employing Explainable AI (XAI) methods to enable visibility and trust in models that farmers see as overly complicated 'black box' systems. Overall, the papers highlight accuracy (almost always greater than or equal to 99% on generic datasets (Kumar & Kumar, 2024; Senapaty et al., 2024), although generalizability and high complexity are limitations.

The majority of limitations identified through an extensive literature review were methodological in nature, including heavily relying on inflated accuracy metrics without adequately discussing the size of the dataset or employing a sound cross-validation strategy. Very high accuracy (e.g. 100%) can indicate possible overfitting models or limitations of the dataset and consequently should be interpreted with caution. In addition, models that trained on hyper-localized data sets often lack the ability to generalize outside of their training area. Thus, for model to be utilized within practical settings, subsequent research teams will need to provide more diverse datasets (IoT and Satellite Images) that can be associated with their specific purposes and/or present model descriptions that are easier for end-users to understand.

MAKING AI TRANSPARENT WITH EXPLAINABLE AI (XAI)

The increasing complexity of AI technologies in agriculture may potentially increase opacity and raise demands for AI technology transparency. Explainable AI (XAI) approaches, which are crucial to developing ethical and practical agricultural AI systems, are then discussed in this section. Finding the 'black box' and offering advice to developers, agronomists, and producers to comprehend and methodically process AI recommendations is the main goal of XAI.

Explainability is significant and multifaceted when it comes to the uptake and efficacy of technology in agriculture. First, confidence is established through explainability. Farmers can transform an untested command into a reliable record of suggestions when they comprehend the reasoning behind an action or recommendation (Shams et al., 2024; Yaganteeswarudu et al., 2025). Second, explanation enables people to use their information and take purposeful, meaningful behaviors. For instance, the user is aware that their next course of action is potash beefed if it is explicitly advised not to cultivate a crop (Srikanth et al., 2023; Turgut et al., 2024). Lastly, explainability is essential for debugging and model verification because agronomists and researchers are using models and assessment. Specifically, explainability helps to find biases, mistakes, and places for improvement, resulting in better, more predictive models (Cartolano et al., 2024; Akkem et al., 2025).

Several XAI methods focus on local explanations that break apart the reasoning of a single prediction to answer the immediate question, 'Why did the model make this recommendation at my location?'. Although local explanations can be valuable for practical decision-making, one of the most recognised local explanation methods is called LIME, which stands for Local Interpretable Model-Agnostic Explanations. LIME works by introducing small perturbations in the input data (for example, small adjustments in the pH or rainfall value) and examining how the model changes. LIME then uses a simpler and more interpretable model (for example, a linear regression) to fit the local area and the output will be a locally linear approximation of a typically complicated model. Yaganteeswarudu et al. (2025) demonstrate how LIME was able to indicate which soil parameters became increasingly important within a location crop recommendation in a very intuitive manner.

Another influential and extensively used approach is the SHAP framework (SHapley Additive exPlanations), which originates from cooperative game theory. SHAP assigns an 'importance value' to each feature indicating how much each feature has contributed to pushing the prediction towards (or away from) the predicted outcome. In local explanations, this is frequently presented with force plots that visually display how nitrogen (N), phosphorus (P), and temperature, for example, led to a recommendation for one specific crop (Shams et al., 2024; Shastri et al., 2025). SHAP's strong theoretical grounding provides a meaningful approach to fairly distributing portions of the model's decision to each of the input features.

Beyond just interpreting individual predictions, it can be helpful to consider the behaviour of the model as a whole. Global explanations provide a macroscopic view of which features are the most important across the full dataset. SHAP is very flexible to provide global explanations in that it can take and simply sum the contributions of the SHAP values for individual observations to generate a global summary plot where features are ranked by importance across the full dataset, and how the model is arguably making general decisions (Shams et al., 2024; Shastri et al., 2025). Global explanations by SHAP can also be elaborated on further and extended with the use of Counterfactual Explanations, which provides a very simple way to describe the constraints which define the model when responding to 'what if' questions. A counterfactual explanation will often state something like 'If your rainfall had been increased by 20%, your recommended crop would have been Soybean instead of Maize,' and provides simple insight into how the model responded to certain characteristics (Turgut et al., 2024; Akkem et al., 2025).

Extending the XAI toolkit: other modalities

Although LIME and SHAP are the most widely used post-hoc explanation techniques used for crop recommendation research (Hasan, 2024; Madharam et al., 2024; Shams et al., 2024). Despite their intuitive nature, LIME's foundational methodology is often hindered by instability. The use of perturbation sampling to generate localized synthetic data points can produce explanations that vary widely based on the data set's distribution. This may lead to conflicting feature importance rankings for a given data point across different runs, causing users to lose faith in critical agricultural use cases and situations (Yaganteeswarudu et al., 2025).

Similarly, SHAP has significant computational challenges when it comes to calculating exact Shapley values since this requires evaluating every possible combination of features. For large-scale agricultural data sets, especially those produced by relatively deep networks with thousands of parameters, this is computationally prohibitive. As a result, researchers are often forced to resort to using approximations (e.g., TreeSHAP or KernelSHAP), which presents a clear trade-off by sacrificing precise interpretability in exchange for limiting extremely high computational costs, which ultimately hinders real-time, on-device deployments (Kumar & Kumar, 2024; Shastri et al., 2025).

Counterfactual explanations offer active recourse beyond merely explaining the predictive models of feature attribution classes (Srikanth et al., 2023; Turgut et al., 2024). While attribute-based approaches inform farmers of features driving a prediction, counterfactual explanations identify the least amount of changes that would result in a different prediction, providing a pragmatic means for farmers to act prescriptively with information presented (Turgut et al., 2024; Akkem et al., 2025).

Causal explanations endeavour to mitigate a limitation associated entirely with correlation, in descriptive models like LIME and SHAP by organising feature relationships through a causal dependency model (Martin et al., 2024; Jagan Mohan et al., 2025; Khaliq et al., 2025). This limitation regarding correlation is a necessary consideration in agriculture, as predictors for crop yield are often based on correlated features based on non-causal proxies, such as NDVI or canopy greenness (Martin et al., 2024; Venugopal et al., 2024). Causal frameworks offer farmers a sense of viability in predicting and enacting a response based on the intervention that may be rooted more in an agronomically based driver instead of coincidental statistical relationships (Jagan Mohan et al., 2025; Khaliq et al., 2025).

Concept-based explanation goes above feature-level function and represents model prediction behaviours to more human-interpretable agronomic concepts like ‘water stress’, ‘nitrogen deficiency’, and ‘leaf discoloration’ rather than equivalent numeric feature scores (Cartolano et al., 2024; Kumar & Kumar, 2024; Shams et al., 2024). Using concept-based explanations enhances interpretability and trust as model explanations are more consistent with how farmer experts cognitively process information resulting in improved decision making compared to raw feature saliency maps (Cartolano et al., 2024; Shams et al., 2024; Shastri et al., 2025).

Another intuitive form of interpretation has gained prominence – Example-Based Explanations (EBE). Instead of attributing a prediction to features, Example-Based Explanations explain a prediction by locating and displaying exemplars (i.e., specific, real-life examples) from the training data that are most similar to the example at hand. For a farmer, this is highly interpretable, converting a complex recommendation to a relatable context; for example, ‘This system recommends maize because with your soil composition (high N, low P) and weather forecast comparison, your field is 95% similar to a case from last season in the neighbouring county that had high-yield’. By basing explanations in concrete, previous instances, these types of explanations help bridge the gap between abstract, noncontextual data with real experiences from farming and they build a sense of trust through analogy and shared experience (Cartolano et al., 2024; Martin et al., 2024; Shams et al., 2024).

Interaction between datasets and XAI

Table 3 provides a comparative summary of these studies that utilize Explainable AI (XAI) in agriculture decision-support systems. In all of these studies the general aim is to increase transparency and trustworthiness of farmers by pairing high performant machine learning models with XAI frameworks, such as SHAP and LIME. The empirical data represented in Table 3 show the theoretical constraints of XAI methods explained before. As an example, LIME is considered unstable and thus creates complication when implementing in practice. In addition, using SHAP requires an additional level of technical overhead when implementing in practice. Consequently, a pathway for future research that spans across all studies is the need to create more intuitive, user-friendly, and accessible XAI methods that enable farmers the ability to receive a practical, understandable sense of the model's product.

Table 3. Comparative analytics of crop recommendation systems using XAI

Ref.	Objective	Methodology	Novelty	Limitation	Future direction
Kumar & Kumar, 2024	Build a trustworthy and transparent crop recommendation system	ML model integrated with an XAI framework (SHAP or LIME)	Adds transparency and trust to standard crop recommendation models	Explanations might be too technical; XAI adds computational overhead	Focus on making XAI techniques more accessible and intuitive for end-users
Chitra et al., 2025	Enhance accuracy while ensuring interpretability	A Stacked Ensemble Model combined with an interpretability layer	Combines a powerful stacking model with interpretability for high performance and transparency	Stacked models are complex; explanations may be less straightforward	Improve performance with a focus on computational efficiency and new data sources
Srikanth et al., 2023	Empower farmers with an explainable soil recommendation model for rice	ML model focused on soil parameters for rice, with XAI to justify recommendations	Hyperspecialisation on rice, providing actionable insights	Not generalisable to other crops	Extend to other crops, improve based on farmer feedback, and collect more data
Shams et al., 2024	Study how XAI integration affects agricultural decision-making and user trust	ML model paired with XAI, focusing on human-computer interaction	Focuses on the impact of XAI on end-users	Emphasis is on qualitative impact rather than advancing ML performance	Improve model scalability
Yaganteeswarudu et al., 2025	Enhance transparency in smart farming with local, case-by-case explanations	ML model using LIME to explain individual predictions	Application of LIME for producing instance-level explanations	LIME explanation can be unstable	Focus on user-centric design and simplified explanations for farmers

RESEARCH GAPS, CHALLENGES, AND FUTURE DIRECTIONS

While much has been accomplished in advancing the use of AI in precision agriculture, significant barriers still remain at a critical intersection between technology and agriculture. Overcoming barriers is vital to creating resilient, reliable and sustainable systems. In this section we highlight the main gaps in research and provide a potential framework for future research to address the gaps.

Selecting data and models is a significant barrier. The agriculture domain negatively is affected by Data Scarcity and Heterogeneity; since across regions and climates, there is no large, standardized public data set, it is difficult to train a model that will generalize well. There is also an Explainability-Accuracy Trade-Off that can be an ongoing conflict regardless of domain where researchers and developers have to select between a high accuracy, but opaque 'black box' models (e.g., deep neural networks) vs lower accuracy, but naturally interpretable models (e.g., simple decision trees) (Cartolano et al., 2024; Jagan Mohan et al., 2025); the tension to resolve the conflict, and recognise performance or trustworthiness is a major hurdle.

Additionally, there is a glaring absence of human-centric considerations in the cases of XAI. To date, very few, maybe even no systems provide User-Centric Explanations. Again, explanations almost always relate to caveats of model features that are technical and not related or meaningful to a farmer. This challenge is also associated with the challenge of Evaluation of Explanations because there are no universally agreed-upon measures to determine 'goodness' of an explanation in practical agricultural or farming contexts. These characteristics; fidelity to the model, usability in the world, a degree of impact on the farmer's trust, are still subjective and problematic (Cartolano et al., 2024).

To fill the existing void between the newer technology-enabled changes in user-centric explanations and the farmer who needs them clearly communicated, the discussion around user-centric explanations must grow. It is critically essential that the XAI output is made applicable by being articulated in clear, practical recommendations that the farmer can immediately relate to. A good example of this transition might be through the development of explanation interfaces that use LLMs (Large Language Models). A LLM can assist in converting highly technical XAI output, such as SHAP values that reflect a significant weight of importance to a feature (for example, Soil pH), to a more user-friendly format (natural language). For example, rather than providing the farmer with a complex force plot, the farmer would see a simple prompt such as, 'The recommendation from the system is to not plant wheat here because the current soil pH is 5.2 (too low) and you may want to apply agricultural lime before planting'.

The limitations to the uptake of XAI related to the models' reliability are accompanied by various social and economic real-world barriers, along with limited digital literacy and infrastructure challenges (Bandara et al., 2020; Musanase et al., 2023; Dhage et al., 2025). One barrier is simply the digital divide and limited AI literacy among farmers, especially full-time farmers in urban and developing sectors, where higher order and complex XAI visualisations will likely not be accessible or useful (Musanase et al., 2023; Baishya & Dutta, 2025; Dhage et al., 2025). Studies have noted that XAI interface designs prioritise data scientists (likely working in urban settings), and therefore mean little for the practical usability of the interfaces by farmers (Kumar & Kumar, 2024; Akkem et al., 2025; Shastri et al., 2025).

Moreover, economic feasibility and material inequity are significant challenges. Agriculture precision modelling frameworks normally entail the use of expensive sensors, drones, cloud computing for data processing, and subscription analytics services to infer and map, and all this may be out of reach for smallholder farmers (Bandara et al., 2020; Musanase et al., 2023; Baishya & Dutta, 2025; Chitra et al., 2025). If these economics are disproportionate, important research in the agricultural space has suggested to modify inequity by using frugal AI, which identifies taking low inputs such as smart phone imagery, low-cost sensor kits, and deploying on edge computable methods with TinyML technology (Musanase et al., 2023; Baishya & Dutta, 2025).

Data governance and trust between owner and product remains equally essential. There is still uncertainty regarding ownership, privacy, and commercial reuse possibilities of sensitive existing yield and soil records (Akkem et al., 2025; Baraian et al., 2025; Khaliq et al., 2025). There are large initiative working together like the European Agricultural Data Space being set up to make an ecosystem of agricultural data interchangeable and to provide equitable ways to share data about agriculture, existing efforts to achieve this includes the SAGE Project which aims to facilitate transparent, secure, and fair data-sharing ecosystems throughout Europe. Emerging solutions include possible models that safeguard ownership such as Federated Learning, which facilitates local model training without the transfer of raw data from the farmer to a cloud platform (Baraian et al., 2025; Khaliq et al., 2025).

Although the literature labels this problem as related to data governance and Federated Learning (FL), the importance of this issue cannot be understated. The entire concept of precision agriculture rests on collecting large amounts of sensitive farm data. This creates a core contradiction: Farmers are typically reluctant to share sensitive farm data about their soil health, yields, and operational data with a central server that they could lose competitive advantage or trustworthiness (Akkem et al., 2025; Baraian et al., 2025; Khaliq et al., 2025).

This importance is precisely where Federated Learning (FL) opens the door as a key future opportunity, or at the least a partial solution to this critical issue. FL stores the models locally on the agricultural producers own devices, either on the edge computer of the tractor (or similar device (e.g., combine, etc.) or on the producers own servers). Each farm will only send its model updates (gradients or weights, not raw data), to a central server for aggregation. In this way, Federated Learning maintains 'privacy-by-design' and retains the agricultural producers data on-premises and private to their farms (Baraian et al., 2025; Khaliq et al., 2025).

Integrating FL with XAI creates its own new research frontier. How can a global model based on federated learned updates generate an explanation for a specific farmer’s field? The approaches to developing SHAP or LIME component values for a federated model is not trivial, or computationally inexpensive. Future work must use FL, for privacy, but also co-design Federated XAI frameworks that can provide meaningful, local explanations for a farmers field but without sacrificing the privacy that FL was designed to protect. The integration of privacy, federated learning, and explainability will be one of the largest technical and ethical barriers to account for in real-world projects (Musanase et al., 2023; Akkem et al., 2025; Khaliq et al., 2025).

Without addressing the economic feasibility associated with inputs, literacy, and governance informs of the potential of widening inequities, as opposed to reducing inequities in agricultural decision-making (Bandara et al., 2020; Musanase et al., 2023; Akkem et al., 2025; Dhage et al., 2025).

Finally, there are significant technical challenges concerning implementation and performance that need to be addressed. One of the most significant challenges is Scalability and Real-Time Performance. Even if AI can make sense of cultivars and environmental variables, for it to be effective in practice, it needs to produce insights instantaneously. Still, engineering this approach and running computationally expensive, XAI approaches on low-power, resource-constrained edge devices (i.e., via TinyML), and then generating explanations in real-time is a challenge to engineering that will make or break on-farm feasibility.

To tackle these concerns, the research community must focus on a few strategic directions. First, improving foundational models and benchmarks is a highest priority. This means developing Hybrid and Naturally Interpretable Models that are both accurate, and designed to be transparent, instead of relying on potentially dubious, post-hoc explanation methods (Jagan Mohan et al., 2025). This direction must arise from a community-wide effort to develop agricultural XAI standards where agricultural researchers develop shared public datasets, and standardized evaluation approaches to encourage collaborative and comparative research.

The future of agricultural AI should also involve more interactivity and intelligence. The next important step is designing Human-in-the-Loop (HITL) and Interactive XAI systems, whereby farmers will question the AI through 'what-if?' inquiries and explore different assumptions to aid in comprehending the systems rationale. This interactivity will be even more crucial while we increase the Integration of Multimodal Data with XAI. A primary research frontier is developing methods for explaining models that integrate complex data streams, such as tabular soil data, time-series climate data, IoT sensor data, and satellite data.

A notable advancement in dealing with the 'Domain-Specific Explanation Language' could derive from outside the conventional XAI. Generative AI and Large Language Models (LLMs) can really help to supplement the explanation process. The difficulty doesn’t lie in creating a SHAP plot, but how we communicate its technical meaning into action-oriented advice to human(s). This is precisely what Generative AI does very well. A future XAI structure could be conceived as a two-stage process:

1. An ML model (e.g., Gradient Boosting) makes a crop prediction.
2. An XAI method (e.g., SHAP) explains 'Why?' (e.g., 'Potassium = 45 mg kg^{-1} is the highest contributing negative feature.')

This output then generates a usable explanation for the LLM, trained from domain-specific knowledge base and communicates, in conversational form, grounded in the research-derived technical output, an explanation such as the following: 'Your soil is deficient in Potassium (45 mg kg^{-1}), which is an important nutrient for corn. The model is suggesting you use soybeans since soybeans have lower Potassium needs. Another option is to move ahead with corn, but you will need to add a potassium-based fertiliser.'

I think this 'XAI-to-LLM' pipeline is a potentially powerful merge; they are much more than just showing feature importance; you now have a cooperative and prescriptive experience developing real and insightful dialogue with the farmer, and ultimately creating a truly user-centred and understandable AI system (Cartolano et al., 2024; Shams et al., 2024; Jagan Mohan et al., 2025).

Ultimately, the goal is to bridge the communication gap between the AI and the farmer. This is to create Domain Specific Explanation Languages. It is not enough to simply provide a farmer with a technical output of 'pH value of 5.2 is the largest contributor', but rather translate this into actionable advice, 'this soil is too acidic for this crop'. Learning to speak the language of the end user will allow us to enable systems powered by XAI to be not only intelligent but intelligible; and thus, create trust needed to have a real impact in modern agriculture.

Table 4. Identified research gaps, key challenges, and future research directions in AI-Driven precision agriculture

Category	Key gaps & challenges	Future directions / Opportunities
Data & Modelling	• Data scarcity and heterogeneity (several datasets do not share a standardized format) • Low generalizability • Explainability-integrity-accuracy trade-off	• Build shared public agricultural datasets • Develop hybrid and inherently interpretable models • Build agricultural XAI benchmarks and standards
Explainability (XAI)	• Lack of user-centric explanations • No standard evaluation metrics to denote 'good' explanations • Explanations are too technical for farmers	• Design domain-specific explanation language • Develop interactive and Human-in-the-Loop XAI • Include conversational XAI with LLM (XAI→ LLM channel)
Socio-Economic Barriers	• Digital divide and low AI literacy • Poor infrastructure • Interfaces that are designed for data scientists not the farmer • Costs of sensors, drones, cloud services	• Frugal/low-resource AI (smartphone imagery, low-cost sensors, TinyML, edge computing) • Farmer-centric UI and low complexity visualizations
Privacy & Data Governance	• Lack of trust in data ownership & data producers • Fear of competitive disadvantage • Unclarity on data-sharing policies	• Federated Learning (FL) for on-device training • Privacy-preserving model aggregation (no raw data sharing) • Development of Federated XAI for local explanations
Technical Deployment	• Limited scalability • Expensive compute cost associated with XAI • Absence of real-time inference capabilities on edge devices	• Optimize XAI to run on low-power levels (TinyML) • Scalable inference pipelines that support real-time • Efficiency with explainability for multimodal data (soil, climate, sensor, satellite)
Human-AI Interaction	• Lack of decision support in dialogue-based context • No user-friendly 'actionable insights'	• Interactive AI systems (what-if...) • LLM-powered explanations to translate model outputs into actionable farming recommendations
Equity Risks	• Tech likely to exacerbate inequality for smallholder or developing world farmers	• Prioritize affordable, transparent, and locally deployable AI in order to enable equitable access

Table 4 compiles important research gaps, aspects of real-world challenges, and future possible opportunities in advancing AI to the precision agriculture domain. Recent literature provides considerable evidence about the importance of the gaps that have been identified regarding technical data modeling and evaluation, (Cartolano et al., 2024; Jagan Mohan et al., 2025). Furthermore, there continue to be significant barriers that exist due to socio-economic status and the digital divide (Musanase et al., 2023; Dhage et al., 2025). In addition to these gaps are more pressing issues related to data governance and privacy (Khaliq et al., 2025; Baraian et al., 2025), as well as the persistent difficulties that exist in creating effective Human-AI interaction (Shams et al., 2024).

CONCLUSIONS

This article presents a review of crop recommender systems driven by artificial intelligence (AI) and the increasing need for explainable AI (XAI) in agricultural decision support systems. Although sophisticated algorithms, including Random Forests and Neural Networks, and combinations (ensemble) are capable of producing highly accurate forecasts, their black box form can impede their ability to be used in real-world agricultural applications. We also highlighted that many current XAI models extend beyond conventional feature attribution models (LIME, SHAP) to include counterfactual, causal and concept-based explanation formats, each increasing decision support by offering actionable and human-aligned interpretability.

The review also highlights the urgency of open gaps in data heterogeneity, the explainability-accuracy trade-off, and notably, the barrier toward uses from a non-technical contributor lens including cost, digital literacy, and confidence in farm data governance. We contend that agricultural AI needs to consider trust, equity, accessibility, and economic sustainability in addition to accuracy, all of which are supported by privacy-preserving learning and intuitive explanation design. In order to guarantee that AI recommendations are not only accurate but also interpretable, practical, and socially deployable at scale, future work should give priority to collaborative, human-centered frameworks (such as design thinking).

In the end, what will ultimately determine whether AI is successful in precision agriculture will be its ability to get accepted and trusted in the field, and how useful it is to agriculture, versus simply providing a high degree of accuracy in a laboratory environment. If the agricultural sector incorporates principles of human-centered design, validated systems that are tested and documented as reliable, and has systems that support transparent decision making, then AI can be implemented to help create an agricultural system that is better able to respond to the challenges of feeding the world with an ever-increasing population and to being viable and sustainable.

REFERENCES

Akkem, Y., Biswas, S.K. & Varanasi, A. 2025. Role of Explainable AI in Crop Recommendation Technique of Smart Farming. *International Journal of Intelligent Systems and Applications* **17**(1), 31–52.

Baishya, M. & Dutta, L. 2025. Tiny ML based crop recommendation system for precision agriculture 5.0. *Smart Agricultural Technology* **12**, 101247.

Bandara, P., Weerasooriya, T., Ruchirawya, T.H., Nanayakkara, W.J.M., Dimantha, M.A.C. & Pabasara, M.G.P. 2020. Crop Recommendation System. *International Journal of Computer Applications* **175**(22), 22–25.

Baraian, I., Erdei, R., Tamaian, R., Delinschi, D., Pasca, E.M. & Matei, O. 2025. Trend-Enabled Recommender System with Diversity Enhancer for Crop Recommendation. *Agriculture* **15**(15), 1614.

Cartolano, A., Cuzzocrea, A. & Pilato, G. 2024. Analyzing and assessing explainable AI models for smart agriculture environments. *Multimedia Tools and Applications* **83**, 37225–37246.

Chan, A., Schneider, M. & Körner, M. 2023. XAI for Early Crop Classification. *arXiv preprint* arXiv:2310.06574. Available at https://arxiv.org/abs/2310.06574

Chitra, P., Raghuraman, P., Varsha, K.S. & Mallavaram, M. 2025. Enhancing Precision Agriculture through Stacked Ensemble Model and Interpretability. **In:** *2025 1st International Conference on Secure IoT, Assured and Trusted Computing (SATC)*.

Dey, B., Ferdous, J. & Ahmed, R. 2024. Machine learning based recommendation of agricultural and horticultural crop farming in India under the regime of NPK, soil pH and three climatic variables. *Heliyon* **10**, e25112.

Dhage, S., Bhendarkar, D., Pathan, A. & Shahapurkar, A. 2025. Harvestify: A help towards agriculture. *International Journal of Creative Research Thoughts* **13**(5), d454–d458.

Doshi, Z., Nadkarni, S., Agrawal, R. & Shah, N. 2018. AgroConsultant: Intelligent Crop Recommendation System Using Machine Learning Algorithms. **In:** *2018 Fourth International Conference on Computing Communication Control and Automation (ICCUBEA)*, pp. 1–6.

Hasan, M.R. 2024. AI and Machine Learning for Optimal Crop Yield Optimization in the USA. *Journal of Computer Science and Technology Studies* **6**(2), 48–61.

Jagan Mohan, R.N.V., Rayanoothala, P.S. & Sree, R.P. 2025. Next-gen agriculture: integrating AI and XAI for precision crop yield predictions. *Frontiers in Plant Science* **15**, 1451607.

Khaliq, A., Khan, A., Jan, S., Umair, M., Gulshair, A., Ali, A. & Shah, U.A. 2025. AI-Driven Smart Agriculture: An Integrated Approach for Soil Analysis, Irrigation, and Crop-Fertilizer Recommendations. *IEEE Access* **13**, 141124–141138.

Kulkarni, N.H., Srinivasan, G.N., Sagar, B.M. & Cauvery, N.K. 2018. Improving Crop Productivity Through A Crop Recommendation System Using Ensembling Technique. **In:** *2018 3rd IEEE International Conference on Computational Systems and Information Technology for Sustainable Solutions (CSITSS)*, pp. 114–119.

Kumar, S. & Kumar, M. 2024. Enhancing Agricultural Decision-Making through an Explainable AI-Based Crop Recommendation System. **In:** *2024 International Conference on Signal Processing and Advance Research in Computing (SPARC)*.

Madharam, A., Yerram, R.R. & Kanagaraj, K. 2024. Crop Recommendation and Plant Disease Identification. **In:** *Proceedings of the 6th International Conference on Information Management & Machine Intelligence*, pp. 1–7.

Malashin, I., Tynchenko, V., Gantimurov, A., Nelyub, V., Borodulin, A. & Tynchenko, Y. 2024. Predicting Sustainable Crop Yields: Deep Learning and Explainable AI Tools. *Sustainability* **16**(21), 9437.

Martin, R.J., Mittal, R., Malik, V., Jeribi, F., Siddiqui, S.T., Hossain, M.A. & Swapna, S.L. 2024. XAI-Powered Smart Agriculture Framework for Enhancing Food Productivity and Sustainability. *IEEE Access* **12**, 168412–168427.

Musanase, C., Vodacek, A., Hanyurwimfura, D., Uwitonze, A. & Kabandana, I. 2023. Data-Driven Analysis and Machine Learning-Based Crop and Fertilizer Recommendation System for Revolutionizing Farming Practices. *Agriculture* **13**, 2141.

S, B.K. & Parvathi, R. 2021. Crop Recommendation System by Artificial Neural Network. *Research Square*, Preprint. Available at https://doi.org/10.21203/rs.3.rs-874525/v1

Senapaty, M.K., Ray, A. & Padhy, N. 2024. A Decision Support System for Crop Recommendation Using Machine Learning Classification Algorithms. *Agriculture* **14**(8), 1256.

Shams, M.Y., Gamel, S.A. & Talaat, F.M. 2024. Enhancing crop recommendation systems with explainable artificial intelligence: a study on agricultural decision-making. *Neural Computing and Applications* **36**, 5695–5714.

Sharma, A., Mehetre, N. & Kumbhar, K. 2024. Harvestify- ML and DL-based website for crop recommendations, fertilizer suggestions, and plant disease prediction. *International Research Journal of Modernization in Engineering Technology and Science* **6**(5), 6188–6198.

Shastri, S., Kumar, S., Mansotra, V. & Salgotra, R. 2025. Advancing crop recommendation system with supervised machine learning and explainable artificial intelligence. *Scientific Reports* **15**(1), 25498.

Srikanth, M., Jagan Mohan, R.N.V. & Chandra Naik, M. 2023. Empowering Agriculture: A Soil Recommendation Model For Rice Cultivation Using Explainable AI. *Migration Letters* **20**(S12), 1046–1057.

Turgut, Ö., Kök, İ. & Özdemir, S. 2024. AgroXAI: Explainable AI-Driven Crop Recommendation System for Agriculture 4.0. *arXiv preprint* arXiv:2412.16196.

Venugopal, A., Farnaghi, M. & Zurita-Milla, R. 2024. Comparative Evaluation of XAI Methods for Transparent Crop Yield Estimation Using CNN. *In: 2024 IEEE International Geoscience and Remote Sensing Symposium (IGARSS)*, pp. 7478–7482.

Yaganteeswarudu, A., Biswas, S.K., Aruna, V. & Tripathi, D. 2025. Enhancing Transparency in Smart Farming: Local Explanations for Crop Recommendations Using LIME. *Procedia Computer Science* **258**, 1993–2005.

Agronomy Research **24**(S1), 164–178, 2026
https://doi.org/10.15159/AR.26.028

TMR silage with sugarcane bagasse and urea: effects on intake, digestibility, and feeding behavior in dairy heifers

D.C. Santos*, A.J.V. Pires, F.F. Silva, A.S. Ribeiro, W.R. Andrade, M.L. Albuquerque, I.C. Dutra, G.R.S. Oliveira, M.P. Sousa, R.B. Mendes, M.L.S. Santos and M.V. Amaral

State University of Southwest of Bahia, BR45700-000, Itapetinga, Bahia, Brazil
*Correspondence: amanda.s.ri@hotmail.com

Received: February 2nd, 2026; Accepted: April 27th, 2026; Published: May 12th, 2026

Abstract. This study evaluated the effects of total mixed ration (TMR) silage containing two levels of sugarcane bagasse (40% and 50% of dry matter), with or without urea inclusion (2.5%), on intake, nutrient digestibility, nitrogen balance, microbial protein synthesis, and feeding behavior of dairy heifers. Eight crossbred heifers were assigned to two simultaneous 4×4 Latin squares in a 2×2 factorial arrangement. Urea inclusion reduced ($P < 0.05$) dry matter and neutral detergent fiber intake but improved dry matter and crude protein digestibility. Increasing bagasse level to 50% reduced ($P < 0.05$) intake and digestibility of nutrients, reflecting the higher fiber content and lower energy density of the diets. Nitrogen balance and microbial protein synthesis were not affected by treatments. Higher bagasse levels increased rumination time per unit of NDF and the number of ruminal boli, indicating greater physical demand for fiber processing. Overall, TMR silage containing 40% sugarcane bagasse without urea provided the best balance between intake and nutrient utilization. These results highlight the importance of optimizing fiber levels and nitrogen sources in TMR silage to improve efficiency in dairy heifer feeding systems under tropical conditions.

Key words: bagasse, digestibility, feeding behavior, nitrogen balance, TMR silage.

INTRODUCTION

Ensiling is the predominant forage conservation method in tropical regions, particularly in Brazil, due to its operational efficiency and suitability to climatic conditions. Crops such as corn, sorghum, and sugarcane are widely used in ruminant feeding systems. In recent years, total mixed ration (TMR) silage has gained attention as a strategy to improve feed management by allowing the storage of complete diets, reducing labor, and ensuring uniform nutrient intake (Pinto & Millen, 2018).

The use of TMR silage also facilitates the inclusion of agro-industrial by-products, contributing to cost reduction and sustainable waste utilization. Among these by-products, sugarcane bagasse stands out due to its wide availability in Brazil, the world's largest sugarcane producer (CONAB, 2020). Although bagasse is commonly used as a fiber source, its high lignin content and low digestibility may limit animal performance.

Urea is frequently used as a non-protein nitrogen source to enhance microbial protein synthesis and improve fiber degradation. However, its inclusion may negatively affect feed intake due to palatability issues and changes in fermentation patterns patterns (Ribeiro et al., 2026).

Despite the recognized potential of TMR silage and the availability of sugarcane bagasse, limited information exists on the combined effects of different bagasse levels and urea inclusion on intake, nutrient utilization, nitrogen metabolism, and feeding behavior in dairy heifers. Understanding these interactions is essential to optimize diet formulation and improve the efficiency of feeding systems under tropical conditions.

Therefore, this study aimed to evaluate the effects of TMR silage containing two levels of sugarcane bagasse (40% and 50% of dry matter), with or without urea inclusion, on intake, nutrient digestibility, nitrogen balance, microbial protein synthesis, and feeding behavior of dairy heifers.

MATERIALS AND METHODS

This research was conducted in accordance with the Ethics Committee on the Use of Animals (CEUA), under protocol number 235/2023, approved at the State University of Southwest Bahia - UESB. The experiment was carried out at Fazenda Bela Vista, in the municipality of Encruzilhada - BA, and the samples were analyzed in the Forage and Pasture, Animal Physiology, and Animal Nutrition Laboratories of UESB - Itapetinga Campus, Bahia.

The total mixed rations (TMRs) were produced at Fazenda Bela Vista. Fresh sugarcane bagasse was collected from a still located on the property. This was chopped in a stationary shredder to a particle size of 5 cm. After chopping, the concentrated components (soybean meal, ground corn, and mineral core), urea, and water were added to the bagasse in the proportions specified for each ration. The material was then manually homogenized to ensure it contained approximately 35% dry matter (DM). Subsequently, these mixtures were placed in 200-micron thick plastic bags with a capacity of 30 kg. The material was then manually compacted and sealed with nylon cable ties.

Eight crossbred Girolando heifers, with an average age of 12 months and an average initial body weight of 200 ± 10 kg, were used. The animals were identified at the beginning of the experimental period with plastic ear tags and dewormed (Abamectin-1% - Abmic® Microsules). After weighing, the animals were distributed into two simultaneous 4×4 Latin squares, in a 2×2 factorial design, with two proportions of sugarcane bagasse (40 or 50% dry matter basis) with and without the use of urea replacing soybean meal in the diet.

The animals were housed in individual 6×2 m (12 m^2) partially covered pens with concrete floors, equipped with individual feeders and waterers. The animals received ad libitum feed, divided into two daily meals (7 am and 1 pm) to allow for leftovers of approximately 10% of the feed provided. The diets were calculated to meet the nutritional requirements of crossbred Girolando heifers for a gain of 700 g day^{-1} (NRC 2001).

The sample size (n = 8) was defined based on similar studies using Latin square designs in ruminant nutrition, which allow efficient control of animal and period variability and are widely accepted for metabolism and intake trials (Detmann et al., 2012).

The chemical composition of the ingredients and experimental diets can be seen in Tables 1 and 2.

Parameters evaluated

Samples of the supplied ingredients, feces, and leftovers were analyzed for the following contents: DM (method G-001/1), crude ash (method M-001/1), CP (method N-001/1), EE (method G-004/1), NDF (method F-002/1), NDFap (methods N-004/1 and N-002/1), ADF (method F-004/1), lignin (method F-005/1), and NDFi (method F-009/1), as described in Detmann et al. (2012).

Total carbohydrate (TC) content was calculated using the equation proposed by Sniffen et al. (1992):

$$TC = 100 - (CP\% + EE\% + ash\%) \quad (1)$$

where CP = crude protein, EE = ether extract, and ash = % of the sample. Non-fibrous carbohydrates (NFC) of the samples were calculated according to the formula of Detmann et al. (2012):

$$NFC = 100 - (CP\% + EE\% + MM\% + NDFap) \quad (2)$$

where EE = ether extract, MM = ash, and NDFap = neutral detergent fiber. Total digestible nutrients (TDN) were calculated according to NRC (2001):

$$TDN = DPP + (EDE \cdot 2.25) + NDF + NDFap) \quad (3)$$

where DPP = digestible crude protein; EED = digestible ether extract; NDF = digestible neutral detergent fiber; NDFap = digestible non-fibrous carbohydrates.

Table 1. Chemical composition of the ingredients used in the experimental diets

Composition	Ingredients		
	Raw sugarcane bagasse	Ground corn	Soybean meal
Dry matter (%)	59.4	80.6	84.1
Crude protein[1]	1.3	9.9	52.5
Ether extract[1]	1.5	6.7	1.5
NDFap[1]	80.2	19.4	23.8
NDFi[1]	59.5	3.9	0.9
Ash[1]	1.7	2.1	6.2
Lignin[1]	22.9	1.4	0.7
CNF[1]	16.7	73.2	30.1
NDT[2]	37.0	84.5	83.3

[1]Values as a percentage of dry matter; NDFap – neutral detergent fiber corrected for ash and protein; NDFi – indigestible neutral detergent fiber; NFC – non-fibrous carbohydrates; TDN – total digestible nutrients; [2]estimated according to NRC (2001).

Table 2. Ratio of ingredients and chemical composition of experimental diets after ensiling

Item	40% bagasse		50% bagasse	
	0% Urea	2.5% Urea	0% Urea	2.5% Urea
Ingredient ratios (%)				
Raw sugarcane bagasse	40.0	40.0	50.0	50.0
Ground corn	39.6	50.0	28.0	38.3
Soybean meal	17.5	4.5	19.0	6.2
Urea	-	2.5	-	2.5
Mineral Mixture[1]	3.0	3.0	3.0	3.0
Chemical Composition (%)				
Dry matter	32.8	32.0	29.9	31.2
Crude protein	13.2	13.7	13.4	13.6
Ether extract	2.9	3.1	3.1	3.7
NDFap	38.1	37.9	44.4	44.7
NDFi	15.5	16.5	20.6	21.6
Ash	6.1	5.4	6.3	5.3
Lignin	6.5	6.9	8.8	9.0
CNF	37.5	37.1	29.8	30.2
TDN[2]	66.4	69.7	61.5	63.0

[1]Guaranteed levels (per kg of active elements): calcium – 187 g; phosphorus – 85 g; magnesium – 15 g; sodium – 90 g; sulfur – 18 g; copper – 1,350 mg; cobalt – 80 mg; iron – 1,450 mg; iodine – 90 mg; manganese – 1,700 mg; selenium – 22 mg; zinc – 5,800 mg; fluorine maximum – 850 mg; phosphorus (P) solubility in 2% citric acid – 95% (minimum). [2]Estimated according to NRC (2001).

Dry matter intake and nutrient digestibility

To determine dry matter intake, the amount of feed offered and leftovers for each animal was recorded daily throughout the experimental period. From the 17th to the 21st day of each period, samples of diets, concentrate, and leftovers were collected and stored in plastic bags, identified, and frozen at -10 °C for chemical-bromatological analyses.

The animals were weighed at the beginning and end of each experimental period to estimate nutrient intake. For the purpose of quantifying and evaluating voluntary intake, the feed provided between the 17th and 21st day of each experimental period was considered, with leftovers counted between the 18th and 22nd day. Subsequently, the samples were dried in a forced-air oven at 60 °C for 72 hours, then ground in a knife mill equipped with a 1 mm mesh sieve. The samples were then stored in hermetically sealed and labeled vials for compositional analysis.

For fecal production estimation, indigestible neutral detergent fiber (iNDF) was used as an internal indicator, obtained after ruminal incubation of 0.5 g corresponding to each sample of feed, leftovers, and feces, packaged in bags made of non-woven fabric (TNT) with a grammage of 100 g m^{-2}, 5×5 cm for 288 hours. The residue was considered indigestible (Detmann et al., 2012). The apparent digestibility of nutrients (D) was determined by the formula described by Silva & Leão (1979):

$$D = [(\text{kg nutrient ingested} - \text{kg nutrient excreted})/\text{kg nutrient ingested}] \cdot 100. \quad (4)$$

Balance of nitrogen compounds and microbial synthesis

On the 21st day of each experimental period, spot urine samples were collected from spontaneous urination of the animals, approximately four hours after the morning feeding. The samples were filtered through gauze, and a 10 mL aliquot was diluted with 40 mL of sulfuric acid (0.036 N) (Valadares et al., 1999) for quantification of urinary concentrations of urea, total nitrogen, creatinine, allantoin, and uric acid.

Blood was collected from the jugular vein on the 21st day of each experimental period, approximately four hours after the morning feeding, using 5 mL tubes (Vacutainer substrate) with EDTA. The blood samples were then centrifuged at 3,500 rpm for 10 minutes, and the plasma was stored in eppendorf tubes and kept frozen (-20 °C) until analysis.

Urine creatinine and uric acid concentrations, and urine and plasma urea concentrations, were determined using commercial kits (Bioclin). Urea values were converted to urea nitrogen by multiplying the obtained values by a factor of 0.4667. Urinary allantoin and uric acid levels were determined using a colorimetric method, according to Chen & Gomes (1992) specifications, and total nitrogen content was estimated using the Kjeldahl method.

Nitrogen balance (N-retained, g day^{-1}) was calculated as: N-retained = N ingested (g) – N in feces (g) – N in urine (g).

Creatinine excretion (mg kg^{-1} BW) used to estimate urine volume from spot samples was obtained for each animal according to the equation described by Chizzotti (2004):

$$EC = 32.27 - 0.01093 \cdot BW \quad (5)$$

where EC = daily creatinine excretion (mg kg^{-1} BW); and BW = body weight (kg). However, urine volume was estimated from the ratio between daily creatinine excretion (mg kg^{-1} BW) obtained from the previous equation and the average creatinine concentration (mg L^{-1}) in the spot urine samples, multiplied by the animal's respective BW.

Total purine derivative excretion (TPD) was obtained by summing the amounts of allantoin and uric acid excreted in the urine. The amount of microbial purines absorbed (mmol/day) was estimated from the total purine derivative excretion (mol/day) using the equation proposed by Verbic et al. (1990):

$$\mathrm{PA} = (\mathrm{TPD} - 0.385 \cdot \mathrm{PV}\ 0.75)/0.85 \qquad (6)$$

where PA is the microbial purines absorbed (mmol day^{-1}); TD corresponds to the total purines (mmol day^{-1}); 0.85 = recovery of absorbed purines as purine derivatives in the urine and 0.385 = endogenous excretion of purine derivatives in the urine (mol) per unit of metabolic size.

The intestinal flow of microbial nitrogen (g NM day^{-1}) was estimated from the amount of purines absorbed (mol day^{-1}), according to the equation of Chen & Gomes (1992):

$$\mathrm{NM}\ (\mathrm{g\ day^{-1}}) = (70 \cdot \mathrm{PA})/(0.83 \cdot 0.116 \cdot 1{,}000), \qquad (7)$$

assuming the value of 70 for the nitrogen content in purines (mg mol^{-1}); 0.83 for the intestinal digestibility of microbial purines and 0.116 for the PNURINE: NTOTAL ratio in bacteria.

Ingestive behavior

For the evaluation of ingestive behavior, the eight steers were visually observed for 24 hours on the 20th day of each period, and observations were recorded at 10-minute intervals, including feeding, rumination, and resting time (Mezzalira et al., 2011). On the same day, three observations were made for each animal: in the morning, at noon, and in the evening. Data were collected by trained observers using digital stopwatches. During the nighttime observation, the environment was kept under artificial lighting, and the animals underwent an adaptation period. The dietary variables (feeding, rumination, and resting) were obtained using equations adapted from Bürger et al. (2000).

Statistical analysis

Data were analyzed using analysis of variance (ANOVA) in a 2×2 factorial arrangement within a Latin square design. The model included the fixed effects of bagasse level, urea inclusion, and their interaction, while animal and period were considered random effects. Means were compared using the *F*-test, and significance was declared at $P < 0.05$.

A complete list of abbreviations used is provided in Table 3.

Table 3. List of abbreviations

ADF – Acid Detergent Fiber;	NPN – Non-protein nitrogen;
BW – Body Weight;	NRC – National Research Council;
CP – Crude Protein;	PA – Purines Absorbed;
DM – Dry Matter;	SB – Sugarcane Bagasse;
EE – Ether Extract;	SEM – Standard Error of the Mean;
iNDF – Indigestible Neutral Detergent Fiber;	TDN – Total Digestible Nutrients;
NDF – Neutral Detergent Fiber;	TMR – Total Mixed Ration;
NDFap – Neutral Detergent Fiber corrected for ash and protein;	TPD – Total purine derivatives;
NDFapI – NDF corrected for ash and protein Intake;	UR – Urea;
NFC – Non-Fiber Carbohydrates;	VFAs – volatile fatty acids.
NM – Microbial Nitrogen;	

RESULTS AND DISCUSSION

There was no significant interaction ($P > 0.05$) between bagasse proportion and urea inclusion for the evaluated intake variables (Table 4). Urea inclusion resulted in lower dry matter intake and lower NDFap intake ($P < 0.05$). The reduction in dry matter intake observed with urea inclusion suggests a negative effect on palatability, likely associated with its bitter taste and odor, which may induce aversive responses in ruminants (Detmann et al., 2007). Additionally, elevated ammonia concentrations in silage may contribute to reduced intake (Huhtanen et al., 2002).

Higher bagasse inclusion (50%) reduced intake, which can be attributed to increased dietary fiber concentration. Diets with higher neutral detergent fiber (NDF) levels tend to limit intake due to rumen fill, as fibrous components have slower degradation rates and occupy ruminal space for longer periods (Detmann et al., 2012).

The higher intake of non-fiber carbohydrates and total digestible nutrients observed in diets containing 40% bagasse reflects their greater energy density, reinforcing the importance of balancing fiber and energy sources in TMR silage formulations.

Table 4. Dry matter and nutrient intake of the diet by dairy heifers fed total mixed ration silage containing sugarcane bagasse with or without urea

Item	SB		Urea		SEM[1]	*P*-value		
	40%	50%	0%	2.5%		SB	UR	SB × UR
Consumption (kg day^{-1})								
Dry matter (DM)	5.03	4.66	5.06	4.63	0.1	0.02	0.01	0.06
Crude protein	1.00	0.97	1.01	0.96	0.0	0.52	0.24	0.97
Ether extract	0.17	0.15	0.16	0.16	0.0	0.21	0.59	0.05
NDFap[2]	1.70	1.86	1.88	1.73	0.0	0.04	0.04	0.10
NFC[3]	1.88	1.39	1.71	1.55	0.0	0.00	0.09	0.16
TDN[4]	3.44	2.94	3.09	2.99	0.0	0.00	0.08	0.12
Consumption (% of body weight)								
DM	2.43	2.22	2.43	2.21	0.08	0.04	0.04	0.13
NDFap	0.83	0.89	0.89	0.83	0.03	0.08	0.08	0.11
Consumption (% metabolic weight)								
DM	92.28	85.06	92.39	84.94	2.84	0.04	0.03	0.11

[1]SEM: standard error of the mean; [2]Neutral Detergent Fiber corrected for ash and protein; [3]Non-fiber carbohydrates; [4]Total digestible nutrients; SB = sugarcane bagasse; UR = urea.

And the protein and energy levels expressed as crude protein (CP) and total digestible nutrients (TDN) are within the recommendations of the NRC (2001), thus there was no imbalance in the protein/energy ratio, which could lead to reduced consumption due to low microbial growth (Calsamiglia et al., 2010).

The average dry matter intake (DM) of 4.85 kg day^{-1} for heifers weighing 220 kg was below the estimate of 5.50 kg day^{-1} by the NRC (2001). One factor that may have led to this lower DM intake compared to the NRC (2001) recommendation is the quality of the forage (sugarcane bagasse) and, consequently, higher levels of neutral detergent fiber. This occurred in this study, as the average NDF (neutral detergent fiber) content of the diet was 41.3%, while the value recommended by the NRC (2001) is 28%. Thus, the high fiber content may have limited intake due to filling, with diets with higher bagasse content (50%) resulting in lower DM intake.

Feed restriction due to filling, or physical intake limitation, occurs when the rumen's physical capacity is reached, regardless of whether the animal has satisfied its energy or nutrient needs. This limitation is common in high-fiber, bulky diets, such as low-quality forages like sugarcane bagasse, which have low energy density and occupy a lot of space in the rumen. In these cases, even if the animal wants to consume more to meet its nutritional needs, it cannot due to the limited space in the rumen (Detmann et al., 2012).

Another factor that may have influenced dry matter intake is the urea content, as diets containing urea showed lower dry matter intake compared to diets without urea. According to Detmann et al. (2007), urea emerges as an effective regulator of supplement intake among grazing cattle, thanks to its association with aversive sensations in the animals. The sensory properties of urea, notably its bitter taste and distinctive odor, also exert control over supplement intake.

Some authors have reported lower dry matter intake in cattle fed silages containing high levels of NH3-N (Rook & Gill, 1990; Cushnahan et al., 1995; Huhtanen et al., 2002).

Lazzari et al. (2021) evaluated the intake of beef cattle fed TMR silage with different protein sources, observing lower intake for silage with urea when compared to silage with protein sources from soybean meal and soybean grain, obtaining a negative variation in intake of 10 percentage points. Thus, these data corroborate the data obtained in this work, since diets with urea also obtained lower dry matter intake.

The influence of higher bagasse content (50%) and the inclusion of urea on limiting intake can be confirmed when analyzing DM intake as a percentage of body weight and as a percentage of metabolic weight, where diets containing higher bagasse content and diets with urea inclusion resulted in lower DM intake for these indices.

The level of bagasse influenced NDFap consumption, which can be explained by the fiber content of the diet, since the diet with 50% bagasse has higher levels of NDFap, NDFi and Lignin (Table 2), having 6.55; 5.1; 2.2 percentage points more respectively when compared with diets containing 40% bagasse, consequently diets with 50% bagasse tend to have higher fiber consumption.

Table 5. Dry matter and nutrient digestibility coefficient of the diet of dairy heifers fed total mixed ration silage containing sugarcane bagasse with or without urea

Digestibility coefficient	Bagasse		Urea		SEM[1]	*P*-value		
	40%	50%	0%	2.5%		SB	UR	SB × UR
DM[2]	63.7	53.5	57.7	59.6	1.1	0.00	0.14	0.03
CP[3]	67.8	64.1	63.2	68.6	1.0	0.01	0.00	0.05
EE[4]	73.1	72.7	73.3	72.5	0.8	0.66	0.39	0.57
NDFap[5]	53.9	46.5	50.4	49.9	1.8	0.00	0.79	0.27
NFC[6]	83.9	80.7	82.4	82.2	0.6	0.00	0.77	0.62
TDN[7]	68.5	63.1	64.7	67.0	0.6	0.00	0.01	0.29

[1]SEM: standard error of the mean; [2]Crude protein; [3]Ether extract; [4]Neutral Detergent Fiber corrected for ash and protein; [5]Non-fiber carbohydrates; [6]Total digestible nutrients; SB = sugarcane bagasse; UR = urea.

There was a significant interaction ($P < 0.05$) between the proportion of bagasse and the inclusion of urea for dry matter digestibility (Table 5), with the DM digestibility being higher in the diets with both bagasse levels, 40% and 50%, when urea was included (Table 6). The proportion of bagasse and the inclusion of urea influenced CP digestibility, with higher digestibility observed in the diet containing 40% bagasse and with the inclusion of urea ($P < 0.05$).

The proportion of bagasse influenced the digestibility of CP, NDFap, NFC, and TDN ($P < 0.05$), with diets containing 40% bagasse showing higher digestibility. For CP and TDN digestibility, in addition to the proportion of bagasse, the inclusion of urea also had an influence, with urea inclusion providing higher digestibility ($P < 0.05$).

The improvement in digestibility with urea inclusion is likely associated with its role as a non-protein nitrogen source, stimulating the growth of ruminal microorganisms, particularly fibrolytic bacteria. This effect enhances fiber degradation and increases nutrient availability. Conversely, the reduction in digestibility observed at higher bagasse levels reflects the increased lignin and indigestible fiber content, which limits microbial access to cell wall components. These results highlight the negative impact of excessive low-quality fiber on nutrient utilization.

Additionally, the ensiling process may enhance starch availability through proteolysis, particularly in diets rich in concentrate, contributing to improved digestibility and feed efficiency, providing greater digestibility of CP, NDFap, NFC, and thus an increase in TDN.

Miyaji et al. (2017) reported an increase in ruminal starch degradation in TMR silage containing flaked corn. An increase in starch digestibility is expected for dry ground or dry rolled corn (or sorghum) when ensiled as part of an TMR if stored for at least two months (based on high-moisture corn silage data). Such an increase in starch digestibility has been associated with greater feed efficiency in animals fed TMR silages (Lazzari et al., 2021).

In their research, Xu et al. (2007) partially replaced cattail hay and alfalfa hay with moist coffee husks in a silage of TMR (0, 100, or 200 g per kg DM) and reported a linear increase in NDF and ADF content and a linear decrease in apparent NDF and ADF digestibility with the inclusion of coffee husks. Consequently, cell wall hydrolysis and changes in fiber content and digestibility during ensiling are primarily dependent on the quality of the ingredients included in the TMR.

The inclusion of urea resulted in higher TDN (Total Digestible Nutrients) and CP (Crude Protein) digestibility. This can be explained by the growth-promoting action of urea on proteolytic bacteria during the ensiling process of the total diet. In addition, the diets contained a significant amount of starch-rich concentrates (60% and 50% concentrate for the diets with 40% and 50% bagasse, respectively), with the majority of this concentrate consisting of ground corn. The corn used was flinted corn, i.e., hard corn coated with prolamins; thus, the action of proteolytic bacteria also increases the availability of starch and proteins in the rumen environment.

The inclusion of urea in conventional forage silage can be detrimental due to its buffering capacity, leading to difficulties in pH reduction during the ensiling process, and because it contributes to proteolysis in forages with high crude protein content (e.g., legumes, temperate grasses), it becomes undesirable and leads to lower nitrogen use efficiency (Huhtanen et al., 2008; Hymes-Fecht et al., 2013).

However, in corn and sorghum silages (plant or grain silages), proteolysis has been positively associated with starch digestibility due to the degradation of hydrophobic proteins (prolamins) surrounding the starch granules (Hoffman et al., 2011).

In TMR silages, which are mixtures of ingredients, we found no report that considered the contribution of microorganisms and plant proteases to proteolysis. Meanwhile, enterobacteria, clostridia, and bacilli are the main agents involved in protein degradation during silage storage (McDonald et al., 1991; Pahlow et al., 2003).

Higher DM digestibility (Table 6) was observed in diets with urea inclusion and a lower proportion of bagasse. This is due to the lower proportion of fibrous material in the diet, and these diets showed lower levels of NDFap, NDFi, and lignin when compared to diets with 50% bagasse.

Therefore, lower fiber content and higher concentrate content lead to increased degradation and passage rates because diets with higher concentrate content are more easily degraded in the rumen environment than diets rich in fiber, which are rich in starch and have a higher degradation and passage rate. Diets with higher fiber content, on the other hand, have slower degradation and, due to their composition, present high levels of components with low degradability such as NDFap and components with low or zero degradability such as NDFi and Lignin, consequently reducing their passage rate and digestibility.

Table 6. Dry matter digestibility coefficient of dairy heifers fed total mixed ration silage containing sugarcane bagasse with or without urea

Proportion of bagasse	0% urea	2.5% urea	Average	SEM[1]
	DM digestibility			
40 (%)	63.2 Aa	64.3 Aa	63.7	1,119
50 (%)	51.1 Bb	55.9 Ba	53.5	
Average	57.12	60.10		

[1]SEM: standard error of the mean, means followed by the same lowercase letter in the row and the same uppercase letter in the column do not differ from each other by the *F* test ($P < 0.05$).

The increase in digestibility with urea inclusion may also be associated with ammoniation effects during ensiling, which can partially disrupt lignocellulosic bonds and improve fiber accessibility to ruminal microorganisms.

Although urea inclusion improved nutrient digestibility, its practical application should be carefully considered, as the associated reduction in dry matter intake may limit overall animal performance depending on production goals.

These results reinforce the importance of balancing nitrogen supplementation and intake regulation in diet formulation.

This trade-off highlights the importance of evaluating both intake and digestibility responses when using non-protein nitrogen sources in TMR silage systems.

According to Oliveira et al. (2007), the main purpose of ammoniation is to enrich the nutritional value of forage by providing non-protein nitrogen and improving its digestibility. In this way, ammoniation of forages results in greater degradation of the cell wall, including cellulose and hemicellulose, due to the extension of its molecules, the breaking of hydrogen bonds, and the increased hydration of the fiber.

Urea doses have demonstrated the ability to reduce neutral detergent fiber and acid detergent fiber in sugarcane bagasse. Ammoniation improves the digestibility of sugarcane bagasse as a result of changes in cell wall constituents, since it causes partial solubilization of hemicellulose and breaking of the bond between lignin and carbohydrates in the cell wall, favoring the action of rumen microorganisms (Oliveira et al., 2011), in addition to improving its nutritional value with an increase in crude protein through the availability of NPN (non-protein nitrogen).

In addition to improving fiber solubility, the addition of a non-protein nitrogen (NPN) source, such as urea, increases nitrogen availability in the rumen. This stimulates the growth and activity of ruminal microorganisms, especially fibrolytic bacteria, responsible for the degradation of plant fiber present in fibrous feeds consumed by ruminants. As a result, ruminal kinetics are accelerated, promoting greater degradation of plant fiber and increased production of volatile fatty acids (VFAs), such as acetate, propionate, and butyrate. These VFAs are absorbed by the rumen wall and provide energy for the host animal.

The results obtained in this work corroborate those found by Lazzari et al. (2021), who analyzed digestibility under the effect of protein sources in silages of TMRs, evaluating the inclusion of urea, soybean meal, and soybean grain, and the silages with urea showed greater DM digestibility compared to the true protein sources.

The proportions of sugarcane bagasse and the inclusion of urea did not influence ($P > 0.05$) urinary volume, microbial CP production and microbial efficiency, with average values of 10.83 L day^{-1}, 562.82 g day^{-1} and 177.92 g CP kg^{-1} TDN, respectively (Table 7).

Microbial protein production in ruminants is strongly influenced by the availability of carbohydrates and nitrogen in the rumen (NRC, 2001). Adequate energy supply is crucial, as it is the main limiting factor for microbial growth. The primary function of this growth is to generate ATP, which is essential for the utilization of ammonia in amino acid synthesis and microorganism growth (Possenti et al., 2008).

In other studies, urinary volume was also not influenced by the use of TMR silage with different by-products, (Miyaji et al., 2017) and (Lazzari et al., 2021), being evaluated in lactating cows and Nellore heifers, respectively.

Table 7. Urinary volume, microbial protein synthesis, and microbial efficiency of dairy heifers fed total mixed ration silage containing sugarcane bagasse with or without urea

Item	Bagasse		Urea		SEM[1]	*P*-value		
	40	50	Sem	Com		SB	UR	SB × UR
Urine volume (L day^{-1})	9.8	11.8	10.3	11.4	1.5	0.25	0.50	0.65
Microbial production (g day^{-1})								
Microbial CP	539.4	586.2	556.2	569.4	51.9	0.53	0.85	0.13
Microbial efficiency								
G CP per kg TDN	156.1	198.1	173.2	182.5	24.9	0.14	0.71	0.12

[1]SEM: standard error of the mean; SB = sugarcane bagasse; UR = urea.

Microbial protein synthesis plays a crucial role in ruminant nutrition, providing proteins in the quantity and quality essential for their well-being. Recent studies (Nguyen et al., 2017) have found that this synthesis represents between 50% and 80% of the total protein absorbed by the animal. The microbial efficiency ratio recommended as a minimum ideal by Valadares Filho et al. (2016) is 120 g microbial protein per kg of total digestible nutrients (TDN) as a reference for microbial synthesis efficiency under tropical conditions. In this study, a measured value of 177.92 g microbial protein per kg of TDN was obtained, falling within the premise recommended by Valadares Filho et al. (2016).

This factor is particularly important for the category used in this study, where heifers require a higher protein intake for their growth and muscle development, but with low fat deposition, as this can hinder mammary gland development (Campos & Assis, 2005).

The results obtained for nitrogen balance and urea excretion are presented in (Table 8). Regarding the inclusion of urea, treatments without urea resulted in greater N excretion in feces ($P < 0.05$). The proportion of bagasse influenced the N balance, with the 40% proportion showing the highest N balance ($P < 0.05$). The proportions of sugarcane bagasse and the inclusion of urea did not influence ($P > 0.05$) plasma urea nitrogen, urinary urea, and urinary urea nitrogen.

Table 8. Nitrogen compound balance of dairy heifers fed total mixed ration silage containing sugarcane bagasse with or without urea

Item	Bagasse		Urea		SEM[1]	*P*-value		
	40%	50%	0%	2.5%		SB	UR	SB × UR
N g^{-1} day balance								
N ingested	160.4	156.1	162.4	156.1	6.4	0.52	0.24	0.97
N in feces	52.0	54.7	58.0	50.8	2.6	0.33	0.01	0.15
N in urine	22.2	23.5	22.9	22.9	3.3	0.69	0.99	0.86
N retained	86.2	77.8	81.5	82.5	4.0	0.08	0.81	0.41
Nitrogen balance	53.6	49.3	49.6	53.2	1.6	0.03	0.06	0.13
Percentage of N								
Plasma urea N	2.0	2.6	2.2	2.4	0.3	0.174	0.702	0.678
Urea urine	126.8	129.2	127.6	128.5	27.9	0.931	0.975	0.420
Urine urea N	5.91	6.02	5.99	5.94	1.3	0.933	0.977	0.422

[1]SEM: standard error of the mean; N = Nitrogen; SB = sugarcane bagasse; UR = urea.

When it comes to the balance of nitrogen compounds, it is essential to consider both nitrogen intake and excretion by ruminants. The quantity and quality of nitrogen in the diet affect the efficiency of microbial protein synthesis in the rumen, as well as nitrogen excretion in urine and feces. This is particularly important due to the potential environmental impact of excess nitrogen excreted by animals, such as contributing to the eutrophication of water bodies.

Research indicates that the composition of TMR silage can influence the nitrogen balance in ruminants. For example, Bueno et al. (2020) observed that the inclusion of certain ingredients in TMR silage can affect the rate of digestion and utilization of nitrogen by ruminal microorganisms. Furthermore, the protein-to-energy ratio in the diet can influence the efficiency of microbial synthesis and, consequently, the nitrogen balance in the animal.

Another aspect to consider is the impact of TMR silage fermentation on nitrogen metabolism. The anaerobic fermentation that occurs during the ensiling process can affect the availability and form of nitrogen in the diet, potentially influencing the digestibility and utilization of nitrogen by ruminants.

The results obtained for feeding behavior are presented in Table 9. There was no significant interaction ($P > 0.05$) between the level of bagasse and the inclusion of urea for the variables analyzed. When analyzed separately, the inclusion of urea significantly increased ($P < 0.05$) the rumination and chewing time of DM in min g^{-1} of DM. The 50% bagasse proportion increased the rumination time of NDFap in min g^{-1} of NDFap.

Table 9. Feeding behavior of dairy heifers fed total mixed ration silage containing sugarcane bagasse with or without urea

Item	Bagasse		Urea		SEM[1]	*P*-value		
	40%	50%	0%	2.5%		SB	UR	SB × UR
Feeding								
Min day^{-1}	306.3	345.0	320.0	331.3	28.9	0.22	0.71	0.18
Min kg^{-1} DM	62.1	74.4	64.6	71.9	6.9	0.12	0.33	0.29
Min kg^{-1} NDF ap^{-1}	182.0	186.1	174.9	194.1	20.3	0.87	0.37	0.41
% per day	21.3	24.0	22.2	23.0	2.0	0.22	0.71	0.18
Rumination								
Min day^{-1}	460.0	502.5	467.5	495.0	25.7	0.14	0.32	0.32
Min kg^{-1} DM	99.0	102.4	93.5	107.9	5.4	0.55	0.03	0.08
Min kg^{-1} NDF ap^{-1}	247.8	301.1	253.3	295.7	15.9	0.01	0.37	0.05
% per day	31.9	34.9	32.5	34.4	1.8	0.14	0.32	0.32
Leisure								
Min day^{-1}	654.0	609.3	652.5	613.8	34.1	0.91	0.30	0.65
% day^{-1}	46.8	41.1	45.3	42.6	2.4	0.91	0.30	0.65
Chew								
N per cake	51.5	54.3	56.1	49.7	3.1	0.41	0.08	0.92
s per cake	46.6	49.5	50.8	45.3	3.21	0.40	0.13	0.90
n per day	33,238.2	30,274.3	30,995.1	32,517.5	1,377.4	0.07	0.31	0.27
Min day^{-1}	808.8	805.0	787.5	826.3	34.1	0.91	0.30	0.65
Min kg^{-1} DM	164.5	173.4	158.0	179.9	8.1	0.31	0.03	0.69
Min kg^{-1} NDF ap^{-1}	483.9	434.0	428.1	489.8	25.4	0.09	0.05	0.46

[1]SEM: standard error of the mean; N = Nitrogen; SB = sugarcane bagasse; UR = urea.

The increase in rumination time and number of ruminal boli observed with higher bagasse inclusion reflects the greater physical demand required to process fibrous diets. High NDF content stimulates chewing activity, which is essential to reduce particle size and facilitate microbial digestion.

Urea inclusion increased rumination time per unit of dry matter, possibly due to enhanced microbial activity and greater fiber degradation, which may alter ruminal dynamics and chewing behavior.

These findings reinforce the relationship between dietary fiber characteristics and ingestive behavior, highlighting the importance of fiber quality in TMR silage systems, with fiber effectiveness being a primary factor in stimulating chewing (Grant & Albright, 1995).

According to Oliveira et al. (2007), diets with urea provided greater rumination and dry matter chewing time; ruminant diets that include urea can increase dry matter chewing and rumination time. This occurs because urea is a source of non-protein nitrogen that can be used by rumen microorganisms to synthesize microbial protein. When urea is provided in the diet, rumen microorganisms become more active in the degradation of dietary fiber, which can lead to an increase in the time spent by animals in chewing and rumination activities.

There was no significant interaction ($P > 0.05$) between bagasse level and urea inclusion for the number of periods and average time spent per period on activities (Table 10). When analyzed separately, the 50% bagasse proportion significantly increased ($P < 0.05$) the NDFap rumination time expressed in g NDFap per hour and increased the number of boluses per day (cakes per day). Urea inclusion significantly increased ($P < 0.05$) the number of boluses per day (cakes per day) and reduced the amount of DM rumination in (g DM per hour).

The higher number of ruminal boli observed in diets with 50% bagasse is consistent with increased fiber content, which stimulates rumination as a mechanism to enhance particle breakdown and digestion.

Table 10. Number of periods and average time spent per period on feeding, rumination, and resting activities of dairy heifers fed a total mixed ration silage containing sugarcane bagasse with or without urea

Item	Bagasse		Urea		SEM[1]	*P*-value		
	40%	50%	0%	2.5%		SB	UR	SB × UR
Periods (Number per day)								
Feeding	14.9	15.9	15.5	15.3	1.8	0.59	0.89	0.98
Rumination	14.3	14.8	14.3	14.8	0.8	0.56	0.56	0.12
Idleness	22.8	23.0	22.3	23.5	1.4	0.86	0.39	0.60
Time spent per period (min)								
Feeding	20.6	22.1	20.8	22.0	1.8	0.43	0.53	0.18
Rumination	36.4	31.5	33.3	34.7	2.1	0.05	0.52	0.52
Idleness	27.9	28.4	29.7	26.6	2.9	0.86	0.32	0.36
Feeding								
g DM per hour	1013.0	830.8	975.1	868.9	85.5	0.07	0.26	0.63
g NDF ap per hour	344.3	331.1	358.4	317.8	32.8	0.72	0.26	0.67
Rumination								
Cakes per day	562.9	668.5	566.3	665.2	30.4	0.013	0.017	0.36
g MS per hour	611.2	611.6	655.3	567.5	33.8	0.989	0.047	0.11
g NDFap per hour	207.4	244.6	241.6	210.3	13.4	0.031	0.057	0.12

[1]SEM: standard error of the mean; N = Nitrogen; SB = sugarcane bagasse; UR = urea.

The same relationship occurs for the inclusion of urea, where diets with urea provided a longer rumination time of dry matter (Table 9), consequently leading to an increase in the number of boluses ruminated per day, being used as a strategy to increase fiber degradation and digestion.

CONCLUSIONS

TMR silage containing 40% sugarcane bagasse without urea provided the best balance between intake and nutrient utilization in dairy heifers. Although urea improved digestibility, its negative impact on intake may limit its practical application.

Increasing bagasse levels to 50% negatively affected intake and digestibility, emphasizing the importance of controlling fiber inclusion in TMR silage. Overall, optimizing the combination of fiber sources and nitrogen supplementation is essential to improve feeding efficiency in tropical ruminant production systems.

REFERENCES

Bueno, A.V.I., Lazzari, G., Jobim, C.C. & Daniel, J.L.P. 2020. Ensiling total mixed ration for ruminants: a review. *Agronomy* **10**(6), 879.

Bürger, P.J., Pereira, J.C., Queiroz, A.C., Coelho Da Silva, J.F., Valadares Filho, S.D.C., Cecon, P.R. & Casali, A.D.P. 2000. Ingestive behavior in Holstein calves fed diets with different concentrate levels. *Brazilian Journal of Animal Science* **29**, 23642.

Campos, J. & Assis, A. 2005. Feeding dairy heifers. *Minas Gerais Symposium On Dairy Cattle Nutrition*, **3**(1), 155–176.

Calsamiglia, S., Ferret, A., Reynolds, C., Kristensen, N. & Van Vuuren, A. 2010. Strategies for optimizing nitrogen use by ruminants. *Animal* **4**(7), 1184–196.

Chen, X.B. & Gomes, M.J. 1992. Estimation of microbial protein supply to sheep and cattle based on urinary excretion of purine derivatives - an overview of technical details. *International Feed Research Unit - Bucksburnd: Rowett Research Institute* **21**.

Chizzotti, M.L. 2004. Evaluation of cottonseed hulls for dairy steers and determination of creatinine excretion and microbial protein production in heifers and dairy cows. *Dissertation* (Master's in Animal Science). Federal University of Viçosa, Viçosa, 141 pp.

CONAB. 2020. National Supply Company. Monitoring of the Brazilian harvest. Brasília. 2019/20 Harvest. Available at: <https://www.conab.gov.br/infoagro/safras/cana/boletim-da-safra-de-cana-de-acucar>. Accessed on: November 20, 2024

Cushnahan, A., Mayne, C.S. & Unsworth, E.F. 1995. Effects of ensilage of grass on performance and nutrient utilization by dairy cattle 2. Nutrient metabolism and rumen fermentation. *Animal Science* **60**(3), 347–359.

Detmann, E., Souza, A.L., Garcia, R., Valadares Filho, S.C., Cabral, L.S. & Zervoudakis, J.T. 2007. Evaluation of the "long-term" bias of internal indicators in a ruminant digestion trial. *Brazilian Archives of Veterinary Medicine and Animal Science* **59**, 182–188.

Detmann, E., Souza, M.A., Valadares Filho, S.C., Queiroz, A.C., Berchielli, T.T., Saliba, E.O.S., Cabral, L.S., Pina, D.S., Ladeira, M.M. & Azevedo, J.A.G. 2012. Methods for food analysis. Visconde do Rio Branco: Suprema. (1), 214.

Grant, R.J. & Albrigth, J.L.1995. Feeding behaviour and management factors during the transition period in dairy cattle. *Journal of Animal Science* **73**(12), 2791–2803.

Hoffman, P.C., Esser, N.M., Shaver, R.D., Coblentz, W.K., Scott, M.P., Bodnar, A.L., Schmidt, R.J. & & Charley, R.C. 2011. Influence of ensiling time and inoculation on alteration of the starch-protein matrix in high-moisture corn. *Journal of Dairy Science* **94**(5), 2465–2474.

Huhtanen, P., Khalili, H., Nousiainen, J.I., Rinne, M., Jaakkola, S., Heikkila, T. & Nousiainen, J. 2002. Prediction of the relative intake potential of grass silage by dairy cows. *Livestock Production Science* **73**(2-3), 111–130.

Huhtanen, P., Rinne, M. & Nousiainen, J. 2008. Effects of silage soluble nitrogen components on metabolizable protein concentration: A meta-analysis of dairy cow production experiments. *Journal of Dairy Science* **91**(3), 1150–1158.

Hymes-Fecht, U., Broderick, G., Muck, R. & Grabber, J. 2013. Replacing alfalfa or red clover silage with birdsfoot trefoil silage in total mixed rations increases production of lactating dairy cows. *Journal of Dairy Science* **96**(1), 460–469.

Lazzari, G., Poppi, A.C., Machado, J., Bueno, A.V., Gomes, A.L., Jobim, C.C. & Daniel, J.L. 2021. Effects of protein source and lipid supplementation on conservation and feed value of total mixed ration silages for finishing beef cattle. *Journal of Animal Science* **99**(2), 32.

Mcdonald, P., Henderson .R. & Heron, S.J.E. 1991. *The biochemistry of silage*. Aberystwyth (UK): Chalcombe Publications, **2**, 1–340.

Mezzalira, J.C., Carvalho, P.C.F., Fonseca, L., Bremm, C., Reffatti, M.V., Poli, C.H.E.C. & Trindade, J.K.D. 2011. Methodological aspects of ingestive behavior of grazing cattle. *Brazilian Journal of Animal Science* **40**, 111420.

Miyaji, M., Matsuyama, H. & Nonaka, K. 2017. Effect of ensiling process of total mixed ration on fermentation profile, nutrient loss andin situruminal degradation characteristics of diet. *Animal Science Journal* **88**(1), 134–139.

Nguyen, T.T.G., Wanapat, M., Phesatcha, K. & Kang, S. 2017. Effect of inclusion of different levels of Leucaena silage on rumen microbial population and microbial protein synthesis in dairy steers fed on rice straw. Asian-Australasian *Journal of Animal Sciences* **30**(2), 1–181.

NRC. 2001. *Nutrient requirements of dairy cattle*. 7th ed. Washington (DC): National Academies Press.

Oliveira, V.S., Ferreira, M.A., Guim, A., Modesto, E.C., Lima, L.E. & Silva, F.M. 2007. Total replacement of corn and partial replacement of Tifton hay with forage palm in diets for lactating cows. Intake and digestibility. *Brazilian Journal of Animal Science* **36**(5), 1419–1425.

Oliveira, T.S., Rocha Júnior, V.R., Reis, S.T., Aguiar, E.F., Souza, A.S., Silva, G.W.V., Dutra, E.S., Silva, C.J., Abreu, C.L. & Bonalti, F.K.Q. 2011. Chemical composition of ammoniated sugarcane bagasse with different doses of urea and soybean grain. *Archives of Animal Science* **60**(231), 625–635.

Pahlow, G., Muck, R.E., Driehuis, F., Elferink, S.J.O. & Spoelstra, S.F. 2003. Microbiology of ensiling. *Silage science and technology* **42**(1), 31–93.

Pinto, A.C. & Millen, D.D. 2018. Nutritional recommendations and management practices adopted by feedlot cattle nutritionists: the 2016 Brazilian survey. *Canadian Journal of Animal Science* **99**(2), 392–407.

Possenti, R.A., Franzolin, R., Schammas, E.A., Demarchi, J.J.A.D.A., Frighetto, R.T.S. & Lima, M.A.D. 2008. Effects of diets containing Leucaena leucocephala and Saccharomyces cerevisiae on ruminal fermentation and methane gas emission in cattle. *Brazilian Journal of Animal Science* **37**(1), 1509–1516.

Ribeiro, A.S., Pires, A.J.V., Santos, D.C., Albuquerque, M.L.P., Silva, F.F., Dutra, I.C., Amorim, S.S., Galvao, P.C.S., Santos, M.L.S., Amaral, M.V., Publio, P.P.P. & oliveira, g.r.s. 2026. Productive and feeding performance of dairy cows fed sugarcane bagasse ammoniated with urea and cottonseed. *Agronomy research* **24**(S1), 41–53. doi: 10.15159/AR.25.108

Rook, A.J. & Gill, M. 1990. Prediction of the voluntary intake of grass silages by beef cattle. 1. Linear regression analyses. *Animal Science* **50**(3), 425–438.

Silva, N.V., Pires, A.J.V., Dutra, I.C., Silva, H.S., Santos, B.E.F., Nogueira, M.S., Cruz, N.T., Silva, A.P.G., Teixeira, L.S., Oliveira, G.R.S., Dutra, G.C. & Teixeira, L.S. 2025. The quality and fermentation of the total diet containing BRS capiaçu or sugarcane with or without urea. *Agronomy Research* **23**(S2), 935–947.

Valadares Filho, S.C., Costa e Silva, L.F., Lopes, S.A., Prados, L.F., Chizzotti, M.L., Machado, P.A.S., Bissaro, L.Z. & Furtado, T. 2016. *BR-CORTE 3.0: Nutrient requirements of zebu and crossbred cattle*. Viçosa, MG: UFV, Suprema Gráfica Ltda. (1), 142 pp.

Valadares, R., Broderick, G., Filho, S.D.C.V. & Clayton, M. 1999. Effect of replacing alfalfa silage with high moisture corn on ruminal protein synthesis estimated from excretion of total purine derivatives. *Journal of dairy science* **82**(12), 2686–2696.

Verbic, J., Chen, X.B., MacLeod, N.A. & Orskov, E.R. 1990. Excretion of purine derivatives by ruminants. Effect of microbial nucleic acid infusion on purine derivative excretion by steers. *Journal of Agricultural Science* **114**(3), 243–248.

Xu, C.C., Cai, Y., Zhang, J.G. & Ogawa, M. 2007. Fermentation quality and nutritive value of a total mixed ration silage containing coffee grounds at ten or twenty percent of dry matter. *Journal of animal science* **85**(4), 1024–1029.

Agronomy Research **24**(S1), 179–191, 2026
https://doi.org/10.15159/AR.26.029

Technological properties of Saanen goat's milk in the context of mountain farming in Kabylia

R. Slamani[1], R. Labadi[2], D. Deffairi[3], H. Fadel[4] S, Ait Kaki[5] and S. Akkal[4,*]

[1]National Institute of Agronomic Research (INRAA), Experimental Station of Agronomic research, Food Technology Laboratory, Baraki road, BP 37, Algiers, Algeria
[2]National Higher School of Agronomy (ENSA), Department of Food Science, Chemistry Laboratory, Hassan Badi, 16200, El Harrach, Algeria
[3]University Saad Dahleb of Blida 1, Faculty of Sciences, Laboratory of Sciences, Food Technology and Sustainable Development, Soumaa road, BP 270, Blida, Algeria
[4]Research Unit, Valorization of Natural Resources, Bioactive Molecules, and Physicochemical and Biological Analyses University of the Mentouri Brothers, Constantine, Aïn El Bey road, 25000, Constantine, Algeria
[5]University M'hamed Bougara of Boumerdes (UMBB), Faculty of Sciences, Laboratory of Valorization and Conservation of Biological Resources, Independence Avenue, BP 35000, Algeria
[*]Correspondence: salah4dz@yahoo.fr

Received: February 17th, 2026; Accepted: April 30th, 2026; Published: May 14th, 2026

Abstract. The technological properties of milk are largely determined by its protein and mineral composition, which influence coagulation suitability and curd yield. This study examined the relationships between the composition of Saanen goat's milk produced in mountainous pastoral conditions and technological indicators. Monthly milk samples collected from March to May were analyzed to determine their chemical composition, mineral profile, and coagulation aptitude. Casein content was identified as the main determinant of technological performance, demonstrating strong positive correlations with curd yield efficiency, daily curd yield, and solid recovery, as well as negative correlations with water retention in the curd. Conversely, the casein number showed limited predictive value. Milk fat also significantly contributed to technological ability by enhancing solid recovery and curd yield through its interaction with the protein matrix. Colloidal calcium exhibited moderate associations with coagulation properties. Seasonal effects were observed with improved curd structuring and moisture control from March to May. Overall, the technological aptitude of Saanen milk was moderate, mainly due to relatively low casein content. These findings highlight the importance of milk components in determining processing performance and provide practical insights for improving feeding strategies and milk utilization in similar agro-climatic conditions.

Key words: Saanen goat milk, milk composition, nutrient recovery, curd yield, technological indicators.

INTRODUCTION

The Saanen goat is a dairy breed originating from Switzerland, widely recognized for its high milk yield and its ability to adapt to diverse environmental conditions (Zeljić Stojiljković et al., 2025). It is currently reared in a wide range of production systems, from temperate regions in Northern Europe to Mediterranean and arid environments (Teissier et al., 2024). Under intensive management and optimal conditions, lactation may extend over 300 days, with milk yields reaching 1,000 kg per lactation (Varlyakov et al., 2018).

In Algeria, particularly in the mountainous region of Kabylia, the Saanen breed is increasingly introduced into local farming systems to diversify dairy production and meet the growing demand for goat milk and derived products (Tefiel et al., 2014; Boumediene et al., 2025). However, these systems are predominantly extensive, characterized by limited concentrate supplementation and strong dependence on seasonal forage availability (Kadi et al., 2016). Under such conditions, milk production remains below the genetic potential of the breed, generally not exceeding 2 kg per day (Mouhous et al., 2015).

Beyond milk yield, the technological quality of milk is a key factor determining its suitability for processing, particularly for cheese production. This quality depends largely on milk composition, especially protein, fat, and mineral fractions, which are known to be influenced by feeding conditions, climate, and herd management practices (Inglingstad et al., 2014; Barłowska et al., 2018; Bouderka et al., 2025). In mountain pastoral systems, these factors may lead to specific compositional profiles that directly affect coagulation behavior, curd formation, and nutrient recovery, which in turn can influence the overall quality and yield of cheese produced from this milk.

While previous studies in Algeria have mainly focused on the reproductive performance and adaptation of Saanen goats to local conditions (Mouhous, 2021), limited information is available on the technological properties of their milk and its suitability for dairy processing. The connections between the composition of milk and how well it coagulates are not well understood in large-scale production systems. Addressing this knowledge ga*p* is essential for improving the valorization of goat milk in these regions. A better understanding of the factors affecting curd yield and nutrient recovery could help to optimize feeding strategies, milk selection, and processing conditions in small-scale and artisanal dairy systems.

Therefore, the objective of this study was to evaluate the technological properties of Saanen goat milk produced in a mountainous agroclimatic context by analyzing its physicochemical composition, mineral profile, and coagulation behavior. In addition, the study aimed to quantify curd yield and nutrient recovery and to assess the relationships between milk composition and technological performance.

MATERIALS AND METHODS

Experimental design and sampling

The study was conducted over a period of three months (January to March) at a private artisanal cheese factory. This period was chosen to coincide with the early to mid-lactation stage of Saanen goats, when the milk composition is relatively stable.

Additionally, feeding conditions in the mountainous agroclimatic context of Kabylia are relatively homogenous during winter, helping to limit variability related to seasonal fluctuations.

Three cheese-making trials were carried out each month, at regular intervals, using Saanen goat's milk collected from three family farms in Kabylia (Afir, Makouda, and Mizrana). The herds (60 to 90 head) graze on mountain pastures at an altitude of 300–900 meters. Milk from the evening milking on each farm was collected the next morning by tanker and then mixed. Upon receipt at the cheese factory, a milk sample was taken from the bulk tank, refrigerated at 4 °C, and sent immediately to the laboratory for composition analyses.

Cheese making process

The process is based on a standardized protocol intended for producing uncooked pressed goat cheese without prolonged ripening. This was chosen to enable the rapid technological evaluation of milk clotting ability, independently of maturation. A total of 9 manufacturing tests were carried out (three per month over three consecutive months). For each test, 10 L of pasteurized milk (75 °C for 30 s) was used. The milk was inoculated with a freeze-dried mesophilic culture (FD-DVS R-707, Chr. Hansen, Denmark) at 8 times the recommended dose and maintained at 34 °C. Once the pH had stabilized, commercial rennet (recombinant bovine chymosin, 1,400 IMCU mL^{-1}, Chr. Hansen) was added at a rate of 25%. After coagulation, the curds were cut into cubes (~6 cm^3), stirred to encourage drainage, and then placed in hanging molds. Draining was carried out by gravity before unmolding, salting in brine, and refining in a ventilated chamber (13 °C, 80% H). The study was limited to analyzing the milk, curd, and whey from each test in order to establish a material balance and calculate curd yield and component recoveries (Cipolat-Gotet et al., 2015a).

Compositional analysis of milk, whey and curd

The main components of milk, whey, and curd, including fat, protein, lactose, and ash, were expressed in g kg^{-1} of fresh matter. Total solids content of milk and whey samples were determined by drying 3 g of each sample at 102 °C until a constant weight was reached. Ash content was determined by weighing after combusting each sample at 550 °C for 6 h. The fat content of milk and whey was analyzed using the Gerber method (ISO 19662, 2018). Fatty acid composition of milk was analyzed using gas chromatography (GC-FID) after methylation of fatty acids to fatty acid methyl esters (FAMEs). Separation was performed using a CP-Sil 88 CB capillary column (100 m × 0.25 mm × 0.20 µm; Agilent Technologies). The results were expressed as a percentage of total fatty acids identified. Total nitrogen, non-casein nitrogen, and non-protein nitrogen were determined using the Kjeldahl method. Nitrogen fractions of milk were prepared according to Rowland (1938) by precipitating the casein at pH 4.2 (the isoelectric point of caprine casein). Crude protein content was calculated as total nitrogen content × 6.38. Casein content was determined by difference, and the casein number was calculated as the ratio of casein to protein multiplied by 100. The fat/protein ratio was calculated as the ratio of milk fat content to total protein content. Lactose content was measured using an infrared analyzer (MilkoScan™ Mars, FOSS, Denmark) according to the IDF method (IDF 141B, 1996). Calcium content was estimated by flame emission spectrometry and phosphorus content by spectrophotometry. Soluble fractions were obtained after appropriate separation, and colloidal calcium and phosphorus were estimated by the difference between total and soluble contents, according to Remeuf et al. (1989). Concerning curd samples, fat, protein, lactose, and total solids were determined using a FoodScanTM analyzer (Foss, Denmark), which is based on near-infrared spectroscopy (NIRS). The pH of milk, whey, and curd samples was determined using a pH meter (Hanna Instruments, model HI 2210). Titratable acidity was only determined for milk samples by titration with N/9 NaOH using phenolphthalein as an indicator and expressed in Dornic degrees (°D).

Evaluation of yield and technological efficiency

In addition to physicochemical analyses, several technological indicators were calculated to evaluate coagulation performance (Vacca et al., 2018). For the nutrient recovery (REC, %), the proportion of each nutrient (protein or fat) recovered in the curd relative to its concentration in the initial milk. For curd yield (CY, %), the mass of curd obtained per 100 kg of processed milk. The theoretical curd yield (Th-CY) is calculated based on the initial concentrations of useful substances in the milk (standard formula). Regarding curd yield efficiency (Eff, %), the ratio of CY to Th-CY expresses the real performance relative to the expected yield. For daily curd yield (dCY), the total mass of curd obtained per day of production. These parameters were analyzed in each trial to assess the stability of technological performance over time and its relationshi*p* with the characteristics of the milk used.

Statistical analysis

Descriptive statistics (means and standard deviations [SD]) were performed, and the results are presented as means and coefficients of variation (CV). The effect of the month on the physicochemical composition of the milk was evaluated using one-way analysis of variance (ANOVA). Multiple comparison tests were performed to identify any significant differences between the sampling periods. A Pearson's correlation analysis was performed to examine the relationships between the physicochemical characteristics of milk, curd, and whey. A linear regression model was used to analyze the correlations between milk components (fat, protein, casein, casein number, and calcium) and technological parameters (nutrient components, curd yield, yield efficiency, and daily yield). In this model, milk components were considered as explanatory variables, while technological indicators were treated as dependent variables. Month was included as a fixed effect to account for seasonal variation. The general form of the model was: $Y = \beta_0 + \beta_1 \times + \varepsilon$. Where Y represents the dependent variable, $\times$ the explanatory variable, β_1 the regression coefficient, and ε the residual error. The regression coefficient (β) indicates the magnitude and direction of the relationshi*p* between variables. Statistical significance was set at $p < 0.05$. All statistical analyses were performed using the R software.

RESULTS AND DISCUSSION

Physicochemical characteristics of Saanen goat's milk

The average chemical composition of Saanen goat's milk produced through a traditional, extensive breeding system in the mountainous Kabylia region is characterized by an average fat content of 39.6 g kg^{-1}, total protein content of 30.3 g kg^{-1}, lactose content of 49.9 g kg^{-1}, and ash content of 9.0 g kg^{-1}. The total solids content ranged from 121.1 to 130.5 g kg^{-1}, with an average value of 125.8 g kg^{-1}. Analysis of the main physicochemical characteristics of the samples reveals significant variations depending on the sampling month (Table 1). In particular, titratable acidity showed a highly significant difference ($p < 0.001$), with values increasing from 17°D in March to 18°D in May. The pH of the milk also decreased significantly ($p < 0.001$) in May (to 6.50), compared to previous months (6.56 in March and 6.59 in April), reflecting more pronounced natural acidification. The casein number increased slightly in May (73.03%), constituting a significant difference compared to March (72.41%), reflecting relative variations between casein and total protein rather than a change in overall protein composition. Ash content also varied significantly ($p < 0.05$) from 8.1 g kg^{-1} in March to 9.9 g kg^{-1} in May, potentially indicating greater mineralization towards the end of the season. Similarly, a significant decrease in colloidal calcium was observed ($p < 0.05$), with slightly lower levels in April. Regarding the major constituents of milk's chemical composition, there has been a gradual increase in total solids, rising from 121.1 g kg^{-1} in March to 130.5 g kg^{-1} in May. Similar trends are evident for lactose and protein contents, increasing from 46.3 g kg^{-1} to 51.7 g kg^{-1} and from 29 g kg^{-1} to 33 g kg^{-1}, respectively, during this period. The fat content remained relatively stable. However, descriptive analysis of the monthly averages shows that the differences observed for these main components are not statistically significant ($p > 0.05$). These results illustrate that the chemical composition of Saanen goat's milk produced within an extensive, pastoral, mountain farming system improved in May for most primary constituents. Although the coefficient of variation (CV) was low for most parameters, greater dispersion was observed for ash (CV = 10.06) and casein (CV = 8.01). This variation is linked to the consistency of local pastoral practices and minor changes in diet.

Table 1. Monthly variations in the physicochemical characteristics of Saanen goat's milk from extensive traditional breeding in Kabylia

Milk Traits	March	April	May	Mean ± SD	CV	*p*-value
Acidity (°D)	17.0^{b}	16.0^{a}	18.0^{c}	17.0 ± 0.82	5.88	***
pH	6.56^{b}	6.59^{b}	6.50^{a}	6.55 ± 0.06	0.69	***
Total solids (g kg^{-1})	121.1	125.7	130.5	125.8 ± 0.34	3.74	-
Fat (g kg^{-1})	39.0	39.5	40.3	39.6 ± 0.29	1.65	-
Protein (g kg^{-1})	29.0	29.0	33.0	30.3 ± 0.17	7.61	-
Serum Protein (g kg^{-1})	8.0	7.9	8.0	7.96 ± 0.02	0.72	-
Casein (g kg^{-1})	21.0	21.1	24.1	22.07 ± 0.13	8.01	-
Casein number (%)	72.41^{a}	72.76^{ab}	73.03^{b}	72.73 ± 0.63	0.43	*
Fat / protien ratio	1.34	1.36	1.22	1.30 ± 0.07	5.75	-
Lactose (g kg^{-1})	46.3	51.8	51.7	49.93 ± 0.39	6.30	-
Ash (g kg^{-1})	8.1^{a}	8.9^{ab}	9.9^{b}	8.96 ± 0.01	10.06	*
Total Calcium (g kg^{-1})	1.09	1.08	1.09	1.09 ± 0.01	0.53	-
Colloïdal Calcium (g kg^{-1})	0.95^{b}	0.92^{ab}	0.93^{a}	0.93 ± 0.002	1.64	*
Total Phosphorus (g kg^{-1})	1.05	1.01	1.03	1.03 ± 0.003	1.94	-
Colloïdal Phosphorus (g kg^{-1})	0.77	0.79	0.85	0.80 ± 0.006	5.18	-

Means followed by different letters (a, b, c) within a row indicate significant differences between months according to Tukey's post-hoc test ($p < 0.05$). Significance levels are indicated as follows: * $p < 0.05$; ** $p < 0.01$; *** $p < 0.001$; ns: not significant.

The compositional profile of Saanen goat milk produced in Kabylie differs from that observed in intensive grazing systems in temperate, mountainous regions. As well as having a relatively high fat content and a lower casein content (with a casein index below the international average for this breed, according to Vacca et al. (2018)), it has an above-average colloidal mineral fraction and, more specifically, an above-average colloidal calcium content. The farming system significantly impacts milk composition, consequently affecting its suitability for cheese production, as demonstrated by Pazzola et al. (2018). The mountainous environment of Kabylie, with altitudes ranging from 300 to 900 meters, and extensive resource management appear to induce physiological adaptation in Saanen goats, resulting in an unusual chemical composition that could affect the structure of the curd during coagulation (Fox et al., 2017). In addition to these physiological factors, seasonal factors must also be monitored to ensure the technological quality of milk intended for processing.

Table 2. Fatty acid composition (sum of fatty acids (% of total fatty acids) and nutritional indices of extracted fat from Saanen goat's milk collected during the spring season and analyzed by gas chromatography

Main fatty acids	Mean ± SD
C4 :0 (Butyric Acid)	0.96 ± 0.43
C6 :0 (Caproic Acid)	1.02 ± 0.32
C8 :0 (Caprylic Acid)	1.10 ± 0.28
C10 :0 (Capric Acid)	3.65 ± 0.61
C12 :0 (Lauric Acid)	1.59 ± 0.454
C14 :0 (Myristic Acid)	5.13 ± 0.31
C15 :0 (Pentadécanoic Acid)	0.36 ± 0.025
C16 :0 (Palmitic Acid)	28.15 ± 0.82
C17:0 (Margaric acid)	0.29 ± 0.08
C18 :0 (Stearic acid)	24.19 ± 0.447
C20:0 (Arachidic acid)	0.07 ± 0.085
C14 :1 (Myristoleic Acid)	0.07 ± 0.015
C16 :1 (Palmitoleic acidic)	1.24 ± 0.115
C17 :1 (Heptadecenoic acid)	0.17 ± 0.04
C18 : 1ω9 (Oleic Acid)	24.00 ± 2.03
C20:1n-9 (Gondoic Acid)	0.07 ± 0.035
C18 : 2ω6 (Linoleic acid)	2.21 ± 0.135
C18:3ω3 (α-Linolenic Acid)	1.92 ± 0.39
Sums of fatty acids	
Σ Polyunsaturated Fatty Acids (PUFA)	4.13 ± 0.52
Σ Monounsaturated Fatty Acids (MUFA)	25.57 ± 1.45
Σ Unsaturated Fatty Acids (UFA)	29.70 ± 1.007
Σ Saturated Fatty Acids (SFA)	65.86 ± 0.22
ω-6	2.28 ± 0.025
Ratios of fatty acids	
PUFA/ SFA	0.063 ± 0.004
ω-6/ω-3	1.19 ± 0.38
AI	1.69 ± 0.24
DI14	0.014 ± 0.004
DI16	0.044 ± 0.003
DI18	0.99 ± 0.938

Saanen milk fatty acids profile

Analysis of the fatty acid profile of Saanen goat's milk (Table 2) shows that saturated fatty acids dominate, accounting for 65.86% of the total. By comparison, monounsaturated fatty acids account for 25.6%, while polyunsaturated fatty acids account for just 4.1%. The main fatty acids are palmitic acid (C16:0) at 28.15%, stearic acid (C18:0) at 24.19%, and oleic acid (C18:1 ω9) at 24%. These proportions are consistent with those reported by Yurchenko et al. (2018) for Saanen goat's milk, confirming the predominance of palmitic and oleic acids among the major lipid constituents. Caproic acid (C6:0), caprylic acid (C8:0), and capric acid (C10:0) contribute to the characteristic aroma of goat's milk, representing around 6% of the total fatty acid content. The atherogenicity index (AI), calculated according to the Ulbricht & Southgate (1991) method, and was estimated at 1.69, indicating moderate cardiovascular risk.

The lipid profile observed in this study is consistent with that reported by López et al. (2019) for goats raised on an extensive diet with a high intake of long-chain fatty acids (FAs) of dietary origin, particularly palmitic, stearic, and oleic acids. The lower proportions of medium-chain fatty acids (C10:0, C12:0, and C14:0) observed in this study compared with the values reported for stall-fed goats (Šlyžius et al., 2023) suggest reduced de novo fatty acid synthesis in the mammary gland and an increased contribution from preformed fatty acids derived from dietary intake. The C14:1/C14:0 ratio, which is an indirect indicator of stearoyl-CoA desaturase (SCD) activity, was low at 0.0136, which suggests that endogenous desaturation is limited. This value is comparable to that reported by Tudisco et al. (2014) under summer feeding conditions, when the nutritional quality of forage tends to decline. The presence of oleiferous plants, such as mastic (*Pistacia lentiscus*) and oleaster (*Olea europaea* var. *sylvestris*), in the goats' grazing areas could potentially cause reduced SCD activity. This is consistent with the inhibitory effect observed when diets are supplemented with vegetable oils rich in polyunsaturated fatty acids (Bernard et al., 2009). Finally, the atherogenicity index (AI) obtained in this study fell within or slightly below the range reported by Kasapidou et al. (2023) for goats fed buriti oil (AI = 2.20 - 1.47), suggesting a potentially more favorable fatty acid profile from a cardiovascular health perspective.

Clotting ability of Saanen goat's milk

Material balance: impact of the physicochemical characteristics of milk on those of curd and whey

Clotting Saanen goat's milk (with a dry matter content of 125.8 g kg^{-1}) yielded a curd with a dry matter content of 442.2 g kg^{-1} (based on fresh matter), which mainly contained 166.2 g kg^{-1} and 230.5 g kg^{-1} of protein and fat, respectively. The whey obtained during draining primarily composed lactose, accounting for around half of its dry matter content (37.9 g kg^{-1}). In terms of the coefficient of variation (CV), most parameters showed moderate variation, except for lactose in the curd, which exhibited a higher CV (19%) (Table 3). This indicates relatively low variability among samples. This may be explained by the use of bulk milk from farms operating under similar extensive feeding conditions, resulting in relatively stable milk composition.

A linear regression analysis revealed several significant relationships between milk composition and curd and whey characteristics. Milk fat ($\beta = 2.35$, $p < 0.001$) and protein ($\beta = 1.72$, $p < 0.001$) showed strong positive correlations with their respective concentrations in the curd. This is consistent with the well-established role of caseins in forming a three-dimensional protein network that retains fat and water during coagulation. Similar relationships between milk composition and curd dry matter have been identified using multiple linear regression approaches in dairy systems (Kern et al., 2019), supporting the relevance of relationships observed in the present study. Although these mechanisms have been extensively described in bovine milk, comparable coagulation principles are generally applicable to goat milk, despite differences in casein micelle size and mineralization (Clark & Sherbon, 2000; Park et al., 2007). In contrast, lactose showed a stronger correlation with whey ($\beta = 0.81$; $p = 0.001$) than with curd ($\beta = 0.45$; $p = 0.049$), confirming its preferential partitioning into the liquid phase during coagulation. A significant relationshi*p* was also observed between milk pH and pH of both curd ($\beta = 0.28$, $p = 0.026$) and whey ($\beta = 0.15$, $p = 0.048$), suggesting the influence of initial milk acidity on coagulation behavior and acid–base balance of the resulting products. The presence of residual lactose in the curd (23.9 g kg^{-1}), combined with a relatively high curd pH (~ 6.15), may influence coagulation kinetics. Similar observations have been reported by Pazzola et al. (2018), who showed that elevated pH and residual lactose can slow coagulation and curd firming in small ruminant milk.

Table 3. Effect of milk characteristics on curd and whey properties (β values ± significance; time reference: March)

Traits	Milk		Curd		Whey		Milk/Curd (β ± signif.)	Milk/*Whey (β ± signif.)	Seasonal effect (April/May)
	Mean	CV	Mean	CV	Mean	CV			
Total solids (g kg^{-1})	125.8	3.74	442.2	5.05	75.9	4.72	–	–	–
Fat (g kg^{-1})	39.6	1.65	230.5	7.88	10.5	7.13	2.35***	- 0.10 ns	April: ns May: ns
Protein (g kg^{-1})	30.3	7.61	166.2	6.36	8.0	4.80	1.72***	0.71**	May: +0.37*
Lactose (g kg^{-1})	49.93	6.30	23.9	19.01	37.9	6.28	0.45*	0.81***	May: +0.27*
pH	6.55	0.69	6.15	0.50	6.34	1.56	0.28*	0.15*	April: ns

β: regression coefficient obtained from the linear regression model. It indicates the magnitude and direction of the relationship between milk components (independent variables) and curd or whey characteristics (dependent variables). March was used as the reference level for estimation of seasonal effects. Significance levels are indicated as follows: $p < 0.05$, *$p < 0.01$, ***$p < 0.001$, and ns: not significant ($p > 0.05$).

Seasonal effects were also observed, with significant increases in curd protein (+0.37, $p = 0.022$) and whey lactose (+0.27, $p = 0.024$) in May compared to March. These variations likely reflect improvements in feeding conditions and animal physiological status during spring, which are known to influence milk synthesis. Seasonal changes in milk composition and their impact on technological properties have been widely reported in goat milk (Cipolat-Gotet et al., 2015b; Pereira et al., 2019).

Overall, these results confirm that the chemical composition of raw milk is closely associated with the physicochemical properties of curd and whey. This is consistent with previous studies reporting that variations in milk composition, whether intrinsic or seasonal, significantly influence coagulation behavior and technological properties of dairy products (Marcinkonienė & Ciprovica, 2020; Paschino et al., 2020).

Enzymatic coagulation efficiency: Curd yield and nutriments recovery

In uncooked pressed goat's cheese manufacture, cheese yield and moisture control depend on the ability of the casein network to entrap fat and expel whey. In the present study, seasonal changes in the composition of Saanen goat's milk were reflected in the evolution of the fat-to-protein ratio and the casein number (Table 1). Although both parameters remained within relatively narrow ranges (72 to 73% for casein number and 1.33 to 1.22 for fat/protein ratio), their seasonal trends may be associated with slight improvements in curd structuring and syneresis efficiency towards late spring. This is consistent with a previous study indicating that fat/protein ratio influences cheese yield and water retention through its effect on curd structure (Bojanić Rašović et al., 2013). Following coagulation and subsequent draining of the curd (Table 4), protein and fat recovery rates reached 73.05% and 71.87%, respectively, while total solids recovery remained lower (38.47%), reflecting losses of whey soluble components such as lactose. The average curd yield (CY = 12.26 kg per 100 kg of milk) was characterized by a relatively high proportion of water (55.5%), indicating a moist curd. This technological profile is consistent with the characteristics of enzymatic coagulation in goat milk, which typically leads to moderate solid recovery and higher moisture retention (Vacca et al., 2018; Pazzola et al., 2019; Marcinkonienė & Ciprovica, 2020).

Table 4. Relationships between the composition of Saanen goat's milk and the technological indicators of coagulation and cheese yield (β coefficients ± significance *p*)

Technological indicators	Mean	CV	Fat (β)	Protein (β)	Casein (β)	Casein number (β)	Ca (β)	Effect month (*p*)
Mean			39.6	30.3	22.07	72.73	1.09	
CV			1.65	7.61	8.01	0.43	0.53	
Nutrient recovery (REC, %)								
REC_{FAT}	71.87	2.55	+0.84 ***	+0.42 **	+0.78 ***	ns	+0.38 **	*
$REC_{PROTEIN}$	73.05	2.51	ns	+0.69 ***	+0.85 ***	+0.33 **	+0.34 **	**
REC_{SOLIDS}	38.47	7.97	+0.76 ***	+0.48 **	+0.74 ***	ns	+0.36 **	*
REC_{ENERGY}	59.414	4.38	+0.59 ***	ns	ns	ns	ns	**
Curd yield (CY, %)								
CY_{CURD}	12.26	11.75	+0.91 ***	+0.55 ***	+0.80 ***	ns	+0.42 **	**
CY_{SOLIDS}	5.91	12.18	+0.78 ***	+0.49 ***	+0.76 ***	ns	+0.31 **	**
CY_{WATER}	6.25	12.39	ns	−0.36 **	−0.48 **	ns	ns	*
Theoretical curd yield (Th-CY, %)								
Th-CY_{CURD}	11.14	14.62	+0.67 ***	+0.41 **	+0.70 ***	ns	+0.39 **	**
Th-CY_{SOLIDS}	6.242	10.98	ns	+0.45 **	+0.69 ***	ns	ns	*
Curd yield efficiency (Eff, %)								
Eff-CY_{CURD}	1.114	16.5	ns	ns	+0.37 **	+0.29 **	ns	*
Eff-CY_{SOLIDS}	0.953	13.4	+0.38 **	ns	ns	ns	ns	*
Daily curd yield (dCY, kg d)$^{-1}$								
dCY_{CURD}	0.184	11.66	+0.82 ***	+0.39 **	+0.75 ***	ns	+0.35 **	**
dCY_{SOLIDS}	0.089	12.093	ns	+0.41 **	+0.71 ***	ns	ns	**
dCY_{WATER}	0.094	12.26	ns	− 0.33 **	− 0.44 **	ns	ns	*

β: regression coefficient obtained from linear regression models, indicating the magnitude and direction of the relationshi*p* between milk components (independent variables) and a technological indicator (dependent variable). Positive β values indicate a positive correlation, whereas negative values indicate an inverse relationship. *p*: level of statistical significance: $p < 0.05$; * $p < 0.01$; *** $p < 0.001$; ns: not significant ($p > 0.05$). Month effect: *p*-value of the fixed effect of month included in the regression model.

Linear regression analysis (Table 4) identified casein content as the main factor associated with nutrient recovery and curd yield parameters. In particular, casein showed strong positive correlation with $REC_{PROTEIN}$ (β = +0.85, $p < 0.001$), REC_{FAT} (β = +0.78, $p < 0.001$), CY_{CURD} (β = +0.80, $p < 0.001$), and dCY_{CURD} (β = +0.75, $p < 0.001$). These results confirm the central role of casein in forming the micellar network responsible for curd structure and solid retention, as widely reported in goat milk studies (Stocco et al., 2018; Marcinkonienė & Ciprovica, 2020). In contrast, casein number did not significantly explain the observed variability in curd yield and moisture retention, indicating that the absolute amount of casein is more relevant to coagulation efficiency than its relative proportion to total protein.

Fat emerged as the second most influential factor affecting technological performance. Significant positive correlations were observed between fat content and several technological indicators, including REC_{FAT} ($\beta = +0.84$, $p < 0.001$), REC_{SOLIDS} ($\beta = +0.76$, $p < 0.001$), REC_{ENERGY} ($\beta = +0.59$, $p < 0.001$) and CY_{CURD} ($\beta = +0.91$, $p < 0.001$). These results are consistent with previous studies showing that fat contributes substantially to curd formation through its incorporation into the protein matrix (Vacca et al., 2018; Pazzola et al., 2019). More generally, similar correlations between fat/protein balance and cheese yield have been reported in dairy matrices, where this ratio significantly influences curd composition, dry matter content, and water retention (Bojanić Rašović et al., 2013). However, when combined with moderate to low casein content, higher fat levels may increase water retention and reduce curd firmness. This reflects the limited capacity of a less dense casein network to effectively entrap fat globules and expel whey. The combined effect of relatively high fat content and moderate casein availability therefore explains the observed technological profile, characterized by satisfactory fat recovery but high moisture retention.

Daily curd yield (0.184 kg day^{-1}) confirmed this trend with comparable contributions from solids (0.089 kg day^{-1}) and water (0.094 kg day^{-1}). The relatively high proportion of retained water is consistent with the structural characteristics of goat milk, notably smaller and less aggregated casein micelles compared to cow milk (Clark & Sherbon, 2000; Park et al., 2007), which limit gel firmness and promote moisture retention. Colloidal calcium showed only a moderate contribution to technological parameters. This suggests that, in the presence of moderate to low casein content, calcium alone is insufficient to strengthen the micellar network, suggesting its secondary role compared to protein structure and organization.

Overall, these results indicate that casein primarily governs curd structure and moisture retention, while fat enhances curd yield and nutrient recovery through its interaction with the protein matrix. The combination of moderate casein content, relatively high fat levels, and intrinsic physicochemical characteristics of goat milk results in moist curd with moderate solid recovery. Progressive seasonal variations in milk composition, particularly toward spring, were associated with slight improvement in coagulation efficiency and curd structuring.

CONCLUSIONS

This study reveals that Saanen goat milk produced under an extensive mountain pastoral system in Kabylia presents specific technological properties linked to its composition and seasonal variability. Casein content was identified as the primary factor influencing curd yield and water retention, while fat content contributed to nutrient recovery through its interaction with the protein matrix. Seasonal changes in milk composition were associated with variations in coagulation suitability and technological performance. However, given the limited sample size and study duration, further investigations over longer periods and with larger datasets are required to confirm and extend these results.

ACKNOWLEDGEMENTS. We acknowledge the support of the private cheese dairy Thiwiza (Boumerdes, Algeria).

REFERENCES

Barłowska, J., Pastuszka, R., Rysiak, A., Król, J., Brodziak, A., Kędzierska-Matysek, M., Wolanciuk, A. & Litwińczuk, Z. 2018. Physicochemical and sensory properties of goat cheeses and their fatty acid profile in relation to the geographic region of production. *International Journal of Dairy Technology* **71**, 699–708. https://doi.org/10.1111/1471-0307.12506

Bernard, L., Shingfield, K.J., Rouel, J., Ferlay, A. & Chilliard, Y. 2009. Effect of plant oils in the diet on performance and milk fatty acid composition in goats fed diets based on grass hay or maize silage. *British Journal of Nutrition* **101**, 213–224. https://doi.org/10.1017/S0007114508006533

Bojanić Rašović, M., Nikolić, N., Martinović, A., Katić, V., Rašović, R., Walcer, M. & Domig, K. 2013. Correlation between protein to fat ratio of milk and chemical parameters and the yield of semi-hard cheese. *Biotechnology in Animal Husbandry* **29**(1), 145–159.

Bouderka, G., Nabi, M., Kebbal, S., Hadj-Omar, K., Salhi, O., Khelifi-Touhami, N.A. & Ouchene, N. 2025. Effects of goat breeds on the physicochemical properties of raw goat milk. *Journal of the Saudi Society of Agricultural Sciences* **24**(5), 39. https://doi.org/10.1007/s44447-025-00049-0

Boumediene, F., Meribai, A., Kahlouche, A., Bouchibane, M., Touzout, N. & Belbraouet, S. 2025. Effects of breed and lactation-stage of goat on the composition and lipid fraction of milk in Algeria. *Asian Journal of Dairy and Food Research* **44**(3), 505–510. https://doi.org/10.18805/ajdfr.DRF-446.

Cipolat-Gotet, C., Bittante, G. & Cecchinato, A. 2015a. Phenotypic analysis of cheese yields and nutrient recoveries in the curd of buffalo milk, as measured with an individual model cheese-manufacturing process. *Journal of Dairy Science* **98**(1), 633–645. https://doi.org/10.3168/jds.2014-8308

Cipolat-Gotet, C., Pazzola, M., Ferragina, A., Cecchinato, A., Dettori, M.L. & Vacca, G.M. 2015b. Technical note: Improving modeling of coagulation, curd firming and syneresis of sheep milk. *Journal of Dairy Science* **101**, 5832–5837. https://doi.org/10.3168/jds.2017-14256

Clark, S. & Sherbon, J.W. 2000. Alphas1-casein, milk composition and coagulation properties of goat milk. *Small Ruminant Research* **38**, 123–134. https://doi.org/10.1016/S0921-4488(00)00154-1

Fox, P.F., Guinee, T.P., Cogan, T.M. & McSweeney, P.L. 2017. Fundamentals of Cheese science. Springer New York, NY. P*p* **1**, 271. https://doi.org/10.1007/978-1-4899-7681-9

IDF standard 141B. 1996. Whole Milk: Determination of Milk Fat, Protein and lactose content. Guide for the operation of mid-infrared instruments. *International Dairy Federation*, Brussels.

Inglingstad, R.A., Steinshamn, H., Dagnachew, B.S., Valenti, B., Criscione, A., Rukke, E.O., Devold, T.G., Skeie, S.B. & Vegarud, G.E. 2014. Grazing season and forage type influence goat milk composition and rennet coagulation properties. *Journal of Dairy Science* **97**(6), 3800–3814. https://doi.org/10.3168/jds.2013-7542

ISO 19662. 2018. Milk – Determination of fat content – Acido-butyrometric (Gerber method. *International Organization for Standardization*, Switzerland

Kadi, S.A., Djellal, F., Hassini, F. & Mouhous, A. 2016. Pratiques alimentaires dans les élevages caprins dans la région montagneuse de Tizi-Ouzou en Algérie. In M. Napoléone, H. Ben Salem, J.P. Boutonnet, A, López-Francos, D. Gabiña (ed), The value chains of Mediterranean sheep and goat products: Organization of the industry, marketing strategies, feeding and production systems, *Options Méditerranéennes CIHEAM,* 249–252. http://om.ciheam.org/article.php?IDPDF=00007283

Kasapidou, E., Iliadis, I.V., Mitlianga, P., Papatzimos, G., Karatzia, M.A., Papadopoulos, V., Amanatidis, M., Tortoka, V., Tsiftsi, E., Aggou, A. & Basdagianni, Z. 2023. Variations in composition, antioxidant profile, and physical traits of goat milk within the semi–intensive production system in mountainous areas during the post–weaning to end of lactation period. *Animals* **13**(22), 1–19. https://doi.org/10.3390/ani13223505

Kern, C., Stefan, T. & Hinrichs, J. 2019. A Multiple linear regression modeling: Prediction of cheese curd dry matter during curd treatment. *Food Research International* **121**, 471–478. https://doi.org/10.1016/j.foodres.2018.11.061

López, A., Vasconi, M., Moretti, V.M. & Bellagamba, F. 2019. Fatty Acid Profile in Goat Milk from High- and Low-Input Conventional and Organic Systems. *Animals* **9**(7), 1–14. https://doi.org/10.3390/ani9070452

Marcinkonienė, L. & Ciprovica, I. 2020. The influence of milk quality and composition on goat milk suitability for cheese production. *Agronomy Research* **18**(S3), 1796–1703. https://doi.org/10.15159/AR.20.094

Mouhous, A., Kadi, S.A. & Brabez, F. 2015. Adaptation strategies of goat farmers in the mountainous region of Tizi-Ouzou, Algeria. *European Science Journal* **11**(2), 1857–7881 (in French).

Mouhous, A., Kadi, S.A., Guermah, H. & Djellal, F. 2021. The goat meat sector in an Algerian mountain region: analysis of its value chain. In López-Francos, A. (ed.), Jouven, M. (ed.), Porqueddu, C. (ed.), Ben Salem, H. (ed.), Keli, A. (ed.), Araba, A. (ed.), Chentouf, M. (ed.). Efficiency and resilience of forage resources and small ruminant production to cope with global challenges in Mediterranean areas *Options Méditerranéennes*, *CIHEAM* 115–118. http://om.ciheam.org/article.php?IDPDF=00007981

Park, Y.W., Juárez, M., Ramos, M.G.F.W. & Haenlein, G.F.W. 2007. Physico-chemical characteristics of goat and sheep milk. *Small Ruminant Research* **68**, 88–113. https://doi.org/10.1016/j.smallrumres.2006.09.013

Paschino, P., Stocco, G., Dettori, M.L., Pazzola, M., Marongiu, M.L., Pilo, C.E., Cipolat-Gotet, C. & Vacca, G.M. 2020. Characterization of milk composition, coagulation properties, and cheese-making ability of goats reared in extensive farms. *Journal of Dairy Science* **103**, 5830–5843. https://doi.org/10.3168/jds.2019-17805

Pazzola, M., Stocco, G., Dettori, M.L., Bittante, G. & Vacca, G.M. 2019. Effect of goat milk composition on cheese-making traits and daily cheese productions. *Journal of Dairy Sciences* **102**(5), 3947–3955. https://doi.org/10.3168/jds.2018-15397

Pazzola, M., Stocco, G., Paschino, P., Dettori, M.L., Cipolat-Gotet, C., Bittante, G. & Vacca, G.M. 2018. Modeling of coagulation, curd firming, and syneresis of goat milk. *Journal of Dairy Sciences* **101**(8), 7027–7039. https://doi.org/10.3168/jds.2018-14397

Pereira, T.C.J., Ribeiro, L.S.O., Pires, A.J.V., Pereira, M.L.A., Santos, A.B., Silva, H.D.O. & de Carvalho, G.G.P. 2019. Growth performance and apparent digestibility by goats fed diets with peach palm meal replacing maize. *Applied Animal Science* **35**(6), 563–569. https://doi.org/10.15232/aas.2019-01874

Remeuf, F., Lenoir, J. & Duby, C. 1989. Study of the relationship between the physicochemical characteristics of goat's milk and its ability to coagulate with rennet. *Dairy Science & Technology* **69**, 499–518.

Rowland, S.J. 1938. The determination of the nitrogen distribution in milk. *Journal of Dairy Research* **9**(1), 42–46. https://doi.org/10.1017/S0022029900002296

Šlyžius, E., Anskienė, L., Palubinskas, G., Juozaitienė, V., Šlyžienė, B., Juodžentytė, R. & Laučienė, L. 2023. Associations between somatic cell count and milk fatty acid and amino acid profile in Alpine and Saanen goat breeds. *Animals* **13**, 965. https://doi.org/10.3390/ani13060965

Stocco, G., Pazzola, M., Dettori, M.L., Paschino, P., Bittante, G. & Vacca, G.M. 2018. Effect of composition on coagulation, curdfirming and syneresis of goat milk. *Journal of Dairy Science* **101**(11), 9693–9702. https://doi.org/10.3168/jds.2018-15027

Tefiel, H., Ata, N., Chahbar, M., Benyarou, M., Fantazi, K., Yilmaz, O., Cemal, I., Karaca, O., Boudouma, D. & Gaouar, S.B.S. 2018. Genetic characterization of four Algerian goat breeds assessed by microsatellite markers. *Small Ruminant Research* **160**, 65–71. https://doi.org/10.1016/j.smallrumres.2018.01.021

Teissier, M., Brito, L.F., Schenkel, F.S., Bruni, G., Fresi, P., Bapst, B., Robert-Granie, C. & Larroque, H. 2024. Genetic parameters for milk production and type traits in North American and European Alpine and Saanen dairy goat populations. *JDS Communications* **5**(1), 28–32. https://doi.org/10.3168/jdsc.2023-0389

Tudisco, R., Grossi, M., Calabrò, S., Cutrignelli, M.I., Musco, N., Addi, L. & Infascelli, F. 2014. Influence of pasture on goat milk fatty acids and stearoyl-CoA desaturase expression in milk somatic cells. *Small Ruminant Research* **122**(1–3), 38–43. https://doi.org/10.1016/j.smallrumres.2014.07.016

Ulbricht, T.L.V. & Southgate, D.A.T. 1991. Coronary heart disease: seven dietary factors. *The Lancet* **338**(8773), 985–992. https://doi.org/10.1016/0140-6736(91)91846-M

Vacca, G.M., Stocco, G., Dettori, M.L., Summer, A., Cipolat-Gotet, C., Bittante, G. & Pazzola, M. 2018. Cheese yield, cheese-making efficiency, and daily production of 6 breeds of goats. *Journal of Dairy Sciences* **101**(9), 7817–7832. https://doi.org/10.3168/jds.2018-14450

Varlyakov, I., Slavov, T., Radev, V., Nedeva, I. & Nikolov, G. 2018. Milking behaviour of Saanen goats. *Bulgarian Journal of Agricultural Sciences* **24**(1), 109–118.

Yurchenko, S., Sats, A., Tatar, V., Kaart, T., Mootse, H. & Jõudu, I. 2018. Fatty acid profile of milk from Saanen and Swedish Landrace goats. *Food Chemistry* **254**(15), 326–332. https://doi.org/10.1016/j.foodchem.2018.02.041

Zeljić Stojiljković, K., Mićić, N., Bogdanović, V., Đedović, R., Pihler, I., Stojiljković, N. & Stanojević, D. 2025. Genetic evaluation of milk production traits in the Serbian Saanen goat population. *Animals* **15**(20), 3008. https://doi.org/10.3390/ani15203008

Agronomy Research **24**(S1), 192–206, 2026
https://doi.org/10.15159/AR.26.031

Economic viability of different skeleton pruning-based management approaches in coffee (*Coffea arabica* L)

F.C. Silva[1,*], V.R. Paula[2], G.B. Sabino[3], A.L. Belem[1], J.P.B. Cunha[4] and M.M. Barros[4]

[1]Federal Fluminense University, Agricultural and Environmental Engineering Department, 156 Rua Passos da Pátria 156, bloco D, sala 235, 24210-240, Niterói, Brasil
[2]Instituto Federal de Educação, Ciência e Tecnologia do Sul de Minas, Rodovia Machado - Paraguaçu, KM 03 - Santo Antônio, 37750-000, Machado, Brasil
[3]Universidade Federal de Lavras, Departamento de Engenharia Agrícola
[4]Federal Rural University of Rio de Janeiro, Engineering Department, Rodovia BR 465, Km 07, s/n Zona Rural, 23890-000, Seropédica, Brasil
[*]Correspondence: flaviocastro@id.uff.br

Received: January 31st, 2026; Accepted: May 7th, 2026; Published: May 21st, 2026

Abstract. Coffee is one of the most valuable commodities on the international market, and its cultivation is among the most important agricultural activities in Brazil. Skeleton pruning is used in coffee crops to maintain production capacity by promoting the recovery of weakened plants and correcting problems related to plant architecture. This study evaluated the effects of different coffee skeleton-pruning management approaches on operating cost, productivity, and profitability. The experiment was conducted in a 22-year-old field of the cultivar Catuaí Vermelho IAC 144, spaced at 2.8×1.0 m. The treatments were obtained by combining two types of skeletonization and four types of regrowth management, totaling eight treatments plus a control without skeletonization. The experiment was arranged in a randomized block design with six replications, totaling 54 experimental plots. Operational cost was estimated from the time required for each management practice and the corresponding fuel consumption. The results showed that skeletonization restricted to branches between rows stimulated the growth of plagiotropic branches between plants, whereas total skeletonization promoted the greatest vegetative recovery and the highest productivity. Although total skeletonization resulted in higher crop cost, the treatment combining total skeletonization with sprout control showed the best economic performance, with an increase in profitability of up to USD 6,300.00 ha^{-1} compared with the control.

Key words: *Coffea arabica* L, skeleton, semi-mechanized, operating cost, profitability.

INTRODUCTION

In recent decades, global coffee production has increased substantially, making this crop stand out as the second most relevant commercial product worldwide. With an increasingly frequent demand, its production and commercialization have proven essential to the economies of many developing countries (Utrilla-Catalan et al., 2022). Consequently, coffee cultivation currently requires increasingly optimized production processes, mainly due to the still low level of technological adoption, resulting from the difficulties many producers face in accessing modern technologies (Rhiney et al., 2021).

One of the technologies adopted by coffee producers to enhance the sustainability and productivity of coffee plantations is crop management through pruning. The adoption of pruning in coffee plants aims to promote the development of productive branches; this practice allows greater and more continuous direct sunlight incidence (Cerda et al., 2017). Thus, pruning stimulates nutrient translocation to productive branches, resulting not only in greater vegetative growth but also in increased flowering and, consequently, higher productivity (Karim et al., 2021), reflecting improved plant growth and flowering, and enabling greater yield and bean quality.

Traditionally, the systems employed for coffee pruning include skeleton pruning, which renews lateral branches while maintaining the main structure; stumping, used to rejuvenate older or weakened plants aiming at a more advantageous biennial production cycle for plantation renewal; and topping, which stimulates branching and standardizes plant height (Pereira et al., 2013; Silva et al., 2016).

However, when these techniques are applied without proper criteria, they may cause drastic effects on the plants, resulting in reduced productivity, root system reduction, and plant death due to excessive removal of vegetative biomass (Gonçalves et al., 2014).

Especially in mechanically harvested areas, pruning can lead to disorganization of plant architecture, with increased branch density in the lower part of the plant and limited leaf growth in the middle third, altering plant size and geometry. This condition results in losses in the collection mechanisms of harvesting machines currently available on the market (Cunha et al., 2016).

Given this context, several studies have been conducted addressing challenges related to the variability of plant responses, aiming to integrate pruning into crop management strategies while considering physiological aspects (Filho et al., 2016; Pereira et al., 2016), the increased occurrence of abiotic stresses such as water deficit and rising temperatures (Custódio et al., 2013; Nascimento et al., 2014), and improvements in techniques associated with nutritional management, aiming to maximize productive efficiency and the longevity of coffee plantations under irrigated conditions (Souza et al., 2024).

Therefore, given the complexity of adopting pruning practices and the coffee plant's response to them, deepening the understanding of different pruning techniques becomes essential to support more precise technical recommendations. The novelty of this study lies in the integrated assessment of vegetative recovery, crop productivity, operating costs, and profitability under different skeleton pruning-based management strategies in mature coffee plantations, in which pruning decisions must reconcile vegetative recovery, productive performance, and economic return. We hypothesized that more intensive skeleton pruning strategies would promote greater vegetative recovery, higher productivity, and superior economic return than lateral skeletonization or the control treatment. Thus, the objective of the present study was to evaluate the effect of different coffee skeleton-pruning management strategies on production costs, their impact on crop productivity, and the differences in profitability resulting from the adopted management practices.

MATERIAL AND METHODS

Study area and pruning management

The study was conducted in the municipality of Poço Fundo in the southern region of the state of Minas Gerais, Brazil. The site is located at an elevation of 1,038 meters and has geographical coordinates of 21°42' S and 46°00' W. The region has a hot and temperate climate, with an average annual rainfall of 1,508 mm and low rainfall during the winter. According to Koeppen (1948), the climate is classified as Cwa, i.e., a humid subtropical climate with dry winters and hot summers. The experimental crop consisted of 20-year-old Catuaí Vermelho IAC 144 cultivar, with a spacing of 2.8×1.0 m, totaling 3,572 plants per hectare. The soil of the experimental area is classified as a dystrophic Red-Yellow Latosol (Latossolo Vermelho-Amarelo Distrófico, LVAd), a deep, well-drained, and highly weathered tropical soil with low natural fertility and generally medium to clayey texture, which is suitable for agricultural mechanization

The management practices adopted in this experiment were total pruning, in which all the plagiotropic branches were skeletonized and the top was cut 1.80 m from the ground, lateral thinning, in which only the plagiotropic branches that protruded between the crop rows were skeletonized, thinning, in which only two shoots were kept on each orthotropic branch, and removal of all shoots originating from the orthotropic branch above the first two pairs of plagiotropic branches.

The experiment was set up in a randomized block design according to Banzatto & Kronka (2013), with six replications and nine treatments (eight pruning-based management approaches plus the control), totaling 54 experimental plots. Each plot consisted of six plants, of which the two plants at the ends were used as borders and the four central plants were considered for evaluation. Different treatments were obtained by combining 2 types of skeletonization (total and lateral) and 4 types of regrowth management, totaling 8 combinations plus the control, as shown in Table 1 below.

Table 1. Skeletonization and regrowth management adopted in the experiment

Treatment	Skeleton Management	Management of Sprouting
1	Only plagiotropic branches between rows	With saplings
2	All plagiotropic branches	With saplings
3	Only plagiotropic branches between rows	With thinning + capping
4	All plagiotropic branches	With thinning + capping
5	Only plagiotropic branches between rows	With capping
6	All plagiotropic branches	With capping
7	Only plagiotropic branches between rows	No pruning
8	All plagiotropic branches	No pruning
9	No skeletonization	No pruning

Management of the crop began after harvest in October 2019 to allow light to enter the crops and create space for vigorous shoots. The treatments were differentiated into total skeletonization (T2, T4, T6 and T8), lateral skeletonization (T1, T3, T5 and T7) and the control. In all the treatments, the apex of the orthotropic branches were cut using the same methodology. The second intervention occurred 37 days after skeletonization and consisted of cutting the shoots to preserve the apical dominance of the orthotropic branch while the plagiotropic branches sprouted their first shoots, with the objective of facilitating management and reducing the incidence of shoots from the orthotropic branches as described above (Thomaziello & Pereira, 2008).

Beginning in January 2020, quarterly evaluations of shoot growth were performed on plagiotropic branches, followed by thinning management in treatments T1, T2, T3 and T4. The first thinning occurred in January, followed by harvesting in February for treatments T3, T4, T5 and T6, and the second thinning occurred in late March. There was no harvest in any of the plots, including the control, during the 2020 harvest due to the adoption of the 'zero harvest' system, which was a strategy to eliminate the need for harvesting in years of low productivity. In January 2021, when potentially productive branches for the next crop were developed, the last measurement of the new plagiotropic branches was performed.

Statistical analysis

The data were analyzed by analysis of variance (ANOVA) to evaluate the effects of treatment, branch position, evaluation time, and their interactions on plagiotropic branch length, and treatment means were compared using Tukey's test at the 5% probability level, using the SISVAR software in accordance with Ferreira (2019) Because branch growth was evaluated repeatedly over the study period, evaluation time was explicitly incorporated into the ANOVA model as an explanatory factor, together with its interactions with treatment and branch position. In order to ensure the robustness and interpretability of the statistical results, the ANOVA model was first fitted and its residual structure was examined, allowing the identification of possible deviations from the assumptions required for valid inference. More specifically, the residuals obtained from the fitted model were extracted and inspected, and the main assumptions underlying ANOVA were formally assessed by testing residual normality and homogeneity of variances among groups. These procedures were included to verify whether the data reasonably satisfied the statistical requirements of the model, thereby providing greater transparency in the analytical workflow and supporting the reliability of the comparisons among the different skeleton pruning management approaches evaluated in this study. The study did not analyze the treatments as a formal full-factorial design; instead, it compared combined management approaches generated by the association between skeletonization type and regrowth management. The Python-based assumption checks, implemented using statsmodels together with supporting statistical libraries, are available in the repository cited in the Data Availability section.

Operating and total costs

In this study, the economic indicator used was net profitability, calculated as gross revenue minus production cost, where production cost included labour and fuel associated with the evaluated operations. The data regarding operating costs were collected considering the operating time and fuel spent to perform the skeletonization of the plagiotropic branches, cut the orthotropic branches and remove the shoot apex of the orthotropic branch, in addition to the time spent thinning the crops. The calculation of the operating cost was based on the time spent managing the crops, converted into work days ha^{-1}; the daily value of an operator was set at US$ 19.42 day^{-1} plus the fuel cost for each operation. Depreciation of the equipment was not considered due to its low value. As the study was conducted in Brazil, monetary values were originally calculated in Brazilian reais (BRL) and then converted to U.S. dollars (USD) using an exchange rate of 4.12 BRL per USD, consistent with the study period (2019–2021)

The 4 central plants of each plot were harvested separately in a semi mechanized and nonselective manner. The beans from each plot were weighed and transferred to a terrace, where they were conventionally dried in the sun before being sent to a processing plant with an average moisture content close to 11.5% (Borém et al., 2008). After processing, they were weighed again, and the weight was then transformed into productivity per hectare.

RESULTS AND DISCUSSION

Development of plagiotropic branches under different skeletonization management practices

Table 2 shows that there is a significant difference between the treatments, verified by analysis of variance (ANOVA) and the Tukey test at a significance level of 5%. In addition to the treatments, other sources of variation (FV) as well as the interactions between them also showed significant differences. Additionally, the coefficient of variation (CV) had a relatively low value (9.22%), suggesting a low variability in the data collected.

Table 2. Analysis of Variance (ANOVA)

Source of variation	GL	SQ	QM	Fc	Pr>Fc
Treatment	8	45,082.09	5,635.26	855.20	0.00**
Position	1	31,110.65	31,110.65	4,721.35	0.00**
Time	4	138,167.27	34,541.82	5,242.07	0.00**
Treatment * Position	8	7,453.57	931.69	141.39	0.00**
Treatment * Time	32	2,415.38	75.48	11.45	0.00**
Position*Time	4	1,432.74	358.18	54.35	0.00**
error	2,102	13,850.80	6.58		
Corrected total	2,159	239,512.52			
CV (%)	9.22				
Overall average	27.83		No. of observations		2,160

Legend: GL = degrees of freedom; SQ = sum of squares; QM = mean square; Fc = F calculated; Pr = power; **Significant.

Analysis of the fluctuations in the lengths of the plagiotropic branches in different treatments applied to the coffee plants (Fig. 1) showed that there was greater growth of the skeletonized branches in the lateral direction. This indicates that during the evaluation period, the branches showed greater development in this direction than between plants.

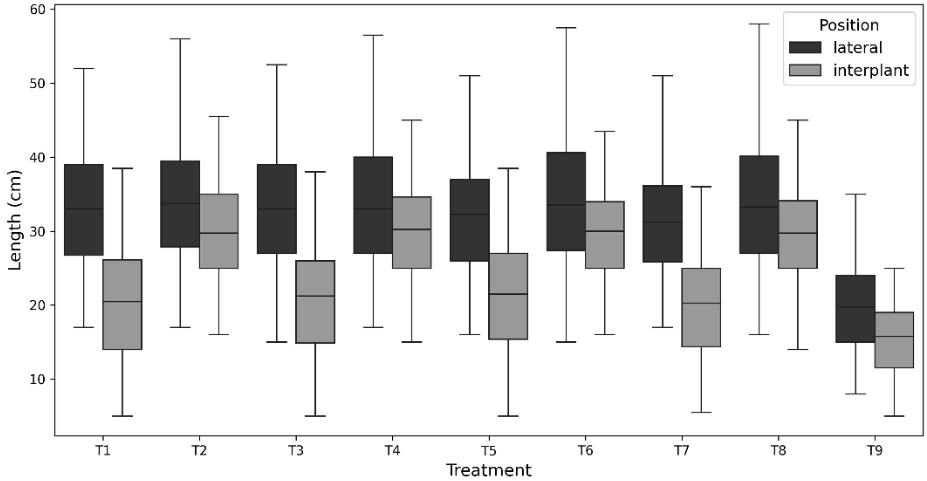

Figure 1. Variation in the observed mean lengths (cm) of plagiotropic branches in each treatment.

Regarding the variation in the average length (cm) of the plagiotropic branches for each treatment throughout the evaluation period (Fig. 2), treatments T2, T4, T6 and T8 stood out compared to the others, for example, although the plants showed greater changes in the lengths of the plagiotropic branches, there was also a lower variation in their size throughout the evaluation period.

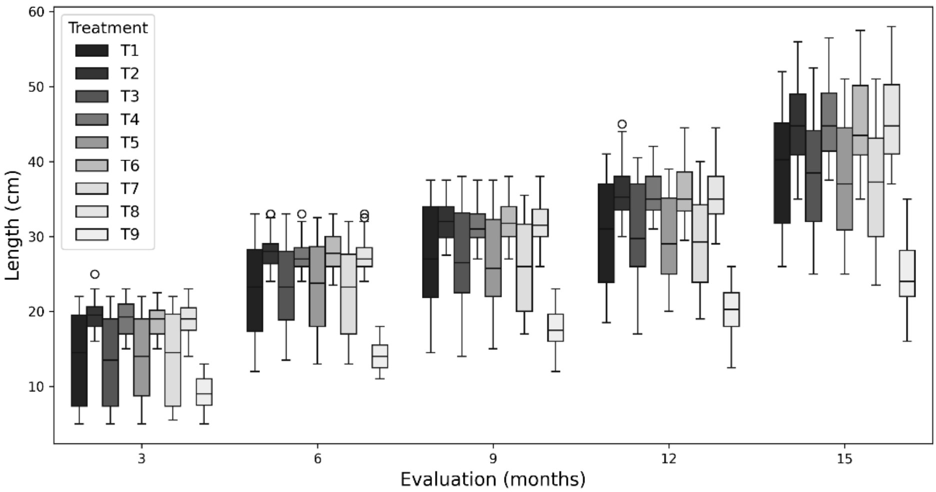

Figure 2. Variation in the mean lengths (cm) of plagiotropic branches in each treatment throughout the evaluation period.

Regarding the variation in the average length (cm) of the plagiotropic branches that underwent lateral skeletonization in each treatment throughout the evaluation period (Fig. 3), treatments T2, T4, T6 and T8 stood out relative to the remaining treatments, i.e., the plants in these treatments had greater changes in plagiotropic branch length throughout the evaluation period. It is noteworthy that the greatest variation in branch length occurred from 12 to 15 months of evaluation. Comparing the treatments with the control (T9), the importance of skeletonization in the renewal and growth of coffee branches is evident.

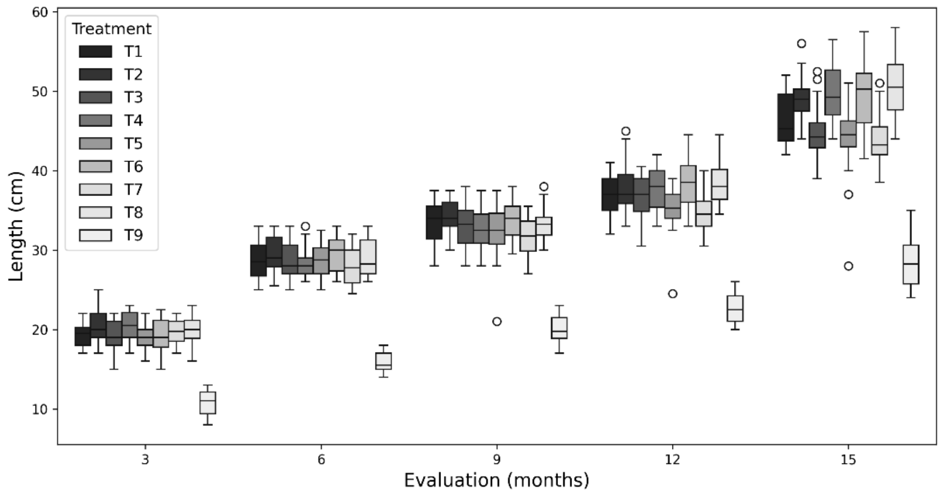

Figure 3. Variation in the mean lengths (cm) of lateral plagiotropic branches in each treatment throughout the evaluation period.

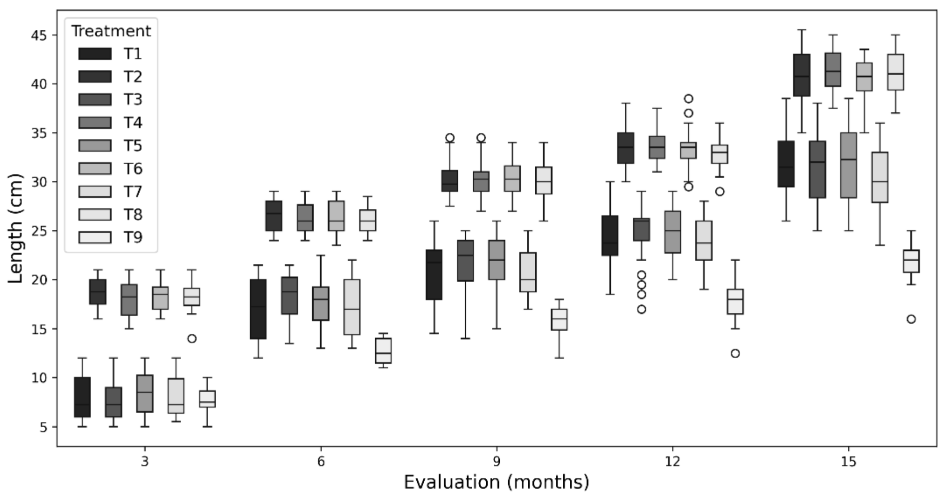

Figure 4. Variation in the mean lengths (cm) of the plagiotropic branches between plants in each treatment throughout the evaluation period.

Regarding the variation in the average length (cm) of the plagiotropic branches between plants that underwent skeletonization in each treatment throughout the evaluation period (Fig. 4), treatments T2, T4, T6 and T8 stood out compared to the others, i.e., the plants in these treatments exhibited greater changes in plagiotropic branch length throughout the evaluation period as well as lower variations in length (minimum and maximum). It is noteworthy that the variations in length among treatments T2, T4, T6 and T8 were higher than those among treatments T1, T3, T5 and T7 when compared with the lengths of branches in the treatments with lateral thinning. This can be verified by comparing the lower and upper limits of branch length in the two skeletonization management approaches for each treatment.

Regarding the average lengths (cm) of the plagiotropic branches in each treatment and with different skeletonization management approaches (Table 3), treatments T2, T4, T6 and T8 presented higher lateral growth rates and were significantly different from the other treatments considering the entire evaluation period. Treatments T2, T4, T6 and T8 showed the highest growth of plagiotropic shoots between plants, with significant differences from the other treatments. There was no significant difference among the other treatments, except for the control, and the lowest values of growth of the plagiotropic branches was observed.

Table 3. Mean lengths (cm) of the plagiotropic branches in each treatment with the different skeletonization management approaches

Treatment	Skeletonization	
	Side	Between plants
T1	32.96 CDb	20.34 Ba
T2	34.21 Eb	29.97 Ca
T3	32.40 BCb	20.66 Ba
T4	33.70 DEb	29.92 Ca
T5	31.85 Bb	20.97 Ba
T6	34.17 Eb	29.77 Ca
T7	31.57 Bb	19.97 Ba
T8	34.28 Eb	29.63 Ca
T9	19.53 Ab	15.12 Aa

Means followed by the same uppercase letter within a column and the same lowercase letter within a row are not significantly different according to Tukey's test at the 5% probability level ($P \leq 0.05$). Uppercase letters compare treatments within each column, whereas lowercase letters compare skeletonization positions within each row.

When comparing lateral shoot growth between rows, for all the treatments, there was greater growth of the branches in the lateral direction, which differed significantly from growth between plants.

When analysing the average lengths (cm) of the plagiotropic branches throughout the evaluation period (Table 4), it was observed that there was an increase in the average branch length and that this increase was significant for all evaluations. It is noteworthy that the greatest variations occurred between 3 and 6 months (8.6 and 8.2 cm for lateral skeletonization and between plants, respectively) and between 12 and 15 months (9.7 and 6.9 cm for lateral skeletonization and between plants, respectively).

Table 4. Mean lengths (cm) of plagiotropic branches throughout the evaluation period in the different skeletonization management treatments

Evaluation	Skeletonization	
	Lateral	Between plants
3 months	18.71 Ab	12.62 Aa
6 months	27.33 Bb	20.87 Ba
9 months	31.55 Cb	24.59 Ca
12 months	35.38 Db	27.59 Da
15 months	45.17 Eb	34.53 Ea

Means followed by the same letter (capital letters in columns and lowercase letters in the rows), did not differ from each other according to Tukey's test at the 5% probability level ($P \leq 0.05$).

When comparing the shoot growth in the lateral skeletonized branches between plants throughout the evaluation period, for all evaluations, there was greater growth of the branches in the lateral direction, which differed significantly from that between plants.

When evaluating the average lengths (cm) of the lateral plagiotropic branches across the different treatments (Table 5), a relatively small growth variation was observed in the control (T9), corresponding to 11.6 cm, which differed significantly from that in the other treatments at all evaluations, except for the 3-month evaluation. In this evaluation, none of the treatments showed a significant difference in branch growth due to weather conditions (low rainfall) and because it was within the initial recovery phase after the branches were cut.

Among the other treatments, the largest increase in the growth of plagiotropic branches was observed in treatments T6 and T8. Based on the data obtained, the importance of lateral skeletonization of coffee plants to support higher productivity among the plagiotropic branches is evident. This practice allows the development of new more productive floral buds. It is important to note the significant difference in the average lengths of the branches between plants that underwent skeletonization and the control plants that did not undergo skeletonization.

Table 5. Average lengths (cm) of lateral plagiotropic branches throughout the evaluation period in the different treatments

Treatment	Evaluation period (months)				
	3	6	9	12	15
T1	19.56 Aa	28.21 ABb	32.61 Bbc	36.75 Bc	45.75 BCd
T2	18.59 Aa	29.92 Bb	35.44 Bbc	39.00 Bc	50.25 BCd
T3	20.14 Aa	29.61 Bb	34.22 Bbc	37.41 Bc	46.41 BCd
T4	19.77 Aa	27.96 ABb	31.50 ABbc	36.66 Bc	46.91 BCd
T5	19.13 Aa	29.07 ABb	33.16 Bbc	36.83 Bc	45.41 BCd
T6	17.18 Aa	28.92 ABb	34.88 Bbc	40.50 Bc	51.83 Cd
T7	20.47 Aa	27.23 ABb	31.11 ABbc	33.66 Bc	42.00 Bd
T8	17.22 Aa	23.71 Ab	29.50 ABbc	39.75 Bc	51.08 Cd
T9	16.95 Aa	23.50 Ab	24.66 Ab	23.00 Aab	28.58 Ab

Means followed by the same letter (capital letters in the columns and lowercase letters in the rows) did not differ from each other according to Tukey's test at the 5% probability level ($P \leq 0.05$).

When evaluating the average lengths (cm) of plagiotropic branches growing between plants in different treatments (Table 6), a relatively small growth variation was observed in the control (T9), corresponding to 14.0 cm, differing significantly from the other treatments in all the evaluations. Among the other treatments, the largest increase in the growth of the plagiotropic branches was observed for treatments T2, T4, T6 and T8, with values that differed significantly from those for the other treatments. Based on the data obtained, the importance of skeletonization both laterally and between coffee plants is evident, as this approach ensures the renewal of all plagiotropic branches, allowing more productive branches and more productive new floral buds.

There was higher growth of the plagiotropic branches in all the treatments in which thinning between plants was applied than in the other treatments. In addition, the results obtained in the control (T9) indicate that the thinning of only the branches located between the rows somehow stimulated the growth of the plagiotropic branches located between plants.

Table 6. Average lengths (cm) of plagiotropic branches growing between plants throughout the evaluation period in the different treatments

Treatment	Evaluation period (months)				
	3	6	9	12	15
T1	8.02 Aa	17.00 Bb	20.85 Bc	24.00 Bd	31.85 Be
T2	18.68 Ba	26.54 Cb	30.29 Cc	33.62 Cd	40.73 Ce
T3	7.70 Aa	18.04 Bb	21.45 Bc	24.66 Bd	31.45 Be
T4	18.12 Ba	26.29 Cb	30.27 Cc	33.60 Cd	41.33 Ce
T5	8.56 Aa	17.77 Bb	21.72 Bc	24.85 Bd	31.93 Be
T6	18.33 Ba	26.35 Cb	30.35 Cc	33.29 Cd	40.54 Ce
T7	8.16 Aa	17.16 Bb	20.64 Bc	23.75 Bd	30.12 Be
T8	18.27 Ba	26.08 Cb	29.95 Cc	32.85 Cd	41.02 Ce
T9	7.72 Aa	12.62 Ab	15.77 Ac	17.68 Ad	21.81 Ae

Means followed by the same letter (capital letters in the columns and lowercase letters in the rows) did not differ from each other according to Tukey's test at the 5% probability level ($P \leq 0.05$).

Productivity in the different treatments

Assessment of the average productivity (sacks ha^{-1}) of processed coffee in each treatment (Fig. 5) revealed that the treatments in which there was total skeletonization (lateral and between plants, here called T2, T4, T8 and T6) were 30.56%, 20.83%, 19.27% and 8.71% more productive than the control (T9), respectively. These treatments were 20.25%, 11.28%, 9.85% and 0.12% more productive than the treatment with the best performance among those in which only lateral skeletonization was applied. Therefore, total skeletonization, despite requiring more time and having a higher cost, demonstrates great agronomic viability in terms of renewing the vegetative and reproductive vigour of the crop.

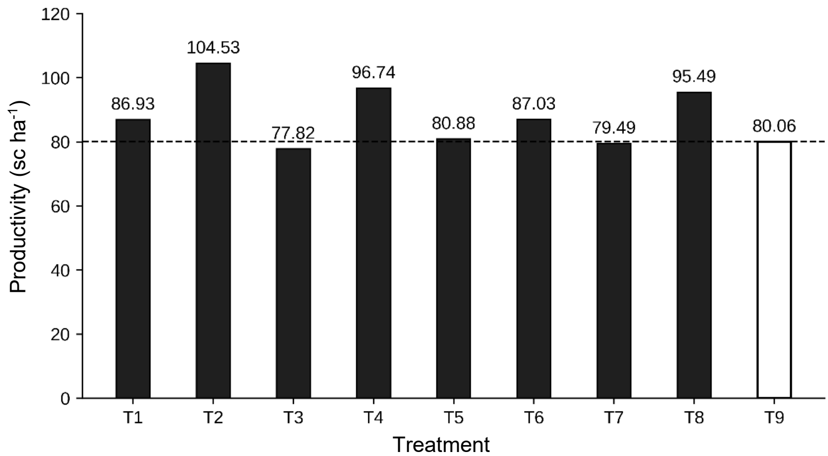

Figure 5. Average productivity of processed coffee (60 kg sacks ha^{-1}) in each treatment, calculated from dry coffee in husk at commercial moisture content using an approximate 2.6:1 conversion from coffee in husk to processed coffee.

Evaluating the vegetative and reproductive recovery capacity of different commercial Arabica coffee cultivars after skeleton pruning in a four-and-a-half-year-old plantation, Silva et al. (2016) observed good recovery capacity following pruning at a young stage, with emphasis on the cultivars Catiguá MG3, Topázio MG1190, and Sabiá 398, which proved to be the most productive and vigorous, presenting a low percentage of empty beans and a high percentage of large-sized beans in the first biennium after pruning.

Additionally, Carvalho et al. (2013), in a study aimed at selecting resistant progenies from the cross between the cultivars Catuaí Amarelo IAC 2077 and Mundo Novo IAC 515-20, verified low percentages of empty and peaberry beans in all evaluated coffee plants, with a high proportion of beans retained on sieve 16 and above. Furthermore, the studied genotypes showed a satisfactory response to pruning.

In contrast, studies demonstrate the complexity of pruning management and the need to adapt pruning practices to different field conditions. Evaluating the 'Zero Yield' system in Arabica coffee plantations, Japiassú et al. (2010) concluded that the use of different pruning cycles did not result in yield gains compared to the unpruned control. Likewise, Reis et al. (2018) reported that the cultivar Catucaí Vermelho 785/15 was not responsive to skeleton pruning, as it exhibited lower productivity, high incidence of coffee leaf rust, and reduced vegetative growth. According to the authors, however, the cultivars Catucaí Amarelo 20/15 cv. 479, Araponga MG1, and Tupi IAC 1669-33 were highly responsive to pruning, showing high productivity associated with high photosynthetic rates.

It is worth noting that, as with Arabica coffee, pruning can also be applied to *Coffea canephora* with the aim of increasing productivity. According to Verdin Filho et al. (2014), seeking to improve existing management recommendations for Conilon coffee cultivation, they concluded that reduced plant spacing combined with an increased number of orthotropic stems per plant has a positive effect on Conilon coffee yield.

The results obtained in the present study are corroborated by Rahman et al. (2024), who, in a study evaluating different pruning methods in *Coffea canephora* plants aimed at controlling plant size and assessing their effects on productivity and quality, reported productivity increases ranging from 34.8% to 49.7%, demonstrating that pruning is an efficient practice to enhance the productive potential of coffee plantations, especially older ones. This pattern is consistent with recent studies showing that pruning can improve vegetative recovery, source-sink balance, branching, and subsequent productive performance, although the magnitude of the response depends on cultivar, pruning intensity, and local growing conditions. This response may be explained by the fact that, after pruning, part of the foliage remains active, allowing the interception of photosynthetically active radiation and the production of photoassimilates required for vegetative recovery and branch renewal. In addition, skeleton pruning may improve source–sink relationships, stimulate branching and leaf development, and modify canopy microclimate, thereby favoring subsequent productive performance.

Production costs, revenue and profit from the applied management practices

Considering the costs involved in each treatment (Fig. 6) and taking into account that in each treatment, there was a different pruning management approach that resulted in a different production cost and yield, the main indicator was the difference in profit (in USD \$ ha^{-1}) compared to that for the control treatment (T9). Treatments T7, T5 and

T6 presented the lowest production costs. When net profitability (gross revenue - production cost) was compared, treatments T2, T8, T4 and T6 showed the highest values. Analysis of the difference in profit (net profitability of the treatment - net profitability of the control) among treatments showed that T2, T4 and T8 had the best results, resulting in an increase in profit of US $ 6,222.71, US $ 4,063.26 and US $ 4,011.17 per hectare, respectively. All the treatments that involved the skeletonization of all the plagiotropic branches resulted in a significant increase in profit compared to the control treatment.

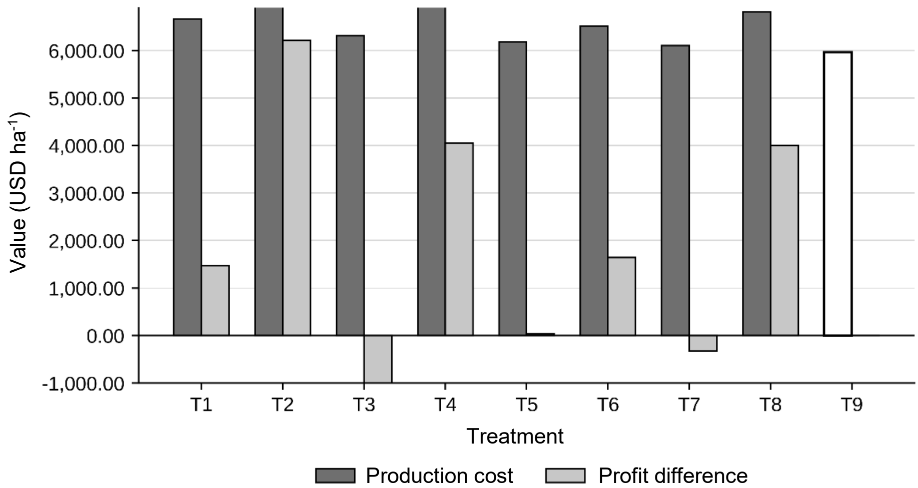

Figure 6. Production cost, net profitability, and profit difference in relation to the control treatment (T9) for each evaluated management approach (USD ha^{-1}).

The results obtained in this study indicate that the use of strategies aimed at management during cultivation and application of appropriate pruning techniques in coffee crops can result in significantly increasing the productivity and profitability of the crop. Similar results were observed in studies by (Viteri Salazar et al., 2018; Dufour et al., 2019). Unlike the observations of (Reis et al., 2018; Dufour et al., 2019), the Catuaí Vermelho IAC 144 variety used in this study responded positively to thinning and pruning management, resulting in gains in productivity and increased profitability.

The thinning and pruning methods used in this study were technically and economically feasible in addition to having great benefits for coffee plants, especially total plant skeletonization. In addition, the modified pruning methods facilitated the vertical growth of coffee plants and thus provided a large margin for the high-density planting system without compromising yield.

Therefore, modified pruning methods may be an option to improve productivity relative to labour in coffee production as well as to facilitate the application of fertilizers, corrective amendments and crop protection products. In addition, the material resulting from skeletonization and pruning can be used to improve soil parameters, as observed by (Musa et al., 2020).

According to (Parreiras Pereira et al., 2007) and (Musa et al., 2020), the best time to prune coffee trees is soon after harvest. Additionally, according to these authors, a reduction in spacing both between rows and between plants in a row increased crop productivity in the first harvest after pruning. It is important to note that higher plant density per area can result in greater shading, especially in the middle and lower thirds of the coffee plants, which can affect both crop quality and productivity, as discussed by Sarmiento-Soler et al. (2020) and Somarriba & Quesada, 2022.

It is also noteworthy that the increase in income due to management practices improves the sustainability of crops and increases market gain, as reported by (Campos et al., 2021) and (Turreira-García, 2022). In this study, it was evident that although there was a higher cost associated with total skeletonization, reflected in the production cost of the crop, this management approach resulted in a much higher profitability compared to treatments in which there was no pruning or only lateral skeletonization, which was performed with tractor-mounted machines.

From a technical-economic perspective, treatments T2 and T8 represented the most advantageous strategies, whereas T3 was not economically justified under the evaluated conditions because its additional management cost was not compensated by gains in productivity or net return. These profitability outcomes should be interpreted in light of the local production conditions and the assumptions adopted in the present study, since formal risk assessment and price-variability analyses were beyond its scope.

Taken together, these results highlight the novelty of the study by showing that the evaluation of skeleton pruning strategies becomes more informative when agronomic performance is interpreted jointly with operational cost and profitability.

CONCLUSIONS

The laterally skeletonized plagiotropic branches developed faster than the skeletonized plagiotropic branches between coffee plants, indicating a stronger vegetative response in the lateral direction during the evaluation period. At the same time, the results showed that skeletonizing only the branches located between rows stimulated the growth of plagiotropic branches between plants, suggesting that partial pruning can also influence branch renewal beyond the directly managed portion of the canopy.

Among the evaluated treatments, total plant skeletonization consistently promoted greater branch development and higher productivity than the treatments based only on lateral skeletonization or the control without skeletonization. This demonstrates that more intensive pruning management can be effective in renewing the vegetative and reproductive vigor of older coffee plantations.

From an economic perspective, although total skeletonization resulted in higher production costs, this additional investment was offset by superior productivity and greater net return. In particular, the treatment combining total plant skeletonization with sprouting control showed the best economic performance, surpassing the treatment without skeletonization and reaching an increase in profitability of up to USD 6,000.00 per hectare. Overall, the results indicate that total skeletonization, especially when associated with adequate sprout management, is both agronomically and economically advantageous under the conditions of this study.

Overall, the results indicate that total skeletonization, especially when associated with adequate sprout management, is both agronomically and economically advantageous under the conditions of this study. In practical terms, this management approach provided the best balance between productivity gains and economic return, making it the most promising strategy among the treatments evaluated.

Data availability: The datasets, analysis notebooks, figures, and tables supporting this study are stored in the GitHub repository https://github.com/andrebelem/coffee-pruning-economics. The repository is currently private for peer-review purposes and will be made publicly available upon acceptance of the manuscript.

REFERENCES

Augusto, A., Custódio, D.P., Lemos, L.B., Luiz, F., Mingotte, C., Pagan, T., Carlos, A., Carmeis de Almeida, A., Barbosa, J.C. & Pierre, C. 2013. Coffee productive and vegetative traits characteristics under different deletions of irrigation and side exposure to sun. *Coffee Science* **8**(4), 411–422.

Banzatto, D.A. & Kronka, S.D. Agricultural Experimentation. 4th ed. Jaboticabal, SP: Funep, 2013 (in Portuguese).

Borém, F.M., Coradi, P.C., Saath, R. & Oliveira, J.A. 2008. Quality of natural and washed coffee after drying on ground and with high temperature. *Ciênc. Agrotecnol.* **32**(5), 1609–1615. doi: 10.1590/S1413-70542008000500038 (in Portuguese).

Campos, A.D.S.N., Satolo, E.G., Mac-Lean, P.A.B. & Júnior, S.S.B. 2021. Economic sustainability analysis of the specialty coffee farmers in Garça/SP. *Coffee Science* 16. doi: 10.25186/.V16I.1993

Carvalho, G.R., Botelho, C.E., Rezende, J.C., Ferreira, A.D., Luz, R. & Pedro, F.C. 2013. Performance of F4 arabic coffee progenies before and after framework pruning. *Coffee Science* **8**(1), 33–42.

Cerda, R., Allinne, C., Gary, C., Tixier, P., Harvey, C., Krolczyk, L., Mathiot, C., Clément, E., Aubertot, J.-N. & Avelino, J. 2017. Effects of shade, altitude and management on multiple ecosystem services in coffee agroecosystems. *Eur. J. Agron.* **82**, 308–319.

Cunha, J.P.B., Silva, F.M., Dias, R.E.B., Lisboa, C.F. & Machado, T.A. 2016. conomic viability for different coffee harvest systems. *Coffee Science* **11**, 416–425 (in Portuguese).

Dufour, B.P., Kerana, I.W. & Ribeyre, F. 2019. Effect of coffee tree pruning on berry production and coffee berry borer infestation in the Toba Highlands (North Sumatra). *Crop Prot.* **122**, 151–158. doi: 10.1016/j.cropro.2019.05.003

Ferreira, D.F. 2019. SISVAR: a computer analysis system to fixed effects split plot type designs. *Rev. Bras. Biometria* **37**(4), 529–535. doi: 10.28951/rbb.v37i4.450

Filho, A.C.V., Tomaz, M.A., Ferrão, R.G., Ferrão, M.A.G., da Fonseca, A.F.A. & Rodrigues, W.N. 2014. Conilon coffee yield using the programmed pruning cycle and different cultivation densities. *Coffee Science* **9**(4), 489–494 (in Portuguese).

Filho, V., Carlos, A., Volpi, P.S., Amélia, M., Ferrão, G., Ferrão, R.G., Mauri, A.L., Almeida da Fonseca, F., Tristão, F.A., de Saul, S. & Júnior, A. 2016. New management technology for arabica coffee: the cyclic pruning program for Arabica coffee. *Coffee Science* **11**(4), 475–483.

Gonçalves, M.A., Cocco, C., Vignolo, G.K., Picolotto, L. & Corrêa Antunes, L.E. 2014. The effect of pruning intensity in the production and quality of peach fruits. *Rev. Bras. Frutic.* **36**(3), 742–747. doi: 10.1590/0100-2945-225/13 (in Portuguese).

Japiassú, L.B., Garcia, A.L.A., Guimarães, R.J., Padilha, L. & Carvalho, C.H.S. 2010. Pruning cycles and nitrogen fertilization of coffee fields conducted in the 'safra zero' system. *Coffee Science* **5**(1), 28–37 (in Portuguese).

Karim, A., Hifnalisa & Manfarizah. 2021. Analysis of arabica coffee productivity due to shading, pruning, and coffee pulp-husk organic fertilizers treatments. *Coffee Science* **16**, e161903. doi: 10.25186/.v16i.1903

Koeppen, W. 1948. Climatology: with a study of the Earth's climates. Fondo de Cultura Econômica, México, 479 pp. (in Spanish).

Musa, Y., Bahrun, A.H. & Rini, A. 2020. Farmers understanding and practices on shading and pruning for Arabica coffee: a survey and analysis on the effects to the yields. IOP Conf. Ser.: *Earth Environ. Sci*. **575**, 012158. doi: 10.1088/1755-1315/575/1/012158

Nascimento, L.M. do, Spehar, C.R. & Sandri, D. 2014. Produtivity of organic coffee orchard in the brazilian savannah after prunning and grown under different water regimes. *Coffee Science* **9**(3), 354–365 (in Portuguese).

Parreiras Pereira, S., Guimarães, R.J., Ferreira Bartholó, G., Tácito, P., Guimarães, G. & Alves, J.D. 2007. Vegetative growth and yield of coffee plants (Coffea arabica L.) in two different pruning times, conducted at different spacings. *Ciênc. Agrotecnol*. **31**(3), 643–649.

Pereira, A.A., de Morais, A.R., Scalco, M.S. & Fernandes, T.J. 2016. Modeling of the diameter of the canopy pruned coffee tree cultivated in different densities and water regimes. *Coffee Science* **11**(4), 495–501 (in Portuguese).

Pereira, S.P., Baliza, D.P. & Santos, M.O. 2013. Influence of cultivation spacing and two pruning times on stem carbohydrate levels in coffee. *Coffee Science* **8**(4), 460–468.

Rahman, G., Malek, A.A., Houssain, A. & Islam, S. 2024. Effect of pruning on growth, yield and quality of coffee. *East Afr. Sch. J. Agric. Life Sci*. **7**(2), 26–30. doi: 10.36349/easjals.2024.v07i02.002

Reis, E.A.C., Freitas, T., Carvalho, M.A.F., Mendes, A.N.G., Rezende, T.T. & Carvalho, J.P.F. 2018. Characterization of coffee cultivars leaf rust-resistant subjected to framework pruning. *Coffee Science* **13**(1), 63–70.

Rhiney, K., Guido, Z., Knudson, C., Avelino, J., Bacon, C.M., Leclerc, G., Aime, C. & Bebber, D.P. 2021. Epidemics and the future of coffee production. *Proc. Natl. Acad. Sci*. **118**, e2023212118. doi: 10.1073/pnas.2023212118

Sarmiento-Soler, A., Vaast, P., Hoffmann, M.P., Jassogne, L., van Asten, P., Graefe, S. & Rötter, R.P. 2020. Effect of cropping system, shade cover and altitudinal gradient on coffee yield components at Mt. Elgon, Uganda. *Agric. Ecosyst. Environ*. **295**, 106887. doi: 10.1016/j.agee.2020.106887

Silva, V.A., de Rezende, J.C., de Carvalho, A.M., Carvalho, G.R., Rezende, T.T. & Ferreira, A.D. 2016. Recovery of coffee cultivars under the 'skeleton cut' pruning after 4.5 years of age. *Coffee Science* **11**(1), 55–64.

Somarriba, E. & Quesada, F. 2022. Modeling age and yield dynamics in Coffea arabica pruning systems. *Agric. Syst*. **201**, 103450. doi: 10.1016/j.agsy.2022.103450

Souza, V.H.S., Carvalho, A.M., Teramoto, É.T., Silva, M.C.S. & Guimarães, R.J. 2024. Yield after intensive pruning of fertigated coffee plants subjected to different macronutrient rates. *Semina: Ciênc. Agrár*. **45**(1), 23–36.

Thomaziello, R.A. & Pereira, S.P. 2008. Pruning and training of Arabica coffee plants. Instituto Agronômico, Campinas, 39 pp. (Série Tecnologia APTA, Boletim Técnico IAC, 203). (in Portuguese).

Turreira-García, N. 2022. Farmers' perceptions and adoption of Coffea arabica F1 hybrids in Central America. *World Dev. Sustain*. 1, 100007. doi: 10.1016/j.wds.2022.100007

Utrilla-Catalan, R., Rodríguez-Rivero, R., Narvaez, V., Díaz-Barcos, V., Blanco, M. & Galeano, J. 2022. Growing inequality in the coffee global value chain: a complex network assessment. *Sustainability* **14**, 672. doi: 10.3390/su14020672

Viteri Salazar, O., Ramos-Martín, J. & Lomas, P.L. 2018. Livelihood sustainability assessment of coffee and cocoa producers in the Amazon region of Ecuador using household types. *J. Rural Stud*. **62**, 1–9. doi: 10.1016/j.jrurstud.2018.06.004

Agronomy Research **24**(S1), 207–224, 2026
https://doi.org/10.15159/AR.26.039

Experimental evaluation of a modified bentleg plough: improving soil structure and water infiltration under South Mediterranean pedo-climatic conditions

K. Laiche[1], I. Guedioura[1], M. Babaousmail[2,*], M. Messaoudi[2], A. Khechkhouch[3] and M. Amara[†,1]

[1]Research laboratory for conservation, management and improvement of forest ecosystems, National higher school of agronomy, ENSA, El Harrach, 16200 Algiers, Algeria
[2]BABDA Laboratory, University of El Oued, Faculty of Nature and life sciences, Department of Agronomy, 39000, El Oued, Algeria
[3]NTD Laboratory, University of El Oued, El Oued 39000, Algeria
[*]Correspondence: mahfoud-babaousmail@univ-eloued.dz

Received: January 13th, 2026; Accepted: May 15th, 2026; Published: May 28th, 2026

Abstract. This study evaluates a mechanically modified Bent leg plough (experimental tool, ET) for deep soil decompaction under low tractor power conditions typical of South Mediterranean cereal systems. The tool integrates a curved blade with a negative rake angle to enhance subsoil loosening while preserving soil horizon integrity and minimizing draft resistance.

A field experiment using a randomized complete block design compared four tillage systems: conventional (CT), minimum (MT), no tillage (NT), and ET. Soil physical properties (penetration resistance and water infiltration) and durum wheat yield were assessed. A second trial related forward speed to specific fuel consumption to derive a Relative Traction Index (RTI), enabling comparison of traction demand and energy efficiency with a mouldboard plough.

Results showed that ET significantly improved infiltration and reduced soil compaction compared to CT, MT, and NT. Mean infiltration rates under ET were 63% higher than CT, 115% higher than MT, and 165% higher than NT ($p < 0.05$). Additionally, penetration resistance was reduced by up to 72% relative to NT, indicating enhanced porosity and structural stability across all soil profiles. Although CT achieved the highest yield (22.5 Qt ha^{-1}), ET produced comparable productivity (18.7 Qt ha^{-1}) with greater soil conservation and lower energy demand. Regression and ANOVA analyses confirmed that ET maintained stable soil conditions over time, unlike CT and MT, which showed rapid reconsolidation.

In term of energy performance, The ET maintained lower fuel consumption (12.6–17.4 L ha^{-1}) at significantly higher speeds than the conventional plough, which required up to 26.7 L ha^{-1}. A Relative Traction Index (RTI) analysis revealed th.

Overall, the modified Bent leg plough enables effective deep loosening with reduced compaction and traction requirements, while maintaining competitive yield under rainfed South Mediterranean conditions.

Key words: bentleg plough, conservation tillage, durum wheat, South Mediterranean region, infiltration, soil compaction, subsoiling.

INTRODUCTION

Modern agriculture faces an existential challenge: feeding a growing global population while managing the accelerating impacts of the climate crisis. In vulnerable regions like the Mediterranean basin, characterized by high rainfall variability and vulnerability to soil erosion (Zdruli et al., 2010; García-Ruiz et al., 2013; Sardans & Peñuelas, 2013). The focus is shifting from land quantity to the soil's ability to manage water and resist structural degradation. Maintaining the physical health of arable land is the primary line of defense against desertification and crop failure. Therefore, innovation in cultural practices and sustainable agricultural mechanization is imperative to ensure the resilience of local cereal systems against the combined threats of drought and compaction.

In response to these challenges, conservation tillage practices (NT, MT) have been widely adopted. However, scientific literature shows that these practices often lead to persistent subsurface compaction (tillage pan), evidenced by increased Penetrometer Resistance (PR) and Bulk Density (BD) in deeper horizons. For instance, long-term no-tillage systems have been found to increase BD in the 5–20 cm layer, leading to a narrower Least Limiting Water Range (LLWR) (Stošić et al., 2020). Furthermore, studies indicate that natural recovery processes struggle to restore the structural integrity of deep soil layers (10–60 cm), even over extended periods, justifying the need for targeted mechanical intervention (Naskar et al., 2025). The hydrological impact of this deep compaction is critical, especially given the intensifying threat of droughts (Shao et al., 2018), as compaction severely alters the pore structure. In this context, the creation of macropores is essential for regulating water retention and mitigating the effects of crucial drying-wetting cycles prevalent in arid climates (Xiao et al., 2022).

To understand these dynamics, a parallel body of research investigates soil-water behaviour at the micro- and pore scales. Pore-scale simulations and imaging studies have demonstrated that pore size distribution and connectivity directly control the hysteresis of water retention curves (Liu et al., 2024; Liu et al., 2025; Zhou et al., 2025). These findings establish that improved water retention is intrinsically linked to enhanced mechanical resistance to compression, highlighting the need to consider soil moisture conditions during tillage (Guedioura et al., 2023; Tan et al., 2025). On the other hand, considerable efforts are directed towards developing materials to enhance unsaturated hydraulic conductivity and water retention. Such findings emphasize that sustainable tillage should aim not only to loosen compacted horizons but also to preserve pore continuity, balance aeration and water storage, and limit structural collapse.

This study experimentally evaluates a newly developed mechanically modified Bentleg plough designed for sustainable tillage under South Mediterranean conditions. The tool features an inclined-share geometry with a negative rake angle, enabling deep soil decompaction while operating efficiently with low-power tractors. Unlike conventional subsoilers, it aims to achieve significant loosening without soil inversion, preserving horizon integrity and reducing draft resistance. The research specifically investigates whether this modified design can improve soil penetration resistance, water infiltration, and crop yield compared to conventional, minimum, and no-tillage systems in South Mediterranean calcareous soils.

MATERIALS AND METHODS

Description of the innovated tool

The developed prototype is a tillage tool inspired by the bentleg plough and specifically adapted to South Mediterranean pedo-climatic conditions. It is designed to achieve effective soil decompaction down to 40 cm without inverting the soil layers, thereby preserving the vertical organization and pedological stratification of the soil profile. To meet these objectives, several design modifications were introduced.

The blade geometry was optimized to minimize draft resistance. The rake angle (α), which is negative compared to that of a conventional bentleg plough (Fig. 1), significantly reduces power requirements while maintaining effective soil fragmentation. This configuration enables the blade to initiate cutting at the surface, where compaction is lowest, and to progressively lift and fracture the soil along the curved cutting line of the blade (Fig. 1). This gradual action reduces draft force and allows higher operating speeds.

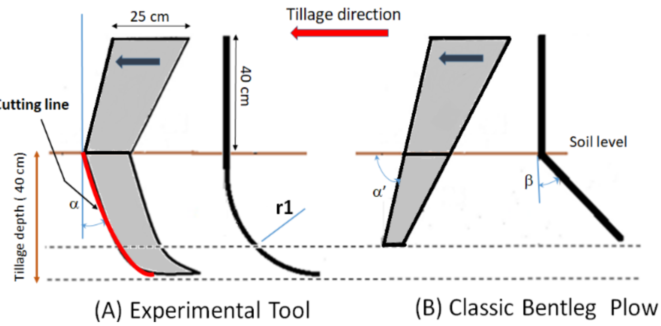

Figure 1. Comparison of blade geometry between (A) the experimental bentleg plough (ET) and (B) the conventional bentleg plough. α and α′ represent the rake angles of the experimental and conventional tools, respectively, while r_1 denotes the curvature radius of the bentleg. The negative rake angle of the ET is designed to reduce draft force while enhancing deep soil loosening without inversion.

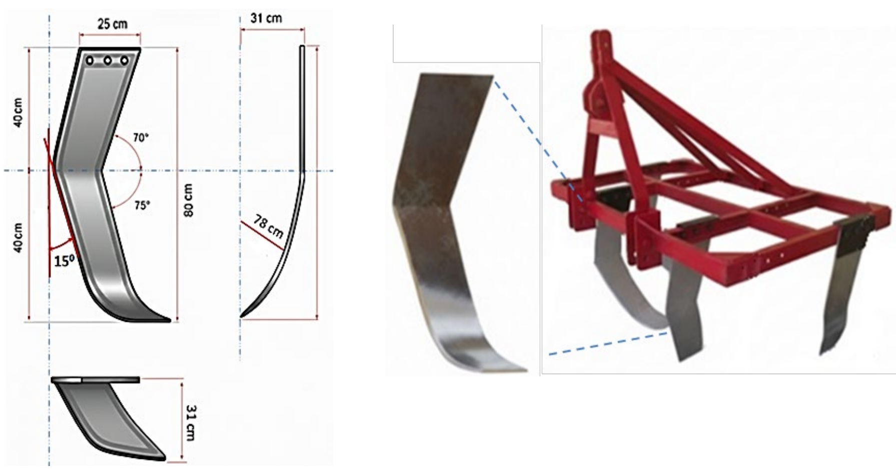

Figure 2. Prototype of the mechanically modified bentleg plough featuring four elements and an adjustable working width of up to 2.1 m.

The prototype features an adjustable working width of of 1.2 m using two elements - 2.1 m using four elements (Fig. 2), an optimal operating speed of 8–12 km h^{-1}, and compatibility with tractors rated between 50 and 80 horsepower.

Thus, the developed tool retains the agronomic advantages of the bentleg plough (alleviating compaction, maintaining natural soil organization, and enhancing both water infiltration and retention) while substantially reducing power demand.

The Fig. 2 shows the full-scale modified bentleg plough equipped with an inclined-share blade and a negative rake angle. The design allows deep soil decompaction while maintaining structural stability and compatibility with low-power tractors. The prototype was fabricated and tested under South Mediterranean field conditions.

Experimental site and design

Experimental site the experiment was conducted at the station of the Technical Institute of Field Crops (ITGC) in Oued Smar (36° 34' N, 3° 48' E, 24 m Alt) (Fig. 3). The site is located 24 meters above sea level, between the 600 mm and 700 mm isohyets.

The experiment was carried out from mid-November to July. The I.T.G.C. station is located in the sub-humid bioclimatic zone characterized by mild, rainy winters and hot, dry summers. During the study period (2020), the mean annual temperature was 21.6∘C, and the average annual precipitation was 30.8 mm (Fig. 4).

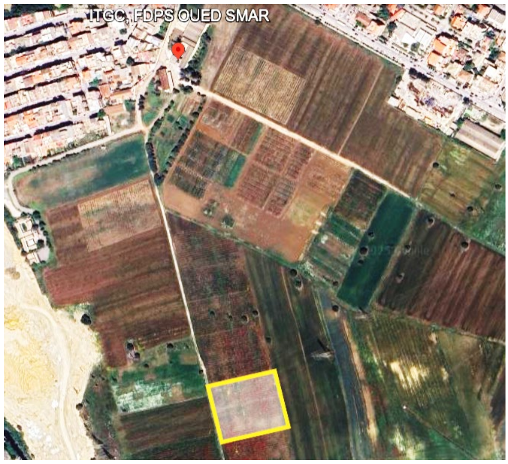

Figure 3. Geographic location of the experimental site at the Technical Institute of Field Crops (ITGC), Oued Smar, Algeria (Google Earth, 2024).

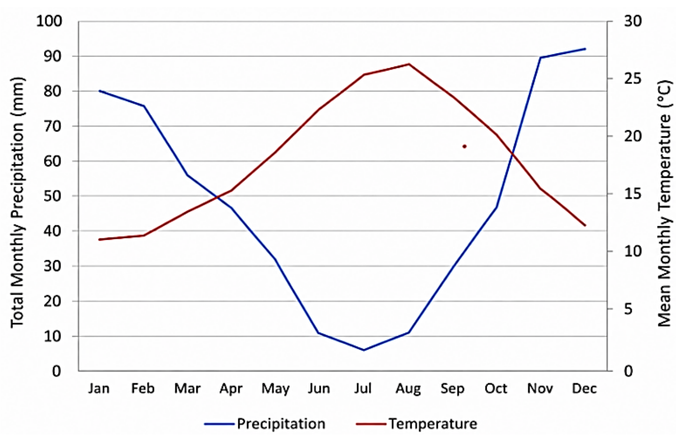

Figure 4. Annual umbrothermal diagram of 2020 at the experimental site, illustrating monthly precipitation and temperature patterns.

Experimental Design The experimental plot was divided into four blocks using a Randomized Complete Block (RCB) design, consisting of four repetitions of four distinct tillage practices (cultural treatments) (Fig. 5).

The experimental design covers a total area of 6,720 m² (96 m × 70 m) and is arranged as a randomized complete block design with four blocks. Each block, with an area of 1,680 m² (24 m × 70 m), is subdivided into four elementary plots corresponding to the treatments (CT, MT, NT, ET). Each plot measures 6 m × 70 m, giving a unit area of 420 m². This design allows comparison of soil management systems while controlling spatial heterogeneity of the experimental site (Fig. 5). The characteristics of the different tillage treatments, including implements used, working depth, and number of operations before sowing, are presented in Table 2 (Conventional tillage CT, Minimum tillage MT, No till NT and experimental tool ET). The used tractor develops a power of 80 hp. ‘

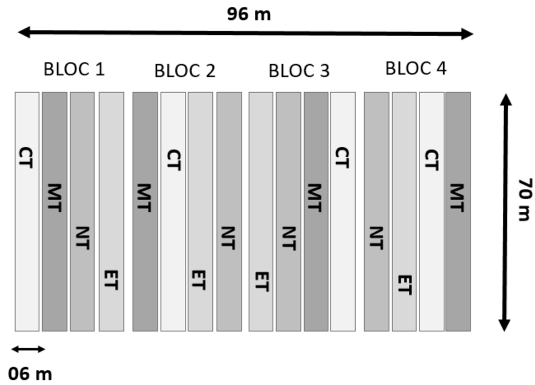

Figure 5. Layout of the experimental field arranged in a randomised complete block design (RCBD). CT: conventional tillage; MT: minimum tillage; NT: no-tillage; ET: experimental tool tillage.

The main characteristics of the experimental site, climatic conditions, soil properties, and experimental design are summarized in Table 1.

Table 1. Main characteristics of the experimental site and field design

Parameter	Description / Value
Location	Technical Institute of Field Crops (ITGC), Oued Smar, Algeria
Geographic coordinates	36°34′ N, 3°48′ E
Altitude	24 m a.s.l.
Bioclimatic zone	Sub-humid, mild rainy winters and hot dry summers
Mean annual temperature (2020)	21.6 °C
Mean annual precipitation (2020)	30.8 mm
Experimental design	Randomized Complete Block Design (RCBD)
Replications	4
Tillage treatments	Conventional (CT), Minimum (MT), No-tillage (NT), Experimental tool (ET)
Experimental period	Mid-November to July
Physical soil characteristics	The soil texture is clay-loam with 46.51% clay; 25.30% silt and 26.79% sand.

Table 2. Description of tillage treatments, implements used, working depth, and number of operations prior to sowing

	Technique	Tools used	Working depth (cm)	Number of operations before sowing
CT	Conventional tillage	- Ploughshare -Spring cultivator -Harrow - Seeder	25	03
MT	Minimum tillage	-Spring cultivator - Seeder	15	01
NT	No Till	- Seeder	00	00
ET	Experimental tool tillage	-Experimental tool - Seeder	40	01

Agricultural management and measurements

The wheat variety used for the experiment belongs to the durum wheat species and is widely cultivated in the region and throughout Algeria. The selected variety was Simeto (pedigree: Capeiti/Valvona), originally developed in Italy. No fertilization programme was applied in order to clearly distinguish the effect of the tillage method and the experimental tool on crop development. The experiment was conducted under rainfed conditions, without supplemental irrigation, for two main reasons: (1) to align with common agricultural practices in the region, where wheat is primarily grown under rainfall, and (2) to better isolate and evaluate the expected effects of the experimental treatment. The parameters analyzed in this experiment were primarily related to the soil condition after the application of the different tillage techniques, with four replications for each measurement.

Measurements included soil penetration resistance, soil infiltration capacity, and crop yield. Soil penetration resistance was measured using a static penetrometer. The penetrometer is a geotechnical instrument used to determine cone resistance and the maximum allowable stress. Measurements were taken after the passage of the tillage tool to quantify the degree of soil crumbling (tillage quality) and evaluate the tool's effectiveness. Soil infiltration capacity was evaluated using a double-ring infiltrometer to characterize the soil's ability to transmit water under ponded, near-saturated conditions. Infiltration capacity was defined as the depth of water infiltrated per unit time, expressed as mm s^{-1}.

Measurements were performed in accordance with the NF EN ISO 22282-5 standard. The infiltrometer consisted of an inner ring with a diameter of 50 cm and an outer ring with a diameter of 70 cm, both inserted vertically into the soil to the same depth. Water was simultaneously applied to both rings in order to establish ponded conditions, while the outer ring was used to limit lateral flow and promote predominantly vertical infiltration beneath the inner ring.

The double-ring infiltrometer measurements were conducted using standard procedures with clearly defined conditions. In each plot, five measurement points were randomly selected to account for spatial variability. The inner and outer rings were inserted into the soil to a depth of 10 cm to minimize lateral water flow. Prior to the test, a pre-saturation phase was applied to stabilize infiltration, and the initial infiltration depth was standardized at 5 cm. Soil moisture content before measurements was recorded and averaged for each mesurment to ensure comparable initial conditions across plots.

Infiltration was determined by recording the time required for a known depth of ponded water in the inner ring to completely infiltrate into the soil. The infiltration rate was calculated as the ratio between the infiltrated water depth and the corresponding infiltration time. This procedure provides an estimate of field infiltration capacity under ponded conditions, which is strongly influenced by soil structure and macroporosity and is therefore particularly suitable for assessing the impact of different tillage techniques on soil hydraulic behavior.

Harvesting was carried out at the end of June using an experimental combine harvester. Yields were calculated by dividing the total production by the cultivated area for each mini-plot, according to the following equation:

$$Yield\ (Qt/\mathrm{h}) = \frac{Total\ Production\ (Qt)}{Cultivated\ Area\ (\mathrm{h})} \tag{1}$$

Assessment of traction power and energetic efficiency

To evaluate the traction power requirements and energetic efficiency of the experimental tool implement, a second series of experimental trials was conducted by correlating forward speed with specific fuel consumption. The trials were carried out using an 80 hp tractor, successively coupled with the experimental tool (two modified bentleg plough elements) and a two-corp mouldboard ploughs. Measurements were taken using a stopwatch, a graduated container, and a measuring ruler.

The experiment was conducted on homogeneous soil, with moisture close to the friable state. Tractor settings were kept constant (≈ 1,800 rpm). Working depths were set at 40 cm (experimental tool) and 25 cm (mouldboard plough).

The trials were performed on 50 m strips, with three replications. Target speeds were 8, 10, and 12 km h^{-1} for the experimental tool, and 3, 4, and 5 km h^{-1} for the plough. The measured variables included travel time, working depth, fuel consumption, and qualitative observations.

The specific fuel consumption Cs (L ha^{-1}) was estimated as:

$$\mathrm{Cs} = \frac{f}{a} \times 10{,}000 \tag{2}$$

where f is the volume of fuel consumed (L), a is the the worked area (m^2).

The speed and consumption parameters were calculated to provide a synthetic indicator of field performance. A relative empirical traction index (RTI) was defined as:

$$\mathrm{RTI} = \frac{s}{\mathrm{Cs}} \tag{3}$$

where s is the forward speed and Cs is the specific fuel consumption.

This index is based on the assumption that fuel consumption serves as a proxy for the energy mobilized by the tractor–implement system, in the absence of direct measurement of draft force (Grisso et al., 2004). Furthermore, the relationship:

$$\mathrm{P} = \mathrm{Ft} \times \mathrm{V} \tag{4}$$

implies that, for a given power, an increase in speed associated with a decrease in fuel consumption indicates a reduction in the required draft force.

Thus, the ratio s/Cs links kinematic performance and energy demand, providing an indirect estimate of traction efficiency. Although empirical, this index allows for consistent relative comparison between implements under controlled experimental conditions.

Statistical analyses

For the agro-pedological effects, a comprehensive multiple regression analysis was carried out using dummy variables to explore the relationships between the dependent variables (infiltration and penetration resistance) within the framework of the Experimental Tool (ET) which was designated as the reference method in this analysis. The objective of this analysis was to quantify and compare the effects of the reference ET method with those of the alternative tillage systems: conventional tillage (CT), no-tillage (NT), and minimum tillage (MT). By applying dummy coding, the model effectively captured variations in performance indicators among the different tillage methods, providing a clearer understanding of their respective impacts on soil physical properties and overall agricultural performance.

A one-way analysis of variance (ANOVA) was conducted to evaluate the differences in average production quantities among various tillage methods. This statistical approach allows us to determine whether there are significant differences between the means of the different groups. Following the ANOVA, post-hoc tests were performed to further analyse the data and identify which specific tillage methods produced significantly different average yields. This rigorous comparison provides clear insight into the effectiveness of each tillage method in enhancing agricultural productivity. In regression and ANOVA analysis, validity tests like model residual normal distribution, residual homogeneity of variances, and linear multiple correlation between independent variables are used to ensure the model's efficiency.

The linear relationships describing soil physical behavior are specified as follows.

For Infiltration Rate (mm s^{-1}):

$$Y_{\text{inf}} = \beta_0 + \beta_{\text{time}} X + \sum(\beta_i D_i) + \sum(\beta_{\text{int},i} D_i X) + \varepsilon_1(02) \quad (5)$$

For Penetration Resistance (N):

$$Y_{\text{pen}} = \alpha_0 + \alpha_{\text{time}} X + \sum(\alpha_i D_i) + \sum(\alpha_{\text{int},i} D_i X) + \varepsilon_2(03) \quad (6)$$

Definition of Terms

- $\beta_0$and α_0 (Intercepts / Baseline levels) These parameters represent the estimated infiltration rate and penetration resistance, respectively, at month zero for the reference evapotranspiration (ET) method.
- $\beta_i$and α_i (Intercept differences) These coefficients quantify the initial deviation of the alternative management methods conventional tillage (CT), minimum tillage (MT), and no-tillage (NT) from the ET baseline.
    - For infiltration, a negative $\beta_i$indicates a lower initial infiltration rate relative to ET.
    - For penetration resistance, a positive $\alpha_i$indicates greater soil strength (i.e., increased compaction) relative to ET.
- $\beta_{\text{time}}$and α_{time} (Baseline temporal trends) These parameters describe the monthly rate of change in infiltration rate and penetration resistance, respectively, for the ET treatment.
- $\beta_{\text{int},i}$and $\alpha_{\text{int},i}$ (Interaction / slope differences) These interaction terms capture differences in temporal trends between the alternative methods and the ET baseline,

indicating whether each method exhibits a faster or slower rate of change over time relative to ET.

- X Time, measured in months.
- D_i Dummy variables identifying the alternative management methods (CT, MT, NT), with ET serving as the reference category.
- $\varepsilon_1$and ε_2 Random error terms associated with the infiltration and penetration resistance models, respectively.

RESULTS AND DISCUSSION

Soil physical responses to the mechanically modified bentleg plough (experimental tool, ET) were evaluated in comparison with conventional tillage (CT), minimum tillage (MT), and no-tillage (NT) using water infiltration rate and soil penetration resistance as key indicators. These variables are widely recognized as integrative measures of soil structural modification and physical quality, as they reflect the combined effects of soil loosening, pore continuity, aggregate stability, and reconsolidation processes over time.

Soil water infiltration

Infiltration performance was strongly influenced by the tillage method. Fig. 6 shows that mean infiltration rates were 0.252 mm s^{-1} for ET, 0.155 mm s^{-1} for CT, 0.117 mm s^{-1} for MT, and 0.095 mm s^{-1} for NT.

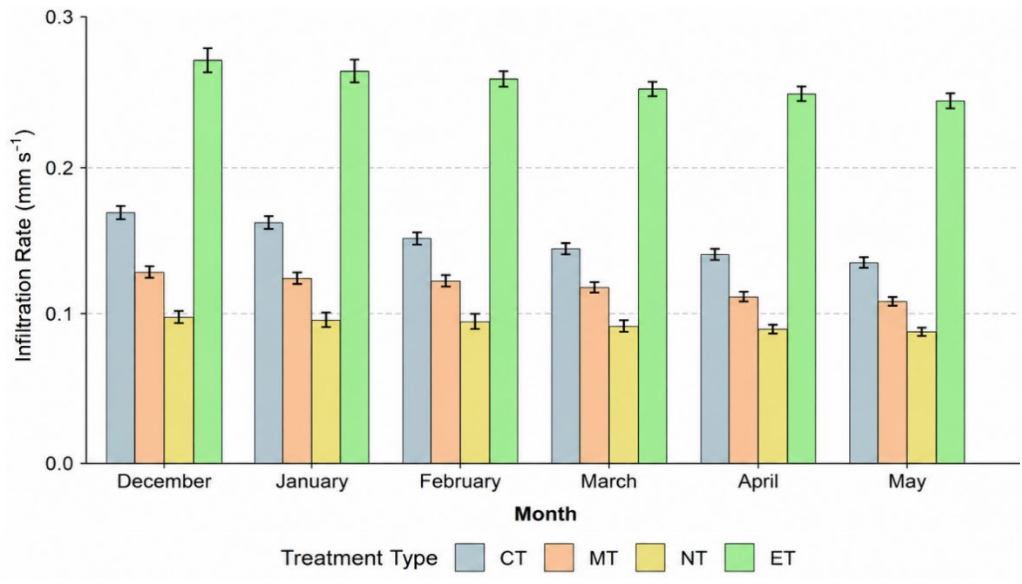

Figure 6. Temporal evolution of soil water infiltration rates over six months under different tillage treatments. Values represent mean infiltration rates measured using a double-ring infiltrometer.

These results confirm that the ET enhanced water infiltration by 63%, 115%, and 165% relative to CT, MT, and NT, respectively. Similar improvements in infiltration following deep, non-inverting tillage have been reported by several studies, which emphasise the restoration of macropore continuity and enhanced percolation through compacted layers (Peña-Sancho et al., 2017; Boincean & Dent, 2019; Wilkes, et al., 2021). The improved behaviour observed under ET can be attributed to its specific mechanical design: the negative attack angle directs shearing forces downward, fragmenting the subsoil and forming continuous vertical fissures while maintaining the natural stratification of the horizons. Such geometry differs from CT, where soil inversion destroys aggregates, disrupts pore continuity, and accelerates reconsolidation (Arriaga et al., 2017; Totsche et al., 2018).

Temporal monitoring over six months revealed that infiltration rates under ET remained relatively stable (0.231–0.283 mm s^{-1}), suggesting the persistence of functional porosity and stable structure even after natural settling. In contrast, CT and MT exhibited progressive decreases in infiltration rates after the third month, indicating pore closure and surface sealing due to mechanical reconsolidation and rainfall impact. NT maintained low but consistent infiltration rates, reflecting the low permeability of undisturbed and compacted soil layers. Similar temporal declines in infiltration under repeated CT operations have been documented in long-term studies of clay loam and sandy soils, where compaction beneath the plough layer reduced infiltration and water storage capacity (Yang et al., 2017; Amami et al., 2021).

The regression analysis confirmed these patterns (Table 3). The infiltration model explained 98% of the variance ($R^2 = 0.98$). ET displayed the highest intercept (0.262 mm·s^{-1}, $p < 0.001$), while NT (−0.163), CT (−0.093), and MT (−0.134) were significantly lower. The small negative time coefficient under ET (B = −0.0028, $p < 0.001$) indicates a slight but significant reduction in infiltration rate over time. However, the significantly steeper decline observed in treatments such as CT and MT (Table 3) reflects the gradual degradation of soil structure and pore closure under conventional management. Conversely, the more stable slope observed under NT ($p = 0.001$ for slope difference) suggests that while undisturbed soil exhibits lower overall permeability, its structure remains more consistent over time.

Table 3. Multiple regression analysis of soil infiltration rate as affected by tillage treatment and time

Predictor	B (Coefficient)	SE	t	*p*
Baseline Rate (ET Intercept)	0.26253	0.0017	157.76	< 0.001
Monthly Rate Change (ET Slope)	−0.00284	0.0004	−6.65	< 0.001
Rate Difference (NT)	−0.16311	0.0024	−69.31	< 0.001
Slope Difference (NT)	0.00209	0.0006	3.47	0.001
Rate Difference (CT)	−0.09304	0.0024	−39.54	< 0.001
Slope Difference (CT)	−0.00059	0.0006	−0.97	0.33
Rate Difference (MT)	−0.13393	0.0024	−56.91	< 0.001
Slope Difference (MT)	0.00059	0.0006	0.97	0.331
R^2	98.25%			

These outcomes are consistent with findings showing that subsoiling or modified bentleg tools, such as the ET used here, maintain soil porosity and hydraulic conductivity more effectively than disc or moldboard ploughing (Solhjou & Alavimanesh, 2023; Reddy et al., 2016).

Soil penetration resistance

Penetrometric resistance data shown in Fig. 7 further supported the infiltration results. The lowest mean resistance was observed under ET (240 N), followed by CT (410 N), MT (690 N), and NT (870 N). ET thus reduced resistance by 41%, 65%, and 72% relative to CT, MT, and NT, respectively. Such reductions indicate a sustained loosening effect in deeper layers, a result frequently reported for conservation-oriented deep tillage techniques that maintain pore continuity and relieve compaction (Vakali et al., 2011; Guedioura et al., 2023). The observed trend suggests that ET effectively minimized mechanical impedance to root growth, a critical determinant of crop establishment and nutrient uptake.

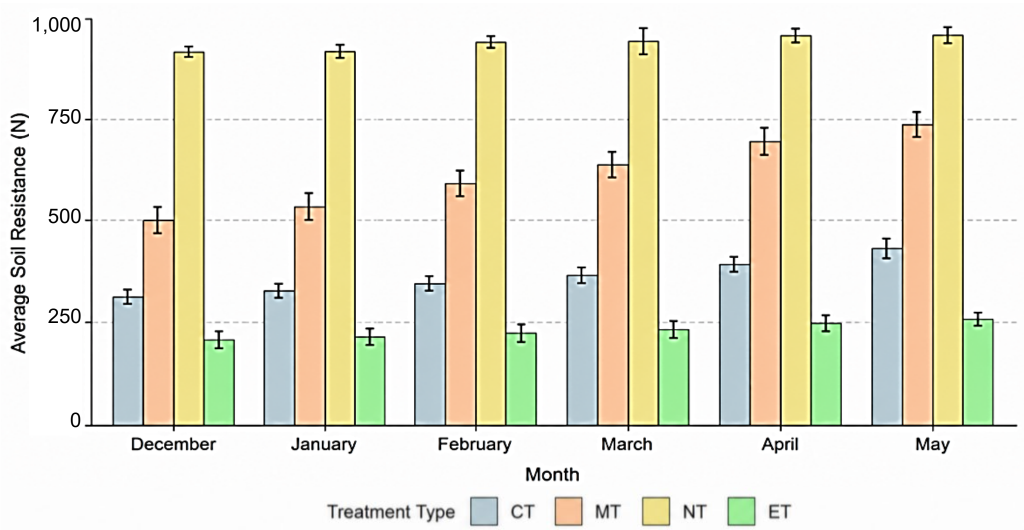

Figure 7. Changes in soil penetration resistance over six months following different tillage treatments, measured using a static penetrometer.

Over time, resistance increased in all treatments due to natural reconsolidation, but the rate of change was smallest under ET (140–390 N). In CT and MT, values increased steadily beyond 500 N and 900 N by the sixth month, consistent with the re-compaction reported in repeated tillage systems (Bogunovic et al., 2018, Özpinar, 2024). NT maintained a stable but high resistance, typical of undisturbed profiles where mechanical penetration remains limited.

Regression analysis demonstrated in Table 4 explained 44.2% of the variance ($R^2 = 0.442$). The baseline ET intercept (582.87) did not differ significantly from other treatments, yet the time coefficient for ET (B = 10.16, $p = 0.047$) confirmed a mild increase in resistance with time. MT displayed a much higher coefficient (B = 40.71, $p < 0.001$), indicating rapid densification, while CT and NT showed no significant trends. Comparable studies have found that minimum tillage often accelerates reconsolidation because the lower disturbance fails to alleviate pre-existing compaction, whereas specialized tools maintain looser conditions deeper in the profile (Bauer et al., 2015).

Table 4. Multiple regression analysis of soil penetration resistance as affected by tillage treatment and time

Predictors	B	SE	t	p
Intercept (ET)	582.87	20.36	28.63	0
Time (ET)	10.16	5.08	2	0.047
Intercept Difference (NT)	21.17	28.8	0.74	0.4625
Time Difference (NT)	-5.13	7.21	-0.7	0.477
Intercept Difference (CT)	-25.18	28.8	-0.87	0.3823
Time Difference (CT)	7.03	7.21	0.98	0.33
Intercept Difference (MT)	-47.8	28.8	-1.66	0.0976
Time Difference (MT)	40.71	7.2	5.64	0
R^2	44.20%			

When both hydraulic and mechanical indicators are considered together, ET provided the most balanced soil condition. CT produced moderate short-term improvements but suffered from fast reconsolidation and decreased infiltration. MT and NT maintained compact profiles characterized by limited pore connectivity and restricted water flow. The dual improvement achieved by ET enhanced infiltration and lower resistance indicates a well-structured soil with stable porosity and efficient internal drainage. This effect aligns with prior observations that moderate, non-inverting deep tillage increases both infiltration and aggregate stability while reducing mechanical resistance (Giannitsopoulos et al., 2019).

Mechanically, the ET geometry plays a key role in this outcome. Its negative attack angle and bentleg configuration direct the shearing force downward, producing deep and uniform fractures without disturbing surface layers. The tool's operational speed allows a single-pass decompaction with reduced traction resistance, limiting fuel consumption and mechanical stress on the soil. These properties correspond with reported advantages of energy-efficient deep tillage systems that loosen subsoil layers while preserving topsoil integrity and minimizing erosion risk (Schneider et al., 2017; Hussein et al., 2019; Ning et al., 2022).

Crop yield response

Average wheat yields under the four tillage systems are presented in Fig. 8. Yield differed significantly among treatments (F = 7.19; df = 3, 12; $p = 0.005$). Average yields were 2.9 Qt ha^{-1} for NT, 12.83 Qt ha^{-1} for MT, 18.68 Qt ha^{-1} for ET, and 22.50 Qt ha^{-1} for CT. Although CT achieved the highest yield, ET produced a comparable yield while maintaining superior soil physical conditions and lower energy demand. These results are consistent with previous studies showing that deep, non-inverting tillage improves water availability and root penetration, supporting stable yields under moderate drought stress (Tian et al., 2016; Ning et al., 2022).

The relationship between infiltration, penetration resistance, and yield underscores the central role of soil physical quality in productivity under rainfed conditions. Maintaining macroporosity and low mechanical impedance favors deeper rooting and efficient water uptake, a factor considered more critical for yield stability than temporary surface loosening (Berisso et al., 2012; Yang et al., 2021).

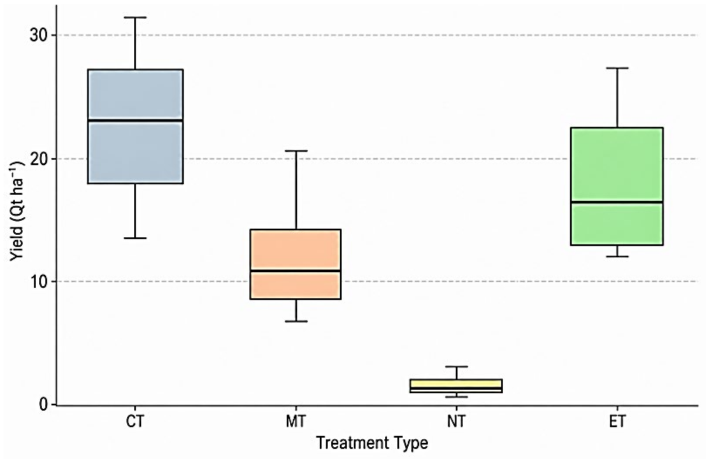

Figure 8. Mean durum wheat grain yield under different tillage treatments at harvest. Error bars indicate standard deviation (*n* = 4).

Integrated agro-pedological performance

As detailed in Table 5 (Comparative Performance Summary), the ET consistently provided the highest infiltration capacity throughout the experimental period, stabilizing around 0.255 mm s^{-1}. These deep structural improvements are crucial, especially since literature shows that deep soil layers struggle to recover their capacity without targeted mechanical intervention.

Table 5. Comparative summary of agro-pedological performance indicators across tillage treatments

Key indicator	ET (Experimental tool)	CT (Conventional tillage)	MT (Minimum tillage)	NT (No tillage)	Justification for ET
Stabilized infiltration (mm s^{-1})	0.255	0.155	0.125	0.098	Best permeability and macroporosity
Stabilized resistance (N)	390	> 500	> 900	Stable but high	Minimization of root impedance
Reconsolidation rate	Lowest rate (minimum b slope)	Rapid	Very rapid	Stable (highly compacted)	Porosity stability (non-inverting mechanism)
Yield (Qt ha^{-1})	18.68	22.50	12.83	2.9	Comparable yield with improved structure

The mechanical benefits of the ET further support its superiority. The penetrometric data confirmed that the experimental tool effectively reduced Penetration Resistance (PR) by 72% relative to NT. This reduction indicates a sustained loosening effect in deeper layers, minimizing mechanical impedance to root growth. A critical aspect of the ET design is its impact on long-term stability. The regression analyses revealed that while all treatments showed signs of natural reconsolidation, the rate of increase in resistance was smallest under ET, which stabilized between 140–390 N. In contrast, MT and CT plots suffered from rapid reconsolidation, with MT exceeding 900 N by the sixth month. This difference is directly attributed to the ET's negative rake angle and bentleg configuration, which induces deep, uniform fractures without inverting the surface horizons, preserving aggregate stability.

The yield results, though not prioritizing maximization, support the ET as an optimal compromise. Conventional Tillage (CT) achieved the highest overall yield at 22.50 Qt ha^{-1}, but the ET produced a comparable yield of 18.68 Qt ha^{-1}. The innovation lies in the fact that this performance is achieved with a low draft requirement. The ET provides a decompaction solution compatible with low-power tractors, rated between 50 and 80 horsepower, directly addressing a technical and socio-economic gap for small and medium farms in the South Mediterranean. This factor strongly favors the ET over CT, which incurs higher energy costs and leads to faster structural degradation and reconsolidation over time. The ET provides a mechanical and structural solution that optimizes the use of *in situ* rainwater and supports stable yields under moderate rainfall conditions, offering a sustainable alternative to complex material amendments like biochar or polymers.

The Modified bentleg plough achieves an optimal balance between the mechanical efficiency required to break the hardpan and ecological structural preservation. By providing superior structural stability, enhanced water infiltration, and a competitive yield with reduced energy input, the ET offers a viable technical path for sustainable soil management and durum wheat resilience in sensitive agricultural systems.

Traction power and energetic efficiency of experimental tool

The mouldboard plough exhibited significantly higher fuel consumption than the experimental tool (ET) at all tested speeds (Table 6). The highest value was recorded at 5 km h^{-1} for the mouldboard plough (26.7 L ha^{-1}), which differed significantly from all Experimental tool (ET) treatments. Analysis of variance revealed a significant effect of implement type and operating speed on fuel consumption per unit area ($p < 0.05$).

Table 6. Comparative analysis of field performance, energy consumption, and traction efficiency of experimental tool (ET) and mouldboard plough implements

Implement	Target speed (km h^{-1})	Actual speed (km·h^{-1})	Working depth (cm)	Time (50 m s^{-1})	Traction load	Fuel consumption (L ha^{-1})	Statistical group	RTI
Experimental tool (ET)	8	8.02 ± 0.15	40.2 ± 0.8	22.4 ± 0.5	Low	12.6 ± 0.7	d	1.56
	10	9.95 ± 0.20	40.1 ± 0.6	18.1 ± 0.6	Moderate	14.9 ± 0.9	cd	1.50
	12	11.48 ± 0.25	39.8 ± 1.0	15.7 ± 0.7	Moderate	17.4 ± 1.1	c	1.52
Mouldboard Plough	3	3.02 ± 0.10	25.3 ± 0.7	59.6 ± 1.2	Moderate	20.2 ± 1.0	b	6.67
	4	3.78 ± 0.15	25.1 ± 0.9	47.5 ± 1.5	High	23.5 ± 1.2	ab	6.13
	5	4.52 ± 0.20	24.8 ± 1.1	39.8 ± 1.8	Very high	26.7 ± 1.4	a	5.91

Values are expressed as mean ± standard deviation ($n = 3$). Means followed by the same letter are not significantly different at $p < 0.05$.

In contrast, the Experimental tool (ET) maintained lower fuel consumption even at higher speeds, with the lowest value observed at 8 km h^{-1} (12.6 L ha^{-1}). These results indicate a significantly lower apparent energy requirement for the Experimental tool (ET) compared to conventional ploughing under similar field conditions.

The performance of both implements was further evaluated using forward speed and fuel consumption measured under field conditions. A relative traction index (RTI), defined as the ratio of speed (km h^{-1}) to fuel consumption (L ha^{-1}), was used as an indirect indicator of draft force.

The results highlight a clear difference between the implements. The Experimental tool (ET) exhibited a stable RTI (1.50–1.56; mean 1.53), whereas the mouldboard plough showed higher values (5.91–6.67; mean 6.24), indicating an approximately fourfold higher traction demand.

This trend is consistent with field observations: the mouldboard plough caused a marked drop in engine speed and a high traction load, particularly at higher speeds, while the Experimental tool (ET) maintained more stable operation with moderate load.

These differences can be explained by soil-tool interaction. The mouldboard plough operates by full inversion, mobilizing a large volume of soil and increasing passive forces, whereas the Experimental tool (ET) primarily induces soil loosening, limiting soil displacement and reducing mechanical resistance.

These findings are consistent with previous studies (Godwin, 2007; Keller et al., 2019), which show that inversion tillage generates higher draft forces, while vertical tillage systems reduce mechanical constraints and energy consumption.

Finally, the relationship $P = Ft \cdot V$ supports this interpretation: higher speed combined with lower fuel consumption (Experimental tool ET) reflects reduced draft force, unlike the mouldboard plough.

Overall, the results highlight the superior energy and mechanical efficiency of the Experimental tool (ET).

CONCLUSIONS

The results of this study demonstrate that the modified Bentleg Plough (ET) offers a measurable improvement in soil physical and hydraulic properties compared to traditional tillage systems in South Mediterranean rainfed conditions.

- Mechanical Performance: The ET tool achieved the most consistent reduction in soil penetration resistance, maintaining values between 140–390 N, which is significantly lower than the critical thresholds found in No-Tillage (NT) and Conventional Tillage (CT) plots.
- Hydraulic Conductivity: Regarding water dynamics, the ET treatment resulted in a stabilized infiltration rate of 10.16×10^{-6} m s^{-1}. This represents a significant technical improvement over NT, facilitating better deep-drainage potential in hardsetting soils.
- Agronomic Viability: Although wheat yields for the ET treatment (1.87 t ha^{-1}) were slightly lower than CT (2.25 t ha^{-1}), the differences were not statistically significant within this single cropping season.
- Technical Implications: These findings suggest that the modified Bentleg geometry, characterized by a negative rake angle, provides a viable technical option for

subsoil decompaction. It offers a mechanical pathway to alleviate soil compaction while requiring lower draft force, making it suitable for the technical constraints of regional farming systems.

Future research should focus on multi-year monitoring to evaluate the long-term stability of these structural improvements and their cumulative effect on crop water-use efficiency.

ACKNOWLEDGEMENTS. This work is dedicated to the memory of my first supervisor, Professor Amara Mahfoud who passed away during the preparation of this study. May his contributions to science be remembered.

REFERENCES

Amami, R., Ibrahimi, K., Sher, F., Milham, P., Ghazouani, H., Chehaibi, S. & Iqbal, H.M. 2021. Impacts of different tillage practices on soil water infiltration for sustainable agriculture. *Sustainability* **13**(6), 3155. doi: 10.3390/su13063155

Arriaga, F.J., Guzman, J. & Lowery, B. 2017. Conventional agricultural production systems and soil functions. In: *Soil health and intensification of agroecosystems*, pp. 109–125. Academic Press. doi: 10.1016/B978-0-12-805317-1.00005-1

Bauer, T., Strauss, P., Grims, M., Kamptner, E., Mansberger, R. & Spiegel, H. 2015. Long-term agricultural management effects on surface roughness and consolidation of soils. *Soil and Tillage Research* **151**, 28–38. doi: 10.1016/j.still.2015.01.017

Berisso, F.E., Schjønning, P., Keller, T., Lamandé, M., Etana, A., de Jonge, L.W. & Forkman, J. 2012. Persistent effects of subsoil compaction on pore size distribution and gas transport in a loamy soil. *Soil and Tillage Research* **122**, 42–51. doi: 10.1016/j.still.2012.02.005

Bogunovic, I., Pereira, P., Kisic, I., Sajko, K. & Sraka, M. 2018. Tillage management impacts on soil compaction, erosion and crop yield in Stagnosols (Croatia). *Catena* **160**, 376–384. doi: 10.1016/j.catena.2017.10.009

Boincean, B. & Dent, D. 2019. Tillage and conservation agriculture. In: *Farming the black earth: Sustainable and climate-smart management of chernozem soils*, pp. 125–149. Springer, Cham. doi: 10.1007/978-3-030-22533-9_6

García-Ruiz, J.M., Nadal-Romero, E., Lana-Renault, N. & Beguería, S. 2013. Erosion in Mediterranean landscapes: Changes and future challenges. *Geomorphology* **198**, 20–36. doi: 10.1016/j.geomorph.2013.05.023

Giannitsopoulos, M.L., Burgess, P.J. & Rickson, R.J. 2019. Effects of conservation tillage systems on soil physical changes and crop yields in a wheat–oilseed rape rotation. *Journal of Soil and Water Conservation* **74**(3), 247–258. doi: 10.2489/jswc.74.3.247

Godwin, R.J. 2007. Advances in labour and machinery management for a profitable agriculture and forestry. Agricultural Engineering International: the CIGR Ejournal 9, Manuscript CIOSTA 07 007.

Google Earth. 2024. Satellite imagery. Google LLC. Available at https://earth.google.com/. Accessed March 2024.

Grisso, R.D., Perumpral, J.V., Vaughan, D.H., Roberson, G.T. & Pitman, R. 2004. *Predicting tractor fuel consumption*. *Applied Engineering in Agriculture* **20**(5), 553–561. doi: 10.13031/2013.17455

Guedioura, I., Rahmoune, B., Khezzaren, A., Dahoumane, A. & Laouar, N. 2023. Combined effect of soil practices and chemical treatments on weed growth, soil features and yield performance in field wheat crop under Mediterranean climate. *Agronomy Research* **21**(1), 62–77. doi: 10.15159/ar.22.079

Hussein, M.A, Muche, H., Schmitter, P., Nakawuka, P., Tilahun, S.A., Langan, S. & Steenhuis, T.S. 2019. Deep tillage improves degraded soils in the (sub)humid Ethiopian Highlands. *Land* **8**(11), 159. doi: 10.3390/land8110159

Keller, T., Sandin, M., Colombi, T., Horn, R. & Or, D. 2019. Historical increase in agricultural machinery weights enhanced soil stress levels and adversely affected soil functioning. *Soil and Tillage Research* **194**, 104293. doi: 10.1016/j.still.2019.06.014

Liu, J., Leung, A.K., Dong, H. & Jiang, Z. 2025. Pore-scale investigation of the hysteretic water retention behaviour of unsaturated soils by tracking preferential water transport. *Computers and Geotechnics* **179**, 107049. doi: 10.1016/j.compgeo.2024.107049

Liu, J., Leung, A.K., Dong, H. & Lai, N.T. 2024. A state-dependent bimodal soil water retention model considering evolutions of pore-scale soil–water interaction. *Computers and Geotechnics* **175**, 106704. doi: 10.1016/j.compgeo.2024.106704

Naskar, J., Kumar Jha, A., Singh, T.N. & Aeron, S. 2025. Climate change and soil resilience: A critical appraisal on innovative techniques for sustainable ground improvement and ecosystem protection. *Journal of Hazardous, Toxic, and Radioactive Waste* **29**(4), 03125002. doi: 10.1061/JHTRBP.HZENG-1465

Ning, T., Liu, Z., Hu, H., Li, G. & Kuzyakov, Y. 2022. Physical, chemical and biological subsoiling for sustainable agriculture. *Soil and Tillage Research* **223**, 105490. doi: 10.1016/j.still.2022.105490

NF EN ISO 22282-5. 2012. *Geotechnical investigation and testing – Geohydraulic testing – Part 5: Infiltrometer tests*. International Organization for Standardization (ISO), Geneva, Switzerland.

Özpinar, S. 2024. Soil compaction effects on soil properties and crop productivity: An overview. *Impact of Climate Change on Agriculture and Ecosystems* **191**.

Peña-Sancho, C., López, M.V., Gracia, R. & Moret-Fernández, D. 2017. Effects of tillage on the soil water retention curve during a fallow period of a semiarid dryland. *Soil Research* **55**(2), 114–123. doi: 10.1071/SR15305

Reddy, P.P. 2016. Agricultural soil compaction. In: *Sustainable intensification of crop production*, pp. 41–52. Springer, Singapore. doi: 10.1007/978-981-10-2702-4_3

Sardans, J. & Peñuelas, J. 2013. Plant–soil interactions in Mediterranean forest and shrublands: Impacts of climatic change. *Plant and Soil* **365**(1), 1–33. doi: 10.1007/s11104-013-1591-6

Schneider, F., Don, A., Hennings, I., Schmittmann, O. & Seidel, S.J. 2017. The effect of deep tillage on crop yield – What do we really know? *Soil and Tillage Research* **174**, 193–204. doi: 10.1016/j.still.2017.07.005

Shao, M.A., Wang, Y., Xia, Y. & Jia, X. 2018. Soil drought and water carrying capacity for vegetation in the critical zone of the Loess Plateau: A review. *Vadose Zone Journal* **17**(1), 1–8. doi: 10.2136/vzj2017.04.0077

Solhjou, A. & Alavimanesh, S.M. 2023. Field evaluation of a bent leg tillage implement in dry soil conditions. *Research in Agricultural Engineering* **69**(3). doi: 10.17221/41/2022-RAE

Stošić, M., Brozović, B., Vinković, T., Ravnjak, B., Kluz, M. & Zebec, V. 2020. Soil resistance and bulk density under different tillage system. *Poljoprivreda* **26**(1), 17–24. doi: 10.18047/poljo.26.1.3

Tan, J., Si, B., Zhao, Y., Lu, Y., Chen, Y., An, N. & Yi, Y. 2025. Short-term no-tillage improves soil water retention and maintains soil aeration at high moisture conditions despite reduced macroporosity. *Soil and Tillage Research* **253**, 106677. doi: 10.1016/j.still.2025.106677

Tian, S., Ning, T., Wang, Y., Liu, Z., Li, G., Li, Z. & Lal, R. 2016. Crop yield and soil carbon responses to tillage method changes in North China. *Soil and Tillage Research* **163**, 207–213. doi: 10.1016/j.still.2016.06.005

Totsche, K.U., Amelung, W., Gerzabek, M.H., Guggenberger, G., Klumpp, E., Knief, C. & Kögel-Knabner, I. 2018. Microaggregates in soils. *Journal of Plant Nutrition and Soil Science* **181**(1), 104–136. doi: 10.1002/jpln.201600451

Vakali, C., Zaller, J.G. & Köpke, U. 2011. Reduced tillage effects on soil properties and growth of cereals and associated weeds under organic farming. *Soil and Tillage Research* **111**(2), 133–141. doi: 10.1016/j.still.2010.09.003

Wilkes, T.I., Warner, D.J., Edmonds-Brown, V., Davies, K.G. & Denholm, I. 2021. Zero t illage systems conserve arbuscular mycorrhizal fungi, enhancing soil glomalin and water stable aggregates with implications for soil stability. *Soil Systems* **5**(1), 4. doi: 10.3390/soilsystems5010004

Xiao, T., Li, P., Pan, Z. & Wang, J. 2022. Effect of compaction condition on the water retention capacity, microstructure and its evolution during drying of compacted loess. *Geoenvironmental Disasters* **9**(1), 27. doi: 10.1186/s40677-022-00229-y

Yang, Y., Wu, J., Zhang, J., Pan, X., Wang, Y. & He, F. 2017. Effect of tillage method on soil water infiltration, organic carbon content and structure. *Chinese Journal of Eco-Agriculture* **25**(2), 258–266. doi: 10.13930/j.cnki.cjea.160720 (in Chinese).

Yang, Y., Wu, J., Zhao, S., Mao, Y., Zhang, J., Pan, X. & van der Ploeg, M. 2021. Impact of long-term sub-soiling tillage on soil porosity and soil physical properties in the soil profile. *Land Degradation & Development* **32**(10), 2892–2905. doi: 10.1002/ldr.3874

Zdruli, P., Kapur, S. & Çelik, I. 2010. Soils of the Mediterranean region, their characteristics, management and sustainable use. In: *Sustainable land management: Learning from the past for the future*, pp. 125–142. Springer, Berlin, Heidelberg. doi: 10.1007/978-3-642-14782-1_4

Zhou, Z., Karimzadeh, A.A., Leung, A.K. & Fok, S.Y. 2025. Hysteretic water-retention behaviour of unsaturated hydrophobised soils. *Géotechnique* **75**(3), 337–347. doi: 10.1680/jgeot.23.00195

Agronomy Research **24**(S1), 225–236, 2026
https://doi.org/10.15159/AR.26.047

Early morphogenesis of kopyor coconut (*Cocos nucifera* L.) embryos *in vitro* as affected by light conditions and thidiazuron concentration

S. Susiyanti[1,5,*], W.S. Hamidah[1], A.A. Fatmawaty[1], Z. Millah[1], Kartina A.M.,[1] M. Mirajiani[2], S. Abdullah[3] and S. Sjaifuddin[4]

[1]Department of Agroecotechnology, Faculty of Agriculture, Universitas Sultan Ageng Tirtayasa, Serang, Banten Province, Indonesia
[2]Department of Agribusiness, Faculty of Agriculture, Universitas Sultan Ageng Tirtayasa, Serang, Banten Province, Indonesia
[3]Faculty of Plantation and Agrotechnology, Universiti Teknologi MARA, Malaysia
[4]Department of Environmental Studies, Universitas Sultan Ageng Tirtayasa, Serang, Banten Province, Indonesia
[5]Center of Excellent for Food Security, Universitas Sultan Ageng Tirtayasa, Serang, Banten Province, Indonesia
[*]Correspondence: susiyanti@untirta.ac.id

Received: December 31st, 2025; Accepted: May 7th, 2026; Published: June 10th, 2026

Abstract. Kopyor coconut (*Cocos nucifera* L.) is a high-value coconut variant characterized by a naturally mutated endosperm; however, its propagation is constrained by low seed viability and inconsistent germination. *In vitro* culture offers a promising approach for large-scale propagation. This study evaluated the effects of light conditions and thidiazuron (TDZ) concentrations on the early morphogenesis of kopyor coconut embryos cultured *in vitro*. A split-plot design based on a completely randomized design was applied, with light conditions (dark and continuous light) as the main plot and TDZ concentrations (0, 0.25, 0.50, 0.75, and 1.00 mg L^{-1}) as subplots. The results showed that light conditions did not significantly affect explant height, shoot number and root number, or root length ($p > 0.05$), although plumule formation occurred exclusively under light conditions. In contrast, TDZ significantly influenced explant height ($p < 0.01$), while its effects on other parameters were not significant. The application of 0.25 mg L^{-1} TDZ produced the most favorable response, with explant height reaching 3.00 ± 0.14 cmunder light and 2.60 ± 0.17 cmunder dark conditions, accompanied by 0.95 shoots and 0.86 roots per explant. No significant interaction between light conditions and TDZ was detected. These findings indicate that early morphogenesis of kopyor coconut embryos is primarily regulated by endogenous hormonal balance, with low TDZ concentrations optimizing growth responses, while light plays a critical role in organ differentiation, particularly in plumule formation. The results provide a basis for improving *in vitro* propagation protocols for this economically important coconut variant.

Key words: *Cocos nucifera* L., kopyor coconut, morphogenesis, light conditions, thidiazuron, *in vitro*.

INTRODUCTION

Indonesia is widely recognized as a megadiversity country with tropical agroecological conditions that strongly support perennial crops, particularly coconut (*Cocos nucifera* L.), which plays an important economic and ecological role due to the extensive utilization of its plant parts. Among coconut variants, kopyor coconut represents a unique and high-value type resulting from a natural mutation in the endosperm. This mutation produces a soft, friable endosperm with a distinctive aroma, attributes that significantly increase its commercial value and consumer demand (Mu et al., 2024).

Despite its high economic potential, kopyor coconut production in Indonesia remains limited, particularly in key regions such as Pati, Central Java, due to the scarcity of viable planting materials and the instability of seedling supply. Low seed viability and the unpredictable outcomes of conventional propagation often result in poor germination and inconsistent plant performance, thereby constraining large-scale cultivation and commercialization (Long et al., 2022). Therefore, alternative propagation strategies are required to produce uniform and reliable planting materials.

In vitro culture has been widely applied as an alternative propagation approach for perennial crops, including coconut, due to its advantages in rapid multiplication, genetic uniformity, and production of pathogen-free plantlets (Nguyen et al., 2016; Kalaipandian et al., 2021). However, coconut is considered a recalcitrant species in tissue culture, with morphogenic responses strongly influenced by basal medium composition, plant growth regulators (PGRs), and environmental conditions. Y3 medium is commonly used as the standard basal medium for coconut tissue culture and is typically supplemented with carbohydrates, vitamins, and growth regulators to compensate for the limited photosynthetic capacity of *in vitro* explants (Zhang et al., 2023; Pokimica et al., 2024).

Plant growth regulators play a central role in controlling *in vitro* morphogenesis. Cytokinins generally promote shoot development, whereas auxins are associated with root and callus formation (Zhang et al., 2023). Thidiazuron (TDZ), a synthetic cytokinin, has been widely reported to be highly effective in stimulating shoot proliferation in coconut and other woody species. However, its effects are strongly dependent on concentration, explant type, and culture conditions (Wilms et al., 2021; Kong et al., 2025). High TDZ concentrations may inhibit growth or induce abnormal morphogenesis, highlighting the need for precise optimization. In kopyor coconut, available studies remain limited and primarily focus on embryogenic callus induction using auxin-cytokinin combinations, while information on optimal TDZ concentrations for early morphogenesis is still lacking (Chandrakala et al., 2019).

In addition to PGRs, light conditions are an important environmental factor influencing *in vitro* morphogenesis through their effects on chlorophyll synthesis, cell elongation, and organ differentiation. Although light regimes have been reported to enhance plantlet growth and acclimatization (Bett et al., 2019; Mu et al., 2025), information regarding the role of light during early developmental stages of kopyor coconut embryos remains limited and inconsistent, particularly in relation to cytokinin-mediated responses.

Therefore, this study aimed to evaluate the effects of light conditions (light and dark) and different TDZ concentrations (0, 0.25, 0.50, 0.75, and 1.00 mg L^{-1}) on early morphogenesis of kopyor coconut embryos cultured *in vitro*. This study addresses the existing gap in understanding the interaction between hormonal regulation and light-mediated developmental processes and provides a basis for optimizing efficient and standardized propagation protocols for this high-value coconut variant.

MATERIALS AND METHODS

Experimental site and duration

The experiment was conducted from September to December 2025 at the Laboratory of Physiology and Biotechnology, Universitas Sultan Ageng Tirtayasa, Indonesia, under controlled laboratory conditions.

Plant materials and experimental design

Zygotic embryos of kopyor coconut (*Cocos nucifera* L.) obtained from Pati, Central Java, Indonesia, were used as explants. The embryos were derived from fruits characterized by brown-colored exocarp and yellow petiole, which are typical morphological traits of the selected kopyor type. The experiment was arranged in a split-plot completely randomized design (CRD) with two factors. Light condition was assigned as the main plot, consisting of complete darkness (C_0) and continuous light (C_1). TDZ concentration was designated as the subplot factor, with five levels: 0, 0.25, 0.50, 0.75, and 1.00 mg L^{-1}. Each treatment combination was replicated three times, with each experimental unit consisting of one explant (one embryo), resulting in a total of 30 experimental units in the experiment.

Culture media preparation

The basal medium used in this study was Y3 medium following Eeuwens formulation. The medium was supplemented with 15 g L^{-1} sucrose, 1 g L^{-1} activated charcoal, 50 mL L^{-1} coconut water, 7 g L^{-1} agar, and 0.5 mL L^{-1} Plant Preservative Mixture (PPM). TDZ was added according to the respective treatment concentrations. The pH of the medium was adjusted to 5.6 prior to sterilization, and all media were autoclaved at 121 °C for 15 min.

Sterilization and inoculation procedures

All instruments and culture vessels were sterilized by autoclaving. Inoculation was performed aseptically in a laminar airflow cabinet sterilized with ultraviolet light for 30 min. Instruments were disinfected with 70% ethanol and flamed during inoculation. After inoculation, culture vessels were sealed to prevent contamination.

Culture conditions and treatments

Cultures were maintained at 22–26 °C for eight weeks. Two light conditions were applied: complete darkness (0 lux) and continuous illumination at approximately 2,000 lux provided by cool-white fluorescent lamps (2×40 W) positioned approximately 30 cmabove the culture shelves.

Data collection

Observations were conducted until week 8. Parameters recorded included explant height (cm), number of shoots per explant, number of roots per explant, and root length (cm). Additional parameters included the percentage of rooted explants and percentage of plumule emergence.

Statistical analysis

Data were subjected to analysis of variance (ANOVA) at a 5% significance level. When significant differences were detected, Duncan's Multiple Range Test (DMRT) was applied. Statistical analysis was performed using DSAASTAT version 1.101.

RESULTS AND DISCUSSION

The effects of light conditions and TDZ on *in vitro* early shoot development of kopyor coconut were evaluated using multiple growth parameters. Analysis of variance (Table 1) showed that light conditions did not significantly affect explant height, shoot number and root number, or root length. In contrast, TDZ concentration had a highly significant effect ($p < 0.01$) on explant height, while its effects on other parameters were not significant.

Table 1. Analysis of variance (ANOVA) summary of the effects of light conditions and TDZ on early morphogenesis of kopyor coconut (*Cocos nucifera* L.) embryos cultured *in vitro*

Parameter	Light condition (C)	TDZ concentration (T)	Interaction (C × T)	CV main plot (%)	CV subplot (%)
Explant height	ns	**	ns	14.31	20.02
Number of shoots	ns	ns	ns	10.49	16.58
Number of roots	ns	ns	ns	17.79	16.13
Root length	ns	ns	ns	6.20	10.91

Note: ns = not significant ($p > 0.05$); ** = highly significant at $p \leq 0.01$; CV = coefficient of variation.

No significant interaction between light conditions and TDZ concentration was detected, suggesting that TDZ responses were largely independent of light conditions. Coefficients of variation ranging from 6.20% to 20.02% indicate acceptable experimental precision.

Although no significant differences in explant height were observed between light and dark conditions ($p > 0.05$), plumule formation occurred only under light conditions and was absent in cultures maintained in darkness.

Explant height

Explant height increased gradually over the eight-week culture period. Light conditions had no significant effect on explant height, whereas TDZ concentration had a highly significant effect ($p < 0.01$), with no significant interaction between the two factors. The detailed effects of treatments on explant height are presented in Table 2.

The slightly greater explant height observed under dark conditions (2.52 cm) compared to light conditions (2.45 cm) may be associated with etiolation, a typical response to the absence of light that promotes elongation (Armarego-Marriott et al., 2020; Huang et al., 2025). However, this difference was not statistically significant ($p > 0.05$).

Table 2. Effect of light conditions and TDZ on explant height of kopyor coconut (*Cocos nucifera* L.) embryos cultured *in vitro* (cm)

Light condition	TDZ Concentration (mg L^{-1})					Mean
	0.00 (T_0)	0.25 (T_1)	0.50 (T_2)	0.75 (T_3)	1.00 (T_4)	
Dark (C_0)	1.81 ± 0.27	2.60 ± 0.17	2.69 ± 0.52	2.82 ± 0.06	3.11 ± 0.33	2.52
Light (C_1)	1.66 ± 0.33	3.00 ± 0.14	2.55 ± 0.21	2.40 ± 0.08	2.66 ± 0.16	2.45
Mean	1.73^{c}	2.80^{a}	2.62^{b}	2.61^{ab}	2.88^{a}	2.49

Note: Values are expressed as mean ± SEM. Means followed by different letters within the TDZ factor differ significantly according to DMRT at $p \leq 0.05$.

Although light is known to regulate photomorphogenesis through processes such as cell differentiation, chloroplast development, and organ formation (Zhang et al., 2024¸ Wu et al., 2025), the comparable explant height observed in this study suggests that elongation under dark conditions may compensate for reduced photomorphogenic development.

TDZ at 0.25 and 1.00 mg L^{-1} produced the highest explant height (2.80–2.88 cm). DMRT analysis confirmed that 0.25 mg L^{-1} TDZ resulted in explant height statistically comparable to higher concentrations but significantly greater than the control and 0.50 mg L^{-1} treatments. This indicates that low TDZ concentrations are sufficient to promote shoot elongation without inducing inhibitory effects.

TDZ-induced morphogenesis is associated with complex hormonal regulation pathways (Erland et al., 2020; Ghosh et al., 2018). The response of explant height to TDZ was not linear, as similar growth responses were observed at both 0.25 and 1.00 mg L^{-1}. This pattern may reflect interactions between exogenous TDZ and endogenous hormones present in kopyor coconut embryos. Zygotic embryos of coconut are known to contain relatively high endogenous cytokinin levels, and TDZ may further modulate the cytokinin-auxin balance, resulting in a non-linear growth response (Kalaipandian et al., 2021). This finding is consistent with previous reports that TDZ influences plant development through its cytokinin-like activity and regulation of hormonal crosstalk (Ali et al., 2022; Li et al., 2022; Faisal et al., 2023).

Number of shoots per explant

Shoot initiation was observed during the culture period, although its timing was not quantitatively assessed. Overall, shoot formation was not significantly influenced by light conditions, TDZ concentration, or their interaction ($p > 0.05$). The mean number of shoots remained low, ranging from 0.81 to 0.95 shoots per explant across treatments. The response of shoot number across treatments is summarized in Table 3.

The limited shoot induction observed in this study may be attributed to the balance of endogenous auxin and cytokinin (Van Gelderen et al., 2021; Kong et al., 2025), as well as the type of explant used. Zygotic embryos are developmentally programmed to produce a single primary shoot during germination, which inherently limits the capacity for multiple shoot formation under *in vitro* conditions (Nguyen et al., 2016). In addition, the use of zygotic embryos as explants may further contribute to the low shoot formation observed, as these tissues are primarily oriented toward germination rather than proliferation, thereby limiting their morphogenic potential for multiple shoot induction.

Table 3. Effect of light conditions and TDZ on shoot number of kopyor coconut (*Cocos nucifera* L.) embryos cultured *in vitro*

Light condition	TDZ (mg L^{-1})					Mean
	0.00 (T_0)	0.25 (T_1)	0.50 (T_2)	0.75 (T_3)	1.00 (T_4)	
Dark (C_0)	0.81 ± 0.10	0.90 ± 0.10	0.90 ± 0.10	1.00 ± 0.00	0.90 ± 0.10	0.90
Light (C_1)	0.81 ± 0.10	1.00 ± 0.00	0.90 ± 0.10	0.71 ± 0.00	0.81 ± 0.10	0.85
Mean	0.81	0.95	0.90	0.86	0.86	0.87

Note: Values are expressed as mean ± SEM. No significant differences were observed among treatments according to analysis of variance (ANOVA) at $p > 0.05$.

A similar pattern was observed in root-related parameters (Table 4). Overall, these findings indicate that the morphogenic response of kopyor coconut embryos was low and not strongly influenced by the applied treatments.

Table 4. Effect of light conditions and TDZ on number of roots of kopyor coconut (*Cocos nucifera* L.) embryos cultured *in vitro*

Light condition	TDZ (mg L^{-1})					Mean
	0.00 (T_0)	0.25 (T_1)	0.50 (T_2)	0.75 (T_3)	1.00 (T_4)	
Dark (C_0)	0.71 ± 0.00	0.81 ± 0.10	0.81 ± 0.00	0.90 ± 0.10	0.81 ± 0.10	0.81
Light (C_1)	0.71 ± 0.00	0.90 ± 0.10	0.81 ± 0.10	0.71 ± 0.00	0.71 ± 0.00	0.77
Mean	0.71	0.86	0.81	0.81	0.76	0.79

Note: Values are expressed as mean ± SEM. No significant differences were observed among treatments according to analysis of variance (ANOVA) at $p > 0.05$.

Number of roots per explant

The number of roots per explant remained low (<1 root) across all treatments, and statistical analysis showed no significant effects of light conditions, TDZ concentration, or their interaction ($p > 0.05$). Numerically, rooting was slightly higher under dark conditions (mean = 0.81) than under light conditions (0.77), with the highest values observed at 0.75 mg L^{-1} in darkness (0.90) and 0.25 mg L^{-1} under light conditions (0.90). However, these differences were not statistically significant, indicating that light conditions had a limited influence on early rhizogenesis.

The limited rooting response observed in this study suggests that rhizogenesis in coconut is not strongly promoted by cytokinin. TDZ is known to stimulate shoot meristem activity but may inhibit root initiation at higher concentrations (Kalaipandian et al., 2021). Root development in palms is generally auxin-dependent and often requires exogenous auxin, such as indole-3-butyric acid (IBA) or naphthaleneacetic acid (NAA), as well as multi-stage culture systems to achieve effective rooting (Chandrakala et al., 2019).

In addition, the use of zygotic embryos as explants may have contributed to the low rooting response observed. Zygotic embryos are developmentally oriented toward germination rather than organ proliferation, and their endogenous hormonal balance is typically optimized for primary root formation rather than multiple root induction. This intrinsic developmental constraint may limit their responsiveness to exogenous treatments aimed at enhancing rhizogenesis.

Therefore, the low rooting response may be attributed to a combination of limited endogenous auxin levels, the absence of auxin supplementation, and the inherent recalcitrant nature of monocot embryos (Martins et al., 2024).

Root length

Root length was relatively uniform across treatments, and analysis of variance showed no significant effects of light conditions or TDZ concentration ($p > 0.05$), indicating limited variation in root elongation. Root length tended to decrease with increasing TDZ concentration; although this trend was not statistically significant. Root length responses under different treatments are shown in Table 5.

Table 5. Effect of light conditions and TDZ on root length of kopyor coconut (*Cocos nucifera* L.) embryos cultured *in vitro* (cm)

Light condition	TDZ (mg L^{-1}) 0.00 (T_0)	0.25 (T_1)	0.50 (T_2)	0.75 (T_3)	1.00 (T_4)	Mean
Dark (C_0)	1.10 ± 0.01	1.05 ± 0.02	1.07 ± 0.01	0.93 ± 0.05	1.08 ± 0.01	1.05
Light (C_1)	1.10 ± 0.02	1.09 ± 0.05	1.29 ± 0.17	1.10 ± 0.00	1.10 ± 0.00	1.14
Mean	1.10	1.07	1.18	1.01	1.09	1.09

Note: Values are expressed as mean ± SEM. No significant differences were observed among treatments according to analysis of variance (ANOVA) at $p > 0.05$.

The regulatory role of auxin in root formation has been widely reported (Du & Scheres, 2018). Root development occurred in the absence of exogenous auxin, suggesting that endogenous hormonal activity within the embryo was sufficient to support root initiation, potentially enhanced by growth-promoting compounds present in coconut water (Chandrakala et al., 2019; Martins et al., 2024). In palms, root formation is generally auxin-dependent and often requires exogenous auxin supplementation for optimal development (Kalaipandian et al., 2021).

The use of zygotic embryos as explants may have contributed to the observed root elongation pattern, as these tissues are developmentally oriented toward primary root establishment during germination rather than extensive root proliferation (Armenta-Medina et al., 2020; Venglat et al., 2025), which may limit their responsiveness to exogenous treatments (Tian et al., 2020).

Following shoot development, newly formed shoot tissues may have contributed additional endogenous growth regulators that supported subsequent root elongation. Although light conditions can influence auxin sensitivity and root development, these effects are often species-specific and not always significant (Yun et al., 2023). Overall, the results indicate that root elongation in kopyor coconut embryos was primarily regulated by endogenous hormonal balance rather than by light or TDZ treatments.

Root formation was observed at the basal region of the explant under both light and dark conditions at 0.25 mg L^{-1} TDZ (Fig. 1). The roots appeared as whitish, elongated structures emerging from compact root primordia, indicating active rhizogenesis. These observations confirm that the explants were capable of initiating and sustaining root growth under the applied treatment, although the overall rooting response remained limited. Consistent with the quantitative results, rhizogenesis in kopyor coconut embryos appears to be primarily regulated by endogenous hormonal balance rather than by TDZ concentration or light conditions (Pasternak & Steinmacher, 2024; Indrachapa et al., 2025).

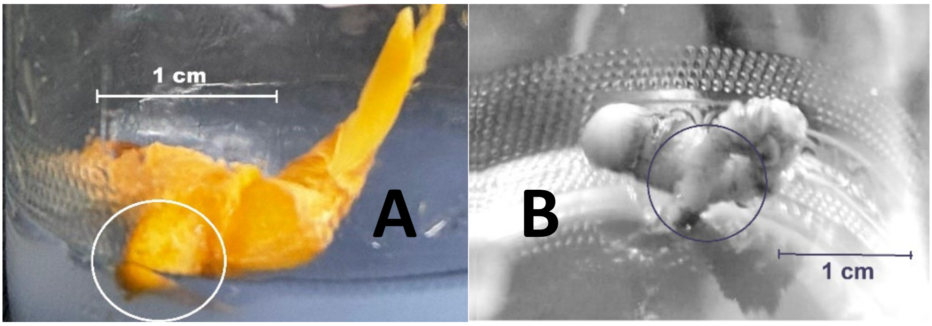

Figure 1. Root formation in kopyor coconut explants cultured under 0.25 mg L^{-1} TDZ under light (A) and dark conditions (B). Root primordia (circled) developed at the basal region and elongated into visible roots, indicating active rhizogenesis. Scale bar = 1 cm.

Percentage of rooted explants

Based on root formation observations, 8 out of 30 explants developed roots, resulting in an overall rooting percentage of 26.67%. Rooting was numerically higher under dark conditions (33.33%) than under light conditions (20%). Under darkness, root formation was observed only in TDZ-treated explants (C_0T_1–C_0T_4), whereas under light conditions it was limited to treatments C_1T_1 and C_1T_2.

The higher rooting percentage observed under dark conditions may be associated with reduced light exposure, which can enhance endogenous auxin activity by limiting its degradation (Van Gelderen et al., 2021). Although fewer explants formed roots under light conditions, those that did tended to produce longer roots, suggesting that light may influence root elongation rather than initiation. However, these patterns were not statistically significant and should therefore be interpreted with caution.

In addition, the use of zygotic embryos as explants may have contributed to the low rooting frequency observed. These embryos are developmentally oriented toward germination rather than organ proliferation, which may limit their responsiveness to treatments aimed at enhancing rhizogenesis.

Overall, these findings suggest that root development in kopyor coconut embryos was primarily regulated by endogenous hormonal balance, particularly auxin activity, while the effects of TDZ and light conditions appeared to be limited under the experimental conditions (Kim et al., 2023). Further studies incorporating exogenous auxin supplementation are required to better elucidate the mechanisms underlying root initiation and development. Similar observations have been reported in other *in vitro* systems, where endogenous hormonal activity was sufficient to support rhizogenesis (Faisal et al., 2023).

Percentage of plumule development

Although no significant differences in explant height were observed between light and dark conditions ($p > 0.05$), plumule formation occurred exclusively under light conditions. This indicates that light had a limited effect on elongation but played a critical role in photomorphogenesis, particularly in regulating organ differentiation and chlorophyll development during early embryo growth (Wu et al., 2025; Manghwar et al., 2026).

Plumules, characterized by leaf-like structures (Fig. 2), were observed only under light conditions, with a maximum frequency of 10%, particularly at low TDZ concentrations (C_1T_0, C_1T_1, and C_1T_2). No plumule formation occurred in explants cultured in darkness, highlighting the importance of light in leaf primordia differentiation (Van Gelderen et al., 2018; Kong et al., 2025).

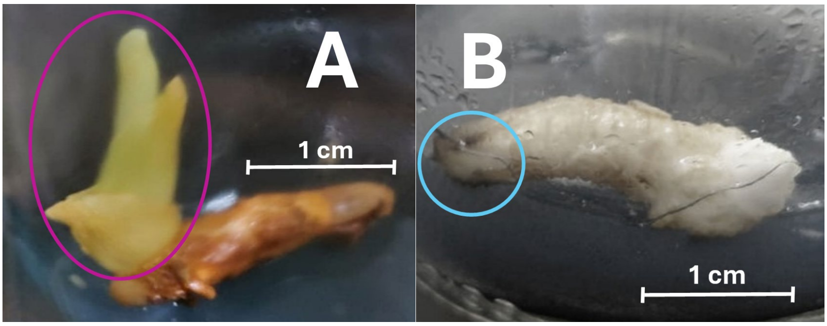

Figure 2. Plumule formation in kopyor coconut embryos cultured under light conditions with 0.5 mg L^{-1} TDZ (A), showing a well-developed shoot structure, and the absence of visible plumule under dark conditions with 0.5 mg L^{-1} TDZ (B). Scale bar = 1 cm.

High TDZ concentrations did not promote plumule formation, which is consistent with previous findings that excessive cytokinin levels may inhibit shoot differentiation (Akbar et al., 2018). In addition, the use of zygotic embryos as explants may have influenced plumule initiation, as their developmental stage is primarily oriented toward germination rather than active shoot proliferation, potentially limiting morphogenic competence (Sun et al., 2025).

Plumule formation was observed only under light conditions (Fig. 2, A), where a distinct, elongated shoot structure developed. In contrast, no visible plumule was formed under dark conditions (Fig. 2, B), and the explants remained morphologically undifferentiated. These observations confirm that light is essential for plumule initiation and shoot differentiation in kopyor coconut embryos.

CONCLUSION

Light conditions did not significantly affect quantitative growth parameters, including explant height, shoot number and root number, and root length of kopyor coconut cultured *in vitro*. However, plumule development occurred exclusively under light conditions, indicating that light plays a critical role in early organ differentiation despite its limited effect on overall growth.

In contrast, TDZ concentration significantly influenced explant height, with 0.25 mg L^{-1} producing the most favorable response. Although similar trends were observed for shoot and root development, these effects were not statistically significant, and no significant interaction between light conditions and TDZ concentration was detected.

These findings demonstrate that early morphogenesis of kopyor coconut embryos is primarily regulated by endogenous hormonal balance, with light acting as a key factor in developmental differentiation rather than growth promotion. This study provides insight into the early developmental constraints of kopyor coconut in vitro and highlights the need to optimize hormonal combinations, particularly through the inclusion of exogenous auxin, to enhance shoot and root development. Future research should further explore the interaction between endogenous hormones and light signaling to improve propagation efficiency.

REFERENCES

Ali, H.M., Khan, T., Khan, M.A. & Ullah, N. 2022. The multipotent thidiazuron: A mechanistic overview of its roles in callogenesis and other plant cultures *in vitro*. *Biotechnology and Applied Biochemistry* **69**(6), 2624–2640. https://doi.org/10.1002/bab.2311

Armarego-Marriott, T., Sandoval-Ibañez, O. & Kowalewska, Ł. 2020. Beyond the darkness: Recent lessons from etiolation and de-etiolation studies. *Journal of Experimental Botany* **71**(21), 6709–6721. https://doi.org/10.1093/jxb/eraa356

Armenta-Medina, A., Gillmor, C.S., Gao, P., Mora-Macias, J., Kochian, L.V., Xiang, D. & Datla, R. 2020. Developmental and genomic architecture of plant embryogenesis: From model plant to crops. *Plant Communications* **2**(1), 100136. https://doi.org/10.1016/j.xplc.2020.100136

Bett, C.C., Mweu, C.M. & Nyende, A.B. 2019. In vitro regeneration of coconut (*Cocos nucifera* L.) through indirect somatic embryogenesis in Kenya. *African Journal of Biotechnology* **18**(32), 1113–1122. https://doi.org/10.5897/AJB2019.16867

Chandrakala, D., Renuka, R. & Sushmitha, D.S. 2019. Influence of 2, 4-d and TDZ on direct organogenesis in coconut var. east coast tall. *Int. J. Chem Stud.* **7**(3). 4111–4115.

Du, Y. & Scheres, B. 2018. Lateral root formation and the multiple roles of auxin. *Journal of Experimental Botany* **69**(2), 155–167. https://doi.org/10.1093/jxb/erx223

Erland, L.A.E., Giebelhaus, R.T., Victor, J.M.R., Murch, S.J. & Saxena, P.K. 2020. The morphoregulatory role of thidiazuron: Metabolomics-guided hypothesis generation for mechanisms of activity. *Frontiers in Plant Science* **11**, 599496. https://doi.org/10.3389/fpls.2020.599496

Faisal, M., Qahtan, A.A. & Alatar, A.A. 2023. Thidiazuron-induced in vitro plant regeneration, phenolic contents, antioxidant potential, GC-MS profiles, and nuclear genome stability of *Plectranthus amboinicus* (Lour.) Spreng. *Horticulturae* **9**(2), 277. https://doi.org/10.3390/horticulturae9020277

Ghosh, A., Igamberdiev, A.U. & Debnath, S.C. 2018. Thidiazuron-induced somatic embryogenesis and changes of antioxidant properties in tissue cultures of half-high blueberry plants. *Scientific Reports* **8**, 16978. https://doi.org/10.1038/s41598-018-35373-7

Huang, Z., Liu, Q., Zou, X., Zhu, L., Ma, X. & Huang, R. 2025. Morpho-physiological responses during dark-induced leaf senescence in *Cunninghamia lanceolata* seedlings. *Forests* **16**(9), 1372. https://doi.org/10.3390/f16091372

Indrachapa, M.T.N., Balasuriya, B.M.I.K., Jayarathna, S.P.N.C., Vidhanaarachchi, V.R.M. & Mu, Z. 2025. Optimizing pulse treatments for enhanced in vitro rooting in coconut micropropagation. *Technology in Horticulture* **5**, e027. https://doi.org/10.48130/tihort-0025-0019

Kalaipandian, S., Mu, Z., Kong, E.Y.Y., Biddle, J., Cave, R., Bazrafshan, A., Wijayabandara, K., Beveridge, F.C., Nguyen, Q. & Adkins, S.W. 2021. Cloning coconut via somatic embryogenesis: A review of the current status and future prospects. *Plants* **10**(10), 2050. https://doi.org/10.3390/plants10102050

Kim, S.-H., Zebro, M., Jang, D.-C., Sim, J.-E., Park, H.-K., Kim, K.-Y., Bae, H.-M., Tilahun, S. & Park, S.-M. 2023. Optimization of plant growth regulators for in vitro mass propagation of a disease-free 'Shine Muscat' grapevine cultivar. *Current Issues in Molecular Biology* **45**(10), 487. https://doi.org/10.3390/cimb45100487

Kong, E.Y.Y., Biddle, J.M., Sisunandar, S., Kalaipandian, S., Bazrafshan, A., Mu, Z. & Adkins, S.W. 2025. Initiation of direct shoot organogenesis in coconut using immature inflorescence. *Plants* **14**(20), 3123. https://doi.org/10.3390/plants14203123

Li, F., Wu, Q., Liao, B., Yu, K., Huo, Y., Meng, L., Wang, S., Wang, B., Du, M., Tian, X. & Li, Z. 2022. Thidiazuron promotes leaf abscission by regulating the crosstalk between ethylene, auxin, and cytokinin in cotton. *International Journal of Molecular Sciences* **23**(5), 2696. https://doi.org/10.3390/ijms23052696

Long, Y., Yang, Y., Pan, G. & Shen, Y. 2022. New insights into tissue culture plant-regeneration mechanisms. *Frontiers in Plant Science* **13**, 926752. https://doi.org/10.3389/fpls.2022.926752

Manghwar, H., Hussain, A., Alam, I., Fan, S., Sun, G. & Liu, F. 2026. Brassinosteroids (BRs) and photomorphogenesis: Hormonal regulation of light-mediated plant development. *Environmental and Experimental Botany* **241**, 106298. https://doi.org/10.1016/j.envexpbot.2025.106298

Martins, J.P.R., Wawrzyniak, M.K., Kalemba, E.M., Ley-López, J.M., Sousa Lira, J.M. & Chmielarz, P. 2024. In vitro rooting of *Quercus robur*: Activated charcoal vs. exogenous auxin—A morphophysiological approach. *Plant Cell, Tissue and Organ Culture* **156**, 24–35. https://doi.org/10.1007/s11240-023-02532-4

Mu, Z., Li, Z., Nulu, N.P.C., Kalaipandian, S., Biddle, J.M., Bazrafshan, A., Kong, E. & Adkins, S.W. 2025. A photomixotrophic system to improve the growth of in vitro cultured seedlings of coconut (*Cocos nucifera* L.). *Horticulturae* **11**(3), 224. https://doi.org/10.3390/horticulturae11030224

Mu, Z., Yang, Z., Xu, H., Khongmaluan, M., Arikit, S., Tran, B.-M.T., Vidhanaarachchi, V.R. M., Sisunandar, S., Yang, S., Peng, H. & Luo, J. 2024. Prospects and challenges of elite coconut varieties in China: A case study of makapuno. *Tropical Plants* **3**, e029. https://doi.org/10.48130/tp-0024-0007

Nguyen, Q.T., Bandupriya, H.D.D., López Villalobos, A., Sisunandar, S., Foale, M. & Adkins, S.W. 2016. Biology, propagation, and utilization of elite coconut varieties. *Plant Physiology and Biochemistry* **109**, 579–589. https://doi.org/10.1016/j.plaphy.2016.10.007

Pasternak, T.P. & Steinmacher, D. 2024. Plant growth regulation in cell and tissue culture *in vitro*. *Plants* **13**(2), 327. https://doi.org/10.3390/plants13020327

Pokimica, N., Cosić, T., Uzelac, B., Ninković, S. & Raspor, M. 2024. Dissecting the roles of the cytokinin signaling network: The case of de novo shoot apical meristem formation. *Biomolecules* **14**(3), 381. https://doi.org/10.3390/biom14030381

Sun, J., Li, J., Zhao, M., Zheng, G., Di, B., Wang, J. & Hu, R. 2025. Successful establishment of somatic embryogenesis and shoot organogenesis systems in *Catalpa bungei*. *Plants* **14**(17), 2688. https://doi.org/10.3390/plants14172688

Tian, R., Paul, P., Joshi, S. & Perry, S.E. 2020. Genetic activity during early plant embryogenesis. *Biochemical Journal* **477**(19), 3743–3767. https://doi.org/10.1042/BCJ20190161

Van Gelderen, K., Kang, C. & Pierik, R. 2018. Light signaling, root development, and plasticity. *Plant Physiology* **176**(2), 1049–1060. https://doi.org/10.1104/pp.17.01207

Van Gelderen, K., Kang, C., Paalman, R., Keuskamp, D., Hayes, S. & Pierik, R. 2021. Regulation of lateral root development by shoot-sensed far-red light via HY5 movement to the root. *Frontiers in Plant Science* **12**, 660870. https://doi.org/10.3389/fpls.2021.660870

Venglat, P., Vijayan, P., Sharbel, T.F., Rahman, A. & Tanino, K. 2025. Phytomers, collet and founder cells: A 'universal' plant embryonic body plan. *Frontiers in Plant Science* **16**, 1521527. https://doi.org/10.3389/fpls.2025.1521527

Wilms, H., De Bièvre, D., Longin, K., Swennen, R., Rhee, J. & Panis, B. 2021. Development of the first axillary in vitro shoot multiplication protocol for coconut palms. *Scientific Reports* **11**, 18367. https://doi.org/10.1038/s41598-021-97888-1

Wu, W., Chen, L., Liang, R., Huang, S., Li, X., Huang, B., Luo, H., Zhang, M., Wang, X. & Zhu, H. 2025. The role of light in regulating plant growth, development and sugar metabolism: A review. *Frontiers in Plant Science* **15**, 1507628. https://doi.org/10.3389/fpls.2024.1507628

Yun, F., Liu, H., Deng, Y., Hou, X. & Liao, W. 2023. The role of light-regulated auxin signaling in root development. *International Journal of Molecular Sciences* **24**(6), 5253. https://doi.org/10.3390/ijms24065253

Zhang, K., Novak, O., Wei, Z., Gou, M., Zhang, X., Yu, Y., Setter, T. & Zhang, J. 2023. Spatially distributed cytokinins: Metabolism, signaling, and transport. *Cell Reports Physical Science* **4**(1), 101075. https://doi.org/10.1016/j.xcrp.2022.101075

Zhang, N., Wang, J., Liu, J., Zhang, P., Kudoyarova, G., Liu, C.J. & Zhang, K. 2024. Photoregulatory protein kinases fine-tune plant photomorphogenesis. *Developmental Cell* **59**(3), 232–245. https://doi.org/10.1016/j.devcel.2024.02.012

INSTRUCTIONS TO AUTHORS

Papers must be in English (British spelling). Authors are strongly urged to have their manuscripts reviewed linguistically prior to submission. Contributions should be sent electronically. Papers are considered by referees before acceptance. The manuscript should follow the instructions below.

Structure: Title, Authors (initials & surname; an asterisk indicates the corresponding author), Authors' affiliation with postal address (each on a separate line) and e-mail of the corresponding author, Abstract (up to 250 words), Key words (not repeating words in the title), Introduction, Materials and methods, Results and discussion, Conclusions, Acknowledgements (optional), References.

Layout, page size and font

- Use preferably the latest version of **Microsoft Word**, doc., docx. format.
- Set page size to **ISO B5 (17.6×25 cm)**, all **margins at 2 cm**. All text, tables, and figures must fit within the text margins.
- Use single line spacing and **justify the text**. Do not use page numbering. Use **indent 0.8 cm** (do not use tab or spaces instead).
- Use font Times New Roman, point size for the title of article **14 (Bold)**, author's names 12, core text 11; Abstract, Key words, Acknowledgements, References, tables, and figure captions 10.
- Use *italics* for Latin biological names, mathematical variables and statistical terms.
- Use single ('…') instead of double quotation marks ("…").

Tables

- All tables must be referred to in the text (Table 1; Tables 1, 3; Tables 2–3).
- Use font Times New Roman, regular, 10 pt. Insert tables by Word's 'Insert' menu.
- Do not use vertical lines as dividers; only horizontal lines (1/2 pt) are allowed. Primary column and row headings should start with an initial capital.

Figures

- All figures must be referred to in the text (Fig. 1; Fig. 1 A; Figs 1, 3; Figs 1–3). Use only black and white or greyscale for figures. Avoid 3D charts, background shading, gridlines and excessive symbols. Use font **Arial, 10 pt** within the figures. Make sure that thickness of the lines is greater than 0.3 pt.
- Do not put caption in the frame of the figure.
- The preferred graphic format is Excel object; for diagrams and charts EPS; for half-tones please use TIFF. MS Office files are also acceptable. Please include these files in your submission.
- Check and double-check spelling in figures and graphs. Proof-readers may not be able to change mistakes in a different program.

References

- **Within the text**

In case of two authors, use '&', if more than two authors, provide first author 'et al.':

Smith & Jones (2019); (Smith & Jones, 2019);
Brown et al. (2020); (Brown et al., 2020)

When referring to more than one publication, arrange them by following keys: 1. year of publication (ascending), 2. alphabetical order for the same year of publication:

(Smith & Jones, 2019; Brown et al., 2020; Adams, 2021; Smith, 2021)

- **For whole books**

Name(s) and initials of the author(s). Year of publication. *Title of the book* (*in italics*). Publisher, place of publication, number of pages.

Behera, K.B. & Varma, A. 2019. *Bioenergy for Sustainability and Security*. Springer International Publishing, Cham, pp. 1–377.

- **For articles in a journal**

Name(s) and initials of the author(s). Year of publication. Title of the article. *Abbreviated journal title* (*in italic*) volume (in bold), page numbers.

Titles of papers published in languages other than English, should be replaced by an English translation, with an explanatory note at the end, e.g., (in Russian, English abstr.).

Bulgakov, V., Adamchuk, V., Arak, M. & Olt, J. 2018. The theory of cleaning the crowns of standing beet roots with the use of elastic blades. *Agronomy Research* **16**(5), 1931–1949. doi: 10.15159/AR.18.213

Doddapaneni, T.R.K.C., Praveenkumar, R., Tolvanen, H., Rintala, J. & Konttinen, J. 2018. Techno-economic evaluation of integrating torrefaction with anaerobic digestion. *Applied Energy* **213**, 272–284. doi: 10.1016/j.apenergy.2018.01.045

- **For articles in collections:**

Name(s) and initials of the author(s). Year of publication. Title of the article. Name(s) and initials of the editor(s) (preceded by In:) *Title of the collection (in italics)*, publisher, place of publication, page numbers.

Yurtsev, B.A., Tolmachev, A.I. & Rebristaya, O.V. 2019. The floristic delimitation and subdivisions of the Arctic. In: Yurtsev, B.A. (ed.) *The Arctic Floristic Region*. Nauka, Leningrad, pp. 9–104 (in Russian).

- **For conference proceedings:**

Name(s) and initials of the author(s). Year of publication. Name(s) and initials of the editor(s) (preceded by In:) *Proceedings name (in italics)*, publisher, place of publishing, page numbers.

Ritchie, M.E. & Olff, H. 2020. Herbivore diversity and plant dynamics: compensatory and additive effects. In: Olff, H., Brown, V.K. & Drent R.H. (eds) *Herbivores between plants and predators. Proc. Int. Conf. The 38th Symposium of the British Ecological Society*, Blackwell Science, Oxford, UK, pp. 175–204.

Please note

- Use '.' (not ',') for decimal point: 0.6 ± 0.2; Use ',' for thousands – 1,230.4;
- Use '–' (not '-') and without space: pp. 27–36, 1998–2000, 4–6 min, 3–5 kg
- With spaces: 5 h, 5 kg, 5 m, 5 °C, C : D = 0.6 ± 0.2; p < 0.001
- Without space: 55°, 5% (not 55 °, 5 %)
- Use 'kg ha^{-1}' (not 'kg/ha');
- Use degree sign ' ° ' : 5 °C (not 5 ^{O}C).